

Geodesic statistics for random network families

Sahil Loomba^{1,*} and Nick S. Jones^{1,2,†}

¹*Department of Mathematics, Imperial College London*

²*EPSRC Centre for the Mathematics of Precision Healthcare,*

Department of Mathematics, Imperial College London

(Dated: November 4, 2021)

A key task in the study of networked systems is to derive local and global properties that impact connectivity, synchronizability, and robustness. Computing shortest paths or geodesics in the network yields measures of node centrality and network connectivity that can contribute to explain such phenomena. We derive an analytic distribution of shortest path lengths, on the giant component in the supercritical regime or on small components in the subcritical regime, of any sparse (possibly directed) graph with conditionally independent edges, in the infinite-size limit. We provide specific results for widely used network families like stochastic block models, dot-product graphs, random geometric graphs, and graphons. The survival function of the shortest path length distribution possesses a simple closed-form lower bound which is asymptotically tight for finite lengths, has a natural interpretation of traversing independent geodesics in the network, and delivers novel insight in the above network families. Notably, the shortest path length distribution allows us to derive, for the network families above, important graph properties like the bond percolation threshold, size of the giant component, average shortest path length, and closeness and betweenness centralities. We also provide a corroborative analysis of a set of 20 empirical networks. This unifying framework demonstrates how geodesic statistics for a rich family of random graphs can be computed cheaply without having access to true or simulated networks, especially when they are sparse but prohibitively large.

Keywords: random networks, shortest path, giant component, percolation, closeness, betweenness, centrality

I. INTRODUCTION

Networks have increasingly become important abstractions for representing a plethora of real-world complex systems. This spans the variety of social networks of friendship connections, ecological networks of predators and preys, biochemical networks of proteins and metabolites, and technological networks like power grids or the internet [1–4]. Often, network structures are not entirely known, and are inferred from partial observations of connections, or of signals generated by the system [5–9]. Inference must account for confounding by many sources of uncertainty, especially measurement errors, which has resulted in a surge of statistical inference methods that yield a probabilistic network model [10]. Moreover, many real-world networks, such as social networks of entire societies, tend to contain a large number of nodes. Estimating properties of very large networks can be computationally prohibitive, especially if one is interested in higher-order properties such as the size of the giant component, or the average distance between any two nodes in the networks. Both of these have impact on overall graph connectivity, network robustness, percolation properties and system synchronizability [11–14], which have been studied deeply for many physical, biological and social systems. The principal motivation for this work is to analytically estimate such network properties by having access either to just an expectation of network realizations,

or to a statistical network model, without simulating networks or obtaining an error-free observation of one. In particular, we focus on geodesic properties of a network, and establish a distribution of shortest path lengths on the giant component in the supercritical regime—when the giant component exists—or on small components in the subcritical regime—when the giant component does not exist.

Problem setting. We consider any random graph wherein edges between any two nodes are independent of one another, perhaps after conditioning on some other node variables. Many popular random graph models are instances of this kind—like the stochastic block model (SBM), random dot-product graph (RDPG), random geometric graph (RGG) or more generally any inhomogeneous random graph. Those explicitly encoding higher-order interactions and dependencies such as exponential random graph models [15] are excluded from this study. We assume network sparsity in the sense that the number of edges varies linearly in the number of nodes. We derive a set of recursive relations in the asymptotic limit that stipulates the full shortest path length distribution (SPLD) between any two nodes on the giant component of a network in the supercritical regime, and on small components otherwise.

Prior work on the SPLD. Previous results on the SPLD have focused almost exclusively on the simplest model of Erdős–Rényi (ER) graphs [16, 17], or average path lengths in degree-configuration models [18, 19] or scalar latent variable models [20], and some results display appreciable discrepancies between theory and empirics in the tail-end of the distribution—especially for net-

* s.loomba18@imperial.ac.uk

† nick.jones@imperial.ac.uk

works with small degrees [16, 17]. Related work has determined the distribution of picking a path between two nodes in a given network [21]—however, this approach does not directly model the distribution of shortest path *lengths* between node pairs. Description of the full SPLD for a general family of network models has, before this work, remained elusive [22].

Our contributions to the SPLD. The proposed approach provides, to the best of our knowledge, the most accurate description of the distribution of shortest path lengths between any node pair for a very general class of (possibly directed) networks. We determine a closed-form lower bound of the SPLD’s survival function which is tight for finite lengths in the asymptotic limit, and has a natural interpretation of traversing independent shortest paths in the graph. The closed-form is specified by an iterated integral operator defined over functions on the node space, whose kernel function indicates the likelihood of an edge existing between two nodes. The integral operator is analogous to the expected adjacency matrix in the finite-dimensional setting, and summarizes the dependence of a node function on all other nodes in the network. If the kernel is symmetric, it leads to an expression for the SPLD in terms of the spectral decomposition of the integral operator. Under specific scenarios, our method recovers known results on geodesics, such as the small-world property of ER graphs [2, 23], or the ultrasmall property of Barabási and Albert (BA) graphs [24]. We provide new results for the illustrative models considered namely SBM, Gaussian RGG, RDPG and sparse graphon, and also apply them to real-world networks. Most prior work in the field has produced analytic results concerning *specific* phenomena on *specific* random graph models. However, our approach to the SPLD unifies the study of shortest paths, and related phenomena of connectedness and centralities, into one theoretical framework. In Tab. I, we include an index for the main analytical results.

Our contributions to network percolation theory. Phenomena related to percolation, i.e. random occupation of sites or bonds, are well-studied in the statistical physics literature. For networks, we can consider the *bond* percolation threshold, at which a giant component exists in the network. There are analytic results on the bond percolation threshold for specific random graph models—graphs with a given degree sequence [25–28], or those with a power law degree distribution [11, 12]. Other notable works have derived thresholds for a more general class of inhomogeneous random graph models with independent edges placed according to symmetric kernels [29–32], and for sparse empirical networks [33, 34], by formulating corresponding branching or message passing processes. Here, we establish a direct relationship between the lower bound of the survival function of the SPLD and the bond percolation threshold. Our formalism adds to the literature by supplying the percolation threshold for the class of sparse random graph models with independent edges, regardless of the symmetry of

the kernel function, which leads to new results and connections on percolation behavior in the models considered. Tab. II summarizes select analytical results on the bond percolation threshold.

Our contributions to geodesic-based centralities. Network centralities are structural measures of importance of nodes in a network, and those based on shortest paths like closeness and betweenness centralities are of great interest when studying real-world networks [35, 36]. Prior work on dense RGGs has derived closed-form expressions for node betweenness [37]. Previous research has also defined spectrum-based centralities for graphons [38] analogous to the eigenvector [39] and Katz centralities [40]. Here, we express closeness in closed-form, and betweenness analytically, for general random graph families that include sparse graphons and RGGs as special cases. In summary, local and global properties of networks, of both empirical and theoretical interest, can be extracted from the SPLD.

The article is organized as follows. In Sec. II we describe the probabilistic framework to derive the SPLD for random graphs defined by an ensemble average model. In Sec. III, we extend this formalism to general random graph families, both directed and undirected, and in Sec. IV we highlight specific cases of popular network models and real-world networks. In Sec. V, we draw a connection between the SPLD and bond percolation threshold, thus deriving a condition for percolation for any random graph model. Then in Sec. VI, we show how path-based statistics like average geodesic lengths, and centralities of node closeness and betweenness can be analytically estimated. Finally, we conclude in Sec. VII with a summary of our results and limitations of this framework.

II. SHORTEST PATH LENGTH DISTRIBUTION

We first derive the distribution of shortest path lengths between two nodes in a network using a recursive approach. In Sec. II A we consider the supercritical regime, describe a lemma that permits the construction of a geodesic via intervening nodes, and discuss a technical condition of sparsity required to generate a set of recursive equations. To supply the initial condition, in Sec. II B we derive the percolation probability of a node. In Sec. II C, the formalism is extended to the subcritical regime. Then in Sec. II D, we extract a closed-form bound of the SPLD.

Definitions. We consider a network of n nodes without self-loops represented by the $n \times n$ adjacency matrix A . That is, for two nodes indexed by i (“source”) and j (“target”), $A_{ij} = 1$ if there is an edge from i to j and $A_{ij} = 0$ otherwise, and $A_{ii} = 0$. We assume knowledge of the expectation in the ensemble average sense: access to the expected adjacency matrix $\langle A \rangle$ such that

$$A_{ij} \sim \text{Bernoulli}(\langle A \rangle_{ij}). \quad (1)$$

TABLE I. Index of equations for main results regarding (A) the shortest path length distribution, (B) percolation behaviour, (C) mean geodesic lengths, (D) closeness centrality, and (E) node betweenness centrality.

Random graph model	Ensemble average	Independent edge models	ER graph	SBM	RDPG	Gaussian RGG	Multiplicative graphon	Scale-free graphon
Exact recursive form $(\Psi_l, \Omega_l), (\psi_l, \omega_l)$	12, 13, 17							35, 36, 37
A Closed-form $(\underline{\Psi}_l, \underline{\Omega}_l), (\underline{\psi}_l, \underline{\omega}_l)$	13, 17, 29							36, 37, 44
Apx. closed-form $(\tilde{\Psi}_l, \tilde{\Omega}_l), (\tilde{\psi}_l, \tilde{\omega}_l)$	30	46	56	55	62	G28, 70		78
B Percolation probability ρ	17	36		52	61	69		77
B Percolation threshold	101	90	95a	99, 100	103	105	93	96
C Mean geodesic length	H4							H5
C Apx. mean geodesic length	H6				107		111, 119 ^a	118
D Node closeness	H9							H10
D Apx. node closeness					123			124
E Node betweenness								125, 126, A3
E Apx. node betweenness								125, 126, A5

^a Multiplicative graphons are equivalent to canonical degree-configuration models (see Sec. IV E) and to rank-1 models (see Sec. V A)

We use the notation $\langle \cdot \rangle$ when averaging over the ensemble. For directed networks, all edges are added independently of each other. For undirected networks, enforce $\langle A \rangle = \langle A \rangle^T$ and, without loss of generality, use node indices as an arbitrary ordering: for $i < j$, A_{ij} is generated independently from Eq. 1, and $A_{ji} = A_{ij}$. Let $\lambda_{ij} \in \mathbb{Z}_{\geq 0}$ be the random variable denoting length of the shortest path from node i to node j .

Node degrees and sparsity. The out- and in-degrees of node i , that respectively encode the number of edges emanating from and incident on i , are given by

$$d_i^+ = \sum_{j \neq i} A_{ij}, \quad (2a)$$

$$d_i^- = \sum_{j \neq i} A_{ji}. \quad (2b)$$

Since edges are added independently, from Eq. 1 the out- and in-degrees of node i follow a Poisson binomial distribution in this ensemble, with the expectation from Eq. 2:

$$\langle d_i^+ \rangle = \left\langle \sum_{j \neq i} A_{ij} \right\rangle = \sum_{j \neq i} \langle A \rangle_{ij}, \quad (3a)$$

$$\langle d_i^- \rangle = \left\langle \sum_{j \neq i} A_{ji} \right\rangle = \sum_{j \neq i} \langle A \rangle_{ji}, \quad (3b)$$

where the second equality in Eqs. 3a, 3b arise by linearity of expectation. We further define the mean network degree as the mean network *out*-degree:

$$\langle d \rangle \triangleq \mathbb{E}[d^+] = \frac{\sum_i \sum_{j \neq i} \langle A \rangle_{ij}}{n}, \quad (4)$$

which we remark can be equivalently defined as the mean network *in*-degree, since both are equal. We use the notation $\mathbb{E}[\cdot]$ when averaging over nodes. For undirected networks we define the degree of node i as:

$$d_i \triangleq d_i^+ = d_i^-, \quad (5)$$

whose expectation is provided by Eq. 3. In this work, we assume that the network is sparse in the sense that nodes have a bounded expected degree asymptotically. From Eq. 3, it is then sufficient that $\forall(i, j)$:

$$\langle A \rangle_{ij} = O(n^{-1}). \quad (6)$$

We remark that due to sparsity, the out- and in-degrees asymptotically follow a Poisson distribution (see Appendix C).

A. Supercritical regime

In this section, we focus on the supercritical regime. We say that a node pair (i, j) is supercritical if asymptotically there can exist a giant component in the network such that there exists a path from i to j going via nodes on that giant component. For an undirected network, a giant component is a connected component whose size is of the order of the number of nodes n in the network, i.e. $O(n)$. Since edges are undirected, if a node i can reach a node j on a giant component, then it can reach *and* be reached from every other node on that giant component. For directed networks the concept of a giant component is more subtle, as it is not necessary for a (directed) path to exist from i to j , even if one exists from j to i . Given this non-trivial difference, we mostly consider networks in an undirected setting in the main text, with results for directed networks reserved for the appendix. We refer the reader to Appendix E for a discussion on directed networks.

Without loss of generality, we assume that $\langle A \rangle$ is not permutation similar to a block diagonal matrix, i.e. it is irreducible. (If $\langle A \rangle$ were reducible, there would exist node subsets that can never have edges between them, and we can simply consider the SPLD separately for subgraphs induced by those node subsets. This assumption is not necessary for our formalism and can be relaxed,

but it simplifies the exposition: if $\langle A \rangle$ is irreducible, then asymptotically there can only exist a unique giant component.) Let ϕ_i be the event that node i is on the giant component, and $\neg\phi_i$ be the event that it is not. We consider the distribution of λ_{ij} conditioned on the source node i being on the giant component. It is useful to define matrices Ω_l, Ψ_l encoding the survival function and conditional probability mass function of the SPLD respectively:

$$[\Psi_l]_{ij} \triangleq P(\lambda_{ij} > l | \phi_i), \quad (7a)$$

$$[\Omega_l]_{ij} \triangleq P(\lambda_{ij} = l | \lambda_{ij} > l - 1, \phi_i), \quad (7b)$$

which we refer to as the ‘‘survival function matrix’’ and ‘‘conditional probability mass function’’ (conditional PMF) matrix respectively. We use the notation $[X]_{ij}$ to refer to the $(i, j)^{th}$ element of a matrix X , to avoid any confusion where it might arise (when X has an associated subscript, or is a product of matrices).

Recursive setup. Since the geodesic being longer than l necessarily implies that it is longer than $l - 1$, modeling recursively for the non-existence of a geodesic from i to j up to some length l is convenient:

$$P(\lambda_{ij} > l | \phi_i) = P(\lambda_{ij} > l | \lambda_{ij} > l - 1, \phi_i) P(\lambda_{ij} > l - 1 | \phi_i). \quad (8)$$

We can write the first factor of the recursive equation as the conditional likelihood of no path of length l existing between i, j , which can be written by accounting for the non-existence of paths of length l from i to j via any node $u \neq (i, j)$ such that there is a direct edge from u to j . Due to sparsity in the asymptotic limit, the probability of existence of a geodesic of any finite length l is asymptotically of $O(n^{-1})$ (Appendix C for details). It then follows that there is vanishing correlation between pairs of shortest paths of length l from i to j via pairs of nodes $u, v \neq (i, j)$, which simplifies the overall likelihood in Eq. 8 into a product of individual likelihoods:

$$P(\lambda_{ij} > l | \lambda_{ij} > l - 1, \phi_i) = \prod_{u \neq (i, j)} [1 - P(\lambda_{iu} = l - 1, \lambda_{uj} = 1 | \lambda_{ij} > l - 1, \phi_i)]. \quad (9)$$

We emphasize that this assumption holds on the giant component for finite geodesic lengths as $n \rightarrow \infty$: as we consider longer geodesics of $O(\log n)$, the likelihood of a node to be at that distance approaches $O(1)$ instead of $O(n^{-1})$, even for sparse networks. This induces finite-size effects on the SPLD, which become incrementally concentrated around the mode of the SPLD as network size increases. See Appendix C for an extended treatment of finite-size effects. To simplify the term on the RHS of Eq. 9, we use Lemma 1 in Appendix A 1, that exploits the assumption of conditionally independent edges in the asymptotic limit to show that:

$$P(\lambda_{iu} = l - 1, \lambda_{uj} = 1 | \lambda_{ij} \geq l, \phi_i) = P(\lambda_{iu} = l - 1 | \phi_i) \times P(A_{uj} = 1). \quad (10)$$

From Eqs. 9, 10 we have $P(\lambda_{iu} = l - 1, \lambda_{uj} = 1 | \lambda_{ij} > l - 1, \phi_i) = P(\lambda_{iu} = l - 1 | \phi_i) P(A_{uj} = 1)$. Finally, note that $P(\lambda_{iu} = l - 1 | \phi_i) = P(\lambda_{iu} = l - 1 | \lambda_{iu} > l - 2, \phi_i) P(\lambda_{iu} > l - 2 | \phi_i)$ to write Eq. 9 as

$$P(\lambda_{ij} > l | \lambda_{ij} > l - 1, \phi_i) = 1 - P(\lambda_{ij} = l | \lambda_{ij} > l - 1, \phi_i) = \prod_{u \neq (i, j)} [1 - P(\lambda_{iu} = l - 1 | \lambda_{iu} > l - 2, \phi_i) \times P(\lambda_{iu} > l - 2 | \phi_i) P(A_{uj} = 1)]. \quad (11)$$

Using the definitions in Eq. 7 we can write Eqs. 8, 11 succinctly in terms of the survival function matrix and conditional PMF matrix of the SPLD:

$$[\Psi_l]_{ij} = (1 - [\Omega_l]_{ij}) [\Psi_{l-1}]_{ij}, \quad (12a)$$

$$[\Omega_l]_{ij} = 1 - \exp \left(\sum_u \log \left(1 - [\Omega_{l-1}]_{iu} [\Psi_{l-2}]_{iu} \langle A \rangle_{uj} \right) \right), \quad (12b)$$

where \exp and \log refer to element-wise exponentiation and natural logarithm respectively. The above pair of recursive equations, together with the initial conditions $[\Omega_1]_{ij} \triangleq P(\lambda_{ij} = 1 | \lambda_{ij} > 0, \phi_i) = P(A_{ij} = 1 | \phi_i)$ and $[\Psi_0]_{ij} \triangleq P(\lambda_{ij} > 0 | \phi_i) = 1$, completely define the distribution of shortest paths, from which other network properties of interest can be extracted. Note that $[\Omega_0]_{ij}$ does not exist, while $1 - [\Psi_\infty]_{ij}$ naturally encodes the probability of the shortest path between i, j being of infinite length, i.e. j not being on the giant component, as i is already on the giant component. Since self-loops are ignored, $[\Psi_l]_{ii} \triangleq 0$ and $[\Omega_l]_{ii} \triangleq 0$.

To define the initial condition $[\Omega_1]_{ij} = P(A_{ij} = 1 | \phi_i)$, we use Lemma 4 in Appendix B which shows that:

$$P(A_{ij} = 1 | \phi_i) = P(A_{ij} = 1) \left\{ 1 + \left[\frac{1}{P(\phi_i)} - 1 \right] P(\phi_j) \right\}. \quad (13)$$

Estimating the RHS of Eq. 13 requires the probability of a node to be on the giant component, i.e. to be ‘‘percolating’’, which we derive in Sec. II B.

B. Percolation probability

To solve Eq. 12, we need to solve Eq. 13 and find percolation probabilities. In this section, we provide two solutions which respectively yield an ‘‘analytic form’’ and an ‘‘approximate analytic form’’ of the SPLD.

Analytic form. In principle, percolation probabilities can be extracted from the survival function of the geodesic length distribution. By continuity of the distribution,

$$P(\lambda_{ij} = \infty | \phi_i) = \lim_{l \rightarrow \infty} P(\lambda_{ij} > l | \phi_i). \quad (14)$$

That is, the steady state of recursive Eq. 12a is indicative of the amount of probability mass at $\lambda_{ij} = \infty$, when i

is on the giant component. Correspondingly, $\forall(i, j)$, we have

$$P(\phi_j) = 1 - P(\lambda_{ij} = \infty | \phi_i). \quad (15)$$

Eqs. 12, 13, 14 and 15 provide us with the full “analytic form” of the SPLD.

Approximate analytic form. At first, computing the RHS of Eq. 15 appears to be a circular problem, since we require the limiting value of the survival function of the SPLD to obtain the initial condition for it. However, we empirically observe that precision in the initial condition is important for agreement of the survival function only for smaller geodesic lengths, whereas we obtain the expected limiting value when using a naïve approximation of the initial condition by setting

$$P(A_{ij} = 1 | \phi_i) = P(A_{ij} = 1). \quad (16)$$

Therefore, running the recursive setup once gives access to $P(\lambda_{ij} = \infty | \phi_i)$, which can then be used to derive the (exact) analytic form of the SPLD from Eqs. 12, 13 and 15 in a second recursion. Henceforth, we refer to the SPLD obtained by using the naïve initial condition in Eq. 16, alongside Eq. 12, as the “approximate analytic form” of the SPLD. We note from Eq. 13 that the approximation in Eq. 16 holds when the network is almost surely connected: $P(\phi_i) \rightarrow 1$. More generally, using the approximation will underestimate the probability mass on short geodesics—refer to Appendix B for details. For an ER graph of mean degree $\langle d \rangle$, where asymptotically $\langle A \rangle_{ij} = \frac{\langle d \rangle}{n}$, Fig. 1 indicates good agreement between the empirical and analytic cumulative distribution functions (CDF) of the SPLD. We note that the approximate analytic CDF remains a good approximation even for shorter geodesics.

Self-consistency equation. Alternatively, we can separately derive percolating probabilities without invoking the SPLD. Consider generating the network edges in some order, such that the edges of node i are generated as the final step, without loss of generality. Due to conditionally-independent edges, in the asymptotic limit, considering the network without edges of i will make vanishing difference to the likelihood of other nodes $j \neq i$ belonging to the giant component. We note that i will be on the giant component only if it connects directly to at least one j —with probability $P(A_{ij} = 1)$ —such that j itself is on the giant component—with probability $P(\phi_j)$. That is

$$\begin{aligned} P(\phi_i) &= 1 - \prod_{j \neq i} [1 - P(A_{ij} = 1)P(\phi_j)] \\ &= 1 - \exp \left(\sum_{j \neq i} \log(1 - P(A_{ij} = 1)P(\phi_j)) \right) \\ &\approx 1 - \exp \left(- \sum_{j \neq i} P(A_{ij} = 1)P(\phi_j) \right), \end{aligned}$$

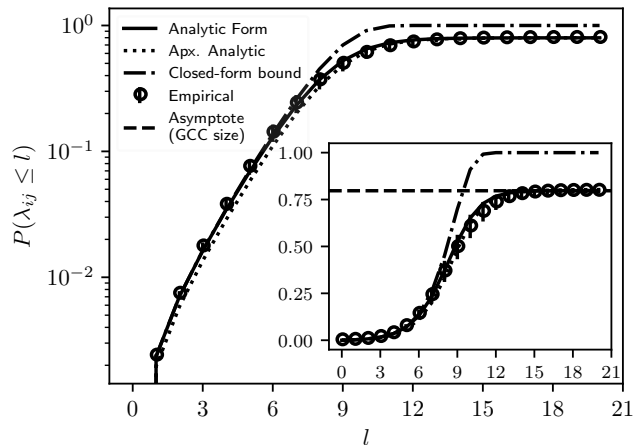


FIG. 1. Analytic cumulative distribution function (CDF) of shortest path lengths for an ER graph agree with the empirical CDF, where the source node is on the giant component. Network size is fixed at $n = 1024$, while mean degree at $\langle d \rangle = 2$. Solid and dotted lines indicate analytic solutions derived from analytic (Eqs. 12, 13, 17) and approximate analytic forms (Eqs. 12, 16) respectively, while dash-dotted line indicates the closed-form bound obtained from Eq. 29. Symbols and bars indicate empirical estimates: mean and standard error over 10 network samples. Dashed asymptote indicates size of the giant component as estimated from the self-consistency Eq. 17. The approximate analytic form marginally underestimates the probability mass for shorter lengths, as is evident on the log-scale (main plot). The closed-form bound shows good agreement for shorter lengths, but deviates strongly for longer ones (inset plot on the linear-scale)—saturating to unity for any percolating graph. There is good agreement between the analytic and empirical estimates, with some deviation around the mode of the distribution, due to finite-size effects—see Appendix C.

where the first-order logarithmic approximation works for sparse networks asymptotically since $\langle A \rangle_{ij} = O(n^{-1})$. Let $\boldsymbol{\rho}$ be the vector encoding $\rho_i \triangleq P(\phi_i)$. Then percolation probability of every node is given by a non-trivial solution to the following transcendental vector equation:

$$\boldsymbol{\rho} = \mathbf{u} - \exp(-\langle A \rangle \boldsymbol{\rho}), \quad (17)$$

where \mathbf{u} is an all-ones vector of length n . For the simplest case of ER graphs, this becomes a scalar equation. In Fig. 17 in Appendix F 1, we demonstrate for ER graphs that there is indeed an agreement between the percolating probabilities observed empirically, from the approximate analytic form (using Eqs. 12, 14, 15 and 16), and from the self-consistency Eq. 17 via function iteration. In all results that follow, we use Eqs. 12, 13, and 17 to yield the “analytic form” of the SPLD in the supercritical regime.

C. Subcritical regime

We now extend the SPLD formalism to the subcritical regime. A node pair (i, j) is subcritical if asymptotically there cannot exist a giant component such that there exists a path from i to j that goes through it. This implies that asymptotically, either there cannot exist *any* path between i, j , in which case $\langle A \rangle$ is reducible and the SPLD trivially has all probability mass at infinity, or i, j can only exist on a small component yielding the subcriticality condition

$$P(\phi_i) = P(\phi_j) = 0, \quad (18)$$

in which case we consider the SPLD on the small component containing i, j .

Analogous to Eq. 7, we can define the conditional PMF and survival function matrices, but without the conditioning on ϕ_i (which is an impossible event). Also, the recursive setup described in Sec. II A, alongside the key result in Lemma 1, can be applied verbatim in the subcritical regime. The only difference is in the initial condition for the conditional PMF:

$$[\Omega_1]_{ij} \triangleq P(\lambda_{ij} = 1 | \lambda_{ij} > 0) = P(A_{ij} = 1), \quad (19)$$

which is completely defined under the ensemble average model. That is, Eqs. 12 and 19 yield the “analytic form” of SPLD when i, j are in the subcritical regime. In the sections that follow, we focus on the supercritical regime, but remark that results for the subcritical regime naturally follow by dropping the conditioning on ϕ_i . In Fig. 18 in Appendix C, we show the empirics and analytics agree for subcritical ER graphs of varying mean degree.

D. Closed-form bound of SPLD

While the recursive formulation in Eq. 12 is powerful, additional approximations allow for analytical progress for both the SPLD and expectation of geodesic lengths. Since the network is sparse, in the infinite-size limit we can use Eq. 6 to apply a first-order approximation for the logarithm in Eq. 12b. Let \odot indicate element-wise product, then

$$\Omega_l \approx \mathbf{u}\mathbf{u}^T - \exp(-(\Omega_{l-1} \odot \Psi_{l-2}) \langle A \rangle). \quad (20)$$

Let $l = 2$, for which $[\Psi_{l-2}]_{iu} \triangleq P(\lambda_{iu} > l - 2 | \phi_i) = P(\lambda_{iu} > 0 | \phi_i) = 1$. Then we can write from Eq. 20:

$$\Omega_2 = \mathbf{u}\mathbf{u}^T - \exp(-\Omega_1 \langle A \rangle). \quad (21)$$

Due to sparsity, from Eqs. 6 and 13 we obtain:

$$\Omega_1 = O(n^{-1}) \implies \Omega_1 \langle A \rangle = O(n^{-1}). \quad (22)$$

Then application of a first-order approximation for the exponential in Eq. 21 yields:

$$\Omega_2 \approx \Omega_1 \langle A \rangle. \quad (23)$$

From Eqs. 12a and 21 we obtain:

$$\Psi_1 = \exp(-\Omega_1 \langle A \rangle). \quad (24)$$

Next, consider Eq. 20 with $l = 3$, for which using Eqs. 22 and 24 we can assume $\Psi_{l-2} = \Psi_1 \approx 1$. This yields an equation for $l = 3$ similar to Eq. 21:

$$\Omega_3 = \mathbf{u}\mathbf{u}^T - \exp(-\Omega_2 \langle A \rangle) = \mathbf{u}\mathbf{u}^T - \exp(-\Omega_1 \langle A \rangle^2), \quad (25)$$

where we have used Eq. 23. Due to sparsity, we can apply identical arguments as above to obtain:

$$\Omega_1 \langle A \rangle^2 = O(n^{-1}) \quad (26a)$$

$$\implies \Omega_3 \approx \Omega_1 \langle A \rangle^2 \quad (26b)$$

$$\implies \Psi_2 = \exp(-\Omega_1 (\langle A \rangle + \langle A \rangle^2)). \quad (26c)$$

In the infinite-size limit, by induction for any finite l , we can propagate through the sparsity assumption

$$\Omega_l = O(n^{-1}), \quad (27)$$

that results in

$$\Omega_l \approx \Omega_{l-1} \langle A \rangle, \quad (28a)$$

$$\Psi_l \approx \exp\left(-\sum_{k=1}^l \Omega_k\right). \quad (28b)$$

We emphasize that this induction relies on assuming $[\Psi_{l-2}]_{iu} \triangleq P(\lambda_{iu} > l - 2 | \phi_i) \approx 1$, which is equivalent to assuming that the conditional PMF $P(\lambda_{ij} = l | \lambda_{ij} > l - 1, \phi_i)$ approximates the PMF $P(\lambda_{ij} = l | \phi_i)$. In the subcritical regime, (and therefore ignoring the conditioning on ϕ_i), this holds for any value of l in a network of finite (but large) size n , since j is almost surely on a different component from i 's, i.e. $P(\lambda_{ij} > l - 1) \approx 1$. In the supercritical regime, this holds for any bounded value of l in the infinite-size limit, since the shortest path between any two arbitrary nodes is almost surely no less than l , and thus the event $\lambda_{ij} > l - 1$ does not inform $\lambda_{ij} = l$. For finite-sized networks in the supercritical regime, this approximation will evidently work only for smaller path lengths. More precisely, for geodesic lengths longer than $O(\log n)$ —which is around the mode of the SPLD—boundary effects due to finite network size become apparent, Eq. 27 no longer holds, and Eq. 28a stops being a tight bound on the actual conditional PMF. (See Appendix C for details.) In fact, the “conditional PMF” encoded by Ω_l may not be a valid probability measure. However, it yields an expression for the survival function matrix from Eq. 28b in terms of sum of powers of $\langle A \rangle$:

$$\underline{\Psi}_l \triangleq \exp\left(-\Omega_1 \sum_{k=1}^l \langle A \rangle^{k-1}\right), \quad (29)$$

which, on its own terms, is a valid probability measure, and alongside Eqs. 13, 17 completely describes

the SPLD. We refer to Eqs. 13, 17 and 29 as the “closed-form” (bound) of the SPLD, and emphasize that these approximations underestimate probability mass on longer geodesics: the closed-form of the survival (cumulative distribution) function of the SPLD is a lower (upper) bound on the analytic form, which is tight for shorter lengths in finite-size networks. These approximations will not be useful if we are interested in computing the size of the giant component, since the closed-form in Eq. 29 will always have a limiting value of 1 in the supercritical regime (see Theorems 1, 3 in Appendix D 2). However, if we are interested in geodesics shorter than the modal length, or the expectation of geodesic lengths rather than the full SPLD, then these are seen to be reasonable approximations. We demonstrate this behaviour for ER graphs in Fig. 2, and for more general random graph models in Sec. IV.

Approximate closed form of the SPLD. Finally, we consider a scenario which produces a helpful interpretation for the survival function of the SPLD. Putting the naïve initial condition from Eq. 16 in Eq. 29 results in an “approximate closed-form” of the survival function of the SPLD:

$$\tilde{\Psi}_l \triangleq \exp\left(-\sum_{k=1}^l \langle A \rangle^k\right). \quad (30)$$

We note that because using Eq. 16 marginally underestimates probability mass for shorter geodesics, while the approximations used to arrive at Eq. 29 vanishingly overestimate it, Eq. 30 does not necessarily define a bound on the survival function. Regardless, Eq. 30 shows that the approximate closed-form of the survival function of the SPLD at length l is encoded by the sum of powers of $\langle A \rangle$ from 1 to l . This is reminiscent of the well-known result that sum of powers of A encodes the number of paths up to length l [41]. We emphasize that if all node pairs are in the subcritical regime, then Eq. 19 yields exactly $\Omega_1 = \langle A \rangle$, i.e. Eq. 30 is an exact and tight closed-form bound on the SPLD, evident in Fig. 18 in Appendix C.

Interpretation. For an alternate comprehension of the expression in Eq. 30, apply a first-order approximation to its RHS—in the sparse infinite-size limit—to obtain for node pair (i, j) : $[\tilde{\Psi}_l]_{ij} \approx 1 - \sum_{k=1}^l [\langle A \rangle^k]_{ij}$. $[\tilde{\Psi}_l]_{ij}$ can be approximated as the probability of i , which is on the giant component, failing to connect to j (in the asymptotic limit) via any of the independent paths of lengths 1 through l . To see how, note that $\langle A \rangle = O(n^{-1}) \implies \langle A \rangle^k = O(n^{-1})$. If all paths of length k between i, j are independent of one another—an independent-path assumption—then $\langle A \rangle_{ij}^k$ encodes the likelihood of a path of length k between them, since higher-order terms cancel out due to the sparsity of $\langle A \rangle^k$ noted above. If paths of length $1, 2, \dots, l$ are independent of one another—an independent-path-length assumption—then $\sum_{k=1}^l [\langle A \rangle^k]_{ij}$ encodes the probability of a path existing between i, j of any length up to l i.e. $P(\lambda_{ij} \leq l | \phi_i)$, since again, higher-order terms cancel out due to spar-

ity. Then $1 - \sum_{k=1}^l [\langle A \rangle^k]_{ij}$ is $P(\lambda_{ij} > l | \phi_i)$, which is exactly the LHS of Eq. 30. This interpretation provides a retrospective derivation for the approximate closed-form of the survival function of the SPLD.

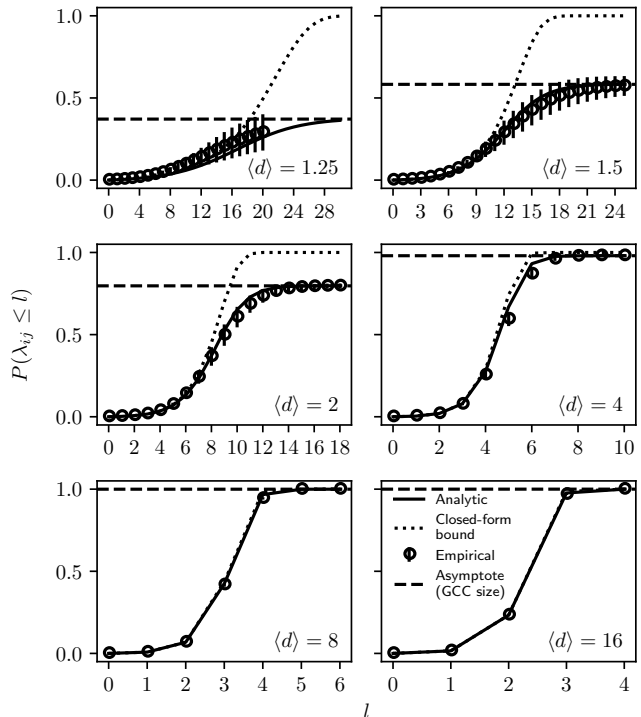


FIG. 2. Empirical, analytic and closed-form cumulative distribution functions (CDF) of shortest path lengths where the source node is on the giant component, for an ER graph with varying connectivity. Network size is fixed at $n = 1024$, while mean degree varies as $\langle d \rangle \in \{1.25, 1.5, 2, 4, 8, 16\}$. Solid and dotted lines indicate analytic (Eqs. 12, 13, 17) and closed-form solutions (Eqs. 13, 29), respectively. Symbols and bars indicate empirical estimates: mean and standard error over 10 network samples. Dashed asymptote indicates size of the giant component as estimated from the self-consistency Eq. 17. While the analytic SPLD is in good agreement for all connectivities at all geodesic lengths, the closed-form SPLD is in good agreement for all connectivities at shorter lengths, while serving as an upper bound to the empirical CDF.

III. GEODESICS IN GENERAL RANDOM GRAPHS WITH INDEPENDENT EDGES

Since $\langle A \rangle$ is representative of any underlying statistical network model (see Appendix E), we can generalize equations for the SPLD when we do not have access to a given network ensemble $\langle A \rangle$, but have knowledge of a (possibly inferred) random graph model that treats both edges and node identities as random variables. In this section, we first derive analogous equations to Sec. II for the expected degree, SPLD and percolation probabilities in this general setting, which will appear as functions instead of

vectors. We also define a linear operator corresponding to $\langle A \rangle$, which will determine key network properties.

Definitions. In its most general form, consider a topological space V of nodes: such as a discrete space for SBMs [42], a Euclidean space for RGGs [43], or an inner-product space for RDPGs [44]. Let μ be a probability measure on it that encodes the distribution of nodes in V , which we refer to as the “node density” in V . Consider the product space $V \times V$ of edges, and their corresponding probability measure ν that encodes the probability of edges conditioned on pairs of node locations in V , e.g. the Euclidean co-ordinates of two nodes in case of an RGG. This function will be referred to as the “connectivity kernel” in $V \times V$. As before, we assume sparsity in the sense that $\nu = O(n^{-1})$ almost everywhere. Lower-case variables will be used to indicate nodes in V . We generate a network of n nodes according to node distribution μ yielding the collection $\mathcal{V} = \{x_i | x_i \sim \mu, i \in \{1, 2 \dots n\}\}$ and add edges between nodes according to a sparse connectivity kernel ν yielding the collection $\mathcal{E} = \{(x_i, x_j) | (x_i, x_j) \sim \nu, (i, j) \in \{1, 2 \dots n\}^2 \text{ s.t. } i \neq j\}$. The result is a graph without self-loops $\mathcal{G} = (\mathcal{V}, \mathcal{E})$ that represents the full network, and may be directed or undirected, contingent on the symmetry of ν . For an undirected network we impose the additional constraints that (1) ν is symmetric, i.e. $\nu(x, y) = \nu(y, x)$, and (2) edges are generated assuming an (arbitrary) ordering of nodes such that $\bar{\mathcal{E}} \triangleq \{(x_i, x_j) | (x_i, x_j) \sim \nu, (i, j) \in \{1, 2 \dots n\}^2 \text{ s.t. } i < j\}$ and $\mathcal{E} = \bar{\mathcal{E}} \cup \{(x_j, x_i) | (x_i, x_j) \in \bar{\mathcal{E}}\}$. We emphasize that while both directed and undirected graphs can be generated using symmetric kernels, graphs generated from asymmetric kernels must necessarily be directed. We also remark that by permitting asymmetric kernels, this model is a moderate extension of the sparse inhomogeneous random graph model [31, 45], which we specifically consider in Sec. IV E.

Degree functions. Some network statistics become immediately apparent for this model with independent edges, such as expected node degrees. For a node located at $x \in V$, let $d^+(x), d^-(x)$ be its out- and in-degree. Recall from Eq. 3a that for the ensemble average model, the expected out-degree for node i is given by $\langle d_i^+ \rangle = \sum_{j \neq i} \langle A \rangle_{ij}$. In the general setting, the sum of expectation over $n-1$ nodes asymptotically translates to n times the expectation over node space V . This yields expressions analogous to Eq. 3 for the expected out- and in-degree at x , and expected network degree:

$$\langle d^+(x) \rangle \triangleq \widehat{d}^+(x) = n \int_V \nu(x, y) d\mu(y), \quad (31a)$$

$$\langle d^-(x) \rangle \triangleq \widehat{d}^-(x) = n \int_V \nu(y, x) d\mu(y), \quad (31b)$$

$$\langle d \rangle \triangleq \mathbb{E}_\mu [\widehat{d}^+(x)] = \int_V \widehat{d}^+(x) d\mu(x), \quad (31c)$$

where we use the convention of defining the mean network degree as the mean network *out*-degree, and the notation $\mathbb{E}_\mu [\cdot]$ when averaging over the node space V .

For undirected networks $\nu(x, y) = \nu(y, x)$ almost everywhere, in which case we define the degree of node at x similarly to Eq. 5 as $d(x) \triangleq d^+(x) = d^-(x)$, yielding:

$$\langle d(x) \rangle \triangleq \widehat{d}(x) = \widehat{d}^+(x) = \widehat{d}^-(x). \quad (32)$$

As before, the sparsity assumption asymptotically implies bounded node degrees and a Poisson degree distribution at x (see Appendix F 1):

$$d(x) \sim \text{Poisson}(\widehat{d}(x)), \quad (33)$$

with similar expressions for the out- and in-degrees, and the network degree distribution is a mixture of Poisson distributions with the expectation $\langle d \rangle$.

Analytic form of the SPLD. Analogous to the survival function matrix Ψ_l and conditional PMF matrix Ω_l of the SPLD defined in Eq. 7, we define the survival function and conditional PMF of the SPLD respectively:

$$\psi_l(x, y) \triangleq P(\lambda_{xy} > l | \phi_x), \quad (34a)$$

$$\omega_l(x, y) \triangleq P(\lambda_{xy} = l | \lambda_{xy} > l - 1, \phi_x), \quad (34b)$$

where the source node is at $x \in V$ and target node at $y \in V$. Then, assuming large n , the sum over all nodes in Eq. 12 becomes n times the integral over the entire node space V .

$$\psi_l(x, y) = [1 - \omega_l(x, y)] \psi_{l-1}(x, y), \quad (35a)$$

$$\omega_l(x, y) = 1 - \exp \left(n \int_V \log(1 - (\omega_{l-1} \cdot \psi_{l-2})(x, z) \nu(z, y)) d\mu(z) \right). \quad (35b)$$

The above set of recursive equations, together with the initial conditions $\omega_1(x, y) \triangleq P(\lambda_{xy} = 1 | \lambda_{xy} > 0, \phi_x) = P(A_{xy} = 1 | \phi_x)$ and $\psi_0(x, y) \triangleq P(\lambda_{xy} > 0 | \phi_x) = 1$, completely define the distribution of shortest path lengths. We remark that $\psi_l(x, x)$ and $\omega_l(x, x)$ encode the distribution of shortest path lengths between nodes with identical locations in V .

To define the initial condition ω_1 , we require percolation probabilities in V . Let $\rho(x)$ be the probability that a node located at x is on the giant component. Following the same argument as for the ensemble average model, and replacing the sum over nodes by n times the integral over node space, we can write $\rho(x) = 1 - \exp(n \int_V \log(1 - \nu(x, y) \rho(y)) d\mu(y))$. Since $\nu = O(n^{-1})$ almost everywhere, we can use a first-order approximation for the logarithm to write ρ as the solution to a self-consistent integral equation:

$$\rho(x) = 1 - \exp \left(-n \int_V \nu(x, y) \rho(y) d\mu(y) \right). \quad (36)$$

This leads to the base case (analogous to Eq. 13):

$$\omega_1(x, y) = \nu(x, y) \left\{ 1 + \left[\frac{1}{\rho(x)} - 1 \right] \rho(y) \right\}, \quad (37)$$

needed to solve Eq. 35.

Closed-form bound of the SPLD. Under the approximations made for the ensemble average model, we obtain a set of equations analogous to Eq. 28 for the closed-form (bound) of the SPLD:

$$\underline{\omega}_l(x, y) \triangleq n \int_V \underline{\omega}_{l-1}(x, z) \nu(z, y) d\mu(z), \quad (38a)$$

$$\underline{\psi}_l(x, y) \triangleq \exp \left(- \sum_{k=1}^l \underline{\omega}_k(x, y) \right), \quad (38b)$$

To our knowledge, there is no alternative means to analytically access the SPLD for sparse general random graph families with independent edges. Substituting the base case of $\omega_1(x, y)$ in Eq. 38a, we can write:

$$\begin{aligned} \underline{\omega}_l(x, y) = n^{l-1} \int_V \int_V \cdots \int_V \omega_1(x, z_1) \nu(z_1, z_2) \cdots \\ \times \nu(z_{l-1}, y) d\mu(z_1) d\mu(z_2) \cdots d\mu(z_{l-1}). \end{aligned} \quad (39)$$

From Eq. 38b, the survival function at length l is encoded by the sum of iterated integrals.

Integral operator. Due to sparsity, we can define a compact integral operator T on the space of functions in V (see Appendix F 1):

$$(Tf)(x) \triangleq n \int_V \nu(x, y) f(y) d\mu(y), \quad (40)$$

that can be viewed as an analogue of the sparse expected adjacency matrix $\langle A \rangle$. It maps a function evaluated at node location x to an expectation of the function evaluated at other node locations y , weighted by the node density at y and the probability of a node at y to connect to a node at x . For example, if $\forall x : f(x) = 1$, then Tf becomes the out-degree function from Eq. 31a. If one applies T to the percolation probability function $\rho(x)$, then the self-consistency Eq. 36 can be written as $\rho(x) = 1 - \exp(-T\rho)(x)$. Therefore, many network quantities of interest can be extracted using T . For the rest of this section, we assume the kernel ν is symmetric, implying that T is self-adjoint, and refer the reader to Appendix E 2 for a discussion on asymmetric kernels. This allows us to apply the spectral theorem for compact self-adjoint operators [46]. Let T have rank N , then there exists an orthonormal system of eigenfunctions of T defined as $\{\varphi_i\}_{i=1}^N$, corresponding to ordered non-zero eigenvalues $\{\tau_i\}_{i=1}^N$, such that $\{|\tau_i|\}_{i=1}^N$ is monotonically non-increasing with index i . Due to compactness of T , either N is finite, or $\lim_{i \rightarrow \infty} \tau_i = 0$. The following eigenfunction expansions hold:

$$(Tf)(x) = \sum_{i=1}^N \tau_i \left(\int_V f(y) \varphi_i(y) d\mu(y) \right) \varphi_i(x), \quad (41a)$$

$$\nu(x, y) = \frac{1}{n} \sum_{i=1}^N \tau_i \varphi_i(x) \varphi_i(y). \quad (41b)$$

Eigenvalues and homophily. Given Eq. 41b, we note that if an eigenvalue τ_i is positive (negative), then it raises the connection probability for node locations having the same (opposite) sign of the eigenfunction φ_i . Since nodes with the same (opposite) sign of an eigenfunction can be seen as being similar (dissimilar) along that “dimension”, positive eigenvalues indicate *homophily*: the phenomenon of similar nodes being more likely to connect to one another, that is widely observed in social networks [47, 48]. Whereas negative eigenvalues indicate *heterophily*: dissimilar nodes being more likely to connect to one another, such as in multipartite graphs.

Closed-form of the SPLD. Substituting Eq. 41b in Eq. 39, we can integrate all intermediate variables from z_{l-1} to z_2 by exploiting the orthonormality of $\{\varphi_i\}_{i=1}^N$:

$$\int_V \varphi_i(x) \varphi_j(x) d\mu(x) = \delta_{ij}, \quad (42)$$

where δ_{ij} is the Kronecker delta, which results in

$$\underline{\omega}_l(x, y) = \int_V \sum_{i=1}^N \tau_i^{l-1} \omega_1(x, z) \varphi_i(z) \varphi_i(y) d\mu(z), \quad (43)$$

where we have suppressed the index of z_1 . Putting this in Eq. 38b, we can push the outermost sum over lengths k through due to compactness of T . Let $\tilde{S}_l(a) \triangleq 1 + a + \cdots + a^{l-1}$ be the geometric sum of a starting at 1 up to l terms—where $\tilde{S}_0(a) \triangleq 0$ —then the closed-form of the survival function is described by:

$$\underline{\psi}_l(x, y) = \exp \left(- \int_V \sum_{i=1}^N \tilde{S}_l(\tau_i) \omega_1(x, z) \varphi_i(z) \varphi_i(y) \right). \quad (44)$$

Approximate closed-form of the SPLD. Similarly to Eq. 30, we can solve Eqs. 38a and 38b, with a naïve initial condition analogous to Eq. 16:

$$\omega_1(x, y) = \nu(x, y). \quad (45)$$

Let $S_l(a) \triangleq a + a^2 + \cdots + a^l$ be the geometric sum of a starting at a up to l terms—where $S_0(a) \triangleq 0$. Then from Eq. 44 we obtain the approximate closed-form of the survival function:

$$\tilde{\psi}_l(x, y) \triangleq \exp \left(- \frac{1}{n} \sum_{i=1}^N S_l(\tau_i) \varphi_i(x) \varphi_i(y) \right). \quad (46)$$

Interpretation. Assuming $\tau_i \neq 1 \forall i \in \{1, 2, \dots, N\}$, we can write $S_l(\tau_i) = \tau_i \frac{\tau_i^l - 1}{\tau_i - 1}$. Define $a_i(x, y) \triangleq \frac{\tau_i \varphi_i(x) \varphi_i(y)}{n(\tau_i - 1)}$, $b_i \triangleq \log |\tau_i|$, and $\text{sgn}(\cdot)$ as the sign function. Then we can rewrite Eq. 46 as the product of survival functions of a (discrete version of the) Gompertz distribution, wherein the i^{th} term in the product only depends on the eigenpair (τ_i, φ_i) :

$$\tilde{\psi}_l(x, y) = \prod_{i=1}^N \exp \left(-a_i(x, y) [\text{sgn}(\tau_i)^l e^{b_i l} - 1] \right). \quad (47)$$

The Gompertz distribution is a reflection of the Gumbel distribution around the origin—one of the three extreme value distributions with an exponential tail [49]. It has been previously shown to model lengths of self-avoiding walks in ER graphs [50].

SPLD for a random node pair. We can further define a distribution for the shortest path length between a randomly selected node pair in the network, which should be informative about typical geodesic lengths in the network, by averaging over the source and target nodes

$$\underline{\tilde{\psi}}(l) \triangleq \mathbb{E}_{\mu^2} \left[\underline{\tilde{\psi}}_l(x, y) \right] = \int_V \int_V \underline{\tilde{\psi}}_l(x, y) d\mu(x) d\mu(y). \quad (48)$$

We use the notation $\mathbb{E}_{\mu^2}[\cdot]$ when averaging over $V \times V$. By applying Jensen’s inequality [51] to Eq. 48—in the form $\exp(\mathbb{E}[Z]) \leq \mathbb{E}[\exp(Z)]$ for some random variable Z —we can obtain a lower bound on $\underline{\tilde{\psi}}(l)$, which will be tight if the variance in survival function over different node pairs is small:

$$\underline{\tilde{\psi}}(l) \geq \exp \left(-\frac{1}{n} \sum_{i=1}^N S_l(\tau_i) \mathbb{E}_{\mu} [\varphi_i(x)^2] \right), \quad (49)$$

which permits a description of the network’s expected geodesic length in terms of the eigenvalues and expectation of eigenfunctions of T .

IV. GEODESICS IN SPECIFIC RANDOM GRAPH FAMILIES

In this section, we consider illustrative models that are special cases of the general setting considered in Sec. III. We focus on symmetric kernels, that coincide with the sparse inhomogeneous random graph models of Ref. [31]. In particular, we elaborate on the percolation probability of nodes, and determine the approximate closed-form of the survival function of SPLD between node pairs—which is asymptotically a good approximation for finite lengths in the supercritical regime, and an exact tight bound for all lengths in the subcritical regime.

A. Stochastic block model

Stochastic block models (SBM) have been popularly used for modeling social networks [42, 52], since they directly capture notions of social homophily that “like befriends like” [47, 48], and social segregation [53]. They are a discrete space model wherein nodes are divided into communities or “blocks”, whose probabilistic connections are modeled by block-level parameters. In essence, SBMs are a form of “graph-coarsening” wherein edges between nodes can be aggregated into edges between blocks of nodes [54]. This property can be leveraged to study the SPLD in empirical graphs (see Appendix IV B). Theorem 5 in Appendix F 2 shows that there exists an ϵ -equivalent

SBM for any general random graph model with independent edges. This property can be used to approximate a continuous space model by an SBM via discretization up to a desired level of accuracy. Establishing a framework for the SPLD in SBMs thus yields applications in a wide variety of settings.

Definitions. Consider n nodes, each of them belonging to one of k blocks where $k < n$, according to a categorical distribution given by $\boldsymbol{\pi} \in (0, 1]^k$ such that $\sum_i \pi_i = 1$. We let $Z \in \{0, 1\}^{n \times k}$ represent the assignment matrix where exactly one entry in every row is 1 and the rest are 0. The probability of two nodes connecting to each other depends entirely on the blocks they belong to, i.e. for two nodes indexed by i, j : $P(A_{ij} = 1 | Z_{ix} = 1, Z_{jy} = 1) \triangleq \frac{B_{xy}}{n}$ where $B_{xy} \geq 0$ measures the “affinity” between blocks x and y , where $x, y \in \{1, 2, \dots, k\}$. The “block matrix” B along with the “distribution vector” $\boldsymbol{\pi}$, completely define this probabilistic model. More succinctly, we can write

$$\begin{aligned} Z_i &\sim \text{Categorical}(\boldsymbol{\pi}), \\ A_{ij} &\sim \text{Bernoulli} \left(\frac{[ZBZ^T]_{ij}}{n} \right). \end{aligned} \quad (50)$$

This parametrization ensures sparsity i.e. $\nu = O(n^{-1})$, wherein the expected degree of any node remains the same for sufficiently large values of n —an assumption that holds particularly well for social networks.

Degree and percolation probability. Functions for expected degree \hat{d} , percolation probability ρ , conditional PMF ω_l and survival function ψ_l of the SPLD, too possess a block structure. This translates Eq. 32 into an expression for the length- k “block degree vector”:

$$\hat{\mathbf{d}} = B\boldsymbol{\pi}, \quad (51)$$

where \hat{d}_x is the expected degree for a node in block x , and therefore from Eq. 31c the average network degree is given by $\langle d \rangle = \boldsymbol{\pi}^T B\boldsymbol{\pi}$. Next, from Eq. 36 we obtain an equation for the length- k “block percolation vector” $\boldsymbol{\rho}$ where ρ_x is the percolation probability for a node in block x :

$$\boldsymbol{\rho} = \mathbf{u} - \exp(-B\Pi\boldsymbol{\rho}), \quad (52)$$

where we define $\Pi \triangleq \text{diag}(\boldsymbol{\pi})$ as the diagonal distribution matrix, and \mathbf{u} is the all-ones vector of length k .

Analytic form of the SPLD. From Eq. 35 we get recursive equations for $k \times k$ “block matrices” Ψ_l, Ω_l :

$$\begin{aligned} \Psi_l &= (\mathbf{u}\mathbf{u}^T - \Omega_l) \odot \Psi_{l-1}, \\ \Omega_l &= \mathbf{u}\mathbf{u}^T - \exp \left(n \sum_{x=1}^k \pi_x \right. \\ &\quad \left. \times \log \left(\mathbf{u}\mathbf{u}^T - \frac{[\Omega_{l-1} \odot \Psi_{l-2}]_{:x} [B]_{x:}}{n} \right) \right), \end{aligned} \quad (53)$$

with the initial condition from Eq. 37 yielding:

$$\Omega_1 = \frac{B + (R^{-1} - I)BR}{n}, \quad (54)$$

where $R \triangleq \text{diag}(\boldsymbol{\rho})$, and $\Psi_0 = \mathbf{u}\mathbf{u}^T$. We have used the notation $[X]_{:i}$ to indicate the i^{th} column vector of matrix X , and $[X]_i$ to indicate the i^{th} row vector of X . Fig. 3 shows the distribution of shortest path lengths between nodes in a 2-block SBM with a bipartite structure, obtained by solving Eqs. 53, 54 and 52, which is in good agreement with the empirical SPLD. Refer to Fig. 19 in Appendix C for the SPLD of a bipartite SBM in a subcritical regime.

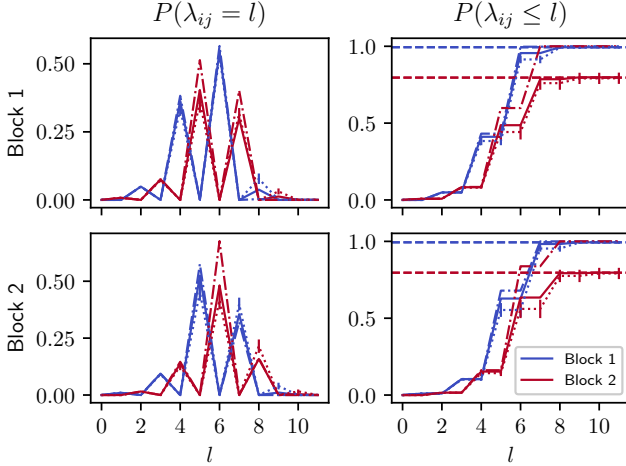


FIG. 3. Empirical, analytic, and approximate closed-form CDF of shortest path lengths where the source node is on the giant component, agree with each other for a bipartite SBM with block matrix $B = \begin{pmatrix} 0 & 8 \\ 8 & 0 \end{pmatrix}$, distribution vector $\boldsymbol{\pi} = (0.2, 0.8)$, and $n = 1024$. Rows correspond to the block membership of source node. Left column depicts the PMF, which highlights bipartitivity of the network, and the right column depicts the CDF, whose tail value agrees with the percolation probability of target node, indicated by the dashed asymptote and calculated from Eq. 52. Solid lines represent analytic form using Eqs. 53, 54, 52, while dash-dotted lines represent approximate closed-form using Eq. 55, and dotted lines with bars represent empirics, i.e. mean and standard error over 10 samples.

Approximate closed-form of the SPLD. Using Eq. 39 yields the survival function of the SPLD as the summation over matrix powers (see Appendix G 1), producing the $k \times k$ survival function block matrix:

$$\tilde{\Psi}_l = \exp\left(-\frac{B}{n} \sum_{i=1}^l (\Pi B)^{i-1}\right). \quad (55)$$

Fig. 3 shows the approximate closed-form of the SPLD between nodes in a 2-block bipartite SBM, obtained by solving Eq. 55. As previously discussed in Sec. IID, the approximate closed-form SPLD agrees with the empirical SPLD for shorter geodesic lengths in finite-size networks. If $\Pi B - I$ is non-singular, we can evaluate the expression in Eq. 55 as a matrix series to obtain

$$\tilde{\Psi}_l = \exp\left(-\frac{B}{n}((\Pi B)^l - I)(\Pi B - I)^{-1}\right).$$

For the special case of an ER graph, where the likelihood of an edge is identical across all node pairs, we have $k = 1$, $B \triangleq \langle d \rangle$, $\Pi \triangleq 1$, and the survival function is scalar valued:

$$\tilde{\psi}(l) = \begin{cases} \exp\left(-\frac{\langle d \rangle (\langle d \rangle^l - 1)}{n(\langle d \rangle - 1)}\right) & \text{if } \langle d \rangle \neq 1, \\ \exp\left(-\frac{l}{n}\right) & \text{otherwise.} \end{cases} \quad (56)$$

Evidently, larger the mean degree, shorter the geodesic lengths in the network. Previous work has demonstrated an analytic expression for the survival function of geodesic lengths in ER graphs, given by Eq. 14 of Ref. [20] as $\tilde{\psi}(l) = \exp\left(-\frac{\langle d \rangle^l}{n}\right)$ which is in slight disagreement with Eq. 56. Particularly at $l = 0$, Eq. 56 will correctly evaluate to 1, while the other to $\exp(-n^{-1})$.

Illustrative examples. For a less trivial example, we consider a k -block SBM with equi-sized blocks and constant mean degree $\langle d \rangle$, such that $B = \delta I + (\langle d \rangle - \delta/k)\mathbf{u}\mathbf{u}^T$, where $\delta \in [-\langle d \rangle k/(k-1), \langle d \rangle k]$ quantifies the amount of homophily—positive δ , wherein nodes are more likely to connect to nodes from the same block—or heterophily—negative δ , wherein nodes are more likely to connect to nodes from other blocks. As before, let $S_l(a)$ be the geometric sum of a starting at a up to l terms, then from Eq. 55 the survival function block matrix is given by (see Appendix G 1)

$$\tilde{\Psi}_l = \exp\left(-\frac{1}{n} \left\{ S_l(\delta/k)kI + [S_l(\langle d \rangle) - S_l(\delta/k)]\mathbf{u}\mathbf{u}^T \right\}\right). \quad (57)$$

The form of $\tilde{\Psi}_l$ is analogous to that of B —naturally $\tilde{\Psi}_1 = B$, but for larger l the off-diagonal (inter-block) elements of the survival function block matrix evolve as the exponential of difference in geometric sums of $S_l(\delta/k)$ and $S_l(\langle d \rangle)$. In particular, consider a 2-block perfectly heterophilous SBM, i.e. $k = 2$ and $\delta/k = -\langle d \rangle$. This would correspond to a bipartite network, since nodes never connect directly with nodes of their own block. Consequently, all paths between nodes of different communities must be of odd length. The expression in Eq. 57 correctly suggests that the inter-block survival function does not change for even values of l due to cancelling out of the even powers of $\langle d \rangle$, that is, there is no probability mass at even values of l .

We next consider a general SBM with a symmetric block matrix B . Let $Q\Lambda Q^T$ be the eigendecomposition of symmetric matrix $\Pi^{\frac{1}{2}}B\Pi^{\frac{1}{2}}$ such that columns of the orthogonal matrix Q encode the eigenvectors and the diagonal matrix Λ encodes the corresponding eigenvalues. Then, we can write $(\Pi B)^{i-1} = \Pi^{\frac{1}{2}}Q\Lambda^{i-1}Q^T\Pi^{-\frac{1}{2}}$. Putting in Eq. 55, we obtain

$$\tilde{\Psi}_l = \exp\left(-\frac{1}{n}\Pi^{-\frac{1}{2}}QS_l(\Lambda)Q^T\Pi^{-\frac{1}{2}}\right), \quad (58)$$

which is the matrix analogue of Eqs. 46 and 56. Evidently, for general block matrices, a weighted geometric sum of eigenvalues of $B\Pi$ governs the whole

distribution, with positive eigenvalues—indicating homophily—and negative eigenvalues—indicating heterophily—contributing differently to the distribution.

B. Labeled empirical graphs

Previous work in estimating dissimilarity measures on empirical graphs has determined a Gibbs–Boltzmann distribution on picking a path between two nodes over a bag-of-paths in a given network [21]. However, this bag-of-paths approach does not directly model the distribution of shortest path *lengths* between node pairs. Our proposed approach provides the desired distribution, but for networks generated from some underlying random graph model with independent edges. One method to apply our approach is to first infer a model given the observed network. Inference can be performed in a myriad of ways [5, 6, 55], but may induce computational overhead if the network is very large.

Another method is to exploit the graph-coarsening property of SBMs described in Sec. IV A, wherein nodes are completely defined by their block membership, to determine the SPLD of empirical graphs. This has the advantage of reducing the parametrization from one in terms of a large number of nodes n , to one in terms of a small number of blocks $k \ll n$. If we have a network represented by the adjacency matrix A , with known node labels indicated by the assignment matrix Z , then assuming that (A, Z) is generated by an SBM permits a maximum likelihood estimate of its parameters from Eq. 50, regardless of how node labels were inferred, and with no computational cost except for summation of node and edge counts. We refer the reader to Appendix I 1 for more details. The SPLD associated with the inferred SBM can then be used to study shortest path lengths in the original network.

Illustrative example. We consider a real-world network of email communications between members of a European research institution [56–58] denoted by the adjacency matrix A_{eue} (see Appendix I 2 for more details on the dataset). Each node has an attribute corresponding to one of the $k = 42$ departments which the individual belongs to, which can serve to provide the assignment matrix Z_{dep} at no additional cost. We can also derive more meaningful community labels for the nodes by applying community detection methods [59, 60], such as modularity maximization [61, 62], which can provide a different assignment Z_{mod} across $k = 5$ modules. We also infer a hierarchical SBM for this network that can infer blocks at multiple levels of coarsening [54, 63], generating a hierarchy of labels yielding assignments Z_{sbm2}, Z_{sbm3} at levels 2 and 3 of the inferred hierarchical SBM, possessing $k = 36$ and $k = 10$ blocks respectively. Using Eq. I 4 we can derive corresponding SBMs, and the analytic form of the SPLD between block pairs using Eq. 53. In Fig. 4 we compare the empirical and analytic means of geodesic lengths for every block pair in this network, which are

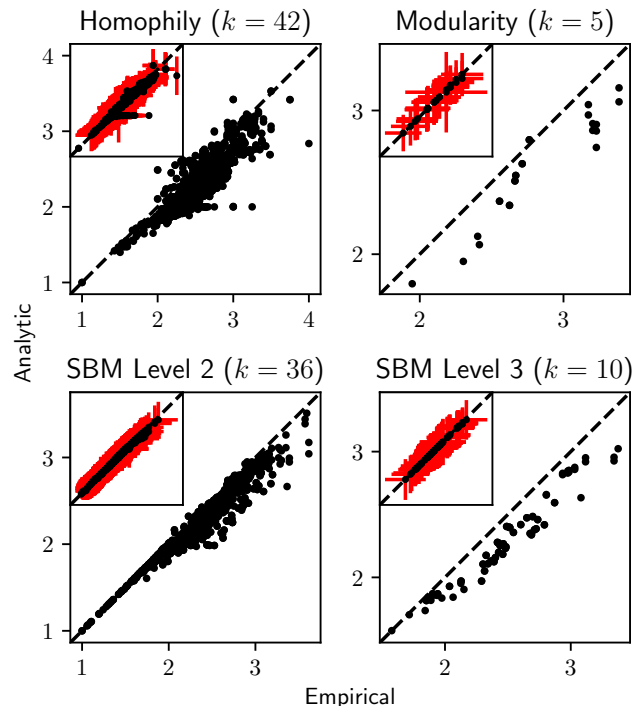


FIG. 4. The empirical average geodesic lengths of a real-world email network A_{eue} (on the x -axis) are well-approximated by the mean obtained from the analytic form of the SPLD (on the y -axis, using Eqs. 52, 53, 54), when nodes with the same “label” are grouped into a single block to form an SBM with k blocks. Subplots correspond to different types of labeling: (top-left) Z_{dep} leverages the homophily assumption by using a node attribute as the label—here, the department of the e-mailer; (top-right) Z_{mod} uses modularity maximization [61, 62] to infer network blocks assigned as the label; (bottom) Z_{sbm2}, Z_{sbm3} use a hierarchical SBM [54, 63] to infer a hierarchy of blocks which allows for multi-level coarsening. Symbols indicate the mean geodesic length between nodes of block pairs. Inset figures indicate the mean (black markers) and standard deviation (red bars) of geodesic lengths between block pairs, averaged over 10 samples of the corresponding SBM established via coarsening. Both the mean and standard deviation of the empirical SPLD are well approximated by the analytic SPLD.

in good agreement for all assignment procedures considered. Notably, this includes Z_{dep} which requires no additional computational overhead. The agreement is stronger for block pairs with shorter geodesics between them. The departure for longer geodesics is likely due to correlations within A_{eue} , wherein longer-than-expected geodesics would beget even longer geodesics, resulting in the analytics mostly underestimating the empirics.

C. Random dot-product graph

While SBMs are commonly used due to their simplicity and ability to model any community structure, they can

be unrealistic in terms of other network attributes. For instance, their degree distribution is a mixture of Poisson distributions which can be restrictive with regards to some real-world networks possessing heavy-tailed degree distributions like power laws [2]. This has led to exploration of other models that can capture modularity alongside arbitrary degree distributions, of which the random dot-product graph (RDPG) [44, 64] is an important example. Here, the connectivity kernel is a function of the dot-product of latent vectors which represent nodes. Consider some k -dimensional bounded real vector space $X \subset \mathbb{R}^k$ wherein nodes are “embedded”, such that the likelihood of $\mathbf{x}, \mathbf{y} \in X$ connecting is proportional to a function of the dot-product of their positions $\mathbf{x}^T \mathbf{y}$. This method of “graph embeddings” is especially popular in statistical machine learning, wherein continuous representations of discrete objects such as graphs are learnt [65–67], making them amenable to downstream predictive tasks. Many approaches for generating such an embedding rely on the dot-product model. For instance, embedding techniques based on matrix factorization, like graph factorization [68], assume that the likelihood of nodes located at \mathbf{x} and \mathbf{y} to connect is proportional to $\mathbf{x}^T \mathbf{y}$, while random-walk based techniques, like “node2vec” [69], assume the likelihood is proportional to $\exp(\mathbf{x}^T \mathbf{y})$.

Symmetric & positive semi-definite kernels. We emphasize that the RDPG is a special case of the general random graph families described in Sec. III when the connectivity kernel is symmetric and positive semi-definite, i.e. all eigenvalues of T , defined in Eq. 40, are non-negative. (Contrary to SBMs, this excludes the possibility of heterophilous structures like bipartitivity, but results in uniform absolute convergence of the kernel’s eigenexpansion in Eq. 41b [46, 70].) In other words, any positive semi-definite kernel can be written as a dot-product in some feature space (see Appendix G 2 c). It is therefore sufficient here to consider the simplest setting of V being Euclidean and the kernel being linear in the dot-product, giving rise to an RDPG. For a kernel that is a non-linear function of the dot-product, we can use random Fourier features [71] to derive an explicit feature map, where a kernel that is linear in the dot-product can be assumed. We refer the reader to Appendix G 2 c for an illustrative example.

Definitions. We consider a non-negative bounded subspace $X \subset \mathbb{R}_{\geq 0}^k$ with the connectivity kernel $\nu(\mathbf{x}, \mathbf{y}) = \beta \mathbf{x}^T \mathbf{y}$ such that $\beta > 0$ and $\beta = O(n^{-1})$ which encodes sparsity. This is a common setting for RDPGs: in the canonical degree-configuration model where $k = 1$, X encodes precisely the expected degree of a node, with the node density μ governing the degree distribution [44]. We define:

$$\phi \triangleq \int_X \mathbf{x} d\mu, \quad (59a)$$

$$\Phi \triangleq n\beta \int_X \mathbf{x} \mathbf{x}^T d\mu, \quad (59b)$$

where ϕ indicates the length- k mean vector in X , and Φ refers to the $k \times k$ matrix of second moments, also known as the autocorrelation matrix, scaled by $n\beta$ that encodes the covariance in space X as per the measure μ and is necessarily positive semi-definite.

Degree and percolation probability. From Eq. 32, it can be seen that the expected degree at \mathbf{x} is given by:

$$\widehat{d}(\mathbf{x}) = n\beta \phi^T \mathbf{x}, \quad (60)$$

and from Eq. 31c the average network degree is given by $\langle d \rangle = n\beta \phi^T \phi$. Given that $\rho(\mathbf{x})$ encodes the percolation probability for a node at \mathbf{x} , define $\boldsymbol{\rho} \triangleq \int_X \mathbf{x} \rho(\mathbf{x}) d\mu$ to be the “mean percolation vector” in X , then Eq. 36 yields:

$$\begin{aligned} \rho(\mathbf{x}) &= 1 - \exp\left(-n\beta \mathbf{x}^T \int_X \mathbf{y} \rho(\mathbf{y}) d\mu(\mathbf{y})\right), \\ &= 1 - \exp(-n\beta \mathbf{x}^T \boldsymbol{\rho}), \end{aligned} \quad (61a)$$

$$\begin{aligned} \int_X \mathbf{x} \rho(\mathbf{x}) d\mu &= \int_X \mathbf{x} d\mu - \int_X \mathbf{x} \exp(-n\beta \mathbf{x}^T \boldsymbol{\rho}) d\mu, \\ \implies \boldsymbol{\rho} &= \phi - \int_X \mathbf{x} \exp(-n\beta \mathbf{x}^T \boldsymbol{\rho}) d\mu, \end{aligned} \quad (61b)$$

where we apply the definition of ϕ from Eq. 59a. Eq. 61b is a self-consistency vector equation for $\boldsymbol{\rho}$ which once solved can be used to solve the self-consistency scalar Eq. 61a for the percolation probability of any node location. To solve the former, we can make use of an m -block SBM approximation of the k -dimensional RDPG—as described in Appendix F 2 b—and solve for $\boldsymbol{\rho}$ numerically via function iteration.

Approximate closed-form of the SPLD. For this and subsequent sections (Sec. IV D and IV E), we focus on the approximate closed-form of the survival function of the SPLD. In particular, Eq. 38a for the conditional PMF would read as $\widetilde{\omega}_l(\mathbf{x}, \mathbf{y}) = \beta \mathbf{x}^T [n\beta \int_X \mathbf{z} \mathbf{z}^T d\mu(\mathbf{z})]^{l-1} \mathbf{y}$, translating Eq. 38b for the survival function into

$$\widetilde{\psi}_l(\mathbf{x}, \mathbf{y}) = \exp\left(-\beta \mathbf{x}^T \left(\sum_{k=0}^{l-1} \Phi^k\right) \mathbf{y}\right), \quad (62)$$

where we use the definition of Φ from Eq. 59b. Since Φ is symmetric, let $Q\Lambda Q^T$ be its eigendecomposition, such that columns of the orthogonal matrix Q encode the eigenvectors and the diagonal matrix Λ encodes corresponding eigenvalues. Let $\widetilde{S}_l(a)$ be the geometric sum of a starting at 1 up to l terms. Then we obtain from Eq. 62:

$$\widetilde{\psi}_l(\mathbf{x}, \mathbf{y}) = \exp\left(-\beta \mathbf{x}^T Q \widetilde{S}_l(\Lambda) Q^T \mathbf{y}\right). \quad (63)$$

This is analogous to the expressions obtained via eigendecomposition for the general random graph family in Eq. 46, for ER graphs in Eq. 56 and for SBMs in Eq.

58. Alternately, consider the expected survival function of the whole network in Eq. 48. By applying Jensen’s inequality [51] to Eq. 62, we obtain a lower bound on $\tilde{\psi}(l)$, similar to the one in Eq. 49, which will be tight if the variance in survival function over different node pairs is small:

$$\tilde{\psi}(l) \geq \exp\left(-\beta \phi^T \tilde{S}_l(\Phi) \phi\right), \quad (64)$$

where we use the definition of ϕ from Eq. 59a. This permits a description of the network’s expected geodesic length entirely in terms of the first and second moments in X , which can be especially useful when we have access to just the sample mean and covariance, instead of the full distribution in X .

Illustrative example. We consider X restricted to the $(k-1)$ -standard simplex in \mathbb{R}^k , and μ corresponding to the Dirichlet distribution on that simplex given by the concentration vector $\alpha \in [0, \infty)^k$. This represents a node $\mathbf{x} \in [0, 1]^k$ such that $\sum_i x_i = 1$, which allows us to interpret the node’s location as the likelihood of belonging to one of k communities located at the corners of the simplex—a continuous analogue of the SBM. Let $\langle d \rangle$ be the mean degree of the network, and $\bar{\alpha} = \alpha^T \mathbf{u}$, then it can be shown that the approximate closed-form of the conditional PMF of the SPLD is given by: $\tilde{\omega}_l(\mathbf{x}, \mathbf{y}) = \frac{\langle d \rangle \bar{\alpha}^2}{n \|\alpha\|^2} \mathbf{x}^T \left\{ \frac{\langle d \rangle \bar{\alpha}}{\|\alpha\|^2 (1 + \bar{\alpha})} [\text{diag}(\alpha) + \alpha \alpha^T] \right\}^{l-1} \mathbf{y}$ (see Appendix G 2). In Fig. 5a, we plot various node and node pair statistics for a “Dirichlet RDPG” when $n = 512$, $\langle d \rangle = 4$ and $\alpha = \{0.8, 0.8, 2\}$ using Eq. 60 for a node’s degree, Eq. 61a for a node’s percolation probability, and the approximate closed-form of the SPLD in Eq. 62 to compute an analytic estimate of expected geodesic length between node pairs using. In Fig. 7 we further show that this analytic estimate is in good agreement with empirical estimates.

D. Gaussian random geometric graph

An inner-product space is a good abstraction when the space of nodes is latent, but for some real-world spaces equipped with distances over which the likelihood of connection decays—like *spatial* networks [72]—it is sensible to consider a metric space of nodes. This notion is precisely captured by random geometric graph (RGG) models [43, 73, 74]. The metric space usually depends on the nature of networks being modeled, such as a Euclidean space for communication networks or a hyperbolic space for social networks [75, 76].

Definitions. In this section, we focus on *soft* random geometric graphs, wherein the probability of connection decays smoothly with distance—specifically, we consider a k -dimensional Euclidean space \mathbb{R}^k , with a squared-exponential decay function [73]. This is akin to having an ellipsoidal connection “bubble” around every node

$\mathbf{x} \in \mathbb{R}^k$, i.e.

$$\nu(\mathbf{x}, \mathbf{y}) = \beta \exp\left(-\frac{1}{2}(\mathbf{x} - \mathbf{y})^T R^{-1}(\mathbf{x} - \mathbf{y})\right), \quad (65)$$

where $\beta = O(n^{-1})$ is the probability of connecting to a node with identical co-ordinates, and R is a $k \times k$ symmetric positive-definite matrix encoding the scale of connections in this node space. For concreteness, assume a standard multivariate Gaussian distribution of nodes centered at the origin:

$$\mu(\mathbf{x}) = (2\pi)^{-\frac{k}{2}} \exp\left(-\frac{1}{2} \mathbf{x}^T \mathbf{x}\right). \quad (66)$$

We remark that this formalism extends to a multivariate Gaussian node distribution through an affine transformation of the node space V and scale matrix R (see Appendix G 3). This is what we refer to as the Gaussian random geometric graph (Gaussian RGG) [77]. (Arguably, this should be termed a *doubly* Gaussian RGG, where both the node distribution and connectivity kernel are Gaussian.)

Degree and percolation probability. Let $|\cdot|$ indicate the matrix determinant. It can be shown that the expected degree at location \mathbf{x} , using Eq. 32, is given by a Gaussian curve:

$$\hat{d}(\mathbf{x}) = \frac{n\beta}{|I + R^{-1}|^{\frac{1}{2}}} \exp\left(-\frac{1}{2} \mathbf{x}^T (I + R)^{-1} \mathbf{x}\right), \quad (67)$$

and correspondingly from Eq. 31c the average network degree is given by

$$\langle d \rangle = n\beta (|I + R^{-1}| \cdot |I + (I + R)^{-1}|)^{-\frac{1}{2}}, \quad (68)$$

see Appendix G 3. If we assume infinitely large connection scales, i.e. $R^{-1} \rightarrow 0$, this results in $\langle d \rangle = n\beta$, which can be seen as the usual ER graph where all spatial structure is lost, since nodes connect to any other node with the same likelihood $\frac{\langle d \rangle}{n}$.

We next consider the percolation probability at location \mathbf{x} . Similar to the discrete approximation used for RDPGs, we can discretize the node space into a fine grid to derive percolation probabilities (see Appendix F 2 b). However, here we apply an ansatz that the percolation probability is given by a generalization of the Gaussian function:

$$\rho(\mathbf{x}) = a \exp\left(-(\mathbf{x}^T C \mathbf{x})^b\right), \quad (69)$$

where $0 \leq a \leq 1$ governs percolation probability at the origin, $b \geq 1$ controls the shape of the percolation surface, and C is a $k \times k$ symmetric positive semi-definite matrix that indicates the scale of the surface. As shown later in Sec. V, C commutes with the scale matrix R , implying that C and R preserve each others eigenspaces. Consequently, we need to infer k non-negative eigenvalues of C , yielding a total of $k + 2$ parameters to fit the percolation surface at grid locations via constrained optimization. We can then use Eq. 69 to obtain percolation probabilities at any node location in \mathbb{R}^k .

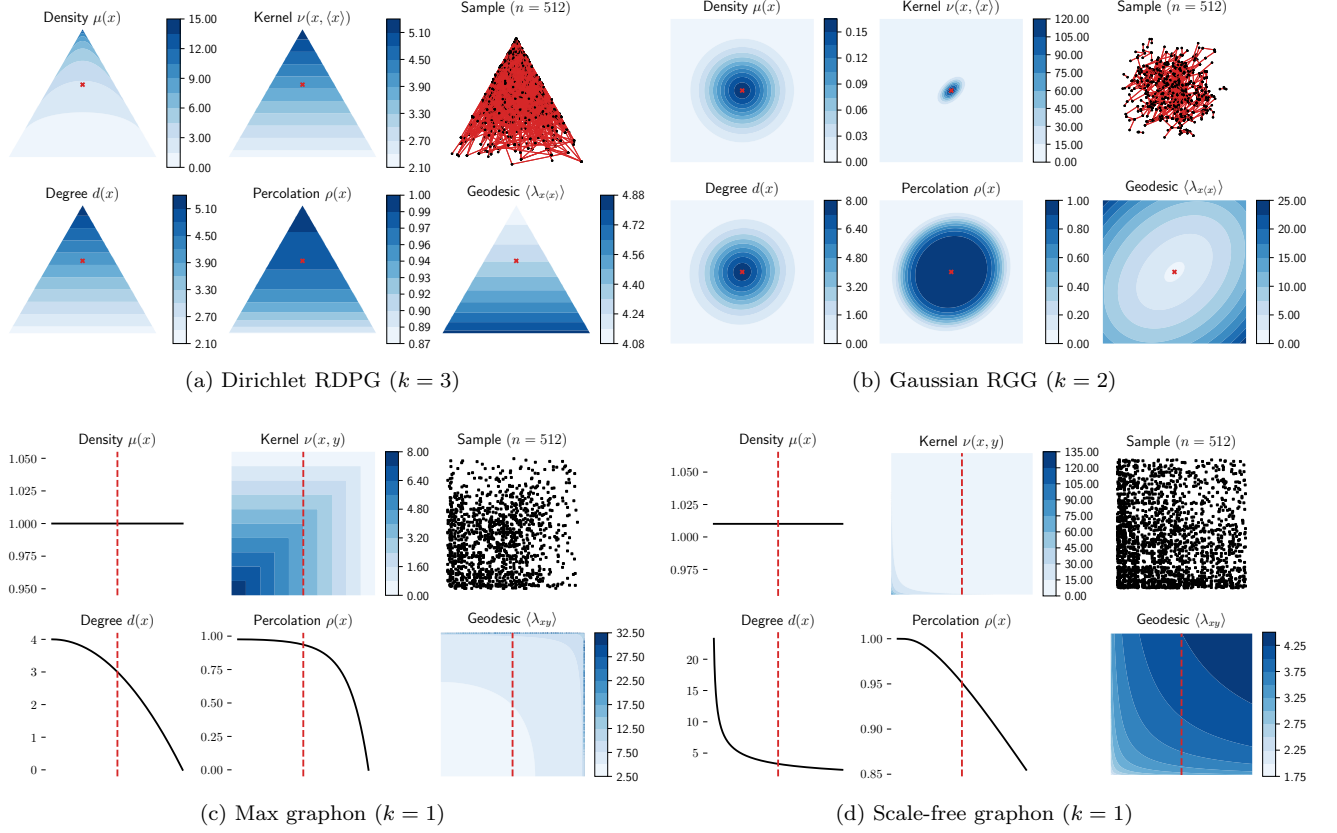


FIG. 5. Node and node pair functions for various random graph models considered in Sec. IV. Density function $\mu(x)$ refers to the distribution of nodes in node space V , connectivity kernel $\nu(x, y)$ refers to likelihood of connection between node pairs, degree function $\hat{d}(x)$ refers to the expected degree of a node at x , percolation function $\rho(x)$ indicates the probability of a node at x to be on the giant component, and geodesic function $\langle \lambda_{xy} \rangle$ refers to the expected shortest path length between node pairs. For one-dimensional models—(c) max graphon ($V = [0, 1]$) and (d) scale-free graphon ($V = [0.01, 1]$)—node functions (μ , ρ , and \hat{d}) are shown on V , while node pair functions (ν and λ) and network sample are shown on $V \times V$. For higher dimensional models—(a) Dirichlet RDPG (functions shown on the standard 2-simplex) and (b) Gaussian RGG (functions shown on $[-3, 3] \times [-3, 3]$)—node pair functions are shown between x and the mean in V indicated by $\langle x \rangle$, which is itself marked by red dashed lines or crosses. Description of model parameters and equations used to compute these functions are in respective subsections. We note that λ is estimated from the approximate closed-form of the SPLD.

Approximate closed-form of the SPLD. Using the expression for the conditional PMF in Eq. 38a, we can write the approximate closed-form of the conditional PMF of the SPLD succinctly via a set of recursive coefficients: see Eq. G28 in Appendix G3. To make further analytical progress, we consider a special scenario of high “spatial homophily” which is the opposite of the ER setting. Here, spatial embedding contributes a lot since the connection scales are very small: $R \rightarrow 0$. Taking this limit in Eq. 68, the mean degree is given by $\langle d \rangle = n\beta\sqrt{\frac{|R|}{2^k}}$. Using Eq. 38a, the approximate closed-form of the conditional PMF of the SPLD can be written as:

$$\tilde{\omega}_l(\mathbf{x}, \mathbf{y}) = \frac{\left(\langle d \rangle 2^{\frac{k}{2}}\right)^l}{n\sqrt{|lR|}} \exp\left(-\frac{1}{2}(\mathbf{x} - \mathbf{y})^T (lR)^{-1}(\mathbf{x} - \mathbf{y})\right), \quad (70)$$

see Appendix G3. Here, we can interpret $\tilde{\omega}_l(\mathbf{x}, \mathbf{y}) \triangleq P(\lambda_{\mathbf{x}\mathbf{y}} = l | \lambda_{\mathbf{x}\mathbf{y}} > l - 1)$ as a “shortest path” connectivity kernel, where a node “inflates” its bubble of nearest neighbours, as defined by the scale matrix R , by a factor of l to potentially form shortest path connections of length l . (For $l = 1$, this simply reduces to the connectivity kernel in Eq. 65.) It then follows that the approximate closed-form of the survival function of the SPLD is given by Eq. 38b as $\tilde{\psi}_l(\mathbf{x}, \mathbf{y}) = \exp\left(-\sum_{q=1}^l \tilde{\omega}_q(\mathbf{x}, \mathbf{y})\right)$ with, as previously, an analogous interpretation to Eq. 30 in terms of independent geodesics. In Fig. 5b, we plot various node and node pair statistics for a Gaussian RGG when $n = 512$, $\langle d \rangle = 4$ and the scale matrix is given by $R = \begin{pmatrix} 0.08 & 0.04 \\ 0.04 & 0.08 \end{pmatrix}$, using Eq. 67 for a node’s degree, Eq. 69 for a node’s percolation probability, and the approximate closed-form of the SPLD in Eq. G28 for the analytic estimate of expected geodesic lengths between

node pairs. We also show in Fig. 7 that this estimate is in good agreement with the empirics, with marginally increasing deviations for longer geodesics, likely because the closed-form of the SPLD overestimates probability mass at shorter geodesic lengths.

E. Sparse graphons

In the most general setting, any conditionally independent edge model with a symmetric connectivity kernel can be expressed by considering a sequence of graphs in some continuum limit, called graph functions or graphon [78–80]. Typically, the node space for a graphon is restricted to the real interval $[0, 1]$ where nodes are distributed according to the standard uniform distribution $\mathcal{U}(0, 1)$. Then all burden of modeling edge probabilities is transferred to the symmetric kernel $W : [0, 1]^2 \rightarrow [0, 1]$, referred to as the “ W -graphon”. Given their flexibility, these functions can get arbitrarily complex. While W -graphons are usually formulated as the dense limit of a graph sequence with $O(n^2)$ edges [78], here we are interested in the sparse limit with $O(n)$ edges, also referred to as the “inhomogeneous random graph model” [45]. For brevity, throughout this paper we refer to $W : [0, 1]^2 \rightarrow [0, 1]$ such that $W = O(n^{-1})$ as a “sparse graphon”, or simply as “graphon”. The SPLD framework of Sec. III translates immediately to sparse graphons, with the simplicity offered by the symmetry of W , and by assuming $x \sim \mathcal{U}(0, 1)$, with regards to numerical integration.

Illustrative example: max graphon. As an example, consider a sparse version of the “max graphon”, that arises as the limit of a uniform attachment process [81, 82] given by $W(x, y) = \beta(1 - \max(x, y))$, where $\beta > 0$ and $\beta = O(n^{-1})$. In Fig. 5c we show various node and node pair functions for this graphon with $n = 512$, $n\beta = 8$, wherein the expected degree, percolation probability, and expected geodesic lengths are all obtained via numerical integration of Eqs. 32, 36 and 46 respectively. In Fig. 7, we show that the empirical and analytic estimates of the geodesic lengths are in good agreement, except for longer path lengths—likely due to the vanishingly low percolation probabilities of the tail-end of the node space as $x \rightarrow 1$. As previously noted, we can discretize any continuous graph model at a chosen scale to obtain an equivalent SBM representation of it—see Appendix F 2a for a discussion on discretizing graphons in particular. In Fig. 7, we also include empirics and analytics for the SBM corresponding to max graphons, that corroborate well with results obtained via numerical integration.

Sparse multiplicative graphons. We next consider a scenario where the formalism simplifies further. Let $f : [0, 1] \rightarrow [0, 1]$ be a function such that $f = O(n^{-\frac{1}{2}})$. Then, we define a sparse multiplicative graphon over a node pair $W_{\times}(x, y)$ to be one which can be written as the

product of that function applied to the nodes separately:

$$W_{\times}(x, y) \triangleq f(x)f(y). \quad (71)$$

We remark that an asymmetric and directed version of this graphon can be obtained by considering two separate functions f and g , but we restrict our discussion here to symmetric multiplicative graphons.

Degree and percolation probability. To derive network properties, it will be useful to define two statistics for the multiplicative graphon:

$$\zeta \triangleq \int_0^1 f(x)dx, \quad (72a)$$

$$\eta \triangleq n \int_0^1 f(x)^2 dx, \quad (72b)$$

which are indicative of the first and second moment of $f(x)$. From Eqs. 32 and 31c, and using the definition in Eq. 72a, the expected degree at x and expected network degree are given by

$$\widehat{d}(x) = nf(x) \int_0^1 f(y)dy = n\zeta f(x), \quad (73a)$$

$$\langle d \rangle = n\zeta \int_0^1 f(x)dx = n\zeta^2. \quad (73b)$$

From 73a, it is evident that $f(x) \propto \widehat{d}(x)$ encodes the expected degree at x , rendering multiplicative graphons as equivalent to canonical degree-configuration models that lack any modularity structure [82]. However, they can still capture degree-related properties of real-world graphs, like “scale-free” networks showcasing power law degree distributions. Using Eq. 73, we can rewrite $f(x)$, ζ and η from Eq. 72 in terms of degree statistics as:

$$f(x) = \frac{\widehat{d}(x)}{\sqrt{n \langle d \rangle}} \quad (74a)$$

$$\zeta = \sqrt{\frac{\langle d \rangle}{n}}, \quad (74b)$$

$$\eta = \frac{\mathbb{E}_{\mu} [\widehat{d}(x)^2]}{\langle d \rangle}. \quad (74c)$$

Recall from Eq. 33 that the degree at x is Poisson distributed with rate $\widehat{d}(x)$. Then the second moment of the degree distribution is given by the law of total expectation:

$$\begin{aligned} \langle d^2 \rangle &= \mathbb{E}_{\mu} [\langle d(x)^2 \rangle] = \mathbb{E}_{\mu} [\widehat{d}(x)^2 + \widehat{d}(x)] \\ \implies \mathbb{E}_{\mu} [\widehat{d}(x)^2] &= \langle d^2 \rangle - \langle d \rangle, \end{aligned} \quad (75)$$

where we apply the definition of mean degree from Eq. 31c. Using Eqs. 75, 74c yields η in terms of the first and second moments of the degree distribution:

$$\eta = \frac{\langle d^2 \rangle}{\langle d \rangle} - 1. \quad (76)$$

We next consider the percolation probability at x . We define $\rho \triangleq \int_0^1 f(x)\rho(x)dx$, then we obtain from Eq. 36 for percolation probability and Eq. 72a:

$$\begin{aligned}\rho(x) &= 1 - \exp\left(-n \int_0^1 f(x)f(y)\rho(y)dy\right), \\ &= 1 - \exp(-n\rho f(x)),\end{aligned}\tag{77a}$$

$$\begin{aligned}\int_0^1 f(x)\rho(x)dx &= \int_0^1 f(x)[1 - \exp(-n\rho f(x))]dx, \\ \implies \rho &= \zeta - \int_0^1 f(x)\exp(-n\rho f(x))dx.\end{aligned}\tag{77b}$$

Eq. 77b is a self-consistency scalar equation for ρ which once solved can be used to solve the self-consistency scalar Eq. 77a for the percolation probability of any node location.

Approximate closed-form of the SPLD. Exploiting the multiplicative nature of the kernel in Eq. 71, we obtain the conditional PMF $\tilde{\omega}_l(x, y)$ and survival function $\tilde{\psi}_l(x, y)$ of the approximate closed-form SPLD from Eqs. 38a, 38b as

$$\tilde{\omega}_l(x, y) = \eta^{l-1} f(x)f(y) = \eta^{l-1} \frac{\hat{d}(x)\hat{d}(y)}{n\langle d \rangle},\tag{78a}$$

$$\tilde{\psi}_l(x, y) = \begin{cases} \exp\left(-\frac{\eta^{l-1}}{\eta-1} \frac{\hat{d}(x)\hat{d}(y)}{n\langle d \rangle}\right) & \text{if } \eta \neq 1, \\ \exp\left(-l \frac{\hat{d}(x)\hat{d}(y)}{n\langle d \rangle}\right) & \text{otherwise,} \end{cases}\tag{78b}$$

where we express $f(x)$ in terms of degree using Eq. 74a. From Eq. 78b we note that the distribution of shortest path length between two nodes in a degree-configuration model is encoded by the product of their expected degree. We also observe that a larger variance in the degree distribution renders a larger value for η from Eq. 76, and therefore shorter geodesic lengths [18]. If we consider the expected survival function of the SPLD for the whole network $\tilde{\psi}(l)$, as defined in Eq. 48, then applying Jensen's inequality [51] to Eq. 78b yields a lower bound on $\tilde{\psi}(l)$, analogous to the bounds in Eqs. 49, 64:

$$\tilde{\psi}(l) \geq \begin{cases} \exp\left(-\frac{\langle d \rangle(\eta^l - 1)}{n(\eta - 1)}\right) & \text{if } \eta \neq 1, \\ \exp\left(-l \frac{\langle d \rangle}{n}\right) & \text{otherwise,} \end{cases}\tag{79}$$

where we have used the definition of mean degree in Eq. 31c. Together, Eqs. 79 and 76 provide a bound for the SPLD in a degree-configuration model entirely in terms of the first and second moments of the degree distribution. This bound is tight when the variance in survival function across node pairs is small. For instance, in an ER graph where every node has the same expected degree $\langle d \rangle$, there is no variance in the survival function across node pairs. Each node has a Poisson degree distribution yielding $\eta = \langle d \rangle$ from Eq. 76, which substituted in Eq. 79 leads precisely to the expression we previously obtained in Eq. 56.

Illustrative example: random regular graphs. Since the SPLD depends only on the first two moments of the degree distribution, we can consider an extreme where the degree distribution has zero variance: the example of random d -regular graphs, wherein every node has the same degree d , and $d \in \mathbb{Z}_{>0}$ such that nd is even, but connections are otherwise random between node pairs [83]. Evidently, the degree constraint on random *regular* graphs prohibits conditionally independent edges, whereas the framework used to derive Eq. 78b assumes a conditionally independent edge model. Remarkably, since Eq. 78b is based only on degree moments, we can still derive an SPLD for random regular graphs. Because every node has the same degree d , we have

$$\forall x \in V : \hat{d}(x) = \langle d \rangle = d,\tag{80a}$$

$$\langle d^2 \rangle = d^2.\tag{80b}$$

Then Eqs. 76 and 80 yield $\eta = d - 1$, and we can rewrite Eq. 78b as:

$$\tilde{\psi}_l(x, y) = \begin{cases} \exp\left(-\frac{d[(d-1)^l - 1]}{n(d-2)}\right) & \text{if } d \neq 2, \\ \exp\left(-\frac{2l}{n}\right) & \text{otherwise.} \end{cases}\tag{81}$$

It is worth analyzing Eq. 81 when $d = 1$: every node in the random regular graph is attached to exactly one other node, thus the graph is composed of $n/2$ disconnected edges and does not have a giant component. Picking a node at random, the likelihood that another random node is directly connected to it is asymptotically n^{-1} , and the probability mass at other shortest path lengths is zero, yielding the survival function of the SPLD as $1 - n^{-1}$ for any $l \geq 1$. This is precisely what we obtain from Eq. 81 by setting $d = 1$ and applying a first-order approximation to the exponential. For $d = 2$, the network is composed of one or more disconnected cycles. Picking a node at random on a cycle of asymptotically large length, there are exactly 2 nodes at a distance of l from it, on either side. Thus, the probability mass at length l is asymptotically $2n^{-1}$, yielding the survival function of the SPLD as $1 - 2ln^{-1}$. As before, we obtain this expression by applying a first-order approximation to the exponential in Eq. 81. In Fig. 6, we show that Eq. 81 is a very good approximation of the SPLD for other degrees too.

Illustrative example: scale-free networks. We next consider the other extreme where the degree distribution has infinite variance. A typical example is of ‘‘scale-free’’ networks, whose nodes follow a power law degree distribution. Although scale-free networks are usually generated by a dynamic process like preferential attachment [2, 84], here we consider a *static* version based on vertex-fitness that permits a model with conditionally independent edges, similar to the stochastic fitness model in Ref. [85]. We define a multiplicative scale-free graphon with $f(x) = \sqrt{\beta} \left(\frac{x}{h}\right)^{-\alpha}$, i.e. $W_x(x, y) = \beta \left(\frac{xy}{h^2}\right)^{-\alpha}$, for some scalars $0 < \alpha \leq 1$, $0 < h \ll 1$, $\beta > 0$, with the node space restricted to the real interval $[h, 1]$ i.e. $\mu(x) = \frac{1}{1-h}$ if $x \in [h, 1]$ and 0 otherwise—a minor modification to

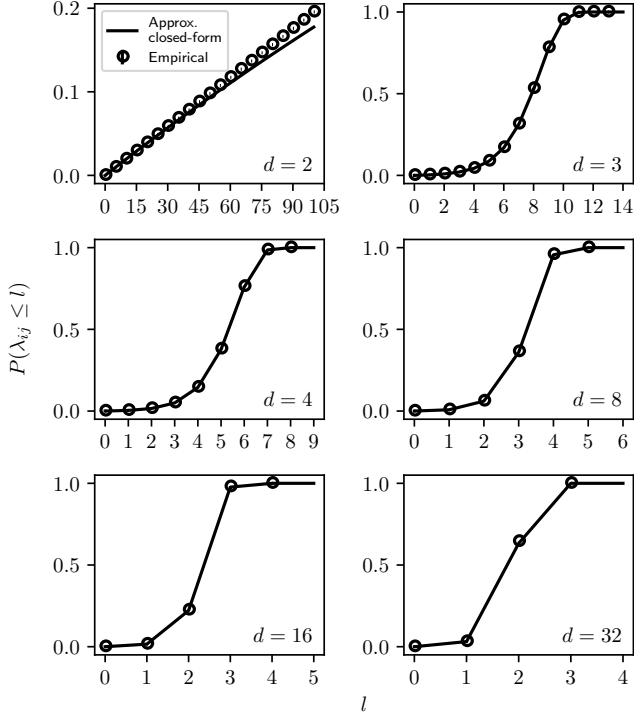


FIG. 6. Empirical and approximate closed-form cumulative distribution functions (CDF) of shortest path lengths for a random d -regular graph. Network size is fixed at $n = 1024$, while degree varies as $d \in \{2, 3, 4, 8, 16, 32\}$. Solid line indicates the approximate closed-form solution (Eqs. 81). Symbols and bars indicate empirical estimates: mean and standard error over 10 network samples. (The variation over samples is negligible.) For $d = 2$, the network is at the phase transition (see Sec. V A), and symbols are shown at every fifth geodesic length for clarity.

the usual assumption of a standard uniform distribution. Here, α controls the exponent of the power law governing the degree distribution: using Eq. 73a, the expected degree at x is $\hat{d}(x) \propto x^{-\alpha}$ which implies a degree distribution $d \propto d^{-\theta}$ where $\theta \triangleq 1 + \frac{1}{\alpha}$. (The distribution is not a *pure* power law, and might show departures from usually studied scale-free graphs in the small θ regime, as shown in the derivation of the degree distribution in Eq. G49 in Appendix G 4.) The definition for η in Eq. 72b yields:

$$\eta = \begin{cases} n\beta \frac{h \log h^{-1}}{1-h} & \text{if } \alpha = 1/2, \\ n\beta \frac{h^{2\alpha} - h}{(1-h)(1-2\alpha)} & \text{otherwise,} \end{cases} \quad (82)$$

and for ζ in Eq. 72a yields:

$$\zeta = \begin{cases} \sqrt{\beta} \frac{h \log h^{-1}}{1-h} & \text{if } \alpha = 1, \\ \sqrt{\beta} \frac{h^\alpha - h}{(1-h)(1-\alpha)} & \text{otherwise,} \end{cases} \quad (83)$$

which can be inserted into Eqs. 73, 78b to obtain the approximate closed-form of the survival function of the SPLD in scale-free graphons. We illustrate with three

special cases based on the power law exponent of the degree distribution: (1) an ER graph (where the power law exponent $\theta \rightarrow \infty \implies \alpha \rightarrow 0$), (2) a BA scale-free graphon (where the power law exponent $\theta = 3 \implies \alpha = \frac{1}{2}$ [84]), and (3) a “highly scale-free” graphon (for which $\theta = 2 \implies \alpha = 1$). We express the degree-controlling parameter h in terms of the mean degree $\langle d \rangle$ (see Appendix G 4 b). Assuming $h \ll 1$, from Eqs. 73b, 82, 83 we obtain:

$$h = \begin{cases} \frac{\langle d \rangle}{4n\beta} & \text{if } \alpha = \frac{1}{2}, \\ \left(\sqrt{\frac{n\beta}{\langle d \rangle}} \log \sqrt{\frac{n\beta}{\langle d \rangle}} \right)^{-1} & \text{if } \alpha = 1, \end{cases} \quad (84)$$

and for the ER graph ($\alpha = 0$) Eqs. 73b, 82 yield:

$$\langle d \rangle = n\beta. \quad (85)$$

Assuming $h \ll 1$, we obtain from Eqs. 82, 84, 85:

$$\eta = \begin{cases} \langle d \rangle & \text{if } \alpha = 0, \\ \frac{\langle d \rangle}{4} \log \left(\frac{4n\beta}{\langle d \rangle} \right) & \text{if } \alpha = \frac{1}{2}, \\ \frac{\sqrt{n\beta\langle d \rangle}}{\log \sqrt{\frac{n\beta}{\langle d \rangle}}} & \text{if } \alpha = 1. \end{cases} \quad (86)$$

From Eq. 86 we note that assuming sparsity—of the form $f(x) = O(n^{-\frac{1}{2}}) \implies \beta = O(n^{-1})$ —yields asymptotically bounded values of η for the BA and highly scale-free graphons, and thus for the degree’s variance, unlike typical scale-free networks. Therefore, we do not assume sparsity here and set $\beta = 1$, while maintaining finite mean degree $\langle d \rangle$, which yields asymptotically unbounded η and variance in the degrees, and permits a check of our formalism when sparsity is not enforced. In Fig. 5d we show various node and node pair functions for the BA scale-free graphon with $n = 512$, $\langle d \rangle = 4$ and $\alpha = 1/2$. The expected degree, percolation probability, and expected geodesic lengths are obtained via Eqs. 73a, 77 and 78b respectively. In Fig. 7, we show that the empirical and analytic estimates of expected geodesic lengths are in good agreement for this scale-free graphon, and its discretized SBM counterpart.

F. Summary of results on the SPLD

In Sec. IV, we have shown how geodesic statistics can be extracted for sparse versions of many popular random graph models, and of empirical networks when coarsened into SBMs. The approximate closed-form of the SPLD reveals further insight for the graph models considered: we showed for

1. SBMs that the survival function is expressed via an eigendecomposition of the block matrix (Eq. 58).
2. RDPGs that the mean vector and covariance matrix of the node distribution can specify a lower bound of the survival function for geodesics between a random node pair (Eq. 64).

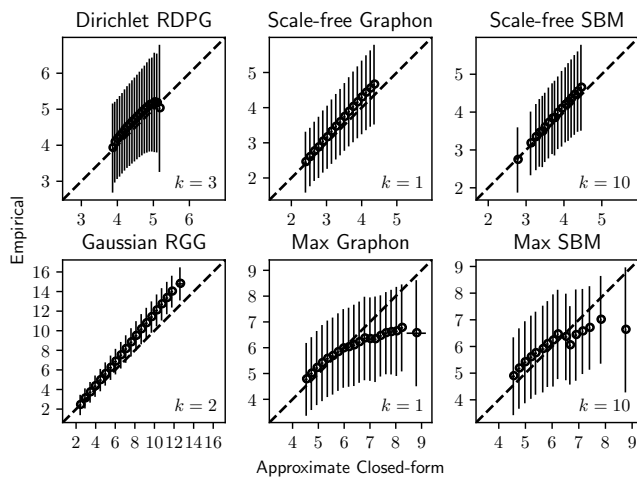


FIG. 7. Estimates of geodesic lengths from the approximate closed-form of the SPLD (on the x -axis) agree with empirical estimates (on the y -axis) for the random graph models considered in Sec. IV. For each model, 10 network samples were generated. For each network sample, the empirical geodesic length and the one derived from their respective closed-forms were computed for every node pair. To prevent clutter, the range of closed-form estimates so-derived was divided into 20 equal partitions, and each node pair of each network sample was placed in the corresponding partition. Then, the mean and standard deviation of closed-form and empirical estimates for each bin were calculated, per network sample. Consequently, each symbol \circ indicates the expected mean over 10 samples, with error bars indicating the expected standard deviation.

3. Gaussian RGGs with high spatial homophily, that the conditional PMF at length l can be interpreted as a “shortest-path” connectivity kernel when changing the connection scales by a factor of l (Eq. 70).
4. multiplicative graphons where the connectivity kernel of a node pair is a product of node functions, (equivalent to canonical degree-configuration models,) that the product of expected degrees of the source and target nodes specifies the survival function (Eq. 78b), and the survival function of the geodesic length between a random node pair can be bounded from below using the first and second moments of the degree distribution (Eqs. 79, 76).

V. SIZE AND EXISTENCE OF GIANT COMPONENT

Once the distribution of geodesic lengths is established, a suite of network properties can be inferred. To our knowledge, there has not yet been an approach that explicitly relates the SPLD to percolation behaviour: here, we draw this direct connection. We show how to estimate the size of the giant component, and obtain the

bond percolation threshold which determines whether a giant component exists in the network, using only the distribution of shortest path lengths.

Size of the giant component. For an undirected network with n nodes, the giant component refers to the largest connected component in the graph and scales in size as $O(n)$. As before, let ϕ_i be the event that node i is on the giant component of the network, then the expected number of nodes on the giant component, denoted by n_{gc} , is given by $n_{gc} = \sum_i P(\phi_i)$. This can be generalized to any graph model, by replacing the sum by an expectation of the percolation probability over the node space scaled by n :

$$n_{gc} = n \int_V \rho(x) d\mu(x), \quad (87)$$

which can be solved using the self-consistency Eq. 36 for the percolation probability. This is evident in Fig. 8, where we plot the analytic mean percolation probability and empirical proportion of nodes on the giant component for three different models in various parameter regimes. However, as described in Sec. II B, the SPLD is sufficient to estimate percolation probabilities using Eqs. 14, 15. Let x and y indicate locations of two nodes in the network such that the node at y is on the giant component. The steady state of Eq. 35a for the survival function of SPLD between nodes at y and x is indicative of $\rho(x)$, which from Eq. 15 results in:

$$n_{gc} = n \left[1 - \int_V \psi_\infty(y, x) d\mu(x) \right], \quad (88)$$

where we define

$$\begin{aligned} \psi_\infty(x, y) &\triangleq P(\lambda_{xy} = \infty | \phi_x) \\ &= \lim_{l \rightarrow \infty} P(\lambda_{xy} > l | \phi_x) = \lim_{l \rightarrow \infty} \psi_l(x, y), \end{aligned} \quad (89)$$

that can be computed as the limit value of ψ_l . (Since nodes are completely identified by their location, with a slight abuse of notation we use λ_{xy} to refer to the geodesic length between nodes at x, y , and ϕ_x to indicate the node at x being on the giant component.) Note that although the RHS of Eq. 88 appears to depend on the source node at y , the limit value $\psi_\infty(y, x)$ should be independent of it, and only depend on the target node at x . Computationally, we do observe close concordance in the limit values regardless of source nodes—as indicated in Fig. 3 for an SBM—but we can take an expectation of Eq. 88 over y for a more robust computation. In practice, the limit is easy to compute as ψ_l saturates quickly with l for a wide range of models. We note that in directed networks, the limiting value of the survival function of the SPLD will similarly yield the size of a node’s out-component (see Appendix E 1 for details).

Bond percolation threshold. There have been a variety of approaches in the literature to find the percolation threshold, which indicates whether a giant component exists in the network. For a graph with a given degree sequence, Ref. [25] established the criterion as when

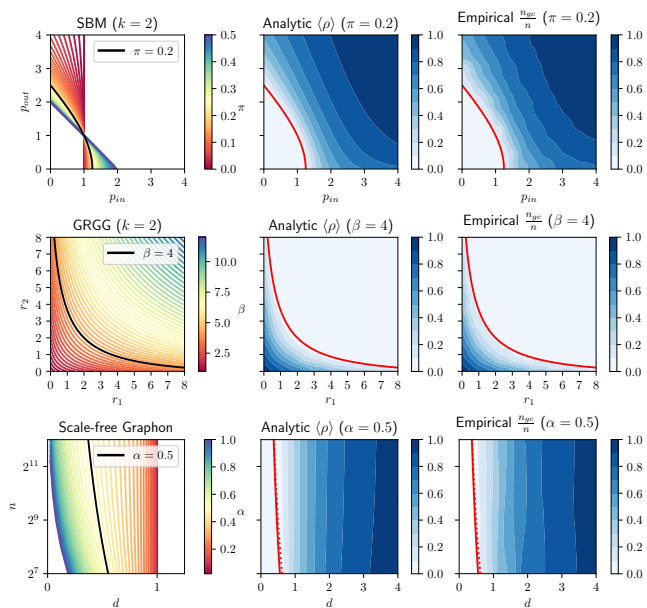


FIG. 8. Percolation thresholds for (a) a 2-block SBM with block matrix $B = \begin{pmatrix} c_{in} & c_{out} \\ c_{out} & c_{in} \end{pmatrix}$ for different values of the proportion of minority community π , computed from Eq. 100, (b) a 2-dimensional Gaussian RGG with scale matrix $R = \begin{pmatrix} r_1^{-1} & 0 \\ 0 & r_2^{-1} \end{pmatrix}$ for different probabilities of connecting to a node with identical co-ordinates β , computed from Eq. 105, and (c) a scale-free graphon with mean degree d and network size n for different values of the exponent α where the power law exponent is given by $\theta \triangleq 1 + \frac{1}{\alpha}$, computed by setting $\eta = 1$ from Eq. 92. The middle column shows the threshold (in red; also marked in black in the corresponding left subplot) alongside the variation in mean percolation probability (in blue) for given values of π, k, α respectively—estimated by taking the expectation of Eqs. 52, 69 and 77a over their respective node spaces. For the BA graphon with $\alpha = 0.5$, the solid and dotted red lines indicate the exact and asymptotic conditions from Eqs. 95b and 96a, respectively. Similarly, the right column shows the empirical proportion of nodes on the giant component—using 1 sample of the model per parameter tuple given by the x and y axes. Evidently, parameter regions indicated by the percolation threshold coincide with those having vanishing mean percolation likelihood $\langle \rho \rangle$ and a vanishing proportion of nodes on the giant component. We remark that the empirical contour plots of all models, and the analytic contour plot for the Gaussian RGG, have been smoothed with a Gaussian filter with unit standard deviation for visual clarity.

nodes are expected to have more neighbors-of-neighbors than neighbors, permitting the nodes to exist on a giant component. For inhomogeneous graphs with hidden colors, which are equivalent to SBMs, Refs. [29, 30] use a branching process to “reveal” the giant component starting from a source node, and determine the percolation threshold as when the trivial solution becomes unstable resulting in infinite trees in the process, yielding a criterion of the largest eigenvalue of a relevant matrix being greater than unity. For graphs with symmetric kernels

more generally, Ref. [31] uses a similar strategy to establish the percolation threshold as when the norm of the integral operator related to the connectivity kernel is greater than unity. More recent work on sparse empirical networks [33] has developed a message passing scheme to determine that the percolation threshold is given by the largest eigenvalue of the Hashimoto or nonbacktracking matrix [86].

In this section, we contribute to the understanding of percolation in graphs—both undirected and directed—generated by sparse connectivity kernels—both symmetric and asymmetric—in the asymptotic limit, by making use of the closed-form bound of the SPLD. We first establish an equivalence between non-existence of the giant component and the closed-form of the conditional PMF of the SPLD. Then, we show a further equivalence of this condition to the spectral radius (the largest absolute eigenvalue) of the integral operator T (which, as defined by Eq. 40, is analogous to $\langle A \rangle$), being less than unity. Finally, we derive percolation thresholds for two classes of random graph models in Sec. V A and Sec. V B.

Theorem 1 (Geodesic condition for percolation). *Consider a network with n nodes in V . Let $\omega_l(x, y; n)$ be the closed-form of the conditional PMF of the SPLD between nodes at $x, y \in V$, as given by Eq. 38a, where we make explicit the dependence on network size n . Then in the asymptotic limit, a giant component does not exist if and only if $\forall x, y \in V : \lim_{n \rightarrow \infty} \limsup_{l \rightarrow \infty} \omega_l(x, y; n) = 0$.*

A proof is enclosed in Appendix D 1. In its essence, Theorem 1 states that the network percolates iff the support of the closed-form of the conditional PMF of the SPLD, defined in Eq. 38a, between a set of nodes (of non-zero measure) is unbounded in the geodesic length. This is in analogy to the study of percolation by setting up an equivalent branching process, and noting that in the supercritical regime the process yields infinite-size trees [31].

From Eq. 43, we can express the conditional PMF of the SPLD for a symmetric connectivity kernel as a function of the eigenvalues of the integral operator defined in Eq. 40. This leads to a more useful condition for percolation.

Theorem 2 (Spectral condition for percolation). *Let T be the integral operator related to a symmetric connectivity kernel, as defined by Eq 40, and $r(T)$ be its spectral radius, i.e. the largest absolute value of its eigenvalues. Then, the network has a giant component if and only if*

$$r(T) > 1, \quad (90)$$

with the phase transition at $r(T) = 1$.

A proof is enclosed in Appendix D 1. While Theorem 2 makes use of the symmetry of the connectivity kernel, this result generalizes to asymmetric connectivity kernels which can lead to more interesting versions of directed graphs. That is, a directed network generated by

TABLE II. Bond percolation threshold for different random graph models considered in text: n refers to number of nodes, g refers to a node function which can be a scalar (g), vector (\mathbf{g} of appropriate length) or otherwise ($g(x)$ or $g(\mathbf{x})$) depending on node space V . T refers to the integral operator in Eq. 40, $r(\cdot)$ indicates the spectral radius, and the bond percolation threshold is given by $r(T)^{-1}$ from Theorem 2.

Model	$(Tg)(x)$	$r(T)$
ER graph ^a	$\langle d \rangle g$	$\langle d \rangle$
SBM ^b	$B\Pi\mathbf{g}$	$r(B\Pi)$
2-block SBM ^c	$\begin{pmatrix} c_{\text{in}}\pi & c_{\text{out}}(1-\pi) \\ c_{\text{out}}\pi & c_{\text{in}}(1-\pi) \end{pmatrix} \mathbf{g}$	$\delta(c_{\text{out}}^2 - c_{\text{in}}^2) + c_{\text{in}}$
Ensemble avg.	$\langle A \rangle \mathbf{g}$	$r(\langle A \rangle)$
Directed rank-1 ensemble ^{a,d}	$\frac{1}{n} \mathbf{a} \mathbf{b}^T \mathbf{g}$	$\frac{\langle d^- d^+ \rangle}{\langle d \rangle}$
RDPG ^{e,f}	$n\beta \int_{\mathbb{X}} \mathbf{x}^T \mathbf{y} \mathbf{g}(\mathbf{y}) d\mu$	$r(\Phi)$
Gaussian RGG ^{e,g,h}	$n \int_{\mathbb{R}^k} \nu(\mathbf{x}, \mathbf{y}; R) g(\mathbf{y}) d\mu$	$\frac{n\beta}{\prod_{i=1}^k \sqrt{\tau_i + \frac{\sqrt{1+4\tau_i+1}}{2}}}$
Unit-scale Gaussian RGG ^{e,g,i}	$n \int_{\mathbb{R}^k} \nu(\mathbf{x}, \mathbf{y}; I) g(\mathbf{y}) d\mu$	$n\beta\varphi^{-k}$
Multiplicative graphon ^j	$n f(x) \int_0^1 f(y) g(y) dy$	$n \int_0^1 f(x)^2 dx$
Degree-config. graphon ^{a,k}	$\frac{\hat{d}(x)}{\langle d \rangle} \int_0^1 \hat{d}(y) g(y) dy$	$\frac{\langle d^2 \rangle}{\langle d \rangle} - 1$
BA graphon ^{a,l}	$\frac{nh}{\sqrt{x}} \int_h^1 \frac{g(y)}{\sqrt{y}} dy$	$\frac{\langle d \rangle (\log n + \log \log n)}{4}$
Highly scale-free graphon ^{a,l}	$\frac{nh^2}{x} \int_h^1 \frac{g(y)}{y} dy$	$\frac{\langle d \rangle n}{(\log n - \log \log n)^2}$

^a mean degree $\langle d \rangle$

^b $k \times k$ block matrix B , distribution vector $\boldsymbol{\pi}$ and $\Pi \triangleq \text{diag}(\boldsymbol{\pi})$

^c π is minority proportion and dispersion $\delta \triangleq \pi(1-\pi)$

^d expected product of in- and out-degrees $\langle d^- d^+ \rangle$

^e $\beta = O(n^{-1})$ scales the connectivity kernel

^f $k \times k$ scaled second-moment matrix $\Phi \triangleq n\beta \int_{\mathbb{X}} \mathbf{x} \mathbf{x}^T d\mu$

^g $\nu(\mathbf{x}, \mathbf{y}; R) = \beta \exp(-\frac{1}{2}(\mathbf{x} - \mathbf{y})^T R^{-1}(\mathbf{x} - \mathbf{y}))$

^h $\{\tau_i\}_{i=1}^k$ are the eigenvalues of R^{-1}

ⁱ $\varphi \triangleq \frac{1+\sqrt{5}}{2}$ is the golden ratio

^j $\nu(x, y) = W_{\times}(x, y) \triangleq f(x)f(y)$

^k mean degree at x : $\hat{d}(x)$, 2^{nd} moment of degree distribution $\langle d^2 \rangle$

^l $h \ll 1$ controls mean degree $\langle d \rangle$

an asymmetric kernel has a giant in-/out-component iff $r(T) > 1$ —see Theorem 4 in Appendix E.

Given the spectral condition, we can derive the bond percolation threshold as $r(T)^{-1}$. The spectral radius of T (as defined in Eq. 40) can be solved for using the eigenvalue equation:

$$Tf = \tau f, \quad (91)$$

where $f \in F$ is an eigenfunction in an appropriate function space F , and τ the corresponding eigenvalue. In the following sections, we show what this general condition for percolation entails for specific graph models, with results on the bond percolation threshold summarized in Tab. II.

A. Percolation in rank-1 models

We first consider the case when the integral operator T has exactly one non-zero eigenvalue: what we refer to as rank-1 models. Special cases of various models discussed in Sec. IV are examples of rank-1 models. In particular, multiplicative graphon defined in Eq. 71 of Sec. IV E, where the connectivity kernel is given by $W_{\times}(x, y) = f(x)f(y)$, is of rank 1. The spectral radius is given by solving the eigenvalue Eq. 91 for the eigenpair (τ, g) , using the definition of T from Eq. 40 and of the multiplicative graphon kernel from Eq. 71:

$$(Tg)(x) = n f(x) \int_0^1 f(y) g(y) dy = \tau g(x) \quad (92)$$

$$\implies g = f, \text{ and } \tau = n \int_0^1 f(y)^2 dy = \eta,$$

where we apply the definition of η from Eq. 72b. Thus, the eigenvalue is given by η , and the eigenfunction by $f(x)$. Note that the normalized eigenfunction is given by $\frac{f(x)}{\sqrt{\int_0^1 f(x)^2 dx}} = \sqrt{\frac{n}{\eta}} f(x)$, which can be put into the kernel's eigenfunction expansion of Eq. 41b to verify that η is the sole eigenvalue: multiplicative graphons are rank-1 models.

Equivalence of rank-1 models and multiplicative graphons The converse is also true: any rank-1 model has an equivalent multiplicative graphon formulation for it (see Theorem 6 in Appendix F 4). We previously observed in Sec. IV E that multiplicative graphons are equivalent to canonical degree-configuration models. This allows us to establish results for multiplicative graphons, but use them for any rank-1 or degree-configuration model. For example, the spectral condition for percolation in multiplicative graphons yields:

$$\eta > 1, \quad (93)$$

with η defined in Eq. 72b. Using Eq. 76, we obtain the percolation condition in degree-configuration models in terms of the first and second moments of the degree distribution [25, 87] as

$$\frac{\langle d^2 \rangle}{\langle d \rangle} - 1 > 1 \implies \frac{\langle d^2 \rangle}{\langle d \rangle} > 2. \quad (94)$$

This result was first obtained using the classic percolation criterion of Molloy and Reed [25] suggesting that a giant component exists in a graph with a given degree sequence when nodes have a higher expectation of number of neighbours at length 2 (“neighbours-of-neighbours”) than at length 1 (“neighbours”). Here, we have shown that this criterion coincides with the spectral condition (Theorem 2) for the simplest class of rank-1 models, but for higher rank models there is a more complicated relationship between Molloy and Reed’s criterion and the spectral condition for percolation (see Appendix F 3). Interestingly, although the result in Eq. 94 has been obtained when assuming conditionally independent edges,

it holds for the random d -regular graph considered in Sec. IV E. Here, $\langle d \rangle = d$ and $\langle d^2 \rangle = d^2$, yielding the percolation condition $d > 2$ from Eq. 94, previously arrived at through other means [33, 87], and evident in Fig. 6.

Illustrative example: scale-free graphon. For scale-free graphons defined in Sec. IV E, the percolation condition is obtained by using the value of η from Eq. 82. Consider the three illustrative examples from Sec. IV E, for which we previously expressed η in terms of the mean degree and network size in Eq. 86. Setting the free parameter $\beta = 1$ as before, it follows that the ER, BA and highly scale-free graphons respectively percolate when

$$\langle d \rangle > 1 \quad \text{if } \alpha = 0, \quad (95a)$$

$$\frac{\langle d \rangle}{4} \log \left(\frac{4n}{\langle d \rangle} \right) > 1 \quad \text{if } \alpha = \frac{1}{2}, \quad (95b)$$

$$\frac{\sqrt{n \langle d \rangle}}{\log \sqrt{\frac{n}{\langle d \rangle}}} > 1 \quad \text{if } \alpha = 1. \quad (95c)$$

In Fig. 8 we plot the condition for BA graphon. For the ER graph, Eq. 95a is the well-studied percolation criterion $\langle d \rangle > 1$ [23]. For scale-free graphons, assuming large n gives an asymptotic condition on $\langle d \rangle$ from Eqs. 95b and 95c (see Appendix G 4 b) as follows:

$$\langle d \rangle > \frac{4}{\log n + \log \log n} \quad \text{if } \alpha = \frac{1}{2}, \quad (96a)$$

$$\langle d \rangle > \frac{(\log n - \log \log n)^2}{n} \quad \text{if } \alpha = 1. \quad (96b)$$

Both of these conditions are decreasing functions of n for large n , converging to zero asymptotically, unlike the constraint for an ER graph which is independent of the network size. We remark that for a BA graph, the RHS of Eq. 96a is a slowly-varying function of n of $O((\log n)^{-1})$, while for a “highly scale-free” graph the RHS of Eq. 96b is a regularly-varying function of n of $O(n^{-1}(\log n)^2)$ with a faster convergence [88]. This phenomenon is evident in the percolation constraints on $\langle d \rangle$ against n for different values of α , as shown in Fig. 8. Altogether, conditions in Eqs. 96a and 96b recapitulate previous results on the resilience of scale-free networks with power law exponent $2 < \theta < 3$ to failure in terms of an asymptotically null percolation threshold [11, 12, 87].

Illustrative example: directed degree-configuration model. We consider a rank-1 ensemble average model where the matrix $\langle A \rangle$ is equivalent to the operator T , when it corresponds to a canonical directed degree-configuration model. Let $\langle A \rangle \triangleq \frac{\mathbf{a}\mathbf{b}^T}{n}$ where $\mathbf{a}, \mathbf{b} \in \mathbb{R}_{\geq 0}^n$, i.e. $\langle A \rangle_{ij} = \frac{a_i b_j}{n}$. Evidently, this is an asymmetric connectivity kernel, for which too the spectral condition holds (see Theorem 4 in Appendix E). From the eigenvalue Eq. 91 we get for the eigenvalue τ and (unnormalized) right eigenvector \mathbf{v} :

$$\begin{aligned} \langle A \rangle \mathbf{v} &= \frac{1}{n} \mathbf{a}\mathbf{b}^T \mathbf{v} = \tau \mathbf{v} \\ \implies \mathbf{v} &= \mathbf{a}, \text{ and } \tau = \frac{\mathbf{a}^T \mathbf{b}}{n}. \end{aligned} \quad (97)$$

From Eqs. 3a, 3b, the expected out-degree of node i is given by $\langle d_i^+ \rangle = \frac{a_i \sum_j b_j}{n}$, and the expected in-degree by $\langle d_i^- \rangle = \frac{b_i \sum_j a_j}{n}$. From Eq. 4, the expected network degree is given by $\langle d \rangle = \frac{\sum_i a_i \sum_j b_j}{n^2}$. Consider the expectation of the product of in- and out-degrees via the law of total expectation: $\langle d^- d^+ \rangle = \mathbb{E}[\langle d^- d^+ \rangle] = \mathbb{E}[\langle d^- \rangle \langle d^+ \rangle]$, where we use the conditional independence of in- and out-degrees given the node identity. We can further write:

$$\begin{aligned} \mathbb{E}[\langle d^- \rangle \langle d^+ \rangle] &= \sum_i \langle d_i^- \rangle \langle d_i^+ \rangle / n \\ &= \sum_i a_i b_i \sum_j a_j \sum_k b_k / n^3 = \tau \langle d \rangle \quad (98) \\ \implies \tau &= \frac{\langle d^- d^+ \rangle}{\langle d \rangle} \end{aligned}$$

where we have used the expression for τ in Eq. 97. By setting $\tau > 1$ for percolation, we recover the percolation condition for the directed configuration model in terms of the expected product of the in- and out-degrees and expected degree [13, 89] as

$$\frac{\langle d^- d^+ \rangle}{\langle d \rangle} > 1.$$

B. Percolation in higher rank models

When the model’s integral operator T does not have a unique non-zero eigenvalue, then we refer to it as a higher rank model. Most higher dimensional independent edge models we have previously considered—ensemble average model, SBM, RDPG, RGG, non-multiplicative graphon like the max graphon—fall in this category. Notable results in percolation theory for models with a symmetric kernel can be recovered from our result on the spectral condition in Theorem 2. Prior work on the sparse stochastic block model with a symmetric block matrix B and diagonal distribution matrix Π has determined that the network percolates when the largest eigenvalue of $B\Pi$, which we note below coincides with the definition of T in Eq. 40, is greater than unity [29, 30]. In general, sparse inhomogeneous graphs with symmetric kernels have been shown to percolate when the 2-norm of an integral operator that describes the model, and coincides with the definition of T in Eq. 40, is greater than unity [31]. Since the kernel is symmetric, T is self-adjoint, and its 2-norm coincides with its spectral radius. Therefore, Theorem 2 recovers the known percolation conditions for sparse symmetric kernels. More generally, when T may not be self-adjoint, its 2-norm is bounded from below by its spectral radius: $\|T\|_2 \geq r(T)$. Therefore $r(T) > 1 \implies \|T\|_2 > 1$, yielding the spectral condition as the “stronger” (and accurate) condition relative to the 2-norm condition when considering asymmetric connectivity kernels (see Appendix E for an example).

Integral operators for various finite-dimensional models considered in this text can be written succinctly. Below, we derive the percolation thresholds for SBMs, ensemble average models, and RDPGs. We also find the threshold for Gaussian RGGs, which disproves a conjecture about the existence of a percolation threshold for RGGs with a non-uniform node density [72].

Illustrative example: SBM. Consider a k -block SBM from Sec. IV A, for which the class of eigenfunctions F becomes the k -dimensional Euclidean vector space. From Eq. 40, the integral operator takes the form of a matrix: $T \triangleq B\Pi$, and $f \in F$ is an eigenvector of T . The spectral condition for percolation suggests:

$$r(B\Pi) > 1. \quad (99)$$

For example, consider a 2-block SBM where the minority community occupies $0 \leq \pi \leq 0.5$ of the share, and a “planted-partition” block matrix given by $B = \begin{pmatrix} c_{\text{in}} & c_{\text{out}} \\ c_{\text{out}} & c_{\text{in}} \end{pmatrix}$, where c_{in} accounts for intra-group affinity whereas c_{out} for inter-group affinity. Then it can be shown (see Appendix G 1c) that T has precisely two (real) eigenvalues:

$\frac{c_{\text{in}}}{2} \left\{ 1 \pm \sqrt{1 + 4\pi(1 - \pi) \left[\left(\frac{c_{\text{out}}}{c_{\text{in}}} \right)^2 - 1 \right]} \right\}$. Setting the larger eigenvalue to be greater than unity, we obtain:

$$\pi(1 - \pi) (c_{\text{out}}^2 - c_{\text{in}}^2) + c_{\text{in}} > 1, \quad (100)$$

when $c_{\text{in}} \leq 2$, which is a hyperbolic constraint on the affinities, while for $c_{\text{in}} > 2$, the network percolates regardless. If $\pi = 0.5$, i.e. there is no minority community, then we obtain the linear constraint $c_{\text{in}} + c_{\text{out}} > 2$ [90]. Whereas if $\pi = 0$, i.e. there is a very strong minority which makes this a 1-block SBM which is equivalent to an ER graph, then we obtain the trivial constraint $c_{\text{in}} > 1$ [23]. In Fig. 8, we show the percolation thresholds for various values of π .

Illustrative example: ensemble average model. For the ensemble average model we have $T \triangleq \langle A \rangle$, resulting in the spectral condition

$$r(\langle A \rangle) > 1 \quad (101)$$

It is known that the spectral radius of the adjacency matrix $r(A)$ has implications for dynamics of processes on the graph, such as the sharp epidemic threshold being given by $r(A)^{-1}$ [91]. Recent work on *dense* graphs has shown the bond percolation threshold to be given by $r(A)^{-1}$ [92]. For *sparse* (and locally tree-like) graphs, the percolation threshold is slightly higher and given by the inverse of the largest eigenvalue of the Hashimoto or nonbacktracking matrix [86]. Eq. 101 adds to this literature by showing that for sparse graphs the inverse of the largest eigenvalue of the *expected* adjacency matrix $r(\langle A \rangle)^{-1}$ gives the bond percolation threshold. Notably, our result yields an asymptotic equivalence between the spectral radius of the nonbacktracking matrix and the corresponding expected adjacency matrix in sparse independent edge models.

Illustrative example: RDPG. We next consider the eigenvalue problem for an RDPG defined in Sec. IV C, for which the integral operator is: $(Tf)(\mathbf{x}) = n\beta \int_X \mathbf{x}^T \mathbf{y} f(\mathbf{y}) d\mu(\mathbf{y})$. Let $F : X \rightarrow \mathbb{R}$ be the space of dot-product operations, i.e. f has the form $f(\mathbf{x}; \mathbf{v}) = \mathbf{x}^T \mathbf{v}$ for some $\mathbf{v} \in \mathbb{R}^k$, which when put in the definition for T leads to:

$$\begin{aligned} (Tf)(\mathbf{x}) &= n\beta \mathbf{x}^T \int_X \mathbf{y} \mathbf{y}^T \mathbf{v} d\mu(\mathbf{y}) \\ &= \mathbf{x}^T \Phi \mathbf{v}, \end{aligned} \quad (102)$$

where we apply the definition of Φ from Eq. 59b. From the eigenvalue Eq. 91 we obtain for the eigenfunction: $(Tf)(\mathbf{x}) = \tau \mathbf{x}^T \mathbf{v}$. Comparing this to the RHS of Eq. 102, it must be the case that $\Phi \mathbf{v} = \tau \mathbf{v}$, i.e. \mathbf{v} is an eigenvector of Φ with eigenvalue τ . If Φ has an eigenpair (τ_i, \mathbf{v}_i) , then T has the eigenpair $(\tau_i, \mathbf{v}_i^T \mathbf{x})$: T has the same spectrum as Φ , which leads to the spectral condition

$$r(\Phi) > 1. \quad (103)$$

Percolation via the approximate closed-form SPLD. For higher rank models considered above, the spectral condition can also be considered through the approximate closed-form of the SPLD. From Theorem 1, the network percolates when the closed-form of the conditional PMF of the SPLD $\omega_l(x, y)$ diverges for some $x, y \in V$. The proof for Theorem 1 holds just as well when using the *approximate* closed-form of the conditional PMF of the SPLD $\tilde{\omega}_l$, since it only differs from the closed-form ω_l in its initial condition (see Corollary 1.1 in Appendix E). Given the definition for the approximate closed-form of the survival function of the SPLD $\tilde{\psi}_l$ in Eq. 38b, we can extract the condition for divergence by observing the expressions for $\tilde{\psi}_l$. In particular, Eq. 30 for ensemble average models, Eq. 55 for SBMs and Eq. 62 for RDPGs, immediately yield the divergence conditions $r(\langle A \rangle) > 1$, $r(B\Pi) > 1$ and $r(\Phi) > 1$, recapitulating percolation conditions in Eqs. 101, 99 and 103 respectively.

Illustrative example: Gaussian RGG. For other models, the percolation threshold may not become apparent from the SPLD alone—like by scrutinizing Eq. 70 for spatially homophilous Gaussian RGGs. Thus, we must consider the eigenvalue problem in Eq. 91 for Gaussian RGGs. Given that the node distribution is Gaussian, let the function space be $F : \mathbb{R}^k \rightarrow \mathbb{R}$ such that the eigenfunction $f \in F$ has the form $f(\mathbf{x}; \alpha, C) = \alpha \exp(-\frac{1}{2} \mathbf{x}^T C^{-1} \mathbf{x})$ for some $\alpha \in \mathbb{R}$ and $C \in \mathbb{R}^k \times \mathbb{R}^k$ where C is positive-definite, which ensures that f vanishes at infinity. Then it can be shown using the eigenvalue Eq. 91 (see Appendix G 3b) that the spectral radius of T is given by

$$r(T) = \frac{n\beta}{|I + C^{-1} + R^{-1}|^{\frac{1}{2}}} \quad (104)$$

where $|\cdot|$ indicates the matrix determinant, and C satisfies $C^2 - RC - R = 0$. Let (τ_i, \mathbf{v}_i) be an eigenpair of R^{-1} , then we can write $|I + C^{-1} + R^{-1}| =$

$\prod_{i=1}^k \left(\tau_i + \frac{\sqrt{1+4\tau_i+1}}{2} \right)$ (see Appendix G 3 b). Plugging into the spectral condition we obtain from Eq. 104:

$$n\beta > \prod_{i=1}^k \left(\tau_i + \frac{\sqrt{1+4\tau_i+1}}{2} \right)^{\frac{1}{2}}, \quad (105)$$

which expresses a percolation constraint on connectivity parameter β —which from Eq. 65 indicates the likelihood of connection to a node with identical co-ordinates—in terms of the connectivity scales. Since R is positive-definite, each factor in the product of this inequality can be no smaller than 1, leading to the minimal requirement that $n\beta > 1$. This also implies that every additional dimension can only raise the percolation threshold in terms of β . The mean degree from Eq. 68 can be written in terms of β and eigenvalues of R^{-1} as $\langle d \rangle = n\beta \prod_{i=1}^k (2\tau_i + 1)^{-\frac{1}{2}}$, which when put in Eq. 105 results in a percolation threshold for the mean degree:

$$\langle d \rangle > \prod_{i=1}^k \left(\frac{1}{2} + \frac{\sqrt{1+4\tau_i}}{2(1+2\tau_i)} \right)^{\frac{1}{2}}, \quad (106)$$

where each factor on the RHS of this inequality lies within the range $[\sqrt{2}^{-1}, 1]$, with the boundary values attained for largest and smallest connection scales: $\tau_i = 0$, $\tau_i = \infty$, respectively. This implies that every additional dimension can only lower the percolation threshold in terms of the mean degree $\langle d \rangle$. For very high-dimensional spaces (large k), the mean degree tends exponentially closer to 0, suggesting increasing robustness of a Gaussian RGG network to failure. This is in sharp contrast to the result for RGGs with uniform distribution [93], wherein although the mean degree constraint decreases with k , it decreases to the fiducial limit of 1 for ER graphs. This difference can be attributed to the nature of higher-dimensional Gaussians, since the expected degree itself is a Gaussian function in the node space, causing nodes close to the origin in \mathbb{R}^k to “bear the burden” of percolation in lieu of peripheral nodes (see Appendix G 3 c). For an illustrative example, consider a “unit-scale” Gaussian RGG where the scale matrix in Eq. 65 is $R = I$, i.e. node connection scales are of the same order as the node distribution’s variances along each dimension, which from Eq. 66 are equal to 1. This sets all eigenvalues of R^{-1} to 1, yielding from Eqs. 105, 106 the percolation conditions:

$$\begin{aligned} n\beta &> \varphi^k, \\ \langle d \rangle &> \left(\frac{\varphi}{\sqrt{3}} \right)^k, \end{aligned}$$

where $\varphi \triangleq \frac{1+\sqrt{5}}{2}$ is the golden ratio.

In Fig. 8, we show the percolation thresholds for a 2-dimensional Gaussian RGG with a diagonal scale matrix $R = \begin{pmatrix} r_1^{-1} & 0 \\ 0 & r_2^{-1} \end{pmatrix}$ for various values of β —with $\tau_1 = r_1, \tau_2 = r_2$. Evidently, for any given value of β ,

longer connection scales encourage percolation. In particular, we remark that our results reject the conjecture in Ref. [72] regarding spatially embedded networks, which suggests that “there is a phase transition only in the case of uniform ensembles”, i.e. where the node distribution is uniform. Here, we provide a counterexample in the form of a Gaussian RGG, by showing that for a non-uniform (Gaussian) node distribution, there still exists a critical value of the connectivity parameter for a giant component to exist.

VI. PATH-BASED STATISTICS

Access to the full geodesic length distribution permits us to compute path-based statistics for the network, like the mean geodesic length which we describe in Sec. VI A. Besides network-level properties, there are some node-level functions—like node centralities measuring the importance of nodes in a networks [36]—which require the computation of shortest paths. In Sec. VIB and Sec. VIC, we show how the general graph framework facilitates estimation of the expectation of two important centrality measures of closeness and betweenness.

A. Mean geodesic length

Since some nodes may have a non-zero likelihood of not being on the giant component, any estimate of the mean geodesic length must condition on the source and target nodes being on the giant component. We refer the reader to Appendix H 1 for obtaining this “analytic estimate” of mean geodesic length, using the analytic form of the SPLD. In this section, we focus on the general random graph model of Sec. III, while describing the use of the approximate closed-form of its SPLD, which (1) facilitates easy computation without numerical integration, and (2) for rank-1 models leads to a closed-form expression for the mean geodesic length.

Mean geodesic length using approximate closed-form of the SPLD. If the network is almost surely connected, then the analytic estimate of the mean geodesic length in Eq. H5 simplifies to the usual mean of a discrete random variable, given by the sum of the survival function of the SPLD:

$$\langle \lambda \rangle = \int_V \int_V \sum_{l=0}^{\infty} \psi_l(x, y) d\mu(x) d\mu(y). \quad (107)$$

Naturally, the RHS of Eq. 107 is finite if and only if $\lim_{l \rightarrow \infty} \psi_l(x, y) = 0$ almost everywhere, signifying that all node pairs have finite mean geodesic lengths, which will be true by assumption of the network being almost surely connected. If the network is not almost surely connected, we can still obtain a finite (albeit approximate) estimate from Eq. 107, when using the (approximate) closed-form of the SPLD, whose survival function $\tilde{\psi}_l(x, y)$

we previously derived for various random graph models. Assume that every node location pair $(x, y) \in V \times V$ is in the supercritical regime, then it can be shown that the approximate closed-form of the survival function of the SPLD, as defined in Eq. 46, has a limiting value of zero: $\lim_{l \rightarrow \infty} \tilde{\psi}_l(x, y) = 0$. We refer the reader to Appendix D2 for more details (including the scenario where not every location pair in $V \times V$ may be supercritical). For nodes at x, y , we define the expectation of their distance λ_{xy} , and consequently expectation of the mean network distance λ , as

$$\langle \lambda_{xy} \rangle \triangleq \sum_{l=0}^{\infty} \tilde{\psi}_l(x, y), \quad (108a)$$

$$\langle \lambda \rangle \triangleq \mathbb{E}_{\mu^2} [\langle \lambda_{xy} \rangle] = \int_V \int_V \langle \lambda_{xy} \rangle d\mu(x) d\mu(y), \quad (108b)$$

which must be finite. In what follows, we focus on computing mean geodesic lengths from Eq. 108, which we refer to as the “approximate closed-form of mean geodesic length”. Since the closed-form for the survival function of the SPLD is a lower bound, it can be used to obtain a lower bound on the mean geodesic length. Also, because it underestimates probability mass at longer lengths, the bound will be tighter for networks with smaller diameters.

Closed-form expression for multiplicative graphons. For sparse graphs in the asymptotic limit, we can make use of the Poisson summation formula—see Eq. H15 in Appendix H3—to write the RHS of Eq. 108a as $\sum_{l=0}^{\infty} \tilde{\psi}_l(x, y) \approx \frac{1}{2} + \int_0^{\infty} \tilde{\psi}_l(x, y) dl$. Then plugging into Eq. 108b, we get

$$\langle \lambda \rangle = \frac{1}{2} + \int_V \int_V \tilde{\psi}_{0 \rightarrow \infty}(x, y) d\mu(x) d\mu(y), \quad (109a)$$

$$\tilde{\psi}_{0 \rightarrow \infty}(x, y) \triangleq \int_0^{\infty} \tilde{\psi}_l(x, y) dl. \quad (109b)$$

To make further analytical progress, we consider the setup of multiplicative graphons with the connectivity kernel in Eq. 71. Eq. 78b yields, in the supercritical regime where from Eq. 92 $\eta > 1$, a closed-form for $\tilde{\psi}_{0 \rightarrow \infty}(x, y)$ —see Appendix H3 for details—as

$$\tilde{\psi}_{0 \rightarrow \infty}(x, y) = \frac{\log(\eta - 1) - \gamma - \log(f(x)f(y))}{\log \eta}, \quad (110)$$

where $\gamma \approx 0.57722$ is the Euler-Mascheroni constant. It then follows from Eq. 109a that:

$$\langle \lambda \rangle = \frac{1}{2} + \frac{\log(\eta - 1) - \gamma - 2\mathbb{E}_{\mu}[\log f(x)]}{\log \eta}. \quad (111)$$

As described in Eqs. 74 and 76, multiplicative graphons are equivalent to a canonical degree-configuration model:

$$\langle \lambda \rangle = \frac{1}{2} + \frac{\log(n \langle d^2 \rangle - 2 \langle d \rangle) - \gamma - 2\mathbb{E}_{\mu}[\log(\hat{d}(x))]}{\log\left(\frac{\langle d^2 \rangle}{\langle d \rangle} - 1\right)} \quad (112)$$

This recapitulates prior results on the average distance in the degree-configuration model varying as $\log_b n$ where $b \triangleq \frac{\langle d^2 \rangle}{\langle d \rangle} - 1$. [18].

Illustrative example: random regular graphs. First, we illustrate this result with the random d -regular graphs considered in Eq. 80, in the supercritical regime $d > 2$:

$$\langle \lambda \rangle = \frac{1}{2} + \frac{\log\left(n\left(1 - \frac{2}{d}\right)\right) - \gamma}{\log(d - 1)}, \quad (113)$$

which exemplifies the logarithmic dependence on n [94]. There is also a close connection here to the degree-diameter problem in graph theory: a graph with maximum degree d and diameter (*longest shortest path length*) k can have no more than

$$M_{d,k} = 1 + \frac{d[(d-1)^k - 1]}{d-2} \quad (114)$$

nodes—an upper bound that is met rarely, and exactly only for Moore graphs that are necessarily d -regular [95, 96]. Then, a d -regular random graph of the (asymptotically large) size $n \approx e^{\gamma} M_{d,k}$ (where $e^{\gamma} \approx 1.78107$) will have, from Eqs. 113 and 114, a mean geodesic length of

$$\langle \lambda \rangle = \frac{1}{2} + k. \quad (115)$$

In Fig. 9a, we plot the closed-form expression of the average geodesic length using Eq. 113 and empirical estimates, which agree well.

Illustrative example: scale-free graphon. We next illustrate with the “scale-free” graphons described in Sec. IVE, where $f(x) = \sqrt{\beta} \left(\frac{x}{h}\right)^{-\alpha}$. This leads to:

$$\begin{aligned} \mathbb{E}_{\mu}[\log f(x)] &= \int_h^1 \log f(x) d\mu(x) \\ &= \log \sqrt{\beta} + \alpha \left(1 + \frac{\log h}{1-h}\right), \end{aligned} \quad (116)$$

which can be inserted into Eq. 111. In Fig. 9b we plot the closed-form expression of the average geodesic length using Eqs. 111 and 116, alongside empirical estimates, for different values of α and network size n , while setting the free parameter $\beta = 1$ to capture asymptotically unbounded degree variance. Focussing on the three scale-free graphons of interest, assuming $h \ll 1$ we can write for the ER, BA and highly-scale-free graphons using Eqs. 84 and 116:

$$\mathbb{E}_{\mu}[\log f(x)] = \begin{cases} -\log \sqrt{\frac{n}{\langle d \rangle}} & \text{if } \alpha = 0, \\ \frac{1}{2} - \log \sqrt{\frac{4n}{\langle d \rangle}} & \text{if } \alpha = \frac{1}{2}, \\ 1 - \log \left(\sqrt{\frac{n}{\langle d \rangle}} \log \sqrt{\frac{n}{\langle d \rangle}} \right) & \text{if } \alpha = 1. \end{cases} \quad (117)$$

Then substituting in Eq. 111 alongside the value for η from Eq. 82, and taking the asymptotic limit for n while

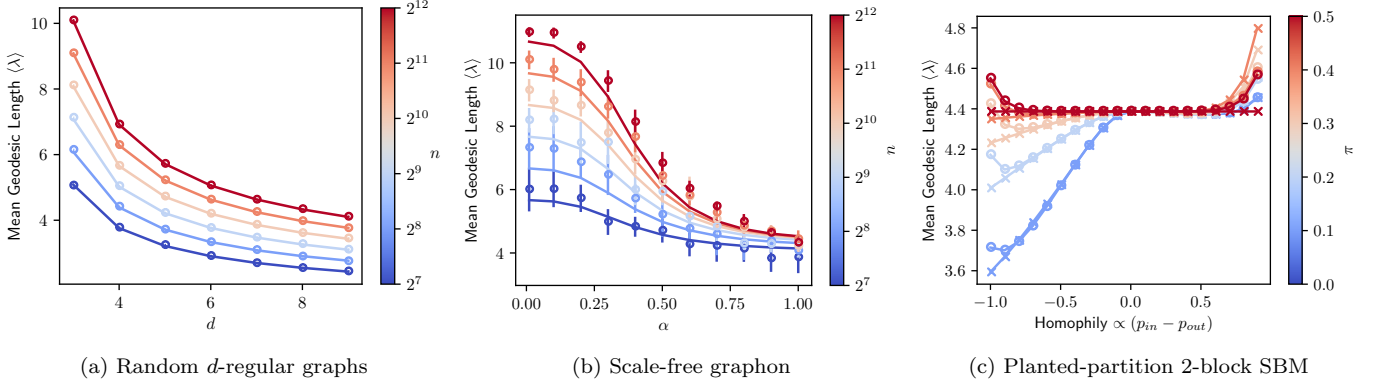


FIG. 9. Mean geodesic length for various random graph models. (a) Closed-form (solid line; Eq. 113) and empirical (o) estimates for random d -regular graphs scale-free graphons show good agreement across different values of d and network size n . (b) Closed-form (solid line; Eqs. 111, 116) and empirical (o) estimates for scale-free graphons show good agreement across different values of the power law exponent $\theta = (1 + \alpha^{-1})$ and network size n , with fixed mean degree $\langle d \rangle = 2$. (c) Analytic (o; Eqs. 108b, 55) and rank-1 closed-form (\times ; Eq. 119) estimates for a planted-partition 2-block SBM, where x -axis corresponds to different levels of homophily scaled to $[-1, 1]$ to facilitate interpretation across different values of the minority community proportion π , with fixed network size $n = 512$ and mean degree $\langle d \rangle = 4$.

holding $\langle d \rangle$ constant (see Appendix G 4 b), we obtain the order of expected geodesic lengths as:

$$\langle \lambda \rangle = \begin{cases} O(\log n) & \text{if } \alpha = 0, \\ O\left(\frac{\log n}{\log \log n}\right) & \text{if } \alpha = \frac{1}{2}, \\ O(1) & \text{if } \alpha = 1. \end{cases} \quad (118)$$

For ER graphons, we obtain the $\log n$ dependence which exemplifies the small-world property: on average, the distance between nodes scales logarithmically with the network size [2, 20]. For BA graphons, we obtain the $\frac{\log n}{\log \log n}$ dependence which marks an “ultra” small-worldness [20, 24]. Finally for “highly scale-free” graphons so-defined, asymptotically the average geodesic lengths does not scale with the network size, in contrast to typical behaviour for highly scale-free graphs [20, 97].

Rank-1 models. We next consider rank-1 models more generally, described in Sec. V A, for which the corresponding integral operator T in Eq. 40 has only one non-zero eigenvalue τ , and corresponding eigenfunction φ . From Theorem 6 in Appendix F 4, it is possible to write for any rank-1 graph model the average geodesic length asymptotically by setting $\eta = \tau$ and $f(x) = \sqrt{\frac{\tau}{n}}\varphi(x)$ in Eq. 111:

$$\langle \lambda \rangle = \frac{1}{2} + \frac{\log(n((1 - \tau^{-1}))) - \gamma - 2\mathbb{E}_\mu[\log \varphi]}{\log \tau}. \quad (119)$$

For large eigenvalue τ , the average geodesic length is governed by the logarithm of the eigenvalue ($\log \tau$) and expectation of logarithm of the corresponding eigenfunction ($\mathbb{E}_\mu[\log \varphi]$). Furthermore, this result also generalizes to the asymmetric kernel setting (see Appendix H 3).

Rank-1 approximations. When the graph model is of a higher rank, then there is no closed-form expression for

the average geodesic length in terms of standard mathematical functions. However, if all but the leading eigenvalue are “small enough” in absolute value, it may be reasonable to use Eq. 119 through a “rank-1 approximation” of the random graph model, by plugging in the leading eigenvalue and eigenfunction of T . We refer to this as the “rank-1 approximate closed-form” of mean geodesic length. Specifically, it can be shown that when the non-leading eigenvalues of T are small and positive, then asymptotically the additive correction to Eq. 119 tends to zero (see Appendix H 3). This allows us to write:

$$\langle \lambda \rangle = O\left((\log r(T))^{-1}\right),$$

where $r(T)$ is the spectral radius. In particular, for the ensemble average model we obtain $\langle \lambda \rangle = O\left((\log r(\langle A \rangle))^{-1}\right)$. Prior work has established the relevance of $\log r(A)$ as being the topological entropy of a graph [98]—where A is the adjacency matrix of the graph—which is the maximal entropy rate that can be achieved by a (biased) random walker on the graph. That is, a distribution over walker’s paths of a fixed length l is uniform up to a constant [99], or in other words, all paths of same length are equi-probable [100]. Here, we show that the expected geodesic length can scale as the inverse of $\log r(\langle A \rangle)$.

Illustrative example: SBM. For a synthetic example, if the random graph model is an SBM, then τ corresponds to the spectral radius of B_{II} , while φ to its corresponding eigenvector—see Appendix G 1 c. In Fig. 9c, we plot the mean geodesic length from Eq. 108b—which makes use of the approximate closed-form of the survival function from Eq. 55—and the rank-1 approximate closed-form of the mean geodesic length from Eq. 119, for the planted-partition 2-block SBM with varying pro-

portions of the minority community π , and varying levels of homophily which scale in proportion to $c_{\text{in}} - c_{\text{out}}$. This is done while holding mean degree and network size constant, so that any variation in geodesic lengths is entirely due to variation in homophily—see Appendix G 1c. We observe that an increase in heterophily induces shorter geodesics in the network under block imbalance, while extreme homophily or heterophily are not the most optimal, with regards to minimizing average geodesic length, for any level of π . The two estimates are in very good agreement when the SBM is close to being of rank 1, with discrepancies arising for extreme levels of homophily or heterophily, when the second eigenvalue and its eigenvector—indicative of block membership—becomes important.

Illustrative example: empirical networks. In Fig. 10, we show the applicability of the rank-1 approximation for empirical networks. First, by coarsening them into corresponding SBMs using the method described in Appendix I 1. Then, by comparing the empirical mean geodesic length to (1) the analytic form obtained from Eq. 108b—computed by using the approximate closed-form of the survival function of the SPLD for an SBM from Eq. 55—and to (2) the rank-1 approximate closed-form of the mean geodesic length from Eq. 119. We observe good agreement for a variety of the real-world networks considered—see Appendix I 2—although the level of agreement depends on selecting an “appropriate” level of coarsening. This demonstrates the power of our approach of coarsening real-world networks, and applying a subsequent rank-1 approximation to obtain average geodesic lengths in closed-form.

B. Closeness centrality

One centrality which can be computed directly from the SPLD is “closeness”, which is motivated by the question of how close, on average, a node is from every other node in the network. Here, we consider the expectation of node closeness in the general random graph model of Sec. III. We also establish a closed-form of closeness for rank-1 graph models, which can credibly approximate closeness for higher rank models.

Closeness from the SPLD. Following the harmonic definition of closeness [102, 103]—which naturally extends to disconnected graphs with infinite distances—the normalized closeness centrality of node k is defined by the expectation of reciprocal distances to the node:

$$\gamma_k = \frac{1}{n} \sum_{i \neq k} \frac{1}{\lambda_{ik}} = \mathbb{E} [\lambda_{ik}^{-1}], \quad (120)$$

where λ_{ik} refers to the length of the shortest path from i to k . Given that we have a random graph model, the closeness centrality of a node is itself a random variable. In Appendix H 2, we derive the “analytic expectation” of closeness using the analytic form of the survival function of the SPLD in Eq. 35a. To make further analytical

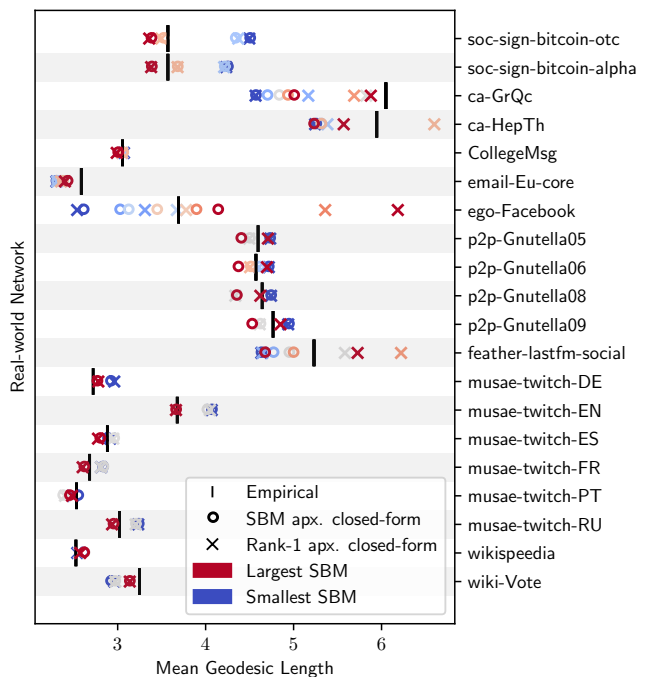


FIG. 10. For multiple real-world networks, the empirical geodesic length (black bars) are in agreement with the approximate closed-form estimates when “coarsened” into SBMs (\circ ; Eq. 108b), and estimates when applying a rank-1 approximation (\times ; Eq. 119). Colors indicate different levels of coarsening obtained from a hierarchical SBM [54], i.e. number of blocks from $k = 1$ (blue) indicating the ER graph to bigger SBMs (red) with a cutoff of 64 blocks. We observe that larger SBMs typically estimate the mean geodesic length better—indicating that a naïve approximation of the network as an ER graph loses information about geodesics in the networks considered. This holds when using either the approximate closed-form SPLD of the corresponding SBM, or when using the rank-1 approximation, with the latter overestimating the length more when excessive homophily (or modularity) is to be expected, such as in the Facebook friendship network [101].

progress, we use the approximate closed-form of the survival function of the SPLD from Eq. 46 in the general random graph setting of Sec. III (in analogy to estimating the closed-form of mean geodesic length in Sec. VI A). Then, assuming every node pair in V is in the supercritical regime and the network is almost surely connected, we define for a node at $z \in V$ its expected closeness:

$$\bar{\gamma}(z) \triangleq \mathbb{E}_\mu [\langle \lambda_{xz}^{-1} \rangle], \quad (121)$$

where the inner expectation over the inverse of the shortest path length between x, z is taken using the approximate closed-form of the survival function in Eq. 46. Since taking the inverse is a convex function for positive variables, from Jensen’s inequality [51] we can write for a random variable Z : $\mathbb{E} [Z^{-1}] \geq \mathbb{E} [Z]^{-1}$, which allows us to propagate the inverse in Eq. 121 outwards, and define

a lower-bound of closeness as defined by Eq. 121

$$\underline{\gamma}(z) \triangleq \mathbb{E}_\mu [\langle \lambda_{xz} \rangle]^{-1}, \quad (122)$$

which should be tight if the variance of geodesic lengths in the network is not too high. We note, this is the exact form we would arrive at by following the original definition of closeness for connected networks by Bavelas [104] as the inverse of farness. Substituting for $\langle \lambda_{xz} \rangle$ in Eq. 122 using Eq. 108a, we obtain in the general setting an approximate expected closeness for a node at z :

$$\underline{\gamma}(z) = \left[\int_V \sum_{l=0}^{\infty} \tilde{\psi}_l(x, z) d\mu(x) \right]^{-1}, \quad (123)$$

which closely resembles Eq. 108b for the mean geodesic length, as the inverse of expected distance to z marginalized over only the source node space.

Rank-1 models and approximations. For rank-1 models with the eigenpair (τ, φ) , we can follow the same approach as in Sec. VIA, to obtain the expected closeness function in closed-form:

$$\underline{\gamma}(z) = \left[\frac{1}{2} + \frac{\log(n(1 - \tau^{-1})) - \gamma - \mathbb{E}_\mu[\log \varphi] - \log \varphi(z)}{\log \tau} \right]^{-1}, \quad (124)$$

where γ is the Euler-Mascheroni constant, analogous to Eq. 119 for expected geodesic lengths, except marginalized only over the source node space. Since $\varphi(z)$ is the leading eigenfunction evaluated at z , it can be interpreted as defining the eigenvector centrality at z [38]. From Eq. 124 we show that for rank-1 models, the logarithm of inverse of eigenvector centrality of a node is proportional to the inverse of its closeness:

$$\underline{\gamma}(z)^{-1} = O(\log(\varphi(z)^{-1})).$$

Similar to Sec. VIA, we can apply here a rank-1 approximation to higher rank models and obtain a closed-form estimate of expected node closeness using Eq. 124 (not presented here).

Illustrative example: Gaussian RGG. To demonstrate the applicability of this framework in computing node closeness, we consider a 1-dimensional Gaussian RGG with different connectivity scales R , and compute its expected closeness centrality after discretization into a 32-block SBM—using the method described in Appendix F 2 a. We plot the empirical as well as various analytic estimates of closeness described here in Fig. 11. We note good agreement between the empirical and analytic estimates of expected closeness, even when using the rank-1 approximate closed-form.

C. Betweenness centrality

We now consider the node betweenness centrality, which is a measure of how important a node is based

on how many other nodes it forms a geodesic “bridge” between. We show how a generalization of Lemma 1 enables us to analytically estimate expected node betweenness using the analytic form of the SPLD.

Betweenness from the SPLD. We formulate betweenness for the ensemble average model of Sec. II, but note that the framework can be extended to the general random graph models of Sec. III. Consider a given network of n nodes, and let ζ_{ij} indicate the number of shortest paths between nodes i and j , and $\zeta_{ij}(k)$ be the number of shortest paths between i, j that pass through a given node k . Then asymptotically, the normalized node betweenness centrality of k as defined by Freeman [105] is given by

$$\beta_k = \frac{1}{n^2} \sum_{(i,j) \neq k} \frac{\zeta_{ij}(k)}{\zeta_{ij}} = \mathbb{E} \left[\frac{\zeta_{ij}(k)}{\zeta_{ij}} \right],$$

where the expectation is over source and target nodes i, j . The computation of β_k would typically necessitate a description of *number* of shortest paths ζ_{ij} between two nodes i, j . However, the original motivation for betweenness is to compute the “probability that k falls on a randomly selected geodesic linking i and j ” [105]. In our random graph framework, through the shortest path length distribution, we can have access to this probability, on average. Let χ_{ijk} indicate the probability that a shortest path between nodes i and j passes through k . We thus propose a probabilistic definition for the expected betweenness centrality as

$$\bar{\beta}_k \triangleq \mathbb{E}[\chi_{ijk}], \quad (125)$$

which in turn requires an expression for χ_{ijk} . Asymptotically, since the size of the giant component scales with network size, k is expected to form a geodesic “bridge” between i and j only if the nodes i, j, k are on the giant component. If we consider k to form a bridge of length l , where l is the geodesic length between i, j , then it can take a single value from $\{2, 3, \dots\}$ since all shortest paths between i, j must be of the same length. Let $\bar{\chi}_{ijk}(l)$ be the probability that the shortest path between i, j is of length l and it passes through k . Also, if the bridge is of length l , then k must be placed at a distance of p from i and $l - p$ from j , where p takes precisely one value from $\{1, 2, \dots, l - 1\}$, since the paths from i to k (and similarly from k to j) must be the shortest between them and therefore all of same length p (and similarly of same length $l - p$). Let $\tilde{\chi}_{ijk}(p; l)$ be the “ l, p -bridging” probability that the shortest path between i, j is of length l , and it passes through k such that k is at a distance p from i . Then, χ_{ijk} can be written as the sum over these

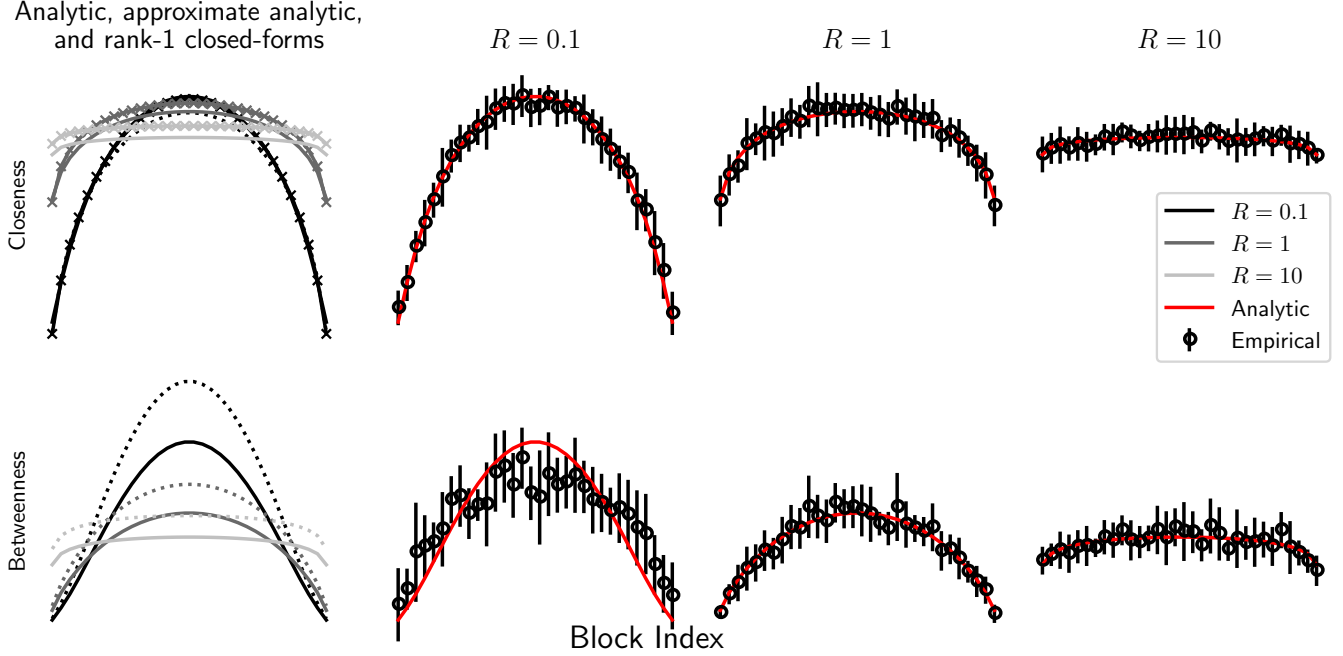


FIG. 11. Analytic and empirical estimates of geodesic-based centralities agree for an exemplar 1-dimensional Gaussian RGG (with fixed mean degree $\langle d \rangle = 2$, network size $n = 512$, varying connectivity scale R , and discretized into 32-block SBMs). Left column shows the analytic (solid), approximate analytic (dotted) and rank-1 closed-form (crosses) estimates of expectation of node centralities, where the node-of-interest is given to be on the giant component. The x -axis indicates block index from 1 to 32; successive block indices encode contiguous segments of \mathbb{R} such that nodes, distributed by a standard Gaussian distribution on \mathbb{R} , are distributed uniformly across the 32 blocks. For “harmonic” closeness (top-row), the analytic estimate is given by Eq. H10, the approximate analytic estimate by Eq. 123, and the rank-1 approximate closed-form estimate by Eq. 124. Evidently, closeness centrality of peripheral nodes massively declines as connection scales become smaller. Also, the rank-1 approximation estimate remains in reasonable agreement with the analytic form. For betweenness (bottom-row), the analytic estimate is given by Eqs. 125 and 126—where the bridging probability is given by Eq. A3 of Lemma 2—and the approximate analytic estimate by Eqs. 125 and 126—where the bridging probability is given by Eq. A5 of Lemma 3. Here too we see qualitatively similar behaviour, that nodes on the periphery (at the center) decrease (increase) in betweenness as connection scales lower. We note that the approximate analytic value overestimates betweenness of central nodes, and there is no closed-form estimate for betweenness.

mutually exclusive and exhaustive events:

$$\chi_{ijk} = \sum_{l=2}^{\infty} \bar{\chi}_{ijk}(l), \text{ where} \quad (126a)$$

$$\bar{\chi}_{ijk}(l) = \sum_{p=1}^{l-1} \tilde{\chi}_{ijk}(p; l) P(\phi_i) P(\phi_j) P(\phi_k), \quad (126b)$$

$$\tilde{\chi}_{ijk}(p; l) \triangleq P(\lambda_{ik} = p, \lambda_{kj} = l - p, \lambda_{ij} = l | \phi_i, \phi_j, \phi_k). \quad (126c)$$

To compute the RHS of Eq. 126c, it is useful to prove a “ l, p -bridging probability” lemma that generalizes Lemma 1, and estimates $\tilde{\chi}_{ijk}(p; l)$ using the SPLD, which can be inserted in Eq. 126 to compute the expected betweenness of any node from Eq. 125. We refer the reader to Lemma 2 in Appendix A 1, and note here that estimating $\tilde{\chi}_{ijk}(p; l)$ from the SPLD involves a recursion over values of p given l . We also consider an approximation to this lemma, and refer the reader to Lemma 3 in Appendix A 1. The approximation is asymptotically

tight for finite “bridge” lengths in infinite-size networks, works well for shorter “bridge” lengths in finite-size networks, and yields a succinct closed-form of the bridging probabilities, thus avoiding the recursion.

Lemmas 2, 3, and consequently the expression for betweenness from Eqs. 125, 126, can be re-written in the notation for the general random graph framework of Sec. III, where we estimate the expected betweenness at a node location $x \in V$, the expectation is taken over V , and sums over nodes are replaced by integrals over V scaled by n . However, unlike for closeness, we do not obtain closed-form approximations for betweenness centrality. Regardless, we emphasize that the recursive method remains computationally easy to apply in practice, as the mode of the SPLD is not too large for finite-sized networks. In Fig. 12, we plot the expected bridging probability for a node k given by $\mathbb{E}[\bar{\chi}_{ijk}(l)]$ in (1) ER graphs of varying degree, and (2) a bipartite SBM—computed both empirically and analytically using the bridging probability Lemma 2 and its approximate version Lemma 3.

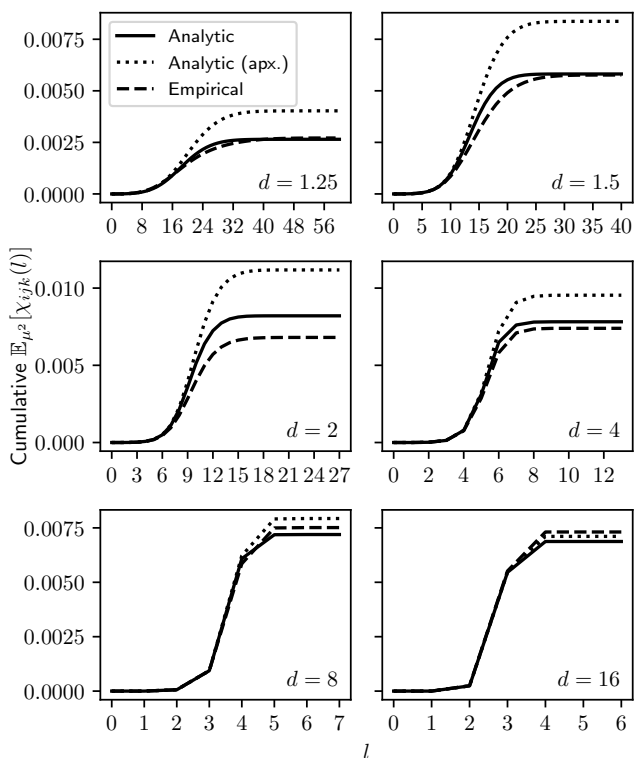
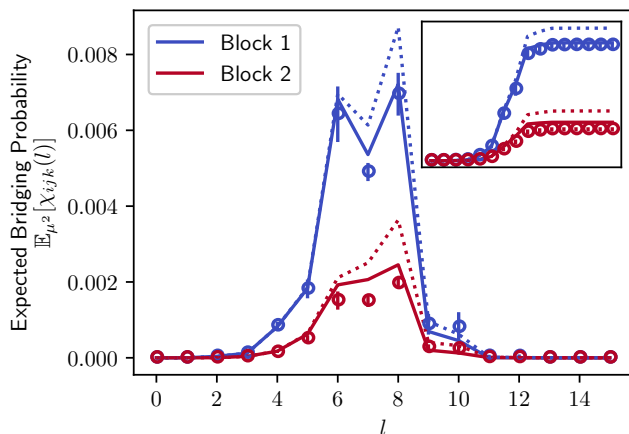
(a) ER Graphs of varying mean degree $\langle d \rangle$, $n = 1024$ (b) Bipartite SBM with $B = \begin{pmatrix} 0 & 8 \\ 8 & 0 \end{pmatrix}$, $\pi = (0.2, 0.8)$, $n = 1024$

FIG. 12. Analytic and empirical estimates of the expected bridging probability (BP) $\mathbb{E}_{\mu^2} [\chi_{ijk}(l)]$, i.e. the likelihood that node k lies on a shortest path of length l in the graph, are in good agreement, as shown here for two random graph models: (a) ER graphs with varying mean degree, where the y -axis indicates cumulative BP, i.e. the likelihood that k forms a shortest path of length up to l , and (b) a bipartite SBM, where the main y -axis indicates BP while the inset plot indicates cumulative BP. Solid (dotted) line correspond to the (approximate) analytic form as given by Lemma 2 (Lemma 3), while the dashed line [in (a)] and markers \circ [in (b)] indicate empirics. Bars in (b) represent the standard deviation over 10 network samples, and have been excluded from (a) for clarity. We remark that the saturating value of the cumulative BP defines betweenness from Eqs. 125, 126.

Illustrative example: Gaussian RGG. Using Eq. 126 and Lemma 2, we can find the expected betweenness of any node from Eq. 125, which is given exactly by the cumulative expected bridging probability. In Fig. 11, we demonstrate this approach to compute expected node betweenness for a 1-dimensional Gaussian RGG with different connectivity scales R , that was previously considered in Sec. VI B. We note good agreement in empirical and analytic expected betweenness, especially when the connection scales are not too small. We also note that the *approximate* bridging probability (from Eq. A5, Lemma 3) consistently overestimates betweenness of nodes, and moreso for nodes with higher betweenness. This is especially apparent at the smallest connection scale of $R = 0.1$, likely because smaller scales induce longer geodesic lengths on average, and the approximation in Lemma 3 works better for shorter geodesic lengths in a finite-size network. However, if the application is only to obtain a ranking of nodes by betweenness, then it may suffice.

Relationship to centralities based on matrix functions. In this section, we have shown how computationally intensive measures of closeness and betweenness can be analytically estimated for large sparse independent edge model using the SPLD framework. We close by drawing a theoretical connection to the centralities literature. From Eq. 29, the approximate closed-form survival function of the SPLD for the ensemble average model is given by a function of sum of powers of $\langle A \rangle$. This is reminiscent of well-studied centralities which can be expressed as matrix functions of the adjacency matrix A [106], i.e. as weighted sums of A^l (and/or $(A^T)^l$, for directed networks). In particular, in the asymptotic limit, we can define weighted versions of closeness and betweenness whose form involves a weighted sum of $\langle A \rangle^l$, akin to the down-weighting of A^l when computing measures like Katz centrality [40], subgraph centrality [107], and other bi-directional measures [108]. We refer the reader to Appendix H 4 for more details.

VII. CONCLUSION

In this work, we have derived an analytic distribution of shortest path lengths (SPLD) for networks, directed or undirected, generated by a sparse random graph model, symmetric or asymmetric, with conditionally independent edges in the asymptotic limit. The distribution describes shortest paths on the giant component when it exists (the supercritical regime), and on the small components otherwise (the subcritical regime). The SPLD is given by a pair of recursive equations which can be easily solved with initial conditions supplied by the form of the random graph model. We have obtained a closed-form lower bound on the survival function of the SPLD. In the supercritical regime, the bound is tight for finite lengths in the asymptotic limit, and for shorter lengths in finite-size networks. In the subcritical regime, it is tight for

all lengths in asymptotically large networks. The lower bound provides an approximate closed-form of the survival function of the SPLD up to length l that resembles the process of hitting a target node j from a source node i via any of the independent geodesics of independent lengths up to l , i.e. it is given by an exponential of the negative likelihood of independent geodesics up to length l . This generalizes previous analytic [16, 17] and closed-form approaches [20] to model the SPLD in ER graphs and scalar latent variable models. Tab. I summarizes an index for these analytical results on the SPLD. We have shown that it is possible to analytically and therefore cheaply compute the expectation of key node-level statistics that use shortest path lengths, namely node closeness and node betweenness centralities. For large real-world graphs like social networks, that may have millions of nodes, the ground truth graph or simulated networks can be prohibitively large. Therefore, computation of pairs of all shortest paths is intractable, but our approach makes such computations much easier.

SPLD in general random graph families. Transitioning away from the ensemble average setting where one has access to the expected adjacency matrix $\langle A \rangle$, we have defined a general framework of random graph models in some node space V which generalizes inhomogeneous random graphs [31] to the asymmetric setting permitting interesting behaviours in directed networks. This encompasses a diverse set of models like stochastic block models (SBM), random geometric graphs (RGG), random dot-product graphs (RDPG) and (sparse) graphons. We have derived a closed-form bound of the survival function of the SPLD in this general setting, whose expression is determined by an iterated integral operator T defined over functions on V , and the connectivity kernel represents the likelihood of an edge existing between two nodes in V . The operator T is analogous to $\langle A \rangle$ in the ensemble average model. For symmetric kernels, this yields an expression for the SPLD in terms of the spectral decomposition of T . In particular, we show for SBMs that the SPLD is expressed as an eigendecomposition of the block matrix. For illustrative examples of each of the above-mentioned models, we have derived the approximate closed-form of the SPLD revealing novel insights, particularly for higher-dimensional models whose shortest paths have not been previously studied analytically. Despite the assumptions involved, we have shown for various models—including “Gaussian RGG”, “Dirichlet RDPG”, random d -regular graphs, and “scale-free graphons”—that there is good agreement in the approximate closed-form and empirical estimates of expected shortest path lengths between node pairs.

Scope of applications. From an applied perspective, we provide empirical corroboration of our framework by demonstrating how real-world networks can be cheaply “coarsened” into SBMs to compute their expected SPLD analytically (see Figs. 10 and 4). Our results on RDPG find relevance in the burgeoning field of statistical machine learning on graphs, wherein nodes are typically em-

bedded in a Euclidean space \mathbb{R}^k equipped with the dot-product. We have shown that the matrix of second moments in \mathbb{R}^k (or in a corresponding feature space \mathbb{R}^d when the kernel is not linear in the dot-product) completely defines the SPLD for nodes located at $\mathbf{x}, \mathbf{y} \in \mathbb{R}^k$. This is particularly useful for sequential learning or querying for distances from individual nodes in prohibitively large networks. More generally, our theoretical framework to analytically estimate the SPLD can aid recent advances in graph representation learning based on graph neural networks (GNN), which incorporate knowledge of inter-node distances beyond immediate neighbours, and are provably more expressive than GNNs which do not [109].

Bond percolation threshold. Many local and global properties of interest can be extracted from the full SPLD. For instance, the expected size of the giant component (and of the in-/out-components for directed networks), can be estimated as the limit of the cumulative distribution function of the SPLD. Notably, there are wider theoretical implications as well. We have shown how the bond percolation threshold, at which the giant component appears, can be determined in the general setting of a conditionally independent edge model using the SPLD, regardless of whether the network is directed, and regardless of the symmetry of the connectivity kernel. Specifically, we have shown that asymptotically a giant (in-/out-)component exists, if and only if the spectral radius of the integral operator is greater than unity, i.e. $r(T) > 1$, with the phase transition at $r(T) = 1$. This draws a connection between the SPLD and percolation behaviour, and extends previous results on the percolation threshold for inhomogeneous graphs with symmetric kernels [29–31]. We have validated this result for both discrete space (2-block SBM) and continuous space network models (2-dimensional Gaussian RGG, scale-free graphon). By proving the existence of a percolation threshold in terms of the connectivity parameter for a non-uniform continuous space ensemble like the Gaussian RGG, we have provided a counterexample to the conjecture in Ref. [72] regarding spatially embedded networks, which had suggested that “there is a phase transition only in the case of uniform ensembles.” In the context of scale-free graphons, our approach yields expressions for the critical mean network degree $\langle d \rangle_c$ as a function of the network size n for percolation to occur, which adds to our understanding of the robustness of scale-free networks to failure [11, 12, 87]. In particular, $\langle d \rangle_c(n)$ is a slowly-decreasing function in n for BA graphs and a regularly-decreasing function in n for “highly scale-free” networks, unlike for ER graphs where $\langle d \rangle_c(n) = 1$ [23]. We have termed a class of “rank-1” random graph models, whose integral operator T has exactly one non-zero (positive) eigenvalue, which is also its spectral radius. We have shown that for any rank-1 graphon, the spectral condition for percolation is equivalent to the well-known Molloy and Reed criterion [25] for percolation, which says that percolation occurs when the expected number of neighbors-of-neighbors of a node

is higher than the expected number of neighbors itself. Tab. II summarizes our analytical results on the bond percolation threshold.

Path-based statistics for nodes and networks. Given the SPLD, we can obtain an estimate of its first moment, i.e. the mean geodesic length. We have shown that the approximate closed-form of the SPLD provides a useful and good approximation of the average shortest path length. For rank-1 models, which are equivalent to the canonical degree-configuration model, it is possible to obtain the mean in closed-form by knowledge of the eigenvalue and expectation of the logarithm of its corresponding eigenfunction. We have demonstrated this approach for random d -regular graphs for varying degrees, and for scale-free graphons spanning all levels of “scale-freeness”. Synthesizing a closed-form estimate of the mean geodesic length for random d -regular graphs also draws a connection to the degree-diameter problem in graph theory via the Moore bound [95]. For higher rank models, we can make a suitable rank-1 approximation and still obtain a good closed-form estimate of the mean geodesic length, as we have shown for 2-block SBMs, and for a wide variety of real-world networks. More generally, for models where eigenvalues that follow the leading eigenvalue are small and positive, this leads to the expected geodesic length scaling as $O\left((\log r(T))^{-1}\right)$. In a similar vein, we have shown how the expected closeness centrality at a node location is related to the logarithm of the leading eigenfunction of T evaluated at that location.

Limitations. The assumptions involved impose limitations on where our approach is applicable, and suggest extensions to be considered for future work. The conditionally-independent-edges assumption might hinder tight local clustering which is found commonly in some graphs like social networks [110, 111], and sparsity constraints may not hold for broad degree distributions over finite network sizes—both being important assumptions for deriving the recursive equations for the SPLD. The approximations involved in obtaining the closed-form lower bound discount probability mass at longer path lengths, and thus may not hold well for some models, particularly for finite-size network with very large diameters. In practice however, we have observed good agreement between analytics and empirics for the statistics we considered, both for Gaussian RGGs that are highly spatial—and thus exhibit some degree of local clustering—and scale-free graphons—that have heavy-tailed degree distributions.

ACKNOWLEDGMENTS

This work has been supported by EPSRC grant EP/N014529/1. The authors would like to thank Mauricio Barahona, Asher Mullokandov, George Cantwell, Florian Klimm, Till Hoffmann and Matthew Garrod for insightful discussions and helpful comments on the

manuscript.

Appendix A: Bridging probability lemmas

In this section, we state and provide brief proof sketches for various bridging probability lemmas.

Lemma 1 (Penultimate bridging probability). *For nodes i, j, k , path length $l > 1$:*

$$P(\lambda_{ik} = l - 1, \lambda_{kj} = 1 | \lambda_{ij} \geq l, \phi_i) = P(\lambda_{ik} = l - 1 | \phi_i) \times P(A_{kj} = 1). \quad (\text{A1})$$

Proof sketch. A full proof for this lemma can be found in Appendix A 1, and exploits the conditionally-independent-edges assumption in the asymptotic limit. However, it is helpful here to understand the lemma by “constructing” a shortest path between i, j , via a penultimate node k . Consider the LHS of Eq. 10:

$$P(\lambda_{ik} = l - 1, \lambda_{kj} = 1 | \lambda_{ij} \geq l, \phi_i) = \frac{P(\lambda_{ik} = l - 1, \lambda_{kj} = 1, \lambda_{ij} = l | \phi_i)}{P(\lambda_{ij} \geq l | \phi_i)}, \quad (\text{A2})$$

using the fact that the shortest path between i and j cannot be longer than l if a path of length l exists between them via k . Consider the numerator, which encodes the likelihood that k is a penultimate node on the shortest path between i, j of length l . Asymptotically, k can do so only if there is no path of length smaller than l existing between them: $\lambda_{ij} \geq l$. And for k to be the penultimate node, it must be true that $(\lambda_{ik} = l - 1) \cap (A_{kj} = 1)$. Asymptotically, these two events are independent. Both observations yield the numerator: $P(\lambda_{ij} \geq l | \phi_i) P(\lambda_{ik} = l - 1 | \phi_i) P(A_{kj} = 1)$, which when substituted in Eq. A2 yields the RHS of Eq. A1. \square

Lemma 2 (l, p -bridging probability). *For nodes i, j, k , path lengths $l > 2, 1 < p < l - 1$, the bridging probability $\tilde{\chi}_{ijk}(p; l)$ can be written as:*

$$\tilde{\chi}_{ijk}(p; l) \triangleq P(\lambda_{ik} = l - p, \lambda_{kj} = p, \lambda_{ij} = l | \phi_i, \phi_j, \phi_k) = P(\lambda_{kj} = p | \phi_k, \phi_j) P(\lambda_{ij} \geq l | \phi_i, \phi_j) \frac{P(\lambda_{ik} \geq l - p | \phi_i)}{P(\phi_k)} \left[1 - \exp \left(\sum_{u \neq (i, j, k)} \log(1 - f_{ijk}(u; p, l)) \right) \right], \quad (\text{A3})$$

where $f_{ijk}(u; p, l) \triangleq$

$$P(\lambda_{iu} = l - p - 1 | \phi_i) P(A_{uk} = 1) P(\lambda_{uj} > p | \phi_u, \phi_j). \quad (\text{A4})$$

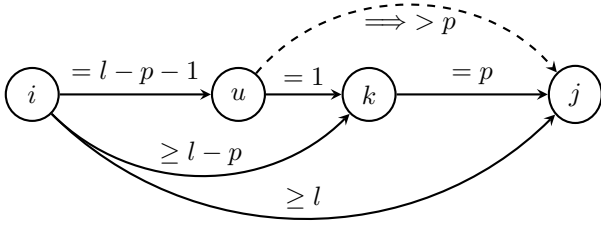
Proof sketch. A full proof for this lemma is enclosed in Appendix A 2, and builds on the proof for Lemma 1 while making use of the conditionally-independent-edges assumption in the asymptotic limit. However, it will be

helpful here to understand the expression of this lemma by “constructing” a bridge between i, j , via k , which serves as a proof sketch. To prevent clutter, we suppress the conditioning on nodes to be on the giant component.

First, construct the path from k to j . Then the first factor on the RHS of Eq. A3, i.e. $P(\lambda_{kj} = p)$, is simply the probability of j being at a distance of p from k . Asymptotically, k can form a bridge of length l only if there is no existing path of length smaller than l between i, j , which contributes the second factor to the RHS: $P(\lambda_{ij} \geq l)$. This leaves us with constructing the geodesic from i to k .

Similar to the derivation for the recursive Eq. 12 for geodesic length distribution, we can construct a shortest path of length $l - p$ from i to k if there is not already a path of a shorter length, which contributes the third factor to the RHS: $P(\lambda_{ik} \geq l - p)$. Such a path exists if there is a penultimate node u on this path, i.e. such that $(\lambda_{iu} = l - p - 1) \cap (A_{uk} = 1)$. This is encoded by the last factor on the RHS: $1 - \exp\left(\sum_{u \neq (i, j, k)} \log(1 - f_{ijk}(u; p, l))\right)$.

Note that the penultimate node u must follow an extra condition of $P(\lambda_{uj} > p)$. For if that were not true, then there would be a path from i to j via u of length shorter than l , which is incompatible with the given events.



Altogether, the constraint $(\lambda_{iu} = l - p - 1) \cap (A_{uk} = 1) \cap (\lambda_{uj} > p)$ is what is encoded by the function $f_{ijk}(u; p, l)$ in Eq. A4. \square

Lemma 3 (Approximate l, p -bridging probability). *For nodes i, j, k , path lengths $l > 2$, $1 < p < l - 1$, an approximate bridging probability $\hat{\chi}_{ijk}(p; l)$ can be written as:*

$$\begin{aligned} P(\lambda_{ik} = l - p, \lambda_{kj} = p, \lambda_{ij} = l | \phi_i, \phi_j, \phi_k) &\approx \hat{\chi}_{ijk}(p; l) \triangleq \\ P(\lambda_{ik} = l - p | \phi_i, \phi_k) P(\lambda_{kj} = p | \phi_k, \phi_j) P(\lambda_{ij} \geq l | \phi_i, \phi_j). \end{aligned} \quad (\text{A5})$$

Proof sketch. The proof for this lemma follows immediately from that of Lemma 2, and is enclosed in Appendix A 2. We can comprehend this expression by similar reasoning as for Lemma 2, with a constraint relaxation in the last step of constructing the geodesic from i to k of length $l - p$. That is, we may ignore the additional constraint of $\lambda_{uj} > l$ on the penultimate node u forming the shortest path between i and k . This can be comfortably done for finite l in infinite-size networks, since asymptotically almost surely $\lambda_{uj} > l$. This implies that the contribution of this geodesic is given simply by $P(\lambda_{ik} = l - p | \phi_i, \phi_k)$,

leading to the expression on the RHS of Eq. A5. We emphasize that in finite-size networks, this constraint-loss will overestimate the likelihood of a geodesic from i to k —especially for longer bridge lengths—and therefore of k forming a bridge between i and j . \square

In this following sections, we provide a full proof for Lemmas 1, 2 and 3.

1. Penultimate bridging probability

We start by restating and proving Lemma 1.

Lemma (Penultimate bridging probability). *For nodes i, j, k , path length $l > 1$:*

$$\begin{aligned} P(\lambda_{ik} = l - 1, \lambda_{kj} = 1 | \lambda_{ij} \geq l, \phi_i) &= P(\lambda_{ik} = l - 1 | \phi_i) \\ &\times P(A_{kj} = 1). \end{aligned}$$

Proof. Consider nodes i, j, k in the graph G , represented by its adjacency matrix A , generated from the sample space Ω . Throughout this proof, we assume the conditioning on i being on the giant component, i.e. ϕ_i , as implicit. With a minor change in notation used in the main text, let $\lambda_{ij}(G)$ represent the shortest path length between nodes i and j in G . Let $G^{\setminus k}$ be the “ k -subgraph” of G , i.e. the subgraph obtained by removing all of k ’s edges. Let Y be the event that the shortest path between i, j in G is of length no less than l (potentially infinite if j is not on the giant component) i.e. $Y \triangleq \{G \in \Omega | \lambda_{ij}(G) \geq l\}$. Let B_p be the event that there exists a path of length l between i, j via the node k , such that k is at a distance p from i and $l - p$ from j for $1 < p < l - 1$, i.e. $B_p \triangleq \{G \in \Omega | \lambda_{ik}(G) = l - p, \lambda_{kj}(G) = p\}$. Let C be the event that the shortest path between i, j that goes via the node k is of length longer than some l , i.e. $C \triangleq \{G \in \Omega | \lambda_{ik}(G) + \lambda_{kj}(G) > l\}$. Note that B_p ’s and C are pairwise disjoint events, i.e. $\forall p : B_p \cap C = \emptyset$ and $\forall p, \forall q \neq p : B_p \cap B_q = \emptyset$. Finally, let Z be the event that in the k -subgraph the shortest path between i, j is of length no less than l , i.e. $Z = \{G^{\setminus k} \in \Omega | \lambda_{ij}(G^{\setminus k}) \geq l\}$, which is analogous to Y but for the k -subgraph. We aim to show that $P(\lambda_{ik}(G) = l - 1, \lambda_{kj}(G) = 1 | \lambda_{ij}(G) \geq l) = P(\lambda_{ik}(G) = l - 1)P(A_{kj} = 1)$. We do so in two steps: first by proving $P(B_1 | Y) \approx P(B_1 | Z)$, and second by proving $P(B_1 | Z) \approx P(\lambda_{ik}(G) = l - 1)P(A_{kj} = 1)$.

Step 1: to show $P(B_1 | Y) \approx P(B_1 | Z)$. We can rewrite Y by considering the corresponding event Z in the k -subgraph, intersected with the union of events that can occur once edges of k are (independently) “added back” to the graph. Since $\lambda_{ij}(G) \geq l$, the addition of k ’s edges will either construct a path between i, j via k that is longer than l (corresponding to C), or one that is exactly of length l (corresponding to one of the B_p ’s). This allows us to write Y as a disjoint union of events that occur when adding k ’s edges back to the graph: it can create a new (possibly shortest) path of length longer than l ($Z \cap C$), or a shortest path of exactly length l —where j is directly

connected to k ($Z \cap B_1$), or where j is at a distance 2 from k ($Z \cap B_2$), etc. up to at a distance $l - 1$ from k ($Z \cap B_{l-1}$)—i.e. $Y = (Z \cap C) \cup \bigcup_{p=1}^{l-1} (Z \cap B_p)$. Consider:

$$P(B_1|Y) = \frac{P(B_1 \cap Y)}{P(Y)} = \frac{P(B_1 \cap Z)}{P((C \cup \bigcup_p B_p) \cap Z)},$$

where the numerator can be written by realizing that B_1 is pairwise disjoint with all other B_p 's and C . Dividing numerator and denominator on RHS by $P(Z)$ leads to

$$\begin{aligned} P(B_1|Y) &= \frac{P(B_1|Z)}{P((C \cup \bigcup_p B_p)|Z)} \\ &= \frac{P(B_1|Z)}{1 - P((C \cup \bigcup_p B_p)^c|Z)}. \end{aligned} \quad (\text{A6})$$

Note that $(C \cup \bigcup_p B_p)^c|Z$ is the event that $\lambda_{ik}(G) + \lambda_{kj}(G) < l$, given that we know $\lambda_{ij}(G^{\setminus k}) \geq l$. In the infinite size limit, the removal of edges of any one node (k) should make vanishing difference to the shortest path length of a pair of different nodes (i, j), i.e. we must have $P((C \cup \bigcup_p B_p)^c|Z) \ll 1$. This translates Eq. A6 into

$$P(B_1|Y) \approx P(B_1|Z).$$

That is, conditioning on $\lambda_{ij}(G) \geq l$ is the same as conditioning on $\lambda_{ij}(G^{\setminus k}) \geq l$, which captures the infinite-size assumption.

Step 2: to show $P(B_1|Z) \approx P(\lambda_{ik}(G) = l - 1)P(A_{kj} = 1)$. We next independently “add” the edges of k back to $G^{\setminus k}$ to form G , which as per B_1 would entail k to be directly connected to j , and at a distance $l - 1$ from i .

We can write:

$$\begin{aligned} P(B_1|Z) &= P(\lambda_{ik}(G) = l - 1, \lambda_{kj}(G) = 1 | \lambda_{ij}(G^{\setminus k}) \geq l) \\ &= \frac{P(\lambda_{ik}(G) = l - 1, \lambda_{kj}(G) = 1, \lambda_{ij}(G^{\setminus k}) \geq l)}{\lambda_{ij}(G^{\setminus k}) \geq l}. \end{aligned} \quad (\text{A7})$$

Consider the numerator of Eq. A7. Due to $(\lambda_{kj}(G) = 1) \cap (\lambda_{ij}(G^{\setminus k}) \geq l)$, we know that k is directly connected to j , and the shortest path between i and j , without having added back the remaining edges of k , is no less than l . Focusing on the event $\lambda_{ik}(G) = l - 1$, we observe that upon addition of the edges of k , the shortest path from i to k cannot pass through j or any of its immediate neighbors, as a shortest path invoking j or its neighbors would be necessarily too long. To be more precise, consider the situations where k uses j or its neighbors as a means of connecting to i in $l - 1$ steps, given $(\lambda_{kj}(G) = 1) \cap (\lambda_{ij}(G^{\setminus k}) \geq l)$. If $\lambda_{ij}(G^{\setminus k}) < \infty$ then j is on the giant component of $G^{\setminus k}$ (recall that we have suppressed writing ϕ_i throughout). Then it is not possible for k to use j as a means of connecting to i in $l - 1$ steps on G , as j is at a distance l or longer from i in $G^{\setminus k}$. Similarly, it is also not possible for k to use any immediate neighbors of j to connect to i in $l - 1$ steps on G , since they must be at a distance $l - 1$ or longer from i in $G^{\setminus k}$. Essentially, while constructing the path of desired length between k and i , we can just as easily “remove” edges which are necessarily forbidden due to the conditioning: let $\eta(j)$ be the set of neighbors of j in $G^{\setminus k}$ (including itself but excluding k)—see Fig. 13. Alternatively, if $\lambda_{ij}(G^{\setminus k}) = \infty$ i.e. j is not on the giant component of $G^{\setminus k}$, then it in no way affects the likelihood of i connecting to k . More precisely, this construction establishes the following equivalence:

$$\begin{aligned} (\lambda_{ik}(G) = l - 1) \cap (\lambda_{kj}(G) = 1) \cap (\lambda_{ij}(G^{\setminus k}) \geq l) &\iff \left[(\lambda_{ik}(G^{\setminus j}) = l - 1) \cap (A_{kj} = 1) \cap (\lambda_{ij}(G^{\setminus k}) = \infty) \right] \cup \\ &\left[(\lambda_{ik}(G^{\setminus \eta(j)}) = l - 1) \cap (A_{kj} = 1) \cap (l \leq \lambda_{ij}(G^{\setminus k}) < \infty) \right]. \end{aligned} \quad (\text{A8})$$

Because of conditionally-independent edges, information about the path length between nodes i, j , in a graph where k 's edges do not exist, asymptotically informs nothing about the path length between nodes i, k in a graph where j 's edges do not exist, and vice-versa:

$$(l \leq \lambda_{ij}(G^{\setminus k}) < \infty) \perp (\lambda_{ik}(G^{\setminus \eta(j)}) = l - 1), \quad (\text{A9a})$$

$$(\lambda_{ij}(G^{\setminus k}) = \infty) \perp (\lambda_{ik}(G^{\setminus j}) = l - 1). \quad (\text{A9b})$$

Similarly, existence of a direct edge between k, j informs nothing about the path lengths between i, j in a graph where k 's edges do not exist, or about the path lengths between i, k in a graph where j 's edges do not exist, and

vice-versa:

$$(A_{kj} = 1) \perp \left(l \leq \lambda_{ij}(G^{\setminus k}) < \infty \right), \quad (\text{A10a})$$

$$(A_{kj} = 1) \perp \left(\lambda_{ij}(G^{\setminus k}) = \infty \right), \quad (\text{A10b})$$

$$(A_{kj} = 1) \perp \left(\lambda_{ik}(G^{\setminus \eta(j)}) = l - 1 \right), \quad (\text{A10c})$$

$$(A_{kj} = 1) \perp \left(\lambda_{ik}(G^{\setminus j}) = l - 1 \right). \quad (\text{A10d})$$

That is, the RHS of Eq. A8 is a disjoint union of intersection of mutually-independent events. Applying the equivalence in Eq. A8 and the independence results in Eqs. A9, A10 to the RHS of Eq. A7 yields:

$$\begin{aligned} & \frac{P(\lambda_{ik}(G^{\setminus \eta(j)}) = l - 1)P(A_{kj} = 1)P(l \leq \lambda_{ij}(G^{\setminus k}) < \infty)}{P(\lambda_{ij}(G^{\setminus k}) \geq l)} \\ & + \frac{P(\lambda_{ik}(G^{\setminus j}) = l - 1)P(A_{kj} = 1)P(\lambda_{ij}(G^{\setminus k}) = \infty)}{P(\lambda_{ij}(G^{\setminus k}) \geq l)}. \end{aligned}$$

Because we assume finite node degrees, addition of the edges of a finite number of nodes in $\eta(j)$ creates no difference to the rest of the network in the asymptotic limit, i.e. $P(\lambda_{ik}(G^{\setminus \eta(j)}) = l - 1) \approx P(\lambda_{ik}(G) = l - 1)$. Similarly, the addition of edges of just one node j also creates no difference asymptotically, i.e. $P(\lambda_{ik}(G^{\setminus j}) = l - 1) \approx P(\lambda_{ik}(G) = l - 1)$. This yields $P(B_1|Z)$ as the product of marginals:

$$P(B_1|Z) \approx P(\lambda_{ik}(G) = l - 1)P(A_{kj}(G) = 1). \quad \square$$

2. l, p -bridging probability

We next prove Lemma 2, which we restate below.

Lemma (l, p -bridging probability). *For nodes i, j, k , path lengths $l > 2$, $1 < p < l - 1$, the bridging probability $\tilde{\chi}_{ijk}(p; l)$ can be written as:*

$$\begin{aligned} \tilde{\chi}_{ijk}(p; l) & \triangleq P(\lambda_{ik} = l - p, \lambda_{kj} = p, \lambda_{ij} = l | \phi_i, \phi_j, \phi_k) = \\ & P(\lambda_{kj} = p | \phi_k, \phi_j) P(\lambda_{ij} \geq l | \phi_i, \phi_j) \frac{P(\lambda_{ik} \geq l - p | \phi_i)}{P(\phi_k)} \\ & \left[1 - \exp \left(\sum_{u \neq (i, j, k)} \log(1 - f_{ijk}(u; p, l)) \right) \right], \end{aligned} \quad (\text{A11})$$

where $f_{ijk}(u; p, l) \triangleq$

$$P(\lambda_{iu} = l - p - 1 | \phi_i) P(A_{uk} = 1) P(\lambda_{uj} > p | \phi_u, \phi_j).$$

Proof. The proof extends the proof for Lemma 1. Consider the LHS of Eq. A11, while keeping implicit the conditioning on ϕ_i :

$$\begin{aligned} & P(\lambda_{ik} = l - p, \lambda_{kj} = p, \lambda_{ij} = l | \phi_j, \phi_k) = \\ & P(\lambda_{ik} = l - p, \lambda_{kj} = p, \lambda_{ij} \geq l | \phi_j, \phi_k) = \\ & P(\lambda_{ik} = l - p, \lambda_{kj} = p | \lambda_{ij} \geq l, \phi_j, \phi_k) P(\lambda_{ij} \geq l | \phi_j) \end{aligned} \quad (\text{A12})$$

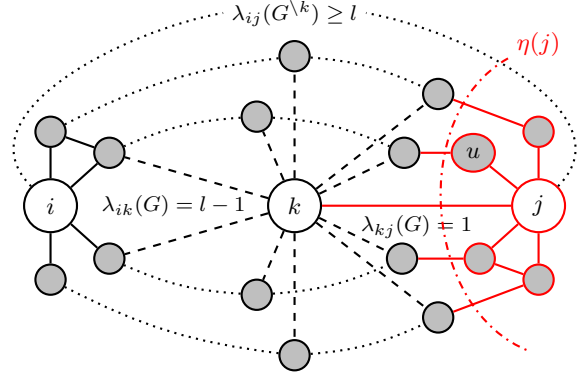


FIG. 13. A schematic depicting the conditioning of the event $\lambda_{ik}(G) = l - 1$ on $\lambda_{jk}(G) = 1, \lambda_{ij}(G^{\setminus k}) \geq l$. Nodes of interest are indicated in white, while gray nodes are other nodes, and solid lines are edges in the network. Dotted lines indicate paths from the source node i to the target node j via any number of intermediate nodes. Node $u \in \eta(j)$ is a node in the set of neighbors of j in $G^{\setminus k}$ (including itself). Since upon addition of edges of k the shortest path between i and k cannot pass through j or any of its immediate neighbors, we can ignore the edges of $\eta(j)$ from being a part of that shortest path, as indicated in red, and therefore consider the $\eta(j)$ -subgraph $G^{\setminus \eta(j)}$ instead. Dashed lines indicate (some of) the potential edges that may be generated when adding k back to the graph, which is essentially an edge to any node except for $\eta(j)$, consequent on which the shortest path between i, k in $G^{\setminus \eta(j)}$ may (or may not) be equal to the desired $l - 1$, and whose probability is given precisely by $P(\lambda_{ik}(G^{\setminus \eta(j)}) = l - 1)$.

Note that the first factor of the final line is equal to the LHS of Eq. 10 of Lemma 1 when $p = 1$ (ignoring the percolation constraints). Then considering the same notation as described in the proof of Lemma 1 in Appendix A1, we are interested in the first factor of the RHS of Eq. A12, which is $P(B_p|Y, \phi_j, \phi_k)$. First, using identical arguments from Appendix A1, it is straightforward to show $P(B_p|Y, \phi_j, \phi_k) \approx P(B_p|Z, \phi_j, \phi_k)$. As before, this conveys the infinite-size assumption, i.e. removing just one node k should have vanishing effect on the shortest path between nodes i, j . Then consider:

$$\begin{aligned} & P(B_p|Z, \phi_j, \phi_k) = \\ & P(\lambda_{ik}(G) = l - p, \lambda_{kj}(G) = p | \lambda_{ij}(G^{\setminus k}) \geq l, \phi_j, \phi_k) = \\ & \frac{P(\lambda_{ik}(G) = l - p, \lambda_{kj}(G) = p, \lambda_{ij}(G^{\setminus k}) \geq l | \phi_j, \phi_k)}{P(\lambda_{ij}(G^{\setminus k}) \geq l | \phi_j, \phi_k)}. \end{aligned} \quad (\text{A13})$$

Consider the numerator of Eq. A13. Due to $(\lambda_{kj}(G) = p) \cap (\lambda_{ij}(G^{\setminus k}) \geq l)$, we know that k is connected to j in p steps, and the shortest path between i and j , without having added back the remaining edges of k , is no less than l . Considering the event $\lambda_{ik}(G) = l - p$, we observe that upon addition of the edges of k , the shortest path from i to k cannot pass through j or any of its neighbors at a distance of up to p from j , as a shortest path invoking

j or this set of neighbors would be necessarily too long. To elaborate, let $\eta(j;p)$ refer to the set of nodes in $G^{\setminus k}$ that are at a distance no more than p to j (including itself but excluding k). Since we condition on ϕ_j , every node in $\eta(j;p)$ is also on the giant component. Consider the scenario where k uses a node u from $\eta(j;p)$ as a means of connecting to i in $l-p$ steps, given $(\lambda_{kj}(G) = p) \cap (\lambda_{ij}(G^{\setminus k}) \geq l)$. Note that $\lambda_{ij}(G^{\setminus k}) \geq l$ implies u , at a distance no more than p to j , must be at a distance no less than $l-p$ from i . Then it is not possible for k to use u as a means of connecting to i in $l-p$ steps on G . Essentially, while constructing the path of desired length between k and i , we can “remove” edges which are necessarily forbidden. This establishes the following equivalence:

$$\begin{aligned} & (\lambda_{ik}(G) = l-p) \cap (\lambda_{kj}(G) = p) \cap (\lambda_{ij}(G^{\setminus k}) \geq l) \\ & \cap \phi_j \cap \phi_k \iff (\lambda_{ik}(G^{\setminus \eta(j;p)}) = l-p) \cap (\lambda_{kj}(G) = p) \\ & \cap (\lambda_{ij}(G^{\setminus k}) \geq l) \cap \phi_j \cap \phi_k, \end{aligned} \quad (\text{A14})$$

which is depicted in Fig. 14.

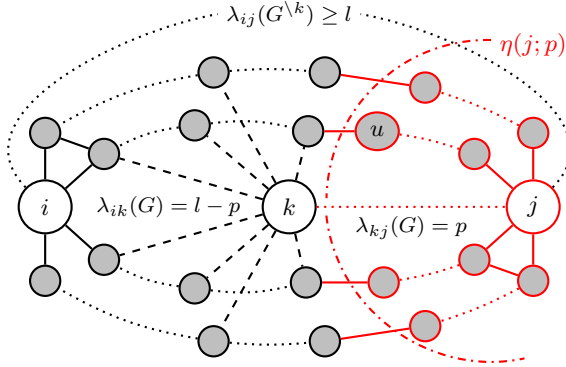


FIG. 14. A schematic depicting the conditioning of the event $\lambda_{ik}(G) = l-p$ on $\lambda_{kj}(G) = p$, $\lambda_{ij}(G^{\setminus k}) \geq l$. Node $u \in \eta(j;p)$ is a node in the set of neighbors of j upto a distance of p to it in $G^{\setminus k}$ (including itself). Analogous to the reasoning for Lemma 1, since the evidence suggests that upon addition of edges of k the shortest path between i and k cannot pass through j or any of its distance- p neighbors, we can ignore the edges of $\eta(j;p)$ from being a part of that shortest path, as indicated in red, and therefore consider the $\eta(j;p)$ -subgraph $G^{\setminus \eta(j;p)}$ instead. Refer to Fig. 13 for figure legend.

Because of conditionally-independent edges, information about the path length between nodes i, j in a graph where k 's edges do not exist asymptotically informs nothing about the path length between nodes i, k in a graph where j 's edges do not exist, and vice-versa:

$$\left(\lambda_{ij}(G^{\setminus k}) \geq l \right) \perp \left(\lambda_{ik}(G^{\setminus \eta(j;p)}) = l-p \right). \quad (\text{A15})$$

Also, the event $\lambda_{kj}(G) = p$ fails to coincide with the event $\lambda_{kj}(G^{\setminus i}) = p$ with a vanishing likelihood in the asymptotic limit.

Therefore, a similar argument can be applied to claim that asymptotically, the geodesic between k, j is independent of (1) the geodesic between i, k in a graph where j 's edges are removed, and of (2) the geodesic between i, j in a graph where k 's edges are removed:

$$(\lambda_{kj}(G) = p) \perp \left(\lambda_{ik}(G^{\setminus \eta(j;p)}) = l-p \right), \quad (\text{A16a})$$

$$(\lambda_{kj}(G) = p) \perp \left(\lambda_{ij}(G^{\setminus k}) \geq l \right). \quad (\text{A16b})$$

Applying the equivalence in Eq. A14 and the independence results in Eqs. A15, A16 to Eq. A13 yields:

$$\begin{aligned} P(B_p | Z, \phi_j, \phi_k) &= P(\lambda_{ik}(G^{\setminus \eta(j;p)}) = l-p | \phi_k, \phi_j) \\ &P(\lambda_{kj}(G) = p | \phi_k, \phi_j). \end{aligned} \quad (\text{A17})$$

To evaluate the first factor of the RHS of Eq. A17, recall the approach for Lemma 1 in Appendix A 1 wherein, asymptotically, the addition of a finite set of nodes $\eta(j)$ back to $G^{\setminus \eta(j)}$ would have made a vanishing difference to the rest of the network. Here, we have the node set $\eta(j;p)$, which will asymptotically be of a finite size for any bounded p . Given that we apply this framework to finite-size networks, this approximation works for small values of p , when the size of $\eta(j;p)$ does not scale with the size of the network n . In such regimes, the approach for Lemma 1 is reasonable—see Appendix A 3. However, for larger values of p of $O(\log n)$, because the probability of a node to be at distance p scales as $O(1)$, the size of $\eta(j;p)$ scales as $O(n)$. Hence, $G^{\setminus \eta(j;p)}$ would be markedly different from the original network G .

Therefore, we pursue a new strategy to estimate $P(\lambda_{ik}(G^{\setminus \eta(j;p)}) = l-p)$, by constructing the geodesic between i, k in $G^{\setminus \eta(j;p)}$ using events defined for G . Let:

$$B_1^u \triangleq \{G \in \Omega | \lambda_{iu}(G) = l-p-1, \lambda_{uk}(G) = 1\}, \quad (\text{A18a})$$

$$X^u \triangleq \{G \in \Omega | \lambda_{uj}(G) > p\}, \quad (\text{A18b})$$

$$W \triangleq \{G \in \Omega | \lambda_{ik}(G) \geq l-p\}. \quad (\text{A18c})$$

Then we can write the equivalence:

$$\left(\lambda_{ik}(G^{\setminus \eta(j;p)}) = l-p \right) \iff W \cap [\exists u (B_1^u \cap X^u)]. \quad (\text{A19})$$

The backward implication of Eq. A19 is seen directly by construction—removal of edges (of nodes in $\eta(j;p)$) cannot reduce the geodesic length between any node pair, and since there exists a node u which is not in $\eta(j;p)$ and forms a geodesic between i, k of length $l-p$, it is retained in the $\eta(j;p)$ -subgraph, therefore maintaining the geodesic between i, k of length $l-p$.

To see the forward implication of Eq. A19, note that if the geodesic between i, k in the $\eta(j;p)$ -subgraph is of length $l-p$, then addition of edges of nodes in $\eta(j;p)$ to construct back G will not reduce the geodesic length between i, k . This is because for all $v \in \eta(j;p)$ we have $\lambda_{iv}(G^{\setminus k}) \geq l-p$ by definition, and since k 's edges can only create paths from i to v of length at least $l-p+1$, this further implies $\lambda_{iv}(G) \geq l-p$. Consequently, addition of

v 's edges cannot create a path between i, k shorter than the existing one, i.e. $\lambda_{ik}(G) = l - p \implies \lambda_{ik}(G) \geq l - p$, i.e. W is true (Eq. A18c). It also follows that there must exist some node $u \notin \eta(j; p)$ which is the penultimate node in the path between i, k in the subgraph, i.e. $\lambda_{iu}(G \setminus \eta(j; p)) = l - p - 1$, and since $\lambda_{ij}(G \setminus k) \geq l$, we have $\lambda_{uj}(G \setminus k) > p$. Since the addition of k 's edges can only create paths from u to j of length at least $p + 1$, this further implies that $\lambda_{uj}(G) > p$, i.e. X^u is true (Eq. A18b). Finally, we note that the reconstruction of G cannot build a shorter path between i, u or u, k than the ones which already exist, i.e. B_1^u is true (Eq. A18a). Altogether, it follows that $W \cap (\exists u B_1^u \cap X^u)$, which is the RHS of Eq. A19.

From the equivalence in Eq. A19, we obtain:

$$\begin{aligned} (\lambda_{ik}(G \setminus \eta(j; p)) = l - p) &\iff W \cap \neg [\exists u (B_1^u \cap X^u)] \\ &\iff W \cap \neg [\forall u \neg (B_1^u \cap X^u)], \end{aligned}$$

which leads to:

$$\begin{aligned} P(\lambda_{ik}(G \setminus \eta(j; p)) = l - p | \phi_k, \phi_j) &= \frac{P(\lambda_{ik}(G \setminus \eta(j; p)) = l - p | \phi_j)}{P(\phi_k)} \\ &= \frac{P(W | \phi_j)}{P(\phi_k)} P(\neg [\forall u \neg (B_1^u \cap X^u)] | W, \phi_j). \end{aligned} \quad (\text{A20})$$

Consider the second factor on the RHS of Eq. A20:

$$\begin{aligned} P(\neg [\forall u \neg (B_1^u \cap X^u)] | W, \phi_j) &= 1 - P(\forall u \neg (B_1^u \cap X^u) | W, \phi_j) \\ &= 1 - \prod_{u \neq (i, j, k)} P(\neg (B_1^u \cap X^u) | W, \phi_j) \\ &= 1 - \exp \left(\sum_{u \neq (i, j, k)} \log(1 - P(B_1^u \cap X^u | W, \phi_j)) \right), \end{aligned} \quad (\text{A21})$$

where in the second equality we use the asymptotic approximation that for any two nodes $u \neq v$ we have negligible correlation between $\neg(B_1^u \cap X^u)$ and $\neg(B_1^v \cap X^v)$ given W . From Eqs. A18c, A20 and A21, we obtain:

$$\begin{aligned} P(\lambda_{ik}(G \setminus \eta(j; p)) = l - p | \phi_k, \phi_j) &= \frac{P(\lambda_{ik}(G) \geq l - p)}{P(\phi_k)} \\ &\left[1 - \exp \left(\sum_{u \neq (i, j, k)} \log(1 - f_{ijk}(u; p, l)) \right) \right] \end{aligned} \quad (\text{A22})$$

where we define:

$$\begin{aligned} f_{ijk}(u; p, l) &\triangleq P(B_1^u \cap X^u | W, \phi_j) = P(\lambda_{iu} = l - p - 1, \\ &\lambda_{uk} = 1, \lambda_{uj} > p | \lambda_{ik} \geq l - p, \phi_j), \end{aligned} \quad (\text{A23})$$

where, because we are only concerned with the full graph G , we drop it from the notation for clarity. Substituting

Eq. A22 into Eq. A17, we obtain the RHS of Eq. A3 in Lemma 2.

Finally, write the RHS of Eq. A23 as:

$$\begin{aligned} &P(\lambda_{uj} > p | \lambda_{iu} = l - p - 1, \lambda_{uk} = 1, \lambda_{ik} \geq l - p, \phi_j) \\ &\times P(\lambda_{iu} = l - p - 1, \lambda_{uk} = 1 | \lambda_{ik} \geq l - p) \\ &= P(\lambda_{uj} > p | \phi_u, \phi_j) P(\lambda_{iu} = l - p - 1) P(A_{uk} = 1), \end{aligned} \quad (\text{A24})$$

where in the last equality we apply Lemma 1 to the second factor, and for the first factor we apply an asymptotic approximation: u forming a geodesic between i, k is uninformative about the geodesic length between u, j , except for supplying the knowledge that u is on the giant component, i.e. ϕ_u (recall that we have suppressed the conditioning on ϕ_i). Rearranging Eq. A24 yields Eq. A4 in Lemma 2. \square

3. Approximate l, p -bridging probability

We next prove Lemma 3, which approximates the bridging probability in a manner that is tight for shorter lengths in finite-size networks. The proof follows similarly to that for Lemma 2 in Appendix A 2, up until Eq. A17. Then, to define the probability of $\lambda_{ik}(G \setminus \eta(j; p)) = l - p$, we follow the same approach as for Lemma 1 in Appendix A 1. For p smaller than $O(\log n)$, $\eta(j; p)$ scales as $O(1)$. Asymptotically, addition of edges of a finite number of nodes in $\eta(j; p)$ creates no difference to the rest of the network in the asymptotic limit, i.e. $P(\lambda_{ik}(G \setminus \eta(j; p)) = l - p | \phi_k, \phi_j) \approx P(\lambda_{ik}(G) = l - p | \phi_k, \phi_j) = P(\lambda_{ik}(G) = l - p | \phi_k)$. Then putting in Eq. A17 yields $P(B_p | Z, \phi_j, \phi_k) \approx P(\lambda_{ik}(G) = l - p | \phi_k) P(\lambda_{kj}(G) = p | \phi_k, \phi_j)$. When plugged into Eq. A12 we obtain:

$$\begin{aligned} &P(\lambda_{ik} = l - p, \lambda_{kj} = p, \lambda_{ij} = l | \phi_j, \phi_k) \approx \\ &P(\lambda_{ik} = l - p | \phi_k) P(\lambda_{kj} = p | \phi_k, \phi_j) P(\lambda_{ij} \geq l | \phi_j), \end{aligned}$$

which is the RHS of Eq. A5 in Lemma 3. This completes the proof.

Appendix B: Connection probability on the giant component

From Sec. II, the initial condition for the recursive equations to derive the SPLD between node i, j in an undirected setting is given by $P(A_{ij} = 1 | \phi_i)$. Here, we show how this conditional likelihood of an edge relates to its marginal likelihood.

Lemma 4 (Connection probability on the giant component). *For nodes i, j , assuming $P(\phi_i) > 0$:*

$$P(A_{ij} = 1 | \phi_i) = P(A_{ij} = 1) \left\{ 1 + \left[\frac{1}{P(\phi_i)} - 1 \right] P(\phi_j) \right\}.$$

Proof. Consider generating the network edges in some order, such that the edge between i, j is generated last of all, without loss of generality (because we consider conditionally independent edge models). We focus on estimating $P(A_{ij} = 1, \phi_i, \phi_j)$. In the asymptotic limit, considering a network with a missing edge should make vanishing difference to the likelihood of a node belonging to the giant component, and to the correlation of two nodes belonging to the giant component. Since edges are added independently of one another, we consider four independent scenarios corresponding to whether i, j were on the giant component before adding the edge between them. In particular, the addition of an edge between i and j can make both nodes belong to the giant component if ϕ_i but $\neg\phi_j$ —with probability $P(\phi_i)[1 - P(\phi_j)]$ —or vice-versa—with probability $P(\phi_j)[1 - P(\phi_i)]$. If the nodes were already on the giant component prior to adding the edge—with probability $P(\phi_i)P(\phi_j)$ —then addition of an edge retains that. Finally, if the nodes were previously not on the giant component, then the addition of an edge will *not* put them on the giant component. Consequently, exploiting the independence arguments above, we have

$$P(A_{ij} = 1, \phi_i, \phi_j) = P(A_{ij} = 1) \times [P(\phi_i) + P(\phi_j) - P(\phi_i)P(\phi_j)].$$

Also, we can write

$$P(A_{ij} = 1, \phi_i, \phi_j) = P(\phi_j|A_{ij} = 1, \phi_i)P(A_{ij} = 1|\phi_i)P(\phi_i) = P(A_{ij} = 1|\phi_i)P(\phi_i),$$

since $(A_{ij} = 1) \cap \phi_i \implies \phi_j$, i.e. $P(\phi_j|A_{ij} = 1, \phi_i) = 1$. Substituting the value derived for $P(A_{ij} = 1, \phi_i, \phi_j)$ from above then gives us the desired expression. \square

Thus, to fix the initial condition for the SPLD, we need to compute percolation probability $P(\phi_i)$ i.e. the likelihood of being on the giant component for all nodes of the network. However, under some circumstances, we need not compute $P(\phi_i)$. In particular, from Lemma 4, it is evident that in the case where (1) i is very likely to percolate i.e. $P(\phi_i) \rightarrow 1$, or when (2) j is very likely to *not* percolate i.e. $P(\phi_j) \rightarrow 0$, then we have $P(A_{ij} = 1|\phi_i) \rightarrow P(A_{ij} = 1)$, i.e. the conditional and marginal likelihoods coincide. When (3) both i and j are very likely to not percolate then $P(A_{ij} = 1|\phi_i) \rightarrow P(A_{ij} = 1) \left[1 + \frac{P(\phi_j)}{P(\phi_i)}\right]$. If the ratio of percolating likelihoods is known, then the initial condition is also known. For instance, in an ER graph where every node is equivalent, we have in the just-supercritical regime: $P(\phi_i) = P(\phi_j) \rightarrow 0$, and obtain $P(A_{ij} = 1|\phi_i) \rightarrow 2P(A_{ij} = 1)$. Thus, we need to compute the likelihood of percolating to compute the initial condition in intermediate settings of percolation. We remark that we can also derive the likelihood of an edge when the node is *not* percolating: $P(A_{ij} = 1|\neg\phi_i) = \frac{P(A_{ij}=1, \neg\phi_i)}{P(\neg\phi_i)} = \frac{P(A_{ij}=1) - P(A_{ij}=1, \phi_i)}{1 - P(\phi_i)}$. Then using Lemma 4 we get:

$$P(A_{ij} = 1|\neg\phi_i) = P(A_{ij} = 1)[1 - P(\phi_j)]. \quad (\text{B1})$$

In Fig. 15, we show how the expected degree varies for percolating and non-percolating nodes, for connectives above the percolation threshold of mean degree $d = 1$ [23].

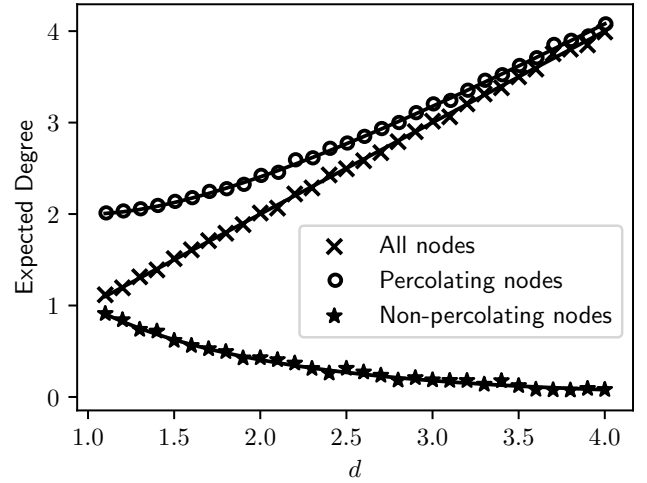


FIG. 15. Expected degree of nodes in the whole network (\times), on the giant component (\circ), and *not* on the giant component (\star) for ER graphs with varying mean connectivity. Network size is fixed at $n = 1024$, while mean degree varies from $d \in [1.1, 4]$. Lines indicate analytics corresponding to the likelihood of connection between two nodes i, j — $P(A_{ij} = 1)$, $P(A_{ij} = 1|\phi_i)$ from Lemma 4 and $P(A_{ij} = 1|\neg\phi_i)$ from Eq. B1, respectively—scaled by n for interpretation as mean degree, while symbols indicate empirical mean estimates over 10 network samples—standard errors are small and not shown to aid legibility. For graphs with high connectivity, $P(A_{ij} = 1|\phi_i) \rightarrow P(A_{ij} = 1)$, while for those with low connectivity, $P(A_{ij} = 1|\phi_i) \rightarrow 2P(A_{ij} = 1)$.

For directed networks, we must define the event ϕ_{ij}^- , indicating that node i is on the giant in-component of j . As shown in Appendix E 1, we require the probability $P(A_{ik} = 1|\phi_{ij}^-)$ to supply the initial condition for the recursive equations of the SPLD. This yields a very similar lemma to Lemma 4 for undirected networks.

Lemma 5 (Connection probability to giant in-component(s)). *For nodes i, j, k , assuming $P(\phi_{ij}^-) > 0$:*

$$P(A_{ik} = 1|\phi_{ij}^-) = P(A_{ik} = 1) \times \left\{ 1 + \left[\frac{1}{P(\phi_{ij}^-)} - 1 \right] P(\phi_{kj}^-) \right\},$$

Proof. The proof is very similar to that of Lemma 4. Because we consider conditionally independent edge models, we can generate the network edges in some order, such that the directed edge between i, k is generated last of all, without loss of generality. We first estimate $P(A_{ik} = 1, \phi_{ij}^-, \phi_{kj}^-)$. In the asymptotic limit, considering a network with a missing edge should make vanishing difference to the likelihood of a node belonging to the

giant in-component of j , and to the correlation of two nodes belonging to that giant in-component. Since edges are added independently of one another, we consider the four independent scenarios corresponding to whether i, k were on the giant in-component of j before adding the edge between them. The addition of a directed edge between i and k can make both nodes belong to the giant in-component of j in only 2 of these scenarios: if ϕ_{ij}^- and ϕ_{kj}^- —with probability $P(\phi_{ij}^-)P(\phi_{kj}^-)$ —or ϕ_{kj}^- but $\neg\phi_{ij}^-$ —with probability $P(\phi_{kj}^-)[1 - P(\phi_{ij}^-)]$. Then, exploiting the independence arguments above, we have

$$P(A_{ik} = 1, \phi_{ij}^-, \phi_{kj}^-) = P(A_{ik} = 1)P(\phi_{kj}^-).$$

Similarly, consider the probability of $P(A_{ik} = 1, \phi_{ij}^-, \neg\phi_{kj}^-)$. This can occur in only 1 of the 4 scenarios: if ϕ_{ij}^- and $\neg\phi_{kj}^-$, yielding

$$P(A_{ik} = 1, \phi_{ij}^-, \neg\phi_{kj}^-) = P(A_{ik} = 1)P(\phi_{ij}^-) \left[1 - P(\phi_{kj}^-)\right]$$

Adding both of the above gives us:

$$\begin{aligned} P(A_{ik} = 1, \phi_{ij}^-) &= P(A_{ik} = 1) \\ &\times \left[P(\phi_{ij}^-) + P(\phi_{kj}^-) - P(\phi_{ij}^-)P(\phi_{kj}^-) \right], \end{aligned}$$

which divided through by $P(\phi_{ij}^-)$ gives the desired equation. \square

Appendix C: Finite-size effects in the SPLD

Given that we assume infinite network size to discount correlations in the network, in this section we analyze finite-size effects for the analytic form of the shortest path length distribution, given by the recursive Eq. 12. We first provide a general asymptotic argument to intuit how the probability mass of a node to be at distance l from a given node scales with network size n . Then, we invoke the approximate closed-form of the SPLD obtained in Eq. 46 of Sec. III to show when this scaling holds, and when it does not, for finite-size networks in the supercritical and subcritical regimes. Finally, we describe how finite-size effects manifest in the analytic form of the SPLD.

Node degrees and sparsity. In Sec. II, we gave the expectation of degree of a given node. In this work, we assume that the network is sparse in the sense that nodes have a bounded expected degree of $O(1)$ asymptotically, as $n \rightarrow \infty$. From Eq. 4, it is then sufficient that $\forall(i, j), \langle A \rangle_{ij} = O(n^{-1})$. (Strictly speaking, it is necessary that the likelihood of an edge is $O(n^{-1})$ almost everywhere, a distinction which becomes more apparent for general models of Sec. III. We further note that our formalism works just as well for a network with self-loops, as long as self-loops are also added sparsely. That is, the chance of a self-loop for any given node is $O(n^{-1})$, and so we can asymptotically ignore self-loops, as we do

here.) We remark that since edges are added independently, the (in-/out-)degree distribution itself for node i will be a Poisson binomial distribution, which by Le Cam's theorem [112] will asymptotically (as $n \rightarrow \infty$) approach the Poisson distribution, whose mean $\langle d_i^+ \rangle, \langle d_i^- \rangle$ is given by Eqs. 3a, 3b. Evidently, the degree distribution for the whole network will be a mixture of Poisson distributions, whose expectation $\langle d \rangle$ is given by Eq. 4.

Asymptotic scaling behaviour of shortest path lengths in sparse networks. Since the network is sparse, probability of two nodes i, j connecting is $O(n^{-1})$. If the nodes have a shortest path of length 2, then (1) they are not directly connected with a likelihood of $1 - O(n^{-1}) = O(1)$, and (2) they have a path of length-2 between them. Consider a node k which forms this length-2 ‘‘bridge’’. Since k has an (independent) likelihood of connecting to i or j of $O(n^{-1})$, it connects with both i and j with a likelihood of $O(n^{-2})$. Since there are $O(n)$ such nodes, the chance of a length-2 bridge is $O(n^{-1})$. Consequently, the likelihood of i and j having a shortest path of length 2 is $O(n^{-1})$. Similarly, if i, j are connected by a length-3 geodesic, then (1) they are not connected by a shorter path with a likelihood of $O(1)$, and (2) they have a path of length-3 between them. Let $\eta(j)$ denote the set of neighbors of j , including itself, and let $k \in \eta(j)$ which may form this length-3 bridge between i, j . For that to be true, k itself must be at a length 2 from i , which we saw above happens with a chance of $O(n^{-1})$. The size of $\eta(j)$ is $O(1)$, i.e. it is bounded due to sparsity. Asymptotically, for two nodes $k, u \in \eta(j)$, it is vanishingly likely for the paths from i to them to coincide. Altogether then, i can reach j via any of its neighbours in 3 hops with a likelihood of $O(n^{-1})$. Then by induction—while assuming asymptotic independence of shortest path from the source node to the neighbors of the target node—it follows that for any *finite* shortest path length l , the probability of two nodes having a shortest path of length l is $O(n^{-1})$ in the asymptotic limit. We emphasize that this argument relies only on sparsity, without assuming anything about the relative probabilities of connection between nodes. That is, it holds regardless of the exact random graph model specification.

The scaling behaviour of shortest path lengths is evident in the expression for the approximate closed-form of the survival function of the SPLD for a general random graph model, as given by Eq. 46, which is asymptotically tight for finite lengths. That is, for nodes x, y :

$$\begin{aligned} P(\lambda_{xy} > l) &= \exp\left(-\frac{1}{n} \sum_{i=1}^N S_l(\tau_i) \varphi_i(x) \varphi_i(y)\right) \\ &\approx 1 - \frac{1}{n} \sum_{i=1}^N S_l(\tau_i) \varphi_i(x) \varphi_i(y) \\ \implies P(\lambda_{xy} = l) &\approx \frac{1}{n} \sum_{i=1}^N \tau_i^l \varphi_i(x) \varphi_i(y) = O(n^{-1}), \end{aligned} \tag{C1}$$

where the first approximation uses a first-order expansion of the exponential, and in the second equality we use $P(\lambda_{xy} = l) = P(\lambda_{xy} > l - 1) - P(\lambda_{xy} > l)$, and the definition of $S_l(a) \triangleq a + a^2 + \dots + a^l$ as the geometric sum of a starting at a up to l terms.

Finite-size effects in the supercritical regime. However, when we begin to consider longer geodesics which scale with the network size n , then we can expect deviations between analytics and empirics in the supercritical regime, due to finite-size effects. If length $l = c \log n$ for some $c > 0$, then from Eq. C1 we obtain

$$P(\lambda_{xy} = l) = O(n^{c \log \tau_1 - 1}), \quad (\text{C2})$$

where τ_1 is the largest eigenvalue. If $\tau_1 > 1$, which from Theorem 2 implies the supercritical regime and vice-versa, then the likelihood of two nodes having a shortest path of length l does not scale as $O(n^{-1})$, and for $c \geq (\log \tau_1)^{-1}$ can scale as $O(n^\epsilon)$ where $\epsilon \geq 0$. Consequently, at such geodesic lengths, we can expect non-vanishing correlations between different geodesics connecting the source and target nodes. To appreciate these finite-size effects, consider the simplest graph model, of an ER graph with mean degree $\langle d \rangle > 1$. From Eq. 56, we know that the approximate closed-form of the survival function of distribution of shortest path lengths λ is a discrete version of the Gompertz distribution, i.e. $P(\lambda > l) = \exp(-a(e^{bl} - 1))$, where $a \triangleq \frac{\langle d \rangle}{n(\langle d \rangle - 1)}$ and $b \triangleq \log \langle d \rangle$. Consequently, this distribution has a mode around $l = \frac{\log \frac{n(\langle d \rangle - 1)}{\langle d \rangle}}{\log \langle d \rangle} = O\left(\frac{\log n}{\log \langle d \rangle}\right)$. Therefore, the finite-size effects should become apparent around the mode of the SPLD.

We plot the error in the analytic (Eqs. 12, 13, and 17) and approximate analytic forms (Eqs. 12 and 16) of the SPLD for an ER graph with $\langle d \rangle = 2$ in Fig. 16, and note that the error in the probability mass function (PMF) stays negligible for short geodesics, but eventually rises to its largest at the analytic mode of the SPLD i.e. where $l = O(\log n)$, regardless of network size—see top row in Fig. 16. However, non-zero errors become more concentrated around the mode as network size is increased, and consequently the absolute error when averaged over the support of the distribution decreases as network size increases—see bottom row in Fig. 16. Notably, we observe that the error in the cumulative distribution function (CDF) as $l \rightarrow \infty$, which is indicative of the size of the giant component, tends to vanish with network size, for both the analytic and approximate analytic forms of the SPLD—see middle row in Fig. 16, and Fig. 17. This implies that while the analytic form marginally overestimates the probability mass around the mode, it compensates for it by commensurately underestimating probability mass elsewhere. In particular, while the analytic form shifts mass away from longer geodesic lengths, the approximate analytic form appears to pull it from either sides of the mode—see top row in Fig. 16.

Subcritical regime. We now consider the subcritical regime, wherein the shortest path between source and

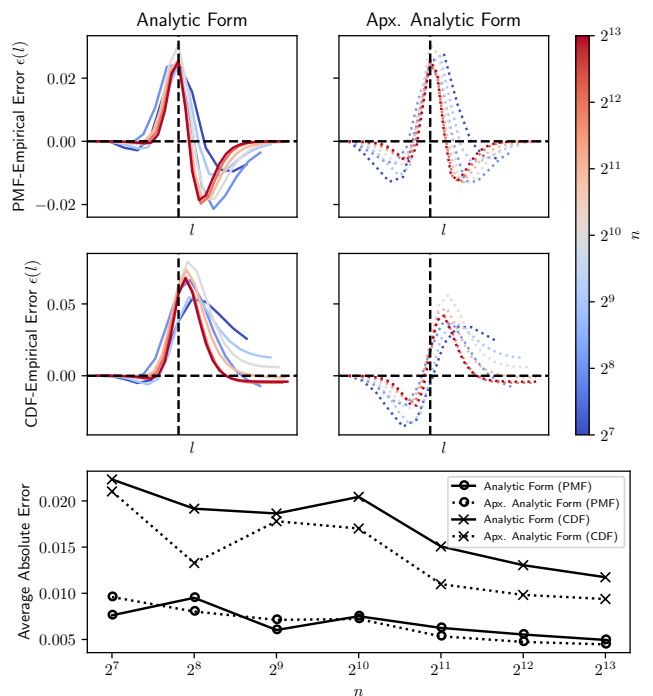


FIG. 16. Average error in analytic and approximate analytic forms of shortest path length distribution vanishes asymptotically. For an ER graph with fixed mean degree $\langle d \rangle = 2$ and varying network size $n \in \{2^7, 2^8, 2^9, 2^{10}, 2^{11}, 2^{12}, 2^{13}\}$, the empirical error is computed by subtracting the (top row) empirical PMF and (middle row) CDF over 10 samples from the respective (left column) analytic and (right column) approximate analytic forms of the SPLD. We remark that error bars are omitted for clarity, and the support of the distribution is scaled by its analytic mode—marked by the vertical dotted line—to aid comparison across network sizes. Bottom row shows the absolute empirical error averaged over the distribution support. Average errors decrease for larger network sizes for either analytic forms of the SPLD.

target nodes cannot pass via nodes on a giant component. From Theorem 2, $\tau_1 \leq 1$ in the subcritical regime, which from Eq. C2 implies that the likelihood of two nodes having a shortest path of length $l = O(\log n)$ scales as $O(n^{-1-\epsilon})$, where $\epsilon \geq 0$. Therefore asymptotically, even when considering geodesic lengths that scale with the network size, the correlations between shortest paths should remain vanishingly small in the subcritical regime, and we expect to observe vanishing finite-size effects. This is evident in Fig. 18 for the SPLD in subcritical ER graphs, and in Fig. 19 for the SPLD in a subcritical bipartite SBM.

Appendix D: Percolation behaviour and the SPLD

In this section, we detail the relationship between percolation behaviour and the distribution of shortest path lengths. In particular, we show that a giant component

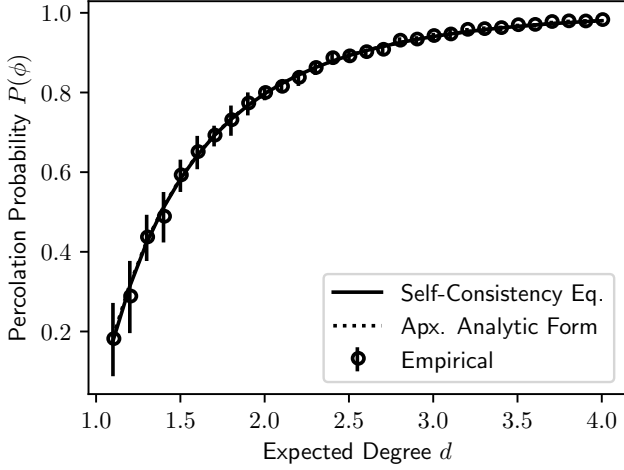


FIG. 17. Percolation probabilities derived from the self-consistency equation agree with estimates derived from the limiting value of the approximate analytic shortest path length distribution. Network size is fixed at $n = 1024$, while mean degree of the ER graph varies from $\langle d \rangle \in [1.1, 4]$. Solid and dotted lines indicate analytic solutions derived from Eq. 17 and Eqs. 12, 14, 15 respectively, while symbols and bars indicate empirical estimates: mean and standard error over 10 network samples. There is good agreement between all three for varying levels of connectivity and therefore percolation probabilities.

exists if and only if asymptotically the closed-form conditional PMF of the SPLD, in Eq. 38a, grows unbounded with the geodesic length l (Theorem 1), and that this is equivalent to the largest absolute eigenvalue of the integral operator T , in Eq. 40, is greater than unity (Theorem 2). For the corresponding result for asymmetric kernels, we refer the reader to Appendix E2b.

1. Geodesic and spectral conditions for percolation

We first restate and prove Theorem 1.

Theorem (Geodesic condition for percolation). *Consider a network with n nodes in V . Let $\underline{\omega}_l(x, y; n)$ be the closed-form of the conditional PMF of the SPLD between nodes at $x, y \in V$, as given by Eq. 38a, where we make explicit the dependence on network size n . Then in the asymptotic limit, a giant component does not exist if and only if $\forall x, y \in V : \lim_{n \rightarrow \infty} \limsup_{l \rightarrow \infty} \underline{\omega}_l(x, y; n) = 0$.*

Proof. First, we show the forward implication that if a giant component does not exist, then $\forall x, y \in V : \lim_{n \rightarrow \infty} \limsup_{l \rightarrow \infty} \underline{\omega}_l(x, y; n) = 0$, via contraposition. Suppose $\exists x, y \in V$ such that $\lim_{n \rightarrow \infty} \limsup_{l \rightarrow \infty} \underline{\omega}_l(x, y; n) \neq 0$. Due to non-negativity of the kernel, the possible initial conditions $\omega_1(x, y; n)$ from Eqs. 37, B1, or 45 must be non-negative, and therefore $\underline{\omega}_l(x, y; n)$ as defined in Eq. 38a

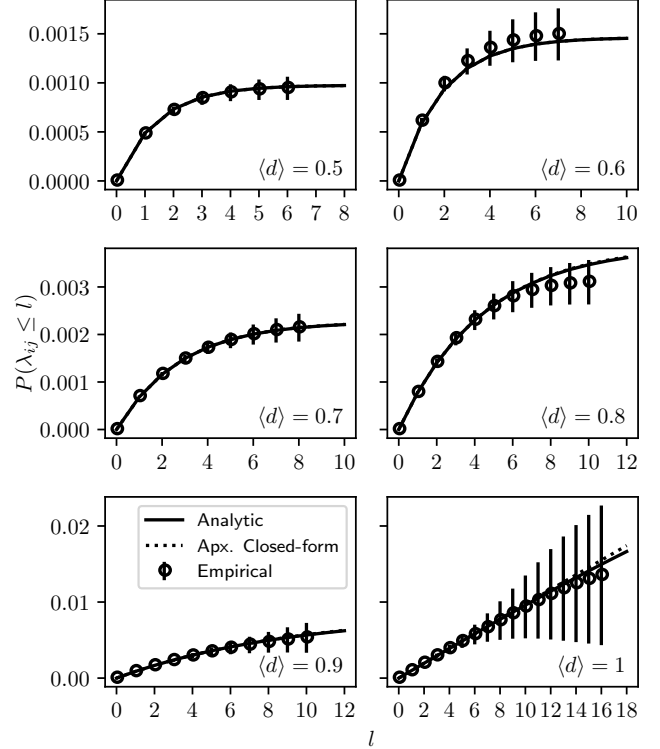


FIG. 18. Empirical, analytic and (approximate) closed-form CDF of shortest path lengths on the small components in the subcritical regime, for an ER graph with varying connectivity. Network size is fixed at $n = 1024$, while mean degree varies as $\langle d \rangle \in \{0.5, 0.6, 0.7, 0.8, 0.9, 1\}$. Solid and dotted lines indicate analytic (Eqs. 12, 16) and (approximate) closed-form solutions (Eqs. 16, 29), respectively. Symbols and bars indicate empirical estimates: mean and standard error over 10 network samples. Both the analytic and (approximate) closed-form SPLD are in good agreement for all subcritical connectivities at all geodesic lengths.

must be non-negative. This leads us to only consider $\lim_{n \rightarrow \infty} \limsup_{l \rightarrow \infty} \underline{\omega}_l(x, y; n) > 0$. We consider three mutually exclusive and exhaustive scenarios under which we can interpret $\underline{\omega}_l(x, y; n)$. If a giant component exists, then the function $\underline{\omega}_l(x, y; n)$ defines the closed-form of the conditional PMF of the SPLD for a source node at x either when (1) the node is on the giant component (with the initial condition in Eq. 37), or when (2) the node is on a small component (with the initial condition in Eq. B1). If a giant component *does not* exist, then (3) the function $\underline{\omega}_l(x, y; n)$ defines the closed-form of the conditional PMF of the SPLD for a source node at x (with the initial condition in Eq. 45) which can only be on a small component. Considering scenarios (1) and (2) entails assuming that the giant component exists, and we obtain the contraposition by tautology. Consider scenario (3), that the giant component does not exist, and the node at x is on a small component. Asymptotically, the target node at y is on a different (small) component with high proba-

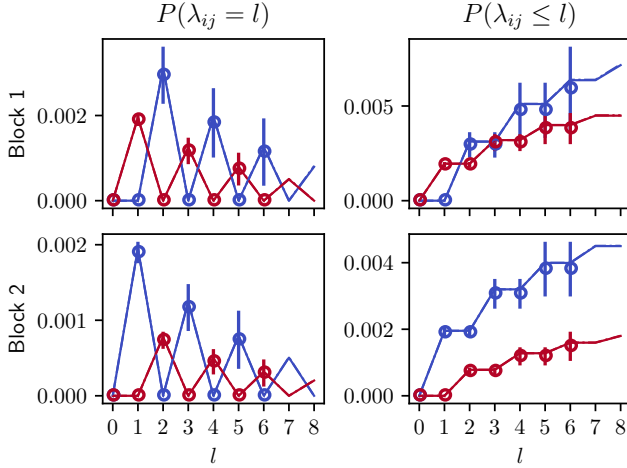


FIG. 19. Empirical, analytic, and (approximate) closed-form CDF of shortest path lengths on the small components in the subcritical regime agree with each other for a bipartite SBM, with block matrix $B = \begin{pmatrix} 0 & 2 \\ 2 & 0 \end{pmatrix}$, distribution vector $\pi = (0.2, 0.8)$, and $n = 1024$. Rows correspond to the block membership of source node. Left column depicts the PMF, and the right column depicts the CDF. Solid lines represent analytic form using Eqs. 53, while dotted lines represent (approximate) closed-form using Eq. 55. Symbols and bars indicate empirical estimates: mean and standard error over 10 network samples.

bility, and arguments for deriving the closed-form of the conditional PMF in Sec. IID will hold for the *entire* support of the SPLD on a small component: $\underline{\omega}_l(x, y; n)$ is a tight bound on the conditional PMF of SPLD on a small component for *all* values of l . Therefore, the function $f(n) \triangleq \limsup_{l \rightarrow \infty} \underline{\omega}_l(x, y; n)$ indicates the (largest) limiting probability of the shortest path length to be l , given that it is longer than $l - 1$, as $l \rightarrow \infty$. The given limit $\lim_{n \rightarrow \infty} f(n) > 0$ suggests that $\exists \epsilon \in \mathbb{R}_{>0}$ such that $\forall N, \exists n > N$ such that $f(n) \geq \epsilon$: we can increase the network size arbitrarily, and there is always a larger network of size n for which $f(n)$ is bounded from below by a positive value. But asymptotically, the conditional PMF of the SPLD on a small component should vanish for longer path lengths, and therefore scenario (3) does not hold. Instead, $\underline{\omega}_l(x, y; n)$ must define the SPLD for when x is on the giant component, and therefore a giant component exists, and scenario (1) holds.

Next, we show the backward implication that $\forall x, y \in V : \lim_{n \rightarrow \infty} \limsup_{l \rightarrow \infty} \underline{\omega}_l(x, y; n) = 0$ implies that a giant component does not exist, via contradiction. Suppose that a giant component indeed exists, and $\forall x, y \in V : \lim_{n \rightarrow \infty} \limsup_{l \rightarrow \infty} \underline{\omega}_l(x, y; n) = 0$. We consider a node at x that is on the giant component, and another node at y for which it is given that $\lim_{n \rightarrow \infty} \limsup_{l \rightarrow \infty} \underline{\omega}_l(x, y; n) = 0$. The limit as $n \rightarrow \infty$ implies $\forall \epsilon \in \mathbb{R}_{>0}, \exists N \in \mathbb{N}$ such that $\forall n > N : \limsup_{l \rightarrow \infty} \underline{\omega}_l(x, y; n) < \epsilon$. By the

definition of limit superior, we get $\exists L \in \mathbb{N}$ such that $\forall l > L : \underline{\omega}_l(x, y; n) < \limsup_{l \rightarrow \infty} \underline{\omega}_l(x, y; n) + \epsilon \implies \underline{\omega}_l(x, y; n) < 2\epsilon$. It then follows that the network size n can be chosen arbitrarily large to render $\underline{\omega}_l(x, y; n)$ arbitrarily small as $l \rightarrow \infty$. Since a giant component exists, $\underline{\omega}_l(x, y; n)$ can be interpreted as describing the closed-form of the conditional PMF of the SPLD for a node at x either when it is on the giant component, or when it is on one of the small components: scenarios (1) and (2) respectively from above. Because $\underline{\omega}_l(x, y; n)$ can be made vanishingly small as $l \rightarrow \infty$, $\underline{\omega}_l(x, y; n)$ is asymptotically a tight bound on the conditional PMF of the SPLD on the giant component. This implies that the probability of the shortest path length to be l , given that it is longer than $l - 1$, tends to 0. But on a giant component, this probability should increase with l asymptotically. Thus, $\underline{\omega}_l(x, y; n)$ cannot describe the SPLD when the node at x is on the giant component, and scenario (2) holds. Because the given limit holds $\forall x, y$, scenario (2) holds for the SPLD between all node pair locations. It then follows that $\underline{\omega}_l(x, y; n)$ may only describe small components. Since the construction of $\underline{\omega}_l(x, y; n)$ makes use of all available nodes, and yet is able to *describe only small components*, it must be the case that *only small components can exist*. This leads to a contradiction, and thus our supposition that the giant component exists was incorrect. \square

We now restate and prove Theorem 2.

Theorem (Spectral condition for percolation). *Let T be the integral operator related to a symmetric connectivity kernel, as defined by Eq 40, and $r(T)$ be its spectral radius, i.e. the largest absolute value of its eigenvalues. Then, the network has a giant component if and only if $r(T) > 1$, with the phase transition at $r(T) = 1$.*

Proof. First, we show the forward implication that if a giant component exists, then $r(T) > 1$, via contraposition. Let us assume that $r(T) \leq 1$. From Eq. 43, we note for nodes at $x, y \in V$ that the closed-form of the conditional PMF of the SPLD can be written as

$$\underline{\omega}_l(x, y; n) = \sum_{i=1}^N \tau_i(n)^{l-1} g_i(x, y; n), \quad (\text{D1})$$

where $\forall x, y$ we define $g_i(x, y; n) \triangleq \int_V \omega_1(x, z; n) \varphi_i(z; n) \varphi_i(y; n) d\mu(z)$ explicating the dependence on network size n , N is the rank of T , $\{\tau_i\}_{i=1}^N$ are the (real) eigenvalues (in non-increasing order) with corresponding orthonormal eigenfunctions $\{\varphi_i\}_{i=1}^N$ of T . The core idea in this proof is that the limiting properties of $\underline{\omega}_l(x, y; n)$ as $l \rightarrow \infty$ are governed by the largest eigenvalue of T : $\tau_1(n)$. Since the spectral radius is no larger than unity, all eigenvalues must be less than or equal to unity in their absolute values. From Eq. D1, $\forall x, y : \limsup_{l \rightarrow \infty} \underline{\omega}_l(x, y; n) < \infty \implies \lim_{n \rightarrow \infty} \limsup_{l \rightarrow \infty} \underline{\omega}_l(x, y; n) = 0$. From Theorem 1, this condition implies that a giant component does not

exist. Thus, if the network has a giant component, then $r(T) > 1$.

Next, we show the backward implication that if $r(T) > 1$, then a giant component exists, via contradiction. Suppose that the network does not contain a giant component. From Theorem 1, this implies that $\forall x, y : \lim_{n \rightarrow \infty} \limsup_{l \rightarrow \infty} \underline{\omega}_l(x, y; n) = 0$. In the proof for Theorem 1, we noted that these limits imply: $\forall \epsilon \in \mathbb{R}_{>0}, \exists N \in \mathbb{N}, \exists L \in \mathbb{N}$ such that $\forall n > N, \forall l > L$ we have $\underline{\omega}_l(x, y; n) < 2\epsilon$. We suppress the conditioning on n from hereon, because it suffices to state that asymptotically the sequence $\underline{\omega}_l(x, y)$ must have a limit as $l \rightarrow \infty$. Since T is compact, it is either of finite rank (N is finite), or the limit of finite rank operators ($\lim_{i \rightarrow \infty} \tau_i(n) = 0$), implying that the RHS of Eq. D1 is finite for finite l . Then for the RHS of Eq. D1 to converge $\forall x, y$ to a finite value as $l \rightarrow \infty$, it is necessary that either (1) $\forall x, y \in V, \forall i \in \{1, 2, \dots, N\} : g_i(x, y) = 0$, or (2) all of the eigenvalues are no larger than unity in their absolute value, or (3) they exist in pairs (τ_i, τ_j) such that $|\tau_i| > 1, |\tau_j| > 1$ and $\forall x, y : \lim_{l \rightarrow \infty} \tau_i^{l-1} g_i(x, y) + \tau_j^{l-1} g_j(x, y) = 0$, i.e. they precisely cancel each others contributions. Scenario (1) can only hold for the trivial zero eigenfunction, and therefore is out of consideration. Let us consider scenario (3), which must require that $\lim_{l \rightarrow \infty} \tau_i^{l-1} = \lim_{l \rightarrow \infty} \tau_j^{l-1} \implies \tau_i = \tau_j$ and $g_i(x, y) = -g_j(x, y)$. We know that T is a non-negative (compact) operator, since the connectivity kernel is non-negative. In particular, if it is positive, i.e. the likelihood of connection between any node pair cannot be precisely 0, then we can apply a generalization of Perron's theorem to positive compact operators. That is, $r(T) > 0$ and is itself an eigenvalue with multiplicity 1 [113, 114]. This implies that there cannot be another eigenvalue which it can be paired with, and therefore scenario (3) is invalidated. If T is non-negative but irreducible, i.e. even if the likelihood of connection between a node pair is 0 but there is a non-zero chance of having a path between them, we can apply Perron-Frobenius theorem [114, 115]. Following this, there can be h eigenvalues of T with the same absolute value $r(T)$, where h is the period of T and each of these eigenvalues is given by a product of $r(T)$ with an h^{th} root of unity. For a symmetric kernel, h can be 1—in which case the largest eigenvalue τ_1 is unique and its pair cannot exist—or 2—in which case too the pair does not exist since the other eigenvalue is given by $-\tau_1$. Thus again, (3) does not hold. Therefore, for T that is positive, or irreducible non-negative, the only condition for non-percolation must be (2), i.e. all eigenvalues are less than or equal to unity in their absolute value. It then follows that $r(T) \leq 1$.

We are yet to consider the case when T is reducible, i.e. there exists a partitioning of the node space V into “connected” subspaces $\{V_1, V_2, \dots\}$ such that the likelihood of a path existing between different subspaces is zero. For instance, in a perfectly homophilous SBM with a diagonal block matrix, the blocks define an exact partitioning with no inter-block edges. Consequently, each of

these subspaces must correspond either to an irreducible operator—where for any two nodes in V_i there is a non-zero likelihood of a path between them—or to the null operator—where for any two nodes in V_i there is zero likelihood of them to connect. This permits an expression for T as the direct sum of (countably many) compact irreducible or null operators: $T = T_1 \oplus T_2 \oplus \dots$ corresponding to each of the node subspaces. In a finite-dimensional setting, this is equivalent to expressing T as a block diagonal matrix. For the network to not have a giant component, none of these node subspaces may contain a giant component. From the above proof for irreducible operators, and noting that for the null operator the spectral radius is 0, we get the condition that $\max(r(T_1), r(T_2), \dots) \leq 1$. Since the spectrum of T is given by the union of spectra of each T_i , we obtain $r(T) \leq 1$. \square

For other analyses, it is useful to observe the following corollary of Theorem 1.

Corollary 1.1 (Percolation condition using approximate closed-form of the conditional PMF of the SPLD). *Consider a network with n nodes in V , and connectivity kernel ν . Let $\tilde{\omega}_l(x, y; n)$ be the approximate closed-form of the conditional PMF of the SPLD between $x \in V$ and $y \in V$, as given by Eq. 38a with the initial condition $\tilde{\omega}_1 = \nu$. Then in the asymptotic limit, a giant component does not exist if and only if $\forall x \in V, \forall y \in V : \lim_{n \rightarrow \infty} \limsup_{l \rightarrow \infty} \tilde{\omega}_l(x, y; n) = 0$.*

Proof. Recall that the approximate closed-form of the conditional PMF differs from the closed-form only in its initial condition. Considering nodes x, y , the initial condition for the closed-form is given from Eq. 37 by $c \triangleq \nu(x, y) \left\{ 1 + \left[\frac{1}{\rho(x)} - 1 \right] \rho(y) \right\}$, and for the approximate closed-form by $\tilde{c} \triangleq \nu(x, y)$. Since the percolation probability $\rho(\cdot)$ is the asymptotic likelihood of being on the giant component, it is independent of network size n and geodesic length l . Also, $c = 0$ iff $\tilde{c} = 0$. Therefore, the limit value of the closed-form of the conditional PMF is strictly zero iff the limit value of the *approximate* closed-form is strictly zero: $\lim_{n \rightarrow \infty} \limsup_{l \rightarrow \infty} \underline{\omega}_l(x, y; n) = 0 \iff \lim_{n \rightarrow \infty} \limsup_{l \rightarrow \infty} \tilde{\omega}_l(x, y; n) = 0$. In other words, the geodesic condition for percolation applies just as well to the approximate closed-form of the distribution. \square

We remark that Corollary 1.1 holds just as well for asymmetric kernels, given the analogous initial condition for the closed-form conditional PMF in Eq. E1 of Appendix E1.

2. Percolative partition of node space

In Sec. VIA, we noted that the mean geodesic length in a network can be computed only after conditioning on the giant component. In the general random graph

framework of Sec. III, it could happen that the node space V has some node subspaces which percolate—and need to be marginalized over when computing the mean geodesic length—and some that do not percolate—and must be ignored. In this section, we define a “percolative partition” of the node space into disconnected subspaces which percolate separately from each other. This allows us to estimate statistics like the mean geodesic length in Eq. D2 by marginalizing separately over each subspace.

Theorem 3 (Percolative partition of node space). *Consider a network in the general random graph model of Sec. III, in a node space V , and let $\underline{\psi}_l(x, y)$ be the closed-form survival function of the distribution of geodesic lengths between nodes $x \in V, y \in V$, as defined in Eq. 38b. Then asymptotically, there exists a countable partition of $V = V_0 \cup \bigcup_{i=1}^m V_i$ such that all of the following conditions hold:*

Disjoint: $V_i \cap V_j = \emptyset$,

Disconnected: $\forall x \in V_i, \forall y \in V_j: \lim_{l \rightarrow \infty} \underline{\psi}_l(x, y) = 1$,

Subcritical: $\forall x, y \in V_0: 1 > \lim_{l \rightarrow \infty} \underline{\psi}_l(x, y) > 0$,

Supercritical: $\forall i > 0, \forall x, y \in V_i: \lim_{l \rightarrow \infty} \underline{\psi}_l(x, y) = 0$.

We remark that it is possible that (a) $V_0 = \emptyset$, when only supercritical subspace(s) exist i.e. $V = \bigcup_{i=1}^m V_i$, or that (b) $V_0 = V$, when no supercritical subspace(s) exist.

Proof. We pursue a proof by construction. Let T be the compact self-adjoint integral operator for the network model, as defined by Eq 40. If T is reducible, then it can be expressed as a direct sum of (countably many) compact irreducible operators $T = \bigoplus_{i=1}^m T_i$, each acting on disjoint node subspaces V_1, V_2, \dots, V_m , such that the likelihood of a path of any finite length between a node at $x \in V_i$, and a node at $y \in V_j$ ($i \neq j$), is 0. It then follows that $\nexists z \in V$ such that there might exist a path of finite length between the node at x and a node at z , and the node at z may be directly connected to the node at y . This yields from Eq. 38 that $\forall x \in V_i, \forall y \in V_j, \forall l \in \mathbb{Z}_{\geq 0} : \underline{\psi}_l(x, y) = 1$. Therefore, $\lim_{l \rightarrow \infty} \underline{\psi}_l(x, y) = 1$, which gives the “disconnected” condition.

Consider the irreducible operator T_i acting on V_i . (If T itself is irreducible, then consider T acting on V .) If $r(T_i) < 1$, then collect all such operators via a direct sum into T_0 , and their corresponding node subspaces via a disjoint union into V_0 . Since the spectra of T is given by the union of spectra of each of the collected operators, we have $r(T_0) < 1$. Since no giant component exists in V_0 , from arguments in the proof for Theorem 1 we know that $\forall x \in V_0, \forall y \in V_0$ it follows that $\limsup_{l \rightarrow \infty} \underline{\omega}_l(x, y) < \infty$. From Eq. 38b, we obtain $\lim_{l \rightarrow \infty} \underline{\psi}_l(x, y) > 0$, which gives the “subcritical” condition.

Finally, if $r(T_i) > 1$, then from Theorem 2 nodes in V_i must form a giant component, making it a “supercritical subspace”. By the same arguments as in the

proof for Theorem 1, for any two nodes $x \in V_i, y \in V_i$ to be on a giant component implies that asymptotically $\limsup_{l \rightarrow \infty} \underline{\omega}_l(x, y) = \infty$, and thus from Eq. 38b $\lim_{l \rightarrow \infty} \underline{\psi}_l(x, y) = 0$, which gives the “supercritical” condition.

The subspaces V_i are pairwise disjoint, and they are also pairwise disjoint with V_0 , which supplies the “disjoint” condition. This exhausts all scenarios. \square

Estimating the mean geodesic length. Theorem 3 essentially partitions V into a non-percolating subspace V_0 (which may be empty), and disconnected yet separately percolating subspaces $\{V_i\}_{i=1}^m$, such that for any given $i \in \{1, 2, \dots, m\}$ it holds that $\forall x \in V_i, \forall y \in V_i$, the closed-form of the survival function of the SPLD—as defined in Eq. 38b—has a limiting value of zero. (Relatedly, this makes clear why we cannot compute the size of the giant component using the closed-form of the SPLD, since using Eq. 88 for the size of the giant component with the closed form $\underline{\psi}_l(x, y)$ instead of the analytic form $\psi_l(x, y)$ would always yield a giant component of size n in the supercritical regime, as previously mentioned in Sec. IID.) We can now obtain the expected geodesic length from Eq. 107 by marginalizing over the percolating subspaces:

$$\langle \lambda \rangle = \frac{\sum_{i=1}^m \int_{V_i} \int_{V_i} \sum_{l=0}^{\infty} \underline{\psi}_l(x, y) d\mu(x) d\mu(y)}{\sum_{i=1}^m \mu(V_i)^2}, \quad (\text{D2})$$

whose RHS is well-defined. We remark that we can establish a corollary for Theorem 3 in terms of the *approximate* closed-form of the survival function of the SPLD, similarly to obtaining Corollary 1.1 regarding the percolation condition in terms of the *approximate* closed-form of the conditional PMF of the SPLD. That is, Eq. D2 is well-defined when using $\tilde{\underline{\psi}}_l(x, y)$ from Eq. 46 instead of $\underline{\psi}_l(x, y)$ from Eq. 38b.

Asymmetric connectivity kernel. Although the proof for Theorem 3 assumes T is self-adjoint, i.e. a symmetric kernel, an analogous proof follows when we have an asymmetric kernel. In particular, from the formalism of Theorem 4 in Appendix E, if supercriticality is symmetric it follows that the percolating subspaces correspond to the “strongly-connected” subspaces $\{\tilde{V}_i\}_{i=1}^m$, which can then be used to compute average geodesic lengths from Eq. D2.

Appendix E: Directed networks and asymmetric connectivity kernels

As discussed in Sec. II A, there can be non-trivial differences between the undirected and directed setting, because the concept of a “giant component” is more subtle for directed networks. Namely, it is not necessary for a (directed) path to exist from i to j , even if one exists from j to i . This yields two generalizations of the giant component: the set of nodes of size $O(n)$ that are reachable from a node constitute its giant out-component, and

those from which a node can be reached constitute its giant in-component [13, 116]. For directed networks, we say that (i, j) is supercritical if asymptotically there can exist a giant in-component of j such that i is on it, or equivalently if asymptotically there can exist a giant out-component of i such that j is on it. The definition of a subcritical node pair arises via negation. We emphasize that supercriticality is symmetric and transitive in an undirected setting, whereas it is (necessarily) only transitive in a directed setting. Consequently, it is possible for (i, j) and (k, j) to be supercritical, but (i, k) and/or (k, i) to be subcritical.

1. Directed networks: ensemble average model

We consider the SPLD on the in-/out-components of a directed network, first in the supercritical regime for node pair (i, j) . By the same argument as in Sec. II A, without loss of generality, we assume that $\langle A \rangle$ is not permutation similar to a block diagonal matrix. (In the directed setting, this is a weaker condition than $\langle A \rangle$ being irreducible, i.e. permutation similar to a block triangular matrix.) Let ϕ_{ij}^- be the event that node i is on the giant in-component of j (note the explicit dependence on both i, j), and ϕ_{ji}^+ be the event that node j is on the giant out-component of i . Analogous to Eq. 7, we can define the conditional PMF and survival function matrices, but when conditioning on ϕ_{ij}^- instead of ϕ_i . The recursive setup of Sec. II A, and the result in Lemma 1, can be applied verbatim to directed networks. However, the initial condition for the conditional PMF matrix $[\Omega_1]_{ik} = P(A_{ik} = 1 | \phi_{ij}^-)$ will be different. As shown in Lemma 5 in Appendix B, we obtain an initial condition analogous to Eq. 13:

$$P(A_{ik} = 1 | \phi_{ij}^-) = P(A_{ik} = 1) \times \left\{ 1 + \left[\frac{1}{P(\phi_{ij}^-)} - 1 \right] P(\phi_{kj}^-) \right\}, \quad (\text{E1})$$

where we remark that $P(\phi_{jj}^-) = P(\phi_{jj}^+)$ is the probability that j is on a giant strongly connected component of the network, which is a connected component of size $O(n)$ such that every node is reachable from every other node on it. Finding the RHS of Eq. E1 requires an estimate of the “directed” percolation probability $P(\phi_{ij}^-)$.

Directed percolation probability via the SPLD. Using arguments of Sec. II B, i.e. by continuity of the SPLD, the amount of probability mass at $\lambda_{ij} = \infty$ when i is on the giant in-component of j is given by the steady state of Eq. 12a:

$$P(\lambda_{ij} = \infty | \phi_{ij}^-) = \lim_{l \rightarrow \infty} P(\lambda_{ij} > l | \phi_{ij}^-). \quad (\text{E2})$$

Since i is already connected to a putative giant in-component of j , the event $\lambda_{ij} = \infty | \phi_{ij}^-$ corresponds to

j not being on the giant out-component of i :

$$P(\phi_{ji}^+) = 1 - P(\lambda_{ij} = \infty | \phi_{ij}^-). \quad (\text{E3})$$

We note that the likelihood of i being on the giant in-component of j , is the same as the likelihood of i being on the giant out-component of j , when the direction of all edges in the network is reversed. With the conditioning on the average adjacency matrix made explicit:

$$P(\phi_{ij}^- | \langle A \rangle) = P(\phi_{ij}^+ | \langle A \rangle^T). \quad (\text{E4})$$

Therefore, Eqs. 12, E1, E2, E3 and E4 provide us with the full analytic form of the SPLD for directed networks. Since precision on the initial condition is not important for the steady state of Eq. 12, we can use the naïve initial condition

$$P(A_{ij} = 1 | \phi_{ij}^-) = P(A_{ij} = 1) \quad (\text{E5})$$

for the recursive setup given the transposed average adjacency matrix $\langle A \rangle^T$ to first obtain the directed percolation probability of every supercritical node pair, and then run the recursive setup a second time given $\langle A \rangle$ and the exact initial condition in Eq. E1.

Asymmetric supercriticality. As described above, a directed setting that permits asymmetric kernels can result in non-trivial deviations from an undirected setting, particularly when supercriticality is asymmetric. For instance, consider a directed “chain” stochastic block model (SBM) with k blocks, whose block matrix has non-zero entries on the diagonal—allowing for nodes to connect to other nodes within the block—and on the upper off-diagonal—allowing for nodes to connect to nodes in the next adjacent block:

$$B = \begin{bmatrix} a & b & & & \\ & a & b & & \\ & & \ddots & \ddots & \\ & & & a & b \\ & & & & a \end{bmatrix}. \quad (\text{E6})$$

Evidently, for $i < j$, (directed) paths can exist from nodes of block i to block i , and block i to block j , but they are entirely prohibited from nodes of block j to block i . Given this directed chain structure, we can expect $P(\phi_{ij}^-) < P(\phi_{ik}^-)$ for block indices $i < j < k$. Fig. 20 shows the variation in directed percolation probabilities in one such chain SBM, using Eqs. 12, E5, E2, E3 and E4.

Symmetric supercriticality. Consider the scenario where supercriticality is symmetric for all node pairs (i, j) : asymptotically, if there can exist a giant in-component of j containing i , then there can exist a giant in-component of i containing j , and vice-versa. This implies that the giant in- and out-components of all nodes constitute a single giant *strongly connected* component, on which every node can reach every other node. Then, we can drop the dependence on the “target node” from the directed percolation events and write

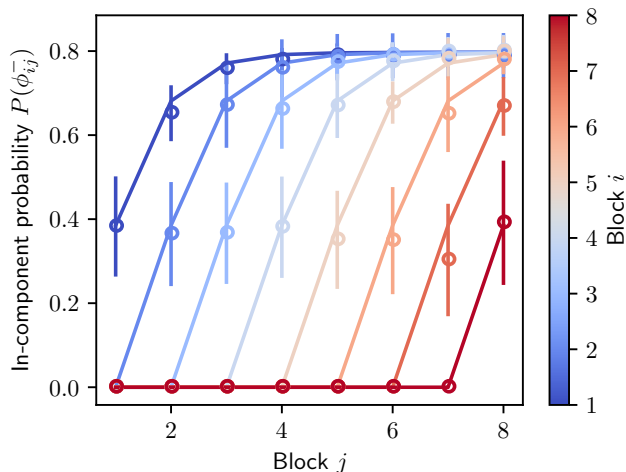


FIG. 20. Empirical and analytic estimates of directed percolation probabilities agree with each other for a “chain” SBM (with 8 equiproportioned blocks, values 10 and 6 on the diagonal and upper off-diagonal entries of the block matrix, respectively). Colors correspond to the block membership of source node, while x -axis corresponds to the block membership of target node. Solid lines represent analytic form using Eqs. 12, E5, E2, E3 and E4, while markers and bars indicate empirical estimates: mean and standard error over 10 network samples.

$\forall j : \phi_{ij}^- = \phi_i^-, \phi_{ij}^+ = \phi_i^+$, where ϕ_i^- (ϕ_i^+) is the event that node i has an edge to (from) the giant strongly connected component. This renders the initial condition for directed networks to be exactly the same as that for undirected networks, Eq. 13, except where ϕ_i is substituted by ϕ_i^- . If we further assume that the average adjacency matrix is symmetric, then Eqs. E4 and E3 yield $P(\phi_j^-) = 1 - P(\lambda_{ij} = \infty | \phi_i^-)$, which is identical to Eq. 15 for undirected networks, except where ϕ_i is substituted by ϕ_i^- . It then follows that the SPLD for a network generated using a symmetric $\langle A \rangle$ does not depend on the network’s directedness. This is evident in Fig. 21, where we plot the empirical and analytic SPLD for a directed network generated with an asymmetric kernel with symmetric supercriticality, by using an SBM with an asymmetric block matrix. We emphasize that if $\langle A \rangle$ is symmetric, (or equivalently kernel ν in the general random graph framework of Sec. III is symmetric,) then supercriticality is symmetric for all node pairs, but the converse need not be true.

Percolation probability via self-consistency equation. We can also derive percolation probabilities without invoking the SPLD. For i to not be on the giant in-component of j , it must not have a directed edge to any node k such that k is on the giant in-component of j . (This exemplifies the transitivity of supercriticality so-defined.) Therefore, the self-consistency Eq. 17 yields percolation probabilities in the directed setting as well, except where $\rho_i \triangleq P(\phi_{ij}^-)$. Given the dependence on j , in the worst case there can be as many non-trivial so-

lutions to the self-consistency equation as the number of nodes, all of which need to be found. However, the SPLD approach to deriving percolation probabilities extracts all solutions in one sweep, encoded in the steady state of the survival function matrix, which is a significant advantage. If supercriticality is symmetric for all node pairs, there can only be a unique giant strongly connected component, and there can exist only a unique non-trivial solution to the self-consistency equation.

Subcritical regime. We now consider a node pair (i, j) that is subcritical, wherein asymptotically there cannot exist a giant in-component of j containing i , or equivalently a giant out-component of i containing j . In the infinite size limit, this yields that either, trivially, there exist no paths from i to j , or that i can reach j through paths only on a small in-/out-component. This results in the subcriticality condition:

$$P(\phi_{ij}^-) = P(\phi_{ji}^+) = 0, \quad (\text{E7})$$

in which case we consider the SPLD on the small in-/out-component containing i, j . By arguments of Sec. II C, the recursive setup remains identical, with the difference arising in the initial condition for the conditional PMF, now given by Eq. 19. That is, we obtain the same expressions for the SPLD—Eqs. 12 and 19—under the subcritical regime in directed and undirected networks.

2. Asymmetric kernel: general random graph models

The shortest path formalism developed in Sec. III for general random graph models works, in principle, for both directed and undirected networks. In this section, we consider asymmetric connectivity kernels in more detail, which permits us to consider asymmetric versions of directed network models. First, we define an ensemble average model which is a finite-size representation of the general model with n nodes. This is the inverse of going from the ensemble average setting to the general setting, and simplifies analyses for asymmetric kernels using accessible results from linear algebra.

Definitions. Consider the general random graph framework with the node space V , and a graph with n nodes generated according to node measure μ given by the collection $\mathcal{V} = \{x_i | x_i \sim \mu, i \in \{1, 2, \dots, n\}\}$ and edges added between them according to connectivity kernel ν given by the collection $\mathcal{E} = \{(x_i, x_j) | (x_i, x_j) \sim \nu, (i, j) \in \{1, 2, \dots, n\}^2 \text{ s.t. } i \neq j\}$. Let $g : \{1, 2, \dots, n\} \rightarrow V$ be the function mapping node indices to their location in the node space. Consequently, we can define the expected adjacency matrix, given g , as:

$$[\langle A \rangle]_{ij} \triangleq \nu(g(i), g(j)), \quad (\text{E8})$$

where $[X]_{ij}$ refers to the corresponding entry in matrix X . We emphasize that g is itself random. However asymptotically, by Borel’s law of large numbers, the collection \mathcal{V} contains a number of nodes from location x in

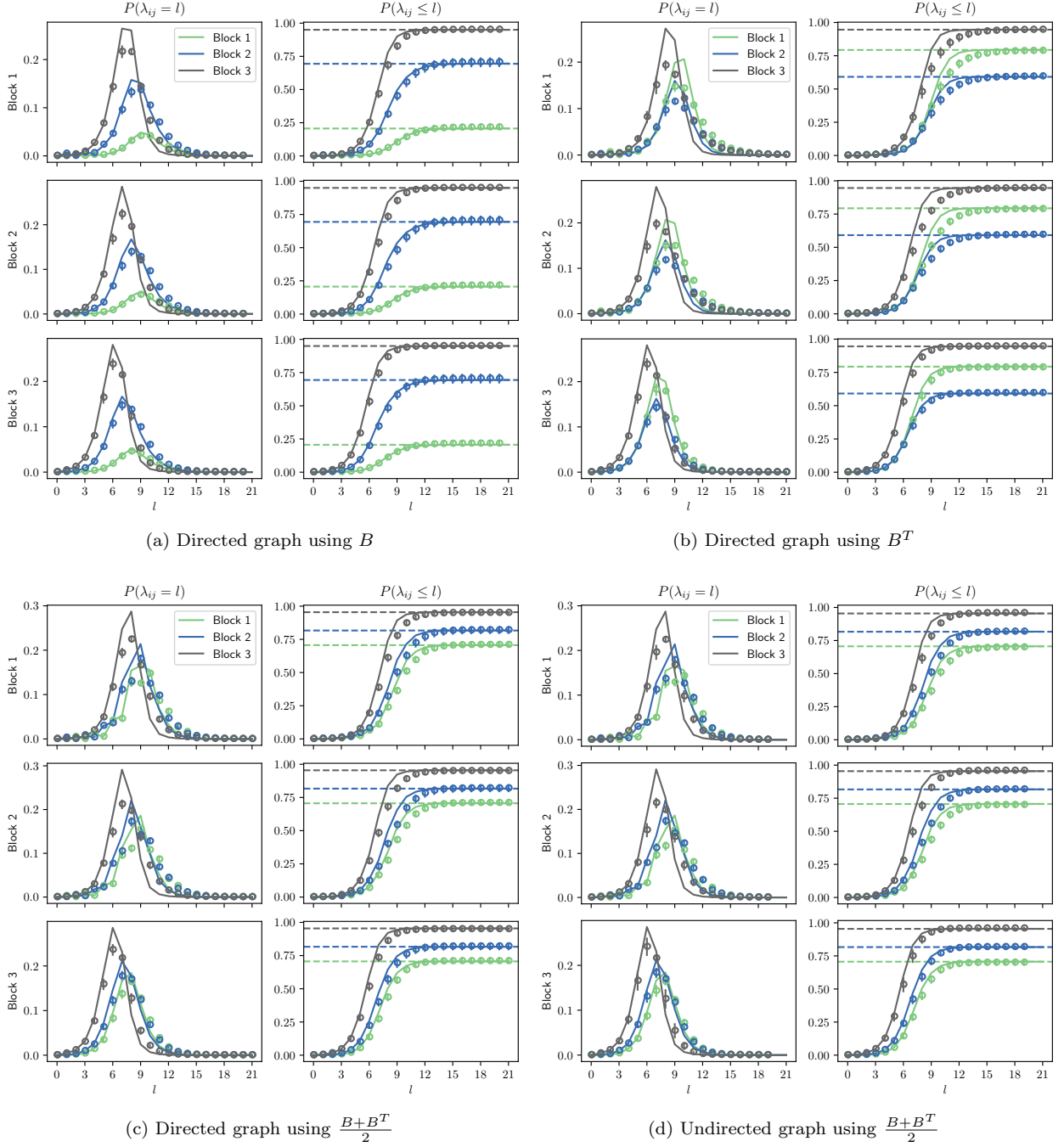


FIG. 21. Empirical and analytic distribution of shortest path lengths for directed (and undirected) graphs generated via stochastic block models with asymmetric (symmetrized) block matrix $B = \begin{pmatrix} 0 & 8 & 0 \\ 1 & 0 & 2 \\ 0 & 2 & 8 \end{pmatrix}$ and distribution vector $\pi = (\frac{1}{3}, \frac{1}{3}, \frac{1}{3})$. In each subplot, rows correspond to the block membership of source node, left column depicts the PMF, and the right column depicts the CDF. Solid lines represent analytic form using Eqs. 12, E1, E2, E3 and E4. Symbols and bars indicate empirical estimates: mean and standard error over 10 network samples.

proportion to $\mu(x)$. This yields asymptotic equivalence between the general random graph model, represented by the integral operator T in Eq. 40, and its corresponding ensemble average model $\langle A \rangle$ in Eq. E8. Asymptotic results on $\langle A \rangle$ can then be extended to those for T . We

further note that because of sparsity:

$$\nu = O(n^{-1}) \implies \langle A \rangle = O(n^{-1}) \implies \langle A \rangle^m = O(n^{-1}). \quad (\text{E9})$$

In this section, we study the closed-form of the survival function of the SPLD and the percolation threshold for

asymmetric kernels via their corresponding asymmetric ensemble average model $\langle A \rangle$.

a. *Closed-form of the SPLD*

From Eq. 29, the closed-form of the survival function matrix for the ensemble average model can be written entirely in terms of powers of $\langle A \rangle$. Since the kernel ν is possibly asymmetric, $\langle A \rangle$ may not be a symmetric matrix. Consequently, $\langle A \rangle$ may not necessarily be a normal matrix, and therefore may not be diagonalized by a unitary matrix. Analogously, in terms of the integral transform operator T defined in Eq. 40, T may not be self-adjoint and therefore the spectral theorem cannot be applied, which prevents us from writing closed-form expressions for the SPLD as in Eqs. 44, 46. However, by making use of the Jordan normal form, the survival function of the SPLD can still be expressed as a weighted sum of powers of eigenvalues over a generalized eigenvector basis.

We consider the Jordan normal form of $\langle A \rangle = PJP^{-1}$, where P is an invertible matrix and J is a block diagonal matrix with k blocks such that the i^{th} block denoted by J_i , of size $n_i \times n_i$, corresponds to the i^{th} eigenvalue of $\langle A \rangle$, denoted by τ_i , and can be written as the sum of a scaled identity matrix and the canonical nilpotent matrix:

$$J_i = \begin{bmatrix} \tau_i & 1 & & & \\ & \tau_i & 1 & & \\ & & \ddots & \ddots & \\ & & & \tau_i & 1 \\ & & & & \tau_i \end{bmatrix}.$$

We remark that for an eigenvalue τ_i , the number of Jordan blocks corresponding to it gives its geometric multiplicity, while the sum of sizes of Jordan blocks corresponding to it gives the algebraic multiplicity [117]. If J is diagonal, then this implies that $\langle A \rangle$ is diagonalizable, and therefore P simply corresponds to the right eigenvectors of $\langle A \rangle$ stacked as column vectors. In that case, the Jordan normal form is simply the eigendecomposition of $\langle A \rangle$. However, since we consider a scenario where $\langle A \rangle$ is not a symmetric matrix, it need not be diagonalized in such a manner. However, the Jordan normal form *almost* diagonalizes it, in which case P then corresponds to a generalized set of eigenvectors of $\langle A \rangle$ [117]. This results in:

$$\langle A \rangle^m = P J^m P^{-1}.$$

Due to the diagonal block structure of J , its powers can be written as the corresponding diagonal-block matrix of the powers of its blocks. Then for the i^{th} block, due to its structure described above, its powers for $m \in \mathbb{Z}_{\geq 0}$ can be written in closed-form as an upper-triangular matrix such that $[J_i^m]_{pq} = \binom{m}{q-p} \tau_i^{m+p-q}$ when $m \geq q-p \geq 0$, and 0 otherwise [118]. Here, $\binom{m}{q-p} = \frac{m!}{(q-p)!(m+p-q)!}$ is the

usual binomial coefficient. We can also express $\langle A \rangle^m$, P and P^{-1} as block matrices:

$$\langle A \rangle^m = \begin{bmatrix} \langle A \rangle_{11}^m & \langle A \rangle_{12}^m & \cdots & \langle A \rangle_{1k}^m \\ \langle A \rangle_{21}^m & \langle A \rangle_{22}^m & \cdots & \langle A \rangle_{2k}^m \\ \vdots & \vdots & \ddots & \vdots \\ \langle A \rangle_{k1}^m & \langle A \rangle_{k2}^m & \cdots & \langle A \rangle_{kk}^m \end{bmatrix},$$

$$P = \begin{bmatrix} P_{11} & P_{12} & \cdots & P_{1k} \\ P_{21} & P_{22} & \cdots & P_{2k} \\ \vdots & \vdots & \ddots & \vdots \\ P_{k1} & P_{k2} & \cdots & P_{kk} \end{bmatrix},$$

$$P^{-1} = \begin{bmatrix} Q_{11} & Q_{12} & \cdots & Q_{1k} \\ Q_{21} & Q_{22} & \cdots & Q_{2k} \\ \vdots & \vdots & \ddots & \vdots \\ Q_{k1} & Q_{k2} & \cdots & Q_{kk} \end{bmatrix}.$$

Therefore, we can express powers of $\langle A \rangle$ in a blockwise manner. For any two nodes a, b we can define their block indices $r, s \in \{1, 2, \dots, k\}$, and within-block indices $u \in \{1, 2, \dots, n_r\}$, $v \in \{1, 2, \dots, n_s\}$, such that:

$$\langle A \rangle_{rs}^m = \sum_{i=1}^k P_{ri} J_i^m Q_{is},$$

$$\implies [\langle A \rangle_{rs}^m]_{uv} = \sum_{i=1}^k \sum_{p=1, q=1}^{n_i} [P_{ri}]_{up} [J_i^m]_{pq} [Q_{is}]_{qv}$$

$$= \sum_{i=1}^k \sum_{p=1}^{n_i} \sum_{q=p}^{\min(p+m, n_i)} \binom{m}{q-p} \tau_i^{m+p-q} [P_{ri}]_{up} [Q_{is}]_{qv}$$
(E10)

Putting Eq. E10 for the powers of $\langle A \rangle$ in Eqs. 29, 30 for the ensemble average model, we have shown that the closed-form of survival function of an asymmetric kernel can be expressed as a sum of powers of eigenvalues over a generalized eigenvector basis. In particular, the approximate closed-form of the conditional PMF and the survival function for the geodesic length between a, b , using Eqs. E10, 28a and 30, is given block-wise by:

$$[(\tilde{\Omega}_l)_{rs}]_{uv} = \sum_{i=1}^k \sum_{p=1}^{n_i} \sum_{q=p}^{\min(p+l, n_i)} \binom{l}{q-p} \times \tau_i^{l+p-q} [P_{ri}]_{up} [Q_{is}]_{qv},$$
(E11a)

$$[(\tilde{\Psi}_l)_{rs}]_{uv} = \exp \left(- \sum_{m=1}^l [(\tilde{\Omega}_m)_{rs}]_{uv} \right).$$
(E11b)

b. *Spectral condition for percolation*

In Theorem 1, we saw the geodesic condition for percolation: in the asymptotic limit, a giant component does not exist iff for all node pairs the limit of closed-form of the conditional PMF is zero. This result holds regardless

of symmetry of the kernel. Then in Theorem 2, we saw the spectral condition for percolation: this condition is equivalent to the spectral radius of the integral operator (of a symmetric kernel) being less than unity. Here, we show that the spectral condition holds for an asymmetric kernel as well.

Theorem 4 (Spectral condition for percolation in asymmetric ensembles). *Let $\langle A \rangle$ be an asymmetric ensemble average model, and $r(\langle A \rangle)$ be its spectral radius. Then, the directed network has a giant (in-/out-)component if and only if $r(\langle A \rangle) > 1$, with the phase transition at $r(\langle A \rangle) = 1$.*

Proof. The proof is analogous to Theorem 2, applied to a (non-negative) matrix instead of a (compact non-negative) self-adjoint operator. Throughout the proof, we use “giant component” to refer to the giant in-/out-component. First, we show the forward implication, that if a giant component exists then $r(\langle A \rangle) > 1$, via contraposition. Let us assume that $r(\langle A \rangle) \leq 1$. Then all eigenvalues of $\langle A \rangle$ must be no larger than unity in their absolute value. Then let us take the limit as $l \rightarrow \infty$ of the approximate closed-form of the PMF of the SPLD from Eq. E11a. For large m , we can use Stirling’s approximation to observe that the binomial coefficient $\binom{m}{k} = O(m^k)$. Consequently for any eigenvalue τ_i , we have:

$$\begin{aligned} \binom{l}{q-p} \tau_i^{l+p-q} &= O(\exp((q-p)\log l + l \log \tau_i)) \\ &= O(\tau_i^l). \end{aligned}$$

Since $|\tau_i| \leq 1$ for all i we have from Eq. E11 that for all combinations of (r, s, u, v) : $\limsup_{l \rightarrow \infty} [(\tilde{\Omega}_l)_{rs}]_{uv} < \infty$. Due to sparsity from Eq. E9, this further implies $\lim_{n \rightarrow \infty} \limsup_{l \rightarrow \infty} [(\tilde{\Omega}_l)_{rs}]_{uv} = 0$. From Corollary 1.1, a giant component does not exist. Thus, if the network has a giant component, then $r(\langle A \rangle) > 1$.

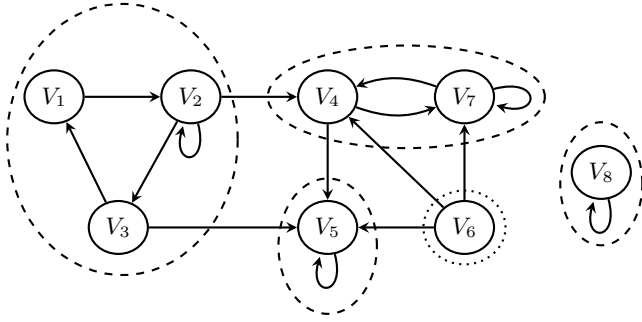
Next, we show the backward implication, if $r(\langle A \rangle) > 1$ then a giant component exists, via contradiction. Let the network not contain a giant component, then from Corollary 1.1, it must be true that for all valid combinations of (r, s, u, v) , $\limsup_{l \rightarrow \infty} [(\tilde{\Omega}_l)_{rs}]_{uv} < \infty$. Considering Eq. E11a for $[(\tilde{\Omega}_l)_{rs}]_{uv}$, since elements of the (invertible) matrix P cannot all be 0, for this to be true either (a) all eigenvalues are no larger than unity in their absolute value, or (b) eigenvalues exist in pairs (τ_i, τ_j) such that $|\tau_i| > 1$, $|\tau_j| > 1$ and yet precisely cancel each other’s contributions out as $l \rightarrow \infty$, i.e. (c) $\limsup_{l \rightarrow \infty} \tau_i^{l+p-q} = \limsup_{l \rightarrow \infty} \tau_j^{l+p-q} \implies \tau_i = \tau_j$ and (d) for all valid node pairs represented by (r, s, u, v) , we have $[P_{ri}]_{up}[Q_{is}]_{qv} = -[P_{rj}]_{up}[Q_{js}]_{qv}$. If $\langle A \rangle$ is a positive matrix, i.e. the likelihood of connection between any node pair cannot be precisely 0, then by Perron’s theorem we know that $r(\langle A \rangle) > 0$ and it is an eigenvalue with multiplicity 1 [113, 114], i.e. it cannot be paired with another eigenvalue, thus invalidating condition (c) and hence (b). If $\langle A \rangle$ is a non-negative but irreducible

matrix, i.e. even if the likelihood of an edge between a node pair is 0 there exists a non-zero chance of having a (directed) path between them, then the Perron-Frobenius theorem can be applied [114, 115]. Consequently, there can be h eigenvalues of $\langle A \rangle$ with the same absolute value $r(\langle A \rangle)$, where h is called the period such that each of these eigenvalues is given by the product of $r(\langle A \rangle)$ with the h^{th} root of unity. That is, if $v \triangleq e^{\frac{2\pi i}{h}}$ is the h^{th} root of unity where $i \triangleq \sqrt{-1}$, then eigenvalues with the largest absolute value are given by the set $\{r(\langle A \rangle)v^t\}_{t=0}^{h-1}$. Evidently, these eigenvalues can be paired within themselves only if h is even, nullifying each other’s contributions out only when $m + p - q$ is an integral multiple of the period h . Thus in the limit, their net contribution remains unbounded, and condition (c) and therefore (b) does not hold. Therefore for $\langle A \rangle$ that is positive, or non-negative irreducible, the only condition for non-percolation must be (a), i.e. all eigenvalues are smaller than or equal to unity in their absolute value. It then follows that $r(\langle A \rangle) \leq 1$.

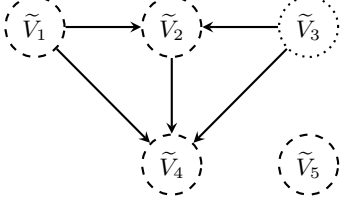
Finally, if $\langle A \rangle$ is reducible, then there exists a partitioning of the “underlying” node space V into q “strongly-connected” subspaces $\{\tilde{V}_1, \tilde{V}_2, \dots, \tilde{V}_q\}$ such that the likelihood of a directed path existing both *from* and *to* different subspace pairs is 0. In other words, it is possible to specify a directed acyclic graph (DAG) structure of node subspaces—akin to the notion of condensation in directed graphs—such that each of these subspaces correspond either to (1) an irreducible ensemble average model $\langle A_i \rangle$ —where for any two nodes in \tilde{V}_i there is a non-zero likelihood of a directed path between them in either direction—or to (2) a strictly-triangular ensemble average model $\langle A_i \rangle$ —where for any two nodes in \tilde{V}_i there is zero likelihood of a directed path between them in both directions. See Fig. 22 for an example. We remark that in terms of the integral operator T of the general random graph framework, for a given node subspace \tilde{V}_i , its corresponding (non-negative) operator T_i is either irreducible, or quasinilpotent. Consequently, we can define a topological ordering of this node space partition, and permute the rows and columns of $\langle A \rangle$ by this ordering, which preserves its spectrum but then can be written as a block upper triangular matrix:

$$\langle A \rangle = \begin{bmatrix} \langle A \rangle_{11} & \langle A \rangle_{12} & \cdots & \langle A \rangle_{1q} \\ 0 & \langle A \rangle_{22} & \cdots & \langle A \rangle_{2q} \\ \vdots & \vdots & \ddots & \vdots \\ 0 & 0 & \cdots & \langle A \rangle_{qq} \end{bmatrix},$$

where the diagonal (possibly strictly-upper triangular) blocks correspond to T_i i.e. intra-subspace connections, and the off-diagonal (possibly strictly-upper triangular) blocks indicate inter-subspace connections. Since inter-subspace connections can alone contribute only to chains of finite length (of upto q), it is necessary and sufficient for no giant components to exist in the whole network that none of the subspaces percolate. From the above



(a) Node subspaces with given directed path structure



(b) Condensation into a DAG subspace structure

FIG. 22. Partitioning of node space V , for an illustrative example of an asymmetric connectivity model with a reducible integral operator, into strongly-connected subspaces operated over by (1) irreducible integral operators (dashed: $\{\tilde{V}_1, \tilde{V}_2, \tilde{V}_4, \tilde{V}_5\}$), and (2) quasinilpotent operators (dotted: $\{\tilde{V}_3\}$). Nodes with solid boundaries indicate subspaces of the node space V with a given path structure, represented by arrows which indicate if there is a likelihood of a (directed) path between the source and target node subspaces. V can be partitioned into strongly-connected subspaces, given here by $\tilde{V}_1 \triangleq V_1 \cup V_2 \cup V_3$, $\tilde{V}_2 \triangleq V_4 \cup V_7$, $\tilde{V}_3 \triangleq V_6$, $\tilde{V}_4 \triangleq V_5$, and $\tilde{V}_5 \triangleq V_8$. Note that the path structure for this partition would be a directed acyclic graph (DAG).

proof for irreducible ensemble average models, and noting that for the “strictly-upper triangular” models the spectrum and thus the spectral radius is 0, we get the condition that $\max(r(\langle A \rangle_{11}), r(\langle A \rangle_{22}), \dots, r(\langle A \rangle_{qq})) \leq 1$. Because $\langle A \rangle$ is block triangular, its spectrum is given by the union of spectra of its diagonal blocks. Therefore, we obtain a contradiction that $r(\langle A \rangle) \leq 1$. \square

In the asymptotic limit, the spectrum of $\langle A \rangle$ will coincide with that of the underlying compact integral operator T for this asymmetric connectivity kernel, as defined by Eq. 40. Therefore, this spectral condition for percolation translates to $r(T) > 1$. That is, we can state Theorem 2 verbatim for any connectivity kernel, regardless of symmetry.

Illustrative example: chain SBM. Consider a directed “chain” SBM with k equiproportioned blocks from Eq. E6, i.e. $[\Pi]_{ii} = 1/k$. We set the diagonal values of the block matrix to 0, and off-diagonals to some parameter $\langle d \rangle$, such that every block has mean in-/out-degree $\langle d \rangle$ —except for the first and last blocks which respectively have expected out- and in-degrees d and expected in-

and out-degrees 0:

$$B = \begin{bmatrix} 0 & \langle d \rangle & & & & & & \\ & 0 & \langle d \rangle & & & & & \\ & & \ddots & \ddots & & & & \\ & & & 0 & \langle d \rangle & & & \\ & & & & & & & \\ & & & & & & & \\ & & & & & & & \\ & & & & & & & 0 \end{bmatrix}.$$

Consequently, directed edges can only exist from one block to its next one, preventing a giant component of asymptotically infinite size to emerge. Evidently, $B\Pi$ is a nilpotent matrix, its spectral radius is 0, and from Theorem 4 it does not have a giant component. (Although, it may contain directed chains of length up to $k - 1$ on its small components.) We note that the 2-norm of $B\Pi$ is given by $\langle d \rangle / k$. Thus, following the 2-norm criterion of sparse inhomogeneous graphs with symmetric kernels [31] would incorrectly suggest that the network percolates when $\langle d \rangle > k$.

Appendix F: General random graph models

1. Sparsity constraint and integral operators

In the general random graph framework of Sec. III, we assume sparsity in the sense that the connectivity kernel $\nu = O(n^{-1})$ almost everywhere, i.e. $\exists m > 0, \exists L > 0$ such that $\forall n \geq m$ we have $\nu(x, y) \leq Ln^{-1}$ almost everywhere on $V \times V$. By almost everywhere, we mean that sparsity holds everywhere except for a subset of V of zero measure, which leads to bounded mean degree for every node in the network asymptotically. Let $U \subset V$ such that $\mu(U) = 0$ and where $\nu(x, y) \neq O(n^{-1})$ for $x \in V, y \in U$, then for $n \geq m$, from Eq. 32:

$$\begin{aligned} \hat{d}(x) &= n \left(\int_{V \setminus U} \nu(x, y) d\mu(y) + \int_U \nu(x, y) d\mu(y) \right)^0 \\ \implies \langle d \rangle &= n \left(\int_{V \setminus U} \int_{V \setminus U} \nu(x, y) d\mu(y) d\mu(x) + \right. \\ &\quad \left. \int_U \int_{V \setminus U} \nu(x, y) d\mu(y) d\mu(x) \right)^0 \\ &\leq n \int_{V \setminus U} \int_{V \setminus U} Ln^{-1} d\mu(x) d\mu(y) = L[\mu(V \setminus U)]^2, \end{aligned}$$

which results in $\lim_{n \rightarrow \infty} \langle d \rangle < \infty$, i.e. a bounded mean degree.

We remark that asymptotically, $n\nu \in \mathcal{L}^2(V \times V, \mu \times \mu)$ (it is square integrable), since:

$$\begin{aligned} \|n\nu\|_2 &= \left(\int_{V^2} (n\nu(x, y))^2 d\mu(x) d\mu(y) \right)^{\frac{1}{2}} \\ &= \left(\int_{(V \setminus U)^2} n^2 (\nu(x, y))^2 d\mu(x) d\mu(y) \right)^{\frac{1}{2}} \\ &\leq L\mu(V \setminus U) < \infty. \end{aligned}$$

This allows us to define the Hilbert-Schmidt integral operator $T : \mathcal{L}^2(V, \mu) \rightarrow \mathcal{L}^2(V, \mu)$ in Eq. 40 that acts on the space of \mathcal{L}^2 functions in V . Being a Hilbert-Schmidt operator, T is compact. That is, T is either finite-rank or the limit of finite-rank operators. Let T have rank N , where if $N = \infty$ then its eigenvalues approach 0. We remark that $n\omega_1 \in \mathcal{L}^2$ by a similar argument as for $n\nu$. Then by Fubini's theorem, this allows for finitely-iterated integrals in Eq. 39 to be computed in any order.

2. Equivalent SBMs for general models

Since the formalism for SBMs allows us to easily deal with the SPLD computationally by using linear algebra toolkits, it is useful to show that for any given general random graph model, there exist equivalent SBMs up to a desirable level of approximation.

Theorem 5 (ϵ -equivalent SBMs of general random graph models). *Consider a general random graph model with n nodes in node space V with node density μ and connectivity kernel ν . Then it has an ϵ -equivalent representation as a stochastic block model (SBM). That is, for any given $\epsilon > 0$ there exist:*

(a) a mapping $f_\epsilon : V \rightarrow \{1, 2, \dots, k\}$ where

$$k \leq \begin{cases} 2^{\lfloor \epsilon^{-1} \rfloor + 1} & \text{if } \nu \text{ is symmetric,} \\ 4^{\lfloor \epsilon^{-1} \rfloor + 1} & \text{otherwise,} \end{cases}$$

(b) a length- k distribution vector π_ϵ , and

(c) a $k \times k$ block matrix B_ϵ such that for any node pair $(x, y) \in V$, we have:

$$n\nu(x, y) - [B_\epsilon]_{f(x)f(y)} = O(\epsilon),$$

almost everywhere.

Proof. The sparsity assumption yields $\nu = O(n^{-1})$ almost everywhere, $\exists m > 0, \exists L > 0$ such that $\forall n \geq m$ we have $\nu(x, y) \leq Ln^{-1}$ almost everywhere on $V \times V$, i.e.

$$n\nu(x, y) \leq L, \quad (\text{F1})$$

where we refer to $n\nu$ as the ‘‘scaled’’ connectivity kernel. For the rest of this proof, we ignore zero measure subsets of V , i.e. use V to indicate $V \setminus U$, where $\mu(U) = 0$.

Let $\epsilon > 0$. Since ν is a non-negative measurable function on $V \times V$, its output (image) can be divided into $p \triangleq \lfloor \epsilon^{-1} \rfloor + 1$ intervals of length ϵL each, where $\lfloor \cdot \rfloor$ is the floor function. That is, define the half-open intervals:

$$I_\epsilon^u \triangleq [(u-1)\epsilon L, u\epsilon L] \quad \text{for } u \in \{1, 2, \dots, p\}. \quad (\text{F2})$$

Then consider the inverse of the scaled connectivity kernel $\nu^{-1} : \mathbb{R}_{\geq 0} \rightarrow V \times V$. Let $\nu^{-1}(I_\epsilon^u) = \vec{V}_\epsilon^u \times \overleftarrow{V}_\epsilon^u$ be the measurable set (of positive measure) in $V \times V$ whose connectivity kernel takes values in I_ϵ^u . Since the intervals

I_ϵ^u are disjoint and cover the image of $n\nu$, it must be true that $\{\vec{V}_\epsilon^u \times \overleftarrow{V}_\epsilon^u\}_{u=1}^p$ forms a partition of $V \times V$. However, the collection $\{\vec{V}_\epsilon^u\}_{u=1}^p$ will be a *cover* of V , and not necessarily a *partition*—i.e. $V = \bigcup_{u=1}^p \vec{V}_\epsilon^u$ but it need not be the case that for any $u \neq v$ we have $\vec{V}_\epsilon^u \cap \vec{V}_\epsilon^v = \emptyset$.

Then consider the following iterative partition refinement process on V . Begin with the trivial partition of the node space $\vec{P}_\epsilon^0 \triangleq \{V\}$. Then for u in the ordered set $\{1, 2, \dots, p\}$:

1. for every node subspace $S_i \in \vec{P}_\epsilon^{u-1}$,
 - (a) remove S_i ,
 - (b) add $S_i \setminus \vec{V}_\epsilon^u$,
 - (c) add $S_i \cap \vec{V}_\epsilon^u$,
2. and obtain the new partition refinement \vec{P}_ϵ^u .

Then the final partition \vec{P}_ϵ^p —after ignoring empty sets—constitutes a partitioning of the node space into k node subspaces. Evidently, since the refinement is done p times, in the worst case the final size of the partition can be no more than 2^p , i.e. $k \leq 2^{\lfloor \epsilon^{-1} \rfloor + 1}$. (We remark that if the kernel ν is symmetric, then the partition $\overleftarrow{P}_\epsilon^p$ obtained by considering the target node space collection $\{\overleftarrow{V}_\epsilon^u\}_{u=1}^p$ will be identical to \vec{P}_ϵ^p . If not, we can consider both collections at the same time in the partition refinement process, in which case the worst case value of k is 2^{2p} , i.e. $k \leq 4^{\lfloor \epsilon^{-1} \rfloor + 1}$.) The final collection of node subspaces can be written as an ordered set $P_\epsilon \triangleq \{V_\epsilon^1, V_\epsilon^2, \dots, V_\epsilon^k\}$. Let $\mathbf{1}_X : V \rightarrow \{0, 1\}$ be the indicator function identifying if $x \in X$, for some $X \subseteq V$. Then define the index-map $f_\epsilon(x) \triangleq \sum_{i=1}^k i \mathbf{1}_{V_\epsilon^i}(x)$. This shows part (a) of the theorem.

Next, define the probability distribution vector $\pi_\epsilon \triangleq \{\mu(V_\epsilon^i)\}_{i=1}^k$. Since we have removed any subspaces of zero measure, and since P_ϵ is a partitioning of V , π_ϵ is a valid distribution vector whose entries are positive-valued and sum up to 1. This shows part (b) of the theorem.

Finally, let $h : \mathcal{P}(V) \times \mathcal{P}(V) \rightarrow \{0, 1\}$ be the indicator function $h(X, Y)$ identifying if $X \subseteq Y$, for some $X, Y \subseteq V$. Then define a $k \times k$ block matrix B_ϵ , such that

$$[B_\epsilon]_{ij} \triangleq \sum_{u=1}^p (u-1)\epsilon L h(V_i, \vec{V}_\epsilon^u) h(V_j, \overleftarrow{V}_\epsilon^u).$$

Since $\{\vec{V}_\epsilon^u \times \overleftarrow{V}_\epsilon^u\}_{u=1}^p$ forms a partition of $V \times V$, and by the construction of P_ϵ , we know that $h(V_i, \vec{V}_\epsilon^u) h(V_j, \overleftarrow{V}_\epsilon^u) = 1$ for exactly one such u , and is 0 otherwise. From the definition of the intervals in Eq. F2, we know that for $x \in V_i$ and $y \in V_j$: $n\nu(x, y) \in I_\epsilon^u$. Consequently, we get for x, y :

$$\begin{aligned} 0 &\leq n\nu(x, y) - [B_\epsilon]_{f(x)f(y)} < \epsilon L \\ \implies n\nu(x, y) - [B_\epsilon]_{f(x)f(y)} &= O(\epsilon) \quad \text{almost everywhere} \end{aligned}$$

This shows part (c) of the theorem. \square

The above theorem provides technical support to the generation of equivalent SBMs by appropriate “discretization” of values that the connectivity kernel can take, and consequently of the node space V . If the node space is Euclidean, say $V \subseteq \mathbb{R}^k$, and the connectivity kernel is “sufficiently regular”, then we could consider a “sufficiently fine” discretization of V such that Theorem F 2, and therefore a good SBM approximation, holds. In particular, if the connectivity kernel ν is Darboux (or equivalently Riemann) integrable on $V \times V$, then for any $\epsilon > 0$ there would exist a sufficiently fine partition P_ϵ of $V \times V$ such that the difference in the supremum and infimum of ν evaluated on each “cell” of P_ϵ is less than ϵ , and the final partition of V can be obtained via the iterative refinement process described in the proof for Theorem F 2. We outline two methods for continuous models in Euclidean space: in one dimension in Appendix F 2 a, and in higher dimensions in Appendix F 2 b

a. MLE-SBM approximation in \mathbb{R}

For continuous models on node space \mathbb{R} , such as graphons described in Sec. IVE, we can define an equivalent m -block SBM with equi-proportioned blocks. Let $F : \mathbb{R} \rightarrow [0, 1]$ be the cumulative distribution function (CDF) for this node space, i.e. $F(x) \triangleq \int_{-\infty}^x \mu(x) dx$. Then using the inverse of F , define a size k partition of \mathbb{R} given by:

$$I_m^i \triangleq \begin{cases} [F^{-1}(\frac{i-1}{m}), F^{-1}(\frac{i}{m})] & \text{if } i \in \{1, 2, \dots, m-1\}, \\ [F^{-1}(\frac{i-1}{m}), F^{-1}(\frac{i}{m})] & \text{if } i = m. \end{cases} \quad (\text{F3})$$

Evidently this is an equi-sized partition:

$$\mu(I_m^i) = F\left(F^{-1}\left(\frac{i}{m}\right)\right) - F\left(F^{-1}\left(\frac{i-1}{m}\right)\right) = m^{-1},$$

which generates the index-map:

$$f_m(x) \triangleq \sum_{i=1}^m i \mathbf{1}_{I_m^i}(x), \quad (\text{F4})$$

where $\mathbf{1}_X$ is the indicator function, and the distribution vector:

$$\boldsymbol{\pi}_m = \frac{1}{m} \mathbf{u}, \quad (\text{F5})$$

where \mathbf{u} is the all-ones vector of size m . We can also define the block matrix B_m , by invoking a likelihood-maximization argument. Consider networks sampled from the original random graph model, and nodes labeled according to f_m , then the maximum likelihood estimate (MLE) of the block matrix—see Eq. I4 and Appendix I1—would asymptotically approach the average affinities between blocks defined by the above partition.

Consequently, define the block matrix B_m as:

$$\begin{aligned} [B_m]_{ij} &\triangleq n \frac{\int_{I_m^i} \int_{I_m^j} \nu(x, y) d\mu(y) d\mu(x)}{\int_{I_m^i} \int_{I_m^j} d\mu(y) d\mu(x)} \\ &= nm^2 \int_{I_m^i} \int_{I_m^j} \nu(x, y) d\mu(y) d\mu(x). \end{aligned} \quad (\text{F6})$$

Then we refer to $(f_m, \boldsymbol{\pi}_m, B_m)$ as the “ m -block MLE-SBM approximation” for the model in \mathbb{R} . As m grows larger, the approximation is expected to become better, but it remains consistent with the MLE for any value of m . In Fig. 23, we show for a one-dimensional Gaussian RGG its 32-block MLE-SBM approximation, and its consequent “rank-1 approximation” (that retains only the leading eigenpair of the model, as in Sec. VIA.

b. SBM approximation in \mathbb{R}^k

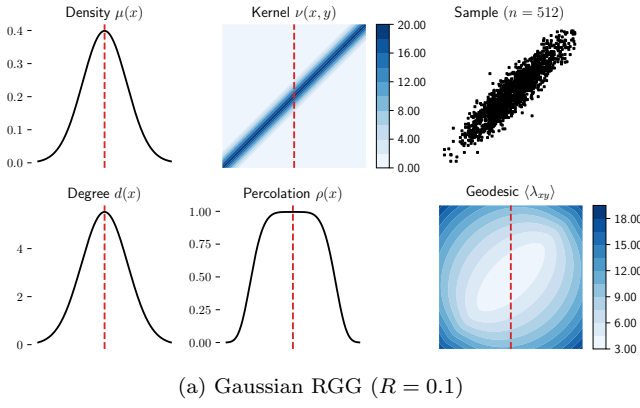
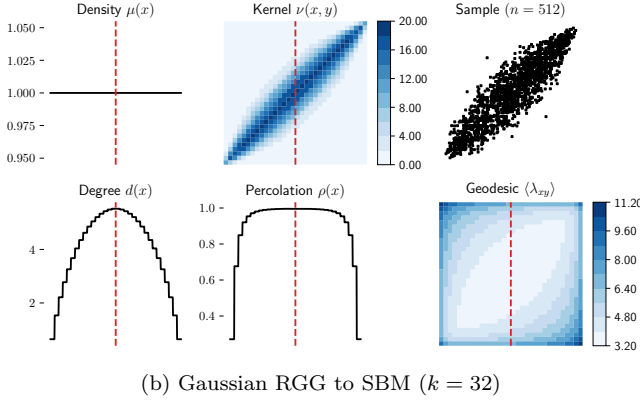
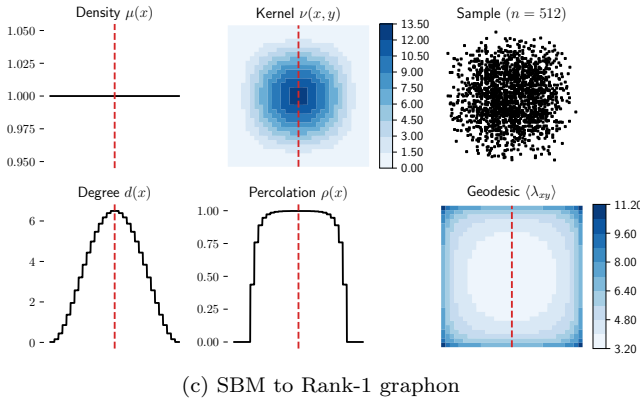
For continuous models in a higher-dimensional node space \mathbb{R}^k , it may be computationally infeasible to integrate the node density μ . However, if we consider a sufficiently fine uniform partition, then assuming smoothness of the node density and connectivity kernel we can consider their point estimates instead. Let $Z_{k \rightarrow m}$ be a $k \times m$ matrix indicating a column-wise collection of m points that defines a uniform partition of a bounded subspace of \mathbb{R}^k , such that negligible probability mass lies outside of it. Define the distribution vector $\boldsymbol{\pi}_{k \rightarrow m}$ such that $[\boldsymbol{\pi}_{k \rightarrow m}]_i \triangleq \frac{\mu([Z_{k \rightarrow m}]_{:i})}{\sum_i \mu([Z_{k \rightarrow m}]_{:i})}$, and kernel matrix $B_{k \rightarrow m}$ such that $[B_{k \rightarrow m}]_{ij} \triangleq n \nu([Z_{k \rightarrow m}]_{:i}, [Z_{k \rightarrow m}]_{:j})$. Then we refer to $(Z_{k \rightarrow m}, \boldsymbol{\pi}_{k \rightarrow m}, B_{k \rightarrow m})$ as the “ m -block SBM approximation” for the model in \mathbb{R}^k . Evidently, as m grows larger, the approximation becomes better. In this paper, we make use of the m -block SBM approximation only for computing average global statistics—like estimating the mean percolation vector for RDPGs, and fitting parameters of the percolation curve for Gaussian RGGs—and thus the errors are expected to be even lower due to averaging.

Illustrative examples. For an RDPG, consider solving Eq. 61b for the mean percolation vector $\boldsymbol{\rho}$. Let $(Z, \boldsymbol{\pi}, B)$ be its m -block SBM approximation. Then the integral in Eq. 61b can be approximated by:

$$\boldsymbol{\rho} = \boldsymbol{\phi} - Z \text{diag}(\boldsymbol{\pi}) \exp(-n\beta Z^T \boldsymbol{\rho}), \quad (\text{F7})$$

which is a vector equation that can be numerically solved via function iteration. We remark that for estimating percolation probabilities for the illustrative example of a 3-dimensional Dirichlet-RDPG, we uniformly partition the 2-simplex—an equilateral triangle—into 4096 equi-triangular partitions.

For a Gaussian RGG, we use the m -block SBM approximation to obtain the percolation probability at the points of the uniform partition. Let $(Z, \boldsymbol{\pi}, B)$ be the Gaussian RGG’s m -block SBM approximation, such that

(a) Gaussian RGG ($R = 0.1$)(b) Gaussian RGG to SBM ($k = 32$)

(c) SBM to Rank-1 graphon

FIG. 23. Node and node pair functions for a (a) 1-dimensional Gaussian RGG, and its (b) discretization into a 32-block SBM, which can be further converted into (c) an (approximate) rank-1 graphon. The functions for Gaussian RGG are viewed on the node space $[-3, 3]$. For description of each node and node pair function, refer to Fig. 5.

negligible probability mass lies outside of the partition defined by Z . Define $\boldsymbol{\rho}$ to be a length m vector indicating the percolation probabilities at m locations in \mathbb{R}^k . Then from Eq. 36, we obtain:

$$\boldsymbol{\rho} = \mathbf{u} - \exp(-nB \text{diag}(\boldsymbol{\pi})\boldsymbol{\rho}), \quad (\text{F8})$$

where \mathbf{u} is the all-ones vector of length k . This is a vector self-consistency equation in $\boldsymbol{\rho}$, whose non-trivial solution

can be obtained via function iteration. Evidently, this equation's form resembles Eq. 52 for percolation probabilities in an SBM. Since $\boldsymbol{\rho}$ defines percolation probabilities on a fine partition, assuming smoothness of the percolation probability function in \mathbb{R}^k , i.e. of $\rho(\mathbf{x})$, we can interpolate for an arbitrary point \mathbf{x} , or infer the parametric form of a percolation surface in \mathbb{R}^k . We remark that, for estimating percolation probabilities for the illustrative example of a 2-dimensional Gaussian RGG, we restrict to the subspace $[-3, 3] \times [-3, 3]$, which includes about 99% of the probability mass [119], divided into 4096 square partitions.

3. Molloy & Reed's criterion and spectral condition for percolation

The classic percolation criterion of Molloy and Reed [25] suggests that a giant component exists in a graph with a given degree sequence when nodes have a higher expectation of number of neighbors at length 2 (“neighbors-of-neighbors”) than at length 1 (“neighbors”). Here, we show that this criterion coincides with Theorem 2 for the simplest class of rank-1 models, wherein the corresponding operator T has precisely one non-zero eigenvalue.

The expectation of number of nodes at length 1 from a node at x is given by the expected degree at x . From Eq. 32 we can write the expected degree function as:

$$\widehat{d}(x) = \sum_{i=1}^N \tau_i \widetilde{\varphi}_i \varphi_i(x), \quad (\text{F9})$$

where we define $\widetilde{\varphi}_i \triangleq \mathbb{E}_\mu[\varphi_i] = \int_V \varphi_i(y) d\mu(y)$. The expected number of nodes at length 2 from the node at x , denoted by $\widehat{d}_2(x)$, is given by the expectation of degrees of neighbors of the node at x :

$$\begin{aligned} \widehat{d}_2(x) &= n \int_V \nu(x, z) \widehat{d}(z) d\mu(z) \\ &= \sum_{i=1}^N \sum_{j=1}^N \tau_i \tau_j \varphi_i(x) \widetilde{\varphi}_j \int_V \varphi_i(z) \varphi_j(z) d\mu(z) \quad (\text{F10}) \\ &= \sum_{i=1}^N \tau_i^2 \widetilde{\varphi}_i \varphi_i(x), \end{aligned}$$

where we use the result in Eq. F9, and exploit the orthonormality of $\{\varphi_i\}_{i=1}^N$ from Eq. 42. From Eqs. F9 and F10, the criterion of Molloy and Reed [25] suggests that a network percolates when:

$$\begin{aligned} \mathbb{E}_\mu[\widehat{d}_2(x)] &> \mathbb{E}_\mu[\widehat{d}(x)] \\ \implies \sum_{i=1}^N \tau_i \widetilde{\varphi}_i^2 (\tau_i - 1) &> 0. \end{aligned} \quad (\text{F11})$$

Using the spectral condition of percolation from Theorem 2 would suggest $r(T) = \tau_1 > 1$. If the network is

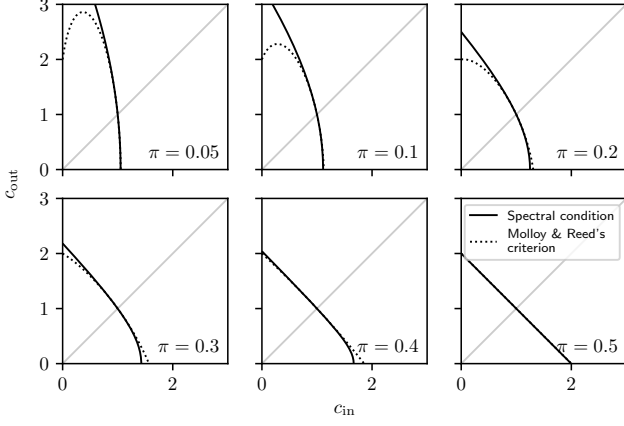


FIG. 24. The criterion of Molloy and Reed [25] coincides with the spectral condition for percolation (Theorem 2) in rank-1 models that exhibit ambiphily, but under/overestimates size of the parameter space permitting percolation in higher rank models that exhibit homophily/heterophily. For a 2-block SBM, with block matrix $B = \begin{pmatrix} c_{in} & c_{out} \\ c_{out} & c_{in} \end{pmatrix}$, and for different values of the proportion of minority community π , we plot the spectral condition for percolation from Eq. 100, and the criterion of Molloy and Reed from Eq. G11.

entirely homophilous such that $\forall i : \tau_i > 0$, then Eq. F11 yields $\tau_1 \leq 1 \implies \mathbb{E}_\mu [\widehat{d}_2(x)] \leq \mathbb{E}_\mu [\widehat{d}(x)]$. By contradiction, Molloy and Reed's criterion implies the spectral condition. On the other hand, consider a network that is entirely heterophilous such that $\tau_1 > 0, \forall i > 1 : \tau_i < 0$. (The largest eigenvalue must still be positive, as described in the proof for Theorem 2.) Then Eq. F11 yields $\tau_1 > 1 \implies \mathbb{E}_\mu [\widehat{d}_2(x)] > \mathbb{E}_\mu [\widehat{d}(x)]$, i.e. the spectral condition implies Molloy and Reed's criterion. Finally, we consider a rank-1 model which has exactly one non-zero eigenvalue: $\tau_1 > 0, \forall i > 1 : \tau_i = 0$. Then Eq. F11 yields $\tau_1 > 1 \iff \mathbb{E}_\mu [\widehat{d}_2(x)] > \mathbb{E}_\mu [\widehat{d}(x)]$. (In fact, using Eqs. F9, F10, we have $\tau_1 > 1 \iff \forall x \in V : \widehat{d}_2(x) > \widehat{d}(x)$.) Hence for rank-1 models, the Molloy and Reed criterion is equivalent to the spectral condition for percolation. However more generally, for higher rank models, the two do not coincide—as illustrated by Fig. F3 for a 2-block SBM.

We emphasize that while it is sufficient for a graph model to have rank-1 to satisfy the criterion of Molloy and Reed, it is not necessary. For instance, consider a k -block planted-partition SBM with equi-sized blocks, mean degree $\langle d \rangle$, and homophily $\delta \in [-\langle d \rangle k / (k-1), \langle d \rangle k]$, as defined in Sec. IV A. Here, every node has the same expected degree $\langle d \rangle$. Then its spectral radius too is given by $\langle d \rangle$, alongside $k-1$ (potentially) non-zero eigenvalues given by $\frac{\delta}{k}$. Therefore the spectral condition for percolation ($\langle d \rangle > 1$) is precisely what the criterion would suggest. But for higher rank models more generally, this is not true.

4. Equivalence of multiplicative graphons and rank-1 models

The formalism of multiplicative graphons allows us to deal with the SPLD, and statistics such as the mean geodesic length analytically. We show here that there is an exact equivalence between multiplicative graphons and rank-1 graph models, which allows us to generalize results on multiplicative graphons to any rank-1 model.

Theorem 6 (Equivalence of rank-1 graph models and multiplicative graphons). *Consider a rank-1 random graph model with a symmetric kernel, i.e. whose integral operator T as defined by Eq. 40 has exactly one non-zero (positive) eigenvalue. Then it has an equivalent representation as a multiplicative graphon. That is, there exists*

- (a) a mapping of the node space $g : V \rightarrow [0, 1]$, and
- (b) a function $f : [0, 1] \rightarrow \mathbb{R}_{\geq 0}$ where $f = O(n^{-\frac{1}{2}})$,

such that for nodes located at $x, y \in V$ with node density μ , we have:

1. $g(x) \sim \mathcal{U}(0, 1)$, and
2. $\nu(x, y) = f(g(x))f(g(y))$.

Proof. The proof constructs a partition of the node space into m subsets, which are mapped to $[0, 1]$. Then, taking the limit of $m \rightarrow \infty$ allows for the multiplicative graphon on $[0, 1] \times [0, 1]$ to approximate the rank-1 model on $V \times V$ to an arbitrary precision.

Let V_1, V_2, \dots, V_m be disjoint measurable and covering subsets of V , i.e. $V = \bigcup_{i=1}^m V_i$ such that $V_i \cap V_j = \emptyset$. Let $\mathbf{1}_X : Y \rightarrow \{0, 1\}$ be the indicator function identifying if $x \in X$, for some $X \subseteq Y$. Define a simple function on V : $s_m(x) \triangleq \sum_i a_i \mathbf{1}_{V_i}(x)$, where $a_i \geq 0$. Essentially, this defines a partition of the node space V such that nodes mapped to the same subset of V have the same value of s_m . This allows for the construction of an equivalent multiplicative graphon.

Define the partition P_m of $[0, 1]$ as:

$$P_m \triangleq \{[u_0, u_1), [u_1, u_2), \dots, [u_{m-1}, u_m)\},$$

such that $u_0 = 0$ and $u_i \triangleq \sum_{j=1}^i \mu(V_j)$, and a node location in V_i is mapped to a location in $[u_{i-1}, u_i)$. It then follows that $u_m \triangleq \mu(V) = 1$, and in the rest of the proof it is implicit that the interval containing 1 is closed. Let $g_m : X \rightarrow [0, 1]$ be a (stochastic) map such that for $x \in V$:

$$g_m(x) \triangleq \sum_{i=1}^m (u_{i-1} + \epsilon \mu(V_i)) \mathbf{1}_{V_i}(x),$$

and $\epsilon \sim \mathcal{U}(0, 1)$. Evidently, g_m is a simple function on V . Consider node $x \in V_i$. Then from its definition, it is clear that $g_m(x)$ follows the uniform distribution over the i^{th}

interval of the partition corresponding to V_i to which x belongs:

$$g_m(x)|_{(x \in V_i)} = u_{i-1} + \epsilon \mu(V_i).$$

Then, the cumulative distribution function of the node locations when mapped to $[0, 1]$ is given by:

$$\begin{aligned} P(g_m(x) \leq p) &= \sum_i P(g_m(x) \leq p)|_{x \in V_i} P(x \in V_i) \\ &= \sum_i \left[\frac{p - u_{i-1}}{\mu(V_i)} \mathbf{1}_{[u_{i-1}, u_i)}(p) + \mathbf{1}_{[u_i, 1)}(p) \right] \mu(V_i) \\ &= \sum_i (p - u_{i-1}) \mathbf{1}_{[u_{i-1}, u_i)}(p) + \sum_i \mu(V_i) \mathbf{1}_{[u_i, 1)}(p) \\ &= \sum_i (p - u_{i-1}) \mathbf{1}_{[u_{i-1}, u_i)}(p) + \sum_i u_{i-1} \mathbf{1}_{[u_{i-1}, u_i)}(p) \\ &= p, \end{aligned}$$

which corresponds to the uniform distribution on $[0, 1]$, i.e. $g_m(x) \sim \mathcal{U}(0, 1)$.

For a rank-1 model, assuming that the kernel is symmetric, we know from Eq. 41b that for nodes $x \in V, y \in V$, the connectivity kernel is of the form $\nu(x, y) = \frac{\tau}{n} \varphi(x) \varphi(y)$, where τ is the eigenvalue of T and φ its corresponding eigenfunction. Then let $f_m : [0, 1] \rightarrow \mathbb{R}_{\geq 0}$ be the map such that for $p \in [0, 1]$:

$$f_m(p) \triangleq \sqrt{\frac{\tau}{n}} \sum_i a_i \mathbf{1}_{[u_{i-1}, u_i)}(p),$$

which is a simple function on $[0, 1]$. Consequently, $f \circ g$ is a simple function on X : $f_m(g_m(x)) = \sqrt{\frac{\tau}{n}} s_m(x)$. For x, y we can define from above:

$$\nu_m(x, y) \triangleq f_m(g_m(x)) f_m(g_m(y)) = \frac{\tau}{n} s_m(x) s_m(y).$$

Since $\nu(x, y)$ is a probability measure on $V \times V$, φ is a non-negative measurable function on V with respect to μ . Therefore, it can be expressed as the pointwise limit of a monotonically increasing sequence of non-negative simple functions s_m . That is, φ can be written as $\lim_{m \rightarrow \infty} s_m$. Since s_m is the composition of simple functions, this also establishes the limits of (g_m) and (f_m) , as $g \triangleq \lim_{m \rightarrow \infty} g_m$ and $f \triangleq \lim_{m \rightarrow \infty} f_m$ respectively, where $f \circ g = \lim_{m \rightarrow \infty} s_m = \varphi$. Therefore, f and g are precisely the functions which will satisfy condition (2). Finally, because $g_m(x) \sim \mathcal{U}(0, 1)$ regardless of m , we obtain condition (1) upon taking the limit. \square

As an application of Theorem 6, a multiplicative graph model with node density μ on the bounded real interval $[a, b] \subset \mathbb{R}$ and connectivity kernel $\nu(x, y) = h(x)h(y)$ can be translated into a multiplicative graphon $W_\times(x, y) = f(x)f(y)$ on $[0, 1]$ via a probability integral transform, i.e. $g(x) = \int_a^x \mu(x) dx$, and $f = h \circ g^{-1}$. The 1-dimensional RDPG of Sec. IV C is an example of such a multiplicative model where $h(x) = \sqrt{\beta x}$.

Asymmetric connectivity kernel. While Theorem 6 makes use of the fact that T is self-adjoint to express the (symmetric) kernel as a product of eigenfunction evaluations i.e. $\nu(x, y) = \frac{\tau}{n} \varphi(x) \varphi(y)$, we can apply the same arguments for an asymmetric kernel of rank 1, as we briefly describe below. Let $\langle A \rangle$ be the non-negative, asymmetric and rank-1 $n \times n$ matrix representing the underlying integral operator T , as in Appendix E. Then, it can be expressed as the outer product of two (non-negative) length- n vectors \mathbf{v}, \mathbf{w} . In fact, assuming $\langle A \rangle$ is irreducible, $\langle A \rangle$ must be strictly positive, since even a single zero value in either \mathbf{v} or \mathbf{w} will render $\langle A \rangle$ as reducible. Thus, applying the Perron theorem [113, 114], these vectors are precisely the right and left eigenvectors of $\langle A \rangle$, i.e. we can write

$$\langle A \rangle = \tau \mathbf{v} \mathbf{w}^T,$$

where τ is the (positive) eigenvalue, and $\mathbf{v}^T \mathbf{w} = 1$. Alternatively, if $\langle A \rangle$ is reducible, then it can be permuted without loss of generality and expressed as the direct sum of a positive matrix and a zero matrix, i.e. $\langle A \rangle = P \text{diag}(\langle A \rangle_1, \langle A \rangle_0) P$, where P is the relevant permutation matrix, $\langle A \rangle_1$ is $q \times q$ rank-1 positive matrix, and $\langle A \rangle_0$ is a $(n - q) \times (n - q)$ zero matrix. Consequently, it can be expressed as an outer product of the direct sum of positive and zero vectors: $\langle A \rangle = \tau (\mathbf{v} \oplus \mathbf{0})(\mathbf{w} \oplus \mathbf{0})^T$, where $\mathbf{0}$ is a zero vector of length $n - q$ and \mathbf{v}, \mathbf{w} are right and left eigenvectors of $\langle A \rangle_1$, and τ the corresponding (positive) eigenvalue. Therefore, it suffices to assume $\langle A \rangle$, and correspondingly T , are positive.

Note that the left eigenvector of $\langle A \rangle$ is the (usual) right eigenvector of its transpose. Analogously, in terms of the integral operator T defined by Eq. 40 on functions on node space V , we can define its adjoint $T^\#$ by [120]:

$$(T^\# f)(x) \triangleq n \int_V \nu(y, x) f(y) d\mu(y). \quad (\text{F12})$$

which is also compact, and of rank 1. Then T and $T^\#$ have the same positive eigenvalue τ , and respective eigenfunctions $\varphi, \varphi^\#$ such that $\int_V \varphi^\#(x) \varphi(x) d\mu(x) = 1$. This allows us to write for the connectivity kernel: $\nu(x, y) = \frac{\tau}{n} \varphi(x) \varphi^\#(y)$. Consequently, we obtain an equivalent asymmetric multiplicative graphon by defining simple functions s_m to converge to φ , and $s_m^\#$ to converge to $\varphi^\#$, resulting in simple functions f_m and $f_m^\#$ which converge to give $\nu(x, y) = f(g(x)) f^\#(g(y))$. That is, Theorem 6 holds for asymmetric kernels, with an additional node function $f^\#$.

Rank-1 approximation. More generally, we remark that we can apply a suitable ‘‘rank-1 approximation’’ to any random graph model, to obtain an estimate of network statistics like the mean geodesic length by making use of the largest eigenvalue τ and its corresponding eigenfunction φ , as we do in Sec. VIA for 2-block SBMs and a variety of real-world networks via graph-coarsening. That is, the theory detailed in Appendices F2 and I1 allows us to convert any random graph model

or real-world network into an equivalent SBM, to which we can apply a rank-1 approximation and obtain approximate closed-form estimates of various geodesic statistics.

Appendix G: Properties of specific graph models

We elaborate below on the key properties and results on expected degree functions, percolation probability function, and the SPLD of random graph models considered in the main text.

1. Stochastic block model

a. General properties

Consider an SBM with k communities, such that a node x belongs to one of the communities $\{1, 2, \dots, k\}$ according to a categorical distribution $x \sim \text{Categorical}(\boldsymbol{\pi})$:

$$\mu(x) = \pi_x, \quad (\text{G1})$$

where the distribution vector $\boldsymbol{\pi}$ encodes the likelihood of being from a community. The connectivity kernel is encoded by the $k \times k$ block matrix B :

$$\nu(x, y) = \frac{B_{xy}}{n}. \quad (\text{G2})$$

Using Eqs. 32 and G2, the expected degree of node in community x is given by:

$$\begin{aligned} \widehat{d}(x) &= n \int_{\{1, 2, \dots, k\}} \nu(x, y) d\mu(y) \\ &= \sum_{y=1}^k B_{xy} \pi_y = [B\boldsymbol{\pi}]_x. \end{aligned} \quad (\text{G3})$$

Similarly the average degree of the network is given from Eq. 31c by:

$$\begin{aligned} \langle d \rangle &= \int_{\{1, 2, \dots, k\}} \widehat{d}(x) d\mu(x) \\ &= \sum_{x=1}^k [B\boldsymbol{\pi}]_x \pi_x = \boldsymbol{\pi}^T B \boldsymbol{\pi}. \end{aligned} \quad (\text{G4})$$

Next, consider the conditional PMF of the SPLD from Eq. 38a, then using Eq. G2:

$$\begin{aligned} \widetilde{\omega}_2(x, y) &= n \int_{\{1, 2, \dots, k\}} \nu(x, z) \nu(z, y) d\mu(z) \\ &= \frac{1}{n} \sum_{z=1}^k B_{xz} B_{zy} \pi_z \\ &= \frac{[B\Pi B]_{xy}}{n} \\ \implies \widetilde{\omega}_l(x, y) &= \frac{[B(\Pi B)^{l-1}]_{xy}}{n}, \end{aligned} \quad (\text{G5})$$

for $l > 0$, where $\Pi \triangleq \text{diag}(\boldsymbol{\pi})$ and the final implication is obtained via induction. Consequently from Eq. 38b we can write the survival function of the SPLD as a ‘‘block matrix’’ containing the survival function of the SPLD between block pairs:

$$\widetilde{\Psi}_l \triangleq \exp\left(-\frac{B}{n} \sum_{i=1}^l (\Pi B)^{i-1}\right). \quad (\text{G6})$$

b. Example: equi-sized planted-partition SBM

For a non-trivial, yet simple, block structure, consider the k -block planted-partition SBM with equi-sized blocks, i.e. $B = \delta I + \beta \mathbf{u}\mathbf{u}^T$ and $\boldsymbol{\pi} = \mathbf{u}/k$, where \mathbf{u} is the all-ones vector of length k . Let the mean degree be $\langle d \rangle$, which from Eq. G4 leads to the constraint:

$$\beta = \langle d \rangle - \frac{\delta}{k}.$$

Here, δ models for the level of homophily (heterophily) in the network. If $\delta > 0$ ($\delta < 0$), communities will connect within each other more (less) strongly than they would outside of each other. B must be a non-negative matrix, which constrains δ to $[-\langle d \rangle k / (k - 1), \langle d \rangle k]$.

We next consider the conditional PMF of geodesic length distribution for this SBM, which from Eq. G5 will involve powers of the matrix ΠB . For any $k \times k$ matrix $M = pI + q\mathbf{u}\mathbf{u}^T$, its matrix powers can be written using a binomial expansion since the matrices I and $\mathbf{u}\mathbf{u}^T$ commute:

$$\begin{aligned} M^n &= (pI + q\mathbf{u}\mathbf{u}^T)^n \\ &= (pI)^n + \sum_{i=1}^n \binom{n}{i} (pI)^{n-i} (q\mathbf{u}\mathbf{u}^T)^i \\ &= p^n I + \sum_{i=1}^n \binom{n}{i} p^{n-i} \frac{(qk)^i}{k} \mathbf{u}\mathbf{u}^T \\ &= p^n I + \frac{(p + qk)^n - p^n}{k} \mathbf{u}\mathbf{u}^T, \\ \sum_{j=1}^l M^j &= \left(\sum_{j=1}^l p^j \right) I + \left[\sum_{j=1}^l (p + qk)^j - \sum_{j=1}^l p^j \right] \frac{\mathbf{u}\mathbf{u}^T}{k}, \\ S_l(M) &= S_l(p)I + \frac{S_l(p + qk) - S_l(p)}{k} \mathbf{u}\mathbf{u}^T, \end{aligned} \quad (\text{G7})$$

where $S_l(a) \triangleq a + a^2 + \dots + a^l = a(a^l - 1)/(a - 1)$ represents the geometric sum of a up to l terms. We can write $\Pi B = \frac{\delta}{k}I + \frac{1}{k}(\langle d \rangle - \frac{\delta}{k})\mathbf{u}\mathbf{u}^T$, then using Eqs. G6 and G7 the survival function block matrix is given by:

$$\widetilde{\Psi}_l = \exp\left(-\frac{1}{n} \{S_l(\delta/k)kI + [S_l(\langle d \rangle) - S_l(\delta/k)]\mathbf{u}\mathbf{u}^T\}\right). \quad (\text{G8})$$

c. Percolation threshold

General SBM. Consider the percolation threshold for a general SBM, which we saw in Sec. V is given by the spectral radius of $B\Pi$. We first show that $B\Pi$ has the same spectrum as $\Pi^{\frac{1}{2}}B\Pi^{\frac{1}{2}}$. Let (τ, \mathbf{v}) be an eigenpair for $\Pi^{\frac{1}{2}}B\Pi^{\frac{1}{2}}$, then we can write:

$$\begin{aligned} \Pi^{\frac{1}{2}}B\Pi^{\frac{1}{2}}\mathbf{v} &= \tau\mathbf{v} \\ \implies B\Pi\Pi^{-\frac{1}{2}}\mathbf{v} &= \tau\Pi^{-\frac{1}{2}}\mathbf{v} \\ \implies B\Pi\mathbf{u} &= \tau\mathbf{u}, \end{aligned}$$

where $\mathbf{u} \triangleq \Pi^{-\frac{1}{2}}\mathbf{v}$ is the corresponding eigenvector with the same eigenvalue τ for $B\Pi$. This allows us to consider the eigendecomposition of the symmetric matrix $\Pi^{\frac{1}{2}}B\Pi^{\frac{1}{2}}$ (if we have a symmetric block matrix B). This is also useful when making a rank-1 approximation of the SBM. That is, if τ is the spectral radius of $\Pi^{\frac{1}{2}}B\Pi^{\frac{1}{2}}$ with the corresponding eigenvector \mathbf{v} , then the affinities between two nodes from blocks x and y is approximately given by

$$B_{xy} \approx \frac{\tau v_x v_y}{\sqrt{\pi_x \pi_y}} \quad (\text{G9})$$

2-block SBM. Consider the 2-block SBM from Sec. V where the minority community occupies $0 \leq \pi < 0.5$ of the share. Consider a planted-partition block matrix given by $B = \begin{pmatrix} c_{\text{in}} & c_{\text{out}} \\ c_{\text{out}} & c_{\text{in}} \end{pmatrix}$, where c_{in} accounts for intra-group affinity whereas c_{out} for inter-group affinity. Then the eigenvalues are given by solving the eigenvalue equation:

$$\begin{aligned} (\Pi^{\frac{1}{2}}B\Pi^{\frac{1}{2}} - \tau I)\mathbf{v} &= 0 \\ \implies \left| \begin{pmatrix} c_{\text{in}}\pi - \tau & c_{\text{out}}\sqrt{\pi(1-\pi)} \\ c_{\text{out}}\sqrt{\pi(1-\pi)} & c_{\text{in}}(1-\pi) - \tau \end{pmatrix} \right| &= 0 \\ \implies \tau^2 - c_{\text{in}}\tau + (c_{\text{in}}^2 - c_{\text{out}}^2)\pi(1-\pi) &= 0, \end{aligned}$$

which gives two (real) eigenvalues:

$$\tau_1, \tau_2 = \frac{c_{\text{in}}}{2} \left\{ 1 \pm \sqrt{1 + 4\pi(1-\pi) \left[\left(\frac{c_{\text{out}}}{c_{\text{in}}} \right)^2 - 1 \right]} \right\}. \quad (\text{G10})$$

To contrast with the Molloy and Reed criterion for percolation (see Appendix F3), one can write for this 2-block SBM the condition for expected number of neighbors-of-neighbors (Eq. F10) to be equal to the expected number of neighbors as (Eq. 32):

$$c_{\text{in}}^2(1-3\tilde{\pi}) + c_{\text{out}}^2\tilde{\pi} - c_{\text{in}}(1-2\tilde{\pi}) - 2c_{\text{out}}\tilde{\pi} + 2c_{\text{in}}c_{\text{out}}\tilde{\pi} = 0, \quad (\text{G11})$$

where $\tilde{\pi} \triangleq \pi(1-\pi)$.

Constant mean degree SBM. Consider the case of an SBM where the mean degree is held constant while its homophily is varied between its extremes. Let $\delta \triangleq c_{\text{in}} -$

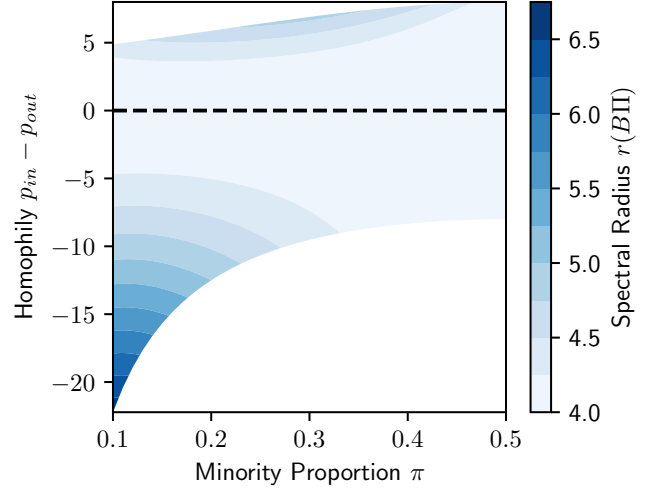


FIG. 25. Spectral radius of a 2-block planted-partition SBM is determined not only by the mean degree—held constant here at $\langle d \rangle = 4$ —but by the level of homophily $\delta = c_{\text{in}} - c_{\text{out}}$ and proportion of minority community π , as given by Eq. G13. Thus, the level of homophily can strongly impact network connectivity, regardless of mean degrees. Horizontal asymptote marks ambiphily—an ER graph.

c_{out} indicate homophily, then from Eq. G4, we know the mean degree $\langle d \rangle$ is given by:

$$\begin{aligned} \langle d \rangle &= c_{\text{in}}[1 - 2\pi(1-\pi)] + 2c_{\text{out}}\pi(1-\pi) \\ &= c_{\text{out}} + \delta[1 - 2\pi(1-\pi)] \\ \implies \delta &= \frac{\langle d \rangle - c_{\text{out}}}{1 - 2\pi(1-\pi)} \quad (\text{G12}) \\ \implies \delta &\in \left[\frac{-\langle d \rangle}{2\pi(1-\pi)}, \frac{\langle d \rangle}{1 - 2\pi(1-\pi)} \right], \end{aligned}$$

where we obtain the constraint on δ by setting the extreme values of perfect heterophily ($c_{\text{in}} = 0$) and perfect homophily ($c_{\text{out}} = 0$). Putting in Eq. G10, and setting $p \triangleq 2\pi(1-\pi)$, we get:

$$\tau_1, \tau_2 = \frac{\langle d \rangle + p\delta \pm \sqrt{(\langle d \rangle - p\delta)^2 + 2p\delta^2(1-2p)}}{2}. \quad (\text{G13})$$

Evidently then, the spectral radius i.e. τ_1 , whose value determines the percolation threshold, is a function of both the mean degree and homophily. In Fig. G1c, we plot the the variation in τ_1 for this 2-block SBM as the proportion of minority community π and the level of homophily δ is varied, while holding the mean degree constant at $\langle d \rangle = 4$.

2. Random dot-product graph

a. General properties

Consider a k -dimensional non-negative bounded subspace $X \subset \mathbb{R}_{\geq 0}^k$ in which the nodes are “embedded” by any distribution $\mu(\mathbf{x})$. We focus on the simplest connectivity kernel here:

$$\nu(\mathbf{x}, \mathbf{y}) = \beta \mathbf{x}^T \mathbf{y}, \quad (\text{G14})$$

where $\beta > 0, \beta = O(n^{-1})$ controls the mean degree. Then using Eqs. 32 and G14, the expected degree at location \mathbf{x} is given by:

$$\begin{aligned} \widehat{d}(\mathbf{x}) &= n \int_X \nu(\mathbf{x}, \mathbf{y}) d\mu(\mathbf{y}) \\ &= n\beta \mathbf{x}^T \int_X \mathbf{y} d\mu(\mathbf{y}) \\ &\triangleq n\beta \mathbf{x}^T \boldsymbol{\phi}, \end{aligned} \quad (\text{G15})$$

where $\boldsymbol{\phi} = \int_X \mathbf{x} d\mu(\mathbf{x})$ is the vector representing mean location of nodes in X . Hence, the degree of a node is given by taking the dot-product of its location with the mean location of all nodes, scaled by $n\beta$. Similarly, using Eq. 31c, the average degree of the whole network is given by:

$$\begin{aligned} \langle d \rangle &= \int_X d(\mathbf{x}) d\mu(\mathbf{x}) \\ &= n\beta \boldsymbol{\phi}^T \int_X \mathbf{x} d\mu(\mathbf{x}) \\ &= n\beta \boldsymbol{\phi}^T \boldsymbol{\phi} = n\beta \|\boldsymbol{\phi}\|^2. \end{aligned} \quad (\text{G16})$$

Consider the conditional PMF of the SPLD from Eq. 38a, then using Eq. G14:

$$\begin{aligned} \widetilde{\omega}_2(\mathbf{x}, \mathbf{y}) &= n \int_X \nu(\mathbf{x}, \mathbf{z}) \nu(\mathbf{z}, \mathbf{y}) d\mu(\mathbf{z}) \\ &= \beta \mathbf{x}^T \left[n\beta \int_X \mathbf{z} \mathbf{z}^T d\mu(\mathbf{z}) \right] \mathbf{y} \\ &\triangleq \beta \mathbf{x}^T \Phi \mathbf{y} \\ \implies \widetilde{\omega}_l(\mathbf{x}, \mathbf{y}) &= \beta \mathbf{x}^T \Phi^{l-1} \mathbf{y}, \end{aligned} \quad (\text{G17})$$

for $l > 0$, where $\Phi \triangleq n\beta \int_X \mathbf{x} \mathbf{x}^T d\mu(\mathbf{x})$ refer to the $k \times k$ matrix of second moments—which essentially encodes the covariance in space X as per the measure μ , and is necessarily positive semi-definite. The last implication can be seen via a simple induction.

b. Example: standard simplex RDPG

As a concrete example, consider X to be restricted to the $(k-1)$ -standard simplex in \mathbb{R}^k , i.e. $X = \{\mathbf{x} \in \mathbb{R}^k : \sum_{i=1}^k x_i = 1, x_i \geq 0 \forall i \in \{1, 2, \dots, k\}\}$ and μ

corresponding to the Dirichlet distribution on that simplex given by the concentration vector $\boldsymbol{\alpha} \in [0, \infty)^k$. Hence a node at $\mathbf{x} \in [0, 1]^k$, constrained to $\mathbf{x}^T \mathbf{u} = 1$, has a location in X that follows the Dirichlet distribution:

$$\mu(\mathbf{x}) = \frac{\prod_{i=1}^k \Gamma(\alpha_i) x_i^{\alpha_i - 1}}{\Gamma\left(\sum_{i=1}^k \alpha_i\right)}, \quad (\text{G18})$$

where $\Gamma(\cdot)$ is the gamma function. This formalism interprets the node’s location as the likelihood of belonging to one of k communities located at the corners of the simplex—a continuous analogue of the SBM. Let $\bar{\alpha} = \boldsymbol{\alpha}^T \mathbf{u}$, then the mean of this distribution is the usual mean of a Dirichlet distribution [121] i.e. $\boldsymbol{\phi} = \frac{\boldsymbol{\alpha}}{\bar{\alpha}}$. Consider the scaled matrix of second moments:

$$\begin{aligned} \Phi &= n\beta \int_X \mathbf{x} \mathbf{x}^T d\mu(\mathbf{x}) \\ &= n\beta \int_X (\mathbf{x} - \boldsymbol{\phi} + \boldsymbol{\phi})(\mathbf{x} - \boldsymbol{\phi} + \boldsymbol{\phi})^T d\mu(\mathbf{x}) \\ &= n\beta \left[\int_X (\mathbf{x} - \boldsymbol{\phi})(\mathbf{x} - \boldsymbol{\phi})^T d\mu(\mathbf{x}) \right. \\ &\quad \left. + \int_X \cancel{\boldsymbol{\phi}(\mathbf{x} - \boldsymbol{\phi})^T} d\mu(\mathbf{x}) + \int_X \cancel{(\mathbf{x} - \boldsymbol{\phi})\boldsymbol{\phi}^T} d\mu(\mathbf{x}) + \boldsymbol{\phi}\boldsymbol{\phi}^T \right] \\ &= n\beta(\Sigma + \boldsymbol{\phi}\boldsymbol{\phi}^T), \end{aligned} \quad (\text{G19})$$

where $\Sigma = \int_X (\mathbf{x} - \boldsymbol{\phi})(\mathbf{x} - \boldsymbol{\phi})^T d\mu(\mathbf{x})$ is the covariance matrix, which for the Dirichlet distribution can be written as $\Sigma = \frac{1}{\bar{\alpha}^2(1+\bar{\alpha})} [\bar{\alpha} \text{diag}(\boldsymbol{\alpha}) - \boldsymbol{\alpha}\boldsymbol{\alpha}^T]$ [121]. Thus using Eq. G19 and the expression $\boldsymbol{\phi} = \frac{\boldsymbol{\alpha}}{\bar{\alpha}}$ leads to $\Phi = \frac{n\beta}{\bar{\alpha}(1+\bar{\alpha})} [\text{diag}(\boldsymbol{\alpha}) + \boldsymbol{\alpha}\boldsymbol{\alpha}^T]$. Let d be the mean degree of the network, then from Eq. G16 we have $\beta = \frac{d\bar{\alpha}^2}{n\|\boldsymbol{\alpha}\|^2}$. Altogether, the expression for conditional PMF of the SPLD for this RDPG from Eq. G17 is given by: $\widetilde{\omega}_l(\mathbf{x}, \mathbf{y}) =$

$$\frac{d\bar{\alpha}^2}{n\|\boldsymbol{\alpha}\|^2} \mathbf{x}^T \left\{ \frac{d\bar{\alpha}}{\|\boldsymbol{\alpha}\|^2(1+\bar{\alpha})} [\text{diag}(\boldsymbol{\alpha}) + \boldsymbol{\alpha}\boldsymbol{\alpha}^T] \right\}^{l-1} \mathbf{y}. \quad (\text{G20})$$

c. Example: non-linear RDPG

In this paper, the SPLD framework for RDPGs assumes that the connectivity kernel $\nu(\mathbf{x}, \mathbf{y})$ is linear in the dot-product $\mathbf{x}^T \mathbf{y}$. As discussed in Sec. IV C, any positive semi-definite kernel can be written as a dot product in some feature space. In particular, the symmetric positive semi-definite kernel $\nu_{\geq 0}(x, y)$ for node locations $x, y \in V$ defines a “feature map” h to a Hilbert space H , i.e. $h : V \rightarrow H$, such that $\nu_{\geq 0}(x, y) = \langle h(x), h(y) \rangle_H$, where $\langle \cdot, \cdot \rangle_H$ indicates the inner-product. In other words, ν is the reproducing kernel for H over the node space: H is a reproducing kernel Hilbert space (RKHS) where

node-wise function evaluation is given by a continuous linear functional. For some kernels—like the polynomial kernel— H is a Euclidean space equipped with the usual dot-product, while for others—like the radial basis or “Gaussian” function kernel—we can derive an explicit map $g : V \rightarrow \mathbb{R}^k$ such that $\nu_{\geq 0}(x, y) = \langle h(x), h(y) \rangle_H \approx g(x)^T g(y)$ [71].

By way of example, consider the “node2vec” graph embedding model of Ref. [69], where the connectivity kernel is proportional to $\exp(\mathbf{x}^T \mathbf{y})$. This can be seen as a “non-linear” RDPG, i.e. an RDPG where the connectivity kernel is a non-linear function of $\mathbf{x}^T \mathbf{y}$. We make use of an explicit randomized feature map $g : \mathbb{R}^d \rightarrow \mathbb{R}^k$ such that the connectivity kernel in \mathbb{R}^d is well-approximated by the corresponding dot-product in \mathbb{R}^k [71], i.e. $\nu(\mathbf{x}, \mathbf{y}) \approx g(\mathbf{x})^T g(\mathbf{y})$. This allows us to apply results from the SPLD framework of “linear” RDPGs to this “exponential” RDPG.

Lemma 6 (Linearization of exponential RDPG). *Let $X \subset \mathbb{R}^d$ be a node space with node density μ and connectivity kernel $\nu(\mathbf{x}, \mathbf{y}) = \beta \exp(\mathbf{x}^T \mathbf{y})$. Then there exists a map $g : \mathbb{R}^d \rightarrow \mathbb{R}^k$ which approximately linearizes this RDPG model i.e. $\nu(\mathbf{x}, \mathbf{y}) \approx \beta g(\mathbf{x})^T g(\mathbf{y})$. There also exist corresponding length- k mean vector ϕ_g , $k \times k$ matrix of second moments Φ_g , and length- k mean percolation vector ρ_g , which can be used to evaluate the percolation probability function and geodesic length distribution functions for this model in \mathbb{R}^k .*

Proof. First, note that the exponential kernel can be expressed as a Gaussian shift-invariant kernel in \mathbb{R}^d :

$$\begin{aligned} \nu(\mathbf{x}, \mathbf{y}) &= \beta \exp(\mathbf{x}^T \mathbf{y}) \\ &= \beta \exp\left(\frac{\|\mathbf{x}\|^2 + \|\mathbf{y}\|^2 - \|\mathbf{x} - \mathbf{y}\|^2}{2}\right) \quad (\text{G21}) \\ &= \beta h(\mathbf{x} - \mathbf{y}) f(\mathbf{x}) f(\mathbf{y}), \end{aligned}$$

where $\beta = O(n^{-1})$, $h(\Delta) \triangleq \exp\left(\frac{-\|\Delta\|^2}{2}\right)$ and $f(\mathbf{x}) \triangleq \exp\left(\frac{\|\mathbf{x}\|^2}{2}\right)$. To obtain an explicit feature map for $\nu(\mathbf{x}, \mathbf{y})$ requires an explicit map for $h(\Delta)$. For that, we use Algorithm 1 in Ref. [71] to compute “random Fourier features” for the Gaussian kernel $h(\Delta)$. More precisely:

1. Draw k i.i.d. samples $\{\mathbf{w}_i\}_{i=1}^k$ from the Fourier transform of the Gaussian function, which is given by the standard multivariate Gaussian distribution:

$$P(\mathbf{w}) = (2\pi)^{-\frac{k}{2}} \exp\left(-\frac{\|\mathbf{w}\|^2}{2}\right).$$

2. Draw k i.i.d. samples $\{b_i\}_{i=1}^k$ from the uniform distribution on $[0, 2\pi]$.

Then for $\mathbf{x} \in \mathbb{R}^d$, the feature map $g(\mathbf{x})$ is given by:

$$g(\mathbf{x}) \triangleq f(\mathbf{x}) \sqrt{\frac{2}{d}} \left(\cos(\mathbf{w}_1^T \mathbf{x} + b_1), \dots, \cos(\mathbf{w}_k^T \mathbf{x} + b_k) \right). \quad (\text{G22})$$

We can thus define a corresponding “linear RDPG” in \mathbb{R}^k , i.e. for nodes $\mathbf{x}, \mathbf{y} \in \mathbb{R}^d$:

$$\nu(\mathbf{x}, \mathbf{y}) \approx \nu_g(\mathbf{x}, \mathbf{y}) \triangleq \beta g(\mathbf{x})^T g(\mathbf{y}), \quad (\text{G23})$$

where the approximation gets better for larger values of k [71].

Recall from Sec. IV C that computing the degree or SPLD in a linear RDPG only requires the mean vector and matrix of second moments, and not the full node distribution. This can be put to use here, by making an m -block SBM approximation of the given non-linear RDPG—see Appendix F 2 b—denoted here by $(Z, \boldsymbol{\pi}, B)$. Since the random Fourier feature map is smooth with high probability [71], the SBM approximation can be used. and we can estimate the random feature mapping of the grid points Z to \mathbb{R}^k given by the $k \times m$ matrix Z_g whose i^{th} column is given by the vector $g(Z_{:,i})$. Consequently, mean vector ϕ_g and matrix of second moments Φ_g in \mathbb{R}^k , and the mean percolation vector from Eq. F7, are given by:

$$\phi_g = Z_g \boldsymbol{\pi} \quad (\text{G24a})$$

$$\Phi_g = n \beta Z_g \text{diag}(\boldsymbol{\pi}) Z_g^T \quad (\text{G24b})$$

$$\boldsymbol{\rho}_g = \phi_g - Z_g \text{diag}(\boldsymbol{\pi}) \exp(-n \beta Z_g^T \boldsymbol{\rho}_g) \quad (\text{G24c})$$

Therefore, geodesic statistics for any node pair $\mathbf{x} \in \mathbb{R}^d, \mathbf{y} \in \mathbb{R}^d$ can be computed by mapping them to \mathbb{R}^k using Eq. G22, and then making use of the connectivity kernel in Eq. G23, and of Eq. G24 to extract statistics from the corresponding linear RDPG. \square

In Fig. 26, we show for an exponential kernel defined on $[-1, 1]$ both the kernel estimate $\nu_g(x, y)$ and corresponding expected geodesic length $\langle \lambda_{xy}^g \rangle$ between nodes $(x, y) \in [-1, 1] \times [-1, 1]$, for varying number of random Fourier features k . Evidently, as the number of features increases, the “linear RDPG approximation” significantly improves, asymptotically matching up to the true connectivity kernel, and corresponding expected geodesic lengths estimated via numerical integration. For other non-linear kernels, the same method follows by using their Fourier transforms.

3. Gaussian random geometric graph

a. General properties

Consider the k -dimensional Euclidean space \mathbb{R}^k , wherein nodes are distributed according to a multivariate Gaussian distribution with mean vector \mathbf{m} and (full-rank) covariance matrix Σ :

$$\mu(\mathbf{x}) = \frac{1}{\sqrt{(2\pi)^k |\Sigma|}} \exp\left(-\frac{1}{2}(\mathbf{x} - \mathbf{m})^T \Sigma^{-1}(\mathbf{x} - \mathbf{m})\right),$$

where $|\Sigma|$ is the determinant of Σ , and (undirected) edges are added according to a Gaussian connectivity kernel

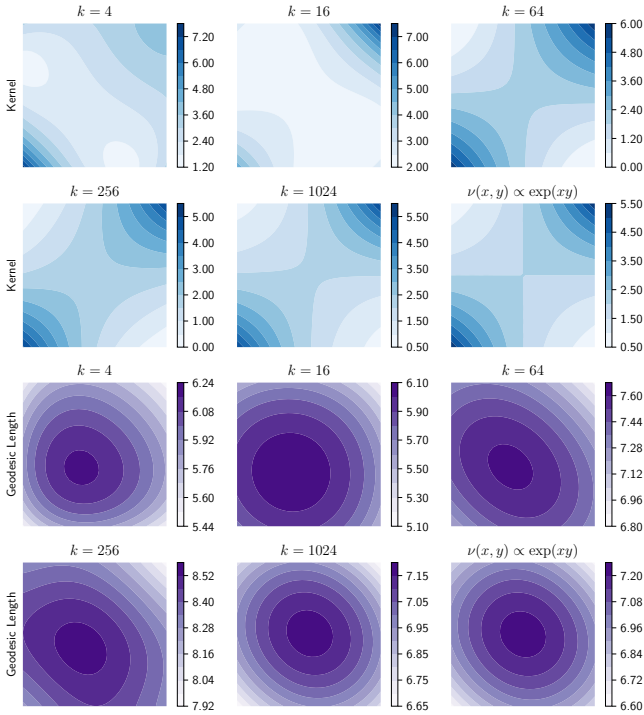


FIG. 26. Linearization of an exponential RDPG using random Fourier features [71] with varying number of features $k \in \{4, 16, 64, 256, 1024\}$. The exponential kernel $\nu(x, y) = \frac{\beta}{n} \exp(xy)$ is defined on $V = [-1, 1]$, with $\beta = 2$, $n = 512$, and where nodes follow a scaled beta distribution with parameters $(0.2, 0.8)$. Upper (blue) subplots correspond to the kernel estimate $\nu_g(x, y)$ on $V \times V$ from Eq. G23 using k features, with the last subplot indicating the original kernel $\nu(x, y)$. Similarly, lower (purple) subplots indicate the expected geodesic length $\langle \lambda_{xy} \rangle$ computed from the approximate closed-form of the geodesic length distribution for a linear RDPG given by Eq. 62—making use of Eqs. G22, G24—with the last subplot using the original kernel $\nu(x, y)$ to obtain the expected geodesic length from the approximate closed-form for a general random graph model as given by Eq. 46, obtained via iterative numerical integration on V . Despite stochasticity in the sampling of Fourier features, larger values of k evidently improve the approximation, with the linear RDPG having $k = 1024$ providing the closest estimates.

with the (positive-definite and symmetric) scale matrix R , as given by Eq. 65. Succinctly, we refer to this as the (\mathbf{m}, Σ, R) Gaussian RGG.

Sufficiency of the standard Gaussian RGG. First, we show that this Gaussian RGG can be uniquely mapped to a “standard Gaussian RGG” given by $(0, I, S)$ where I is the $k \times k$ identity matrix, i.e. where the node distribution is standard multivariate Gaussian. Since Σ is a full-rank covariance matrix, it must be real, symmetric, and with positive eigenvalues. Let us express it via its eigendecomposition: $\Sigma = U\Lambda U^T$, where U is an orthonormal matrix with eigenvectors stacked column-wise, and Λ is the diagonal matrix with corresponding eigenvalues on the diagonal. Then, define the affine whitening

transform $f : \mathbb{R}^k \rightarrow \mathbb{R}^k$

$$f(\mathbf{x}) \triangleq \Lambda^{-\frac{1}{2}} U^T (\mathbf{x} - \mathbf{m}),$$

which maps to values distributed by $\mathcal{N}(0, I)$. We also require a new connectivity kernel $\nu_w(\mathbf{x}, \mathbf{y})$ for the whitened space, which from Eq. 65 will be given by substituting \mathbf{x} with $f^{-1}(\mathbf{x})$ to obtain $\nu_w(\mathbf{x}, \mathbf{y}) =$

$$\begin{aligned} & \beta \exp \left(-\frac{1}{2} [f^{-1}(\mathbf{x}) - f^{-1}(\mathbf{y})]^T R^{-1} [f^{-1}(\mathbf{x}) - f^{-1}(\mathbf{y})] \right) \\ &= \beta \exp \left(-\frac{1}{2} (\mathbf{x} - \mathbf{y})^T \Lambda^{\frac{1}{2}} U^T R^{-1} U \Lambda^{\frac{1}{2}} (\mathbf{x} - \mathbf{y}) \right), \end{aligned}$$

which leads to a standard Gaussian RGG given by $(\mathbf{0}, I, \Lambda^{-\frac{1}{2}} U^T R U \Lambda^{-\frac{1}{2}})$. We remark that if R commutes with Σ , then they have the same eigenvectors—i.e. connectivity directions are oriented along the same axes as the node distribution—and we can write $R = U\Gamma U^T$. Consequently, we obtain a diagonal scale matrix $\Lambda\Gamma$.

In any case, it is sufficient to study a standard Gaussian RGG to obtain geodesic statistics for general Gaussian RGGs, as we do through the rest of this paper. Therefore, while we maintain the connectivity kernel in Eq. 65, we use the standard normal node distribution from Eq. 66. It will be useful to state the following multivariate Gaussian integral:

$$\int_{\mathbb{R}^k} \exp \left(-\frac{\mathbf{x}^T C \mathbf{x}}{2} + \mathbf{v}^T \mathbf{x} \right) d\mathbf{x} = \frac{(2\pi)^{\frac{k}{2}}}{\sqrt{|C|}} \exp \left(\frac{\mathbf{v}^T C^{-1} \mathbf{v}}{2} \right). \quad (\text{G25})$$

Using Eqs. 32, 66, 65 the expected degree at location \mathbf{x} is given by $\hat{d}(\mathbf{x})$

$$\begin{aligned} &= n \int_{\mathbb{R}^k} \nu(\mathbf{x}, \mathbf{y}) d\mu(\mathbf{y}) \\ &= \frac{n\beta}{(2\pi)^{\frac{k}{2}}} \int_{\mathbb{R}^k} \exp \left(-\frac{1}{2} [(\mathbf{x} - \mathbf{y})^T R^{-1} (\mathbf{x} - \mathbf{y}) \right. \\ &\quad \left. + \mathbf{y}^T \mathbf{y}] \right) d\mathbf{y} \\ &= \frac{n\beta}{(2\pi)^{\frac{k}{2}}} \exp \left(-\frac{\mathbf{x}^T R^{-1} \mathbf{x}}{2} \right) \\ &\quad \times \int_{\mathbb{R}^k} \exp \left(-\frac{\mathbf{y}^T (I + R^{-1}) \mathbf{y}}{2} + \mathbf{x}^T R^{-1} \mathbf{y} \right) d\mathbf{y} \\ &= \frac{n\beta}{\sqrt{|I + R^{-1}|}} \exp \left(-\frac{\mathbf{x}^T [R^{-1} - R^{-1} (I + R^{-1})^{-1} R^{-1}] \mathbf{x}}{2} \right) \\ &= \frac{n\beta}{\sqrt{|I + R^{-1}|}} \exp \left(-\frac{\mathbf{x}^T R^{-1} (I + R^{-1})^{-1} \mathbf{x}}{2} \right) \\ &= \frac{n\beta}{\sqrt{|I + R^{-1}|}} \exp \left(-\frac{\mathbf{x}^T (I + R)^{-1} \mathbf{x}}{2} \right), \end{aligned} \quad (\text{G26})$$

where in the fourth equality we use Eq. G25, and in the fifth equality we use a special case of the Woodbury

matrix identity (WMI): $(I + M)^{-1} = I - (I + M)^{-1}M$. Similarly, using Eqs. 31c, G26, 66 the average degree of the whole network is given by

$$\begin{aligned} \langle d \rangle &= \int_{\mathbb{R}^k} d(\mathbf{x}) d\mu(\mathbf{x}) \\ &= \frac{n\beta}{(2\pi)^{\frac{k}{2}} \sqrt{|I + R^{-1}|}} \int_{\mathbb{R}^k} \exp\left(-\frac{\mathbf{x}^T [I + (I + R)^{-1}] \mathbf{x}}{2}\right) d\mathbf{x} \\ &= \frac{n\beta}{\sqrt{|I + R^{-1}| |I + (I + R)^{-1}|}}. \end{aligned} \quad (\text{G27})$$

Next, consider the conditional PMF of the SPLD from Eq. 38a. We apply an ansatz: by symmetry of this function, it will take a form wherein terms of $\|\mathbf{x} - \mathbf{y}\|^2$ are weighted by some functions of l as:

$$\begin{aligned} \tilde{\omega}_l(\mathbf{x}, \mathbf{y}) &= c_l \exp\left(-\frac{1}{2}(\mathbf{x}^T R^{-1} U_l \mathbf{x} + \mathbf{y}^T R^{-1} U_l \mathbf{y} \right. \\ &\quad \left. - 2\mathbf{x}^T R^{-1} W_l \mathbf{y})\right), \end{aligned} \quad (\text{G28})$$

where U_l, W_l are symmetric matrices. Then, using Eqs. 38a, 66, 65, we get $\tilde{\omega}_{l+1}(\mathbf{x}, \mathbf{y})$

$$\begin{aligned} &= n \int_{\mathbb{R}^k} \tilde{\omega}_l(\mathbf{x}, \mathbf{z}) \nu(\mathbf{z}, \mathbf{y}) d\mu(\mathbf{z}) \\ &= \frac{c_l n \beta}{(2\pi)^{\frac{k}{2}}} \int_{\mathbb{R}^k} \exp\left(-\frac{1}{2}(\mathbf{x}^T R^{-1} U_l \mathbf{x} + \mathbf{z}^T R^{-1} U_l \mathbf{z} \right. \\ &\quad \left. - 2\mathbf{x}^T R^{-1} W_l \mathbf{z} + \mathbf{z}^T R^{-1} \mathbf{z} + \mathbf{y}^T R^{-1} \mathbf{y} - 2\mathbf{y}^T R^{-1} \mathbf{z} \right. \\ &\quad \left. + \mathbf{z}^T \mathbf{z})\right) d\mathbf{z} \\ &= \frac{c_l n \beta}{(2\pi)^{\frac{k}{2}}} \exp\left(-\frac{1}{2}(\mathbf{x}^T R^{-1} U_l \mathbf{x} + \mathbf{y}^T R^{-1} \mathbf{y})\right) \\ &\quad \times \int_{\mathbb{R}^k} \exp\left(-\frac{1}{2}[\mathbf{z}^T (I + R^{-1} U_l + R^{-1}) \mathbf{z} \right. \\ &\quad \left. - (\mathbf{x}^T R^{-1} W_l + \mathbf{y}^T R^{-1}) \mathbf{z}]\right) d\mathbf{z} \\ &= \frac{c_l n \beta}{\sqrt{|V_l|}} \exp\left(-\frac{1}{2}[\mathbf{x}^T R^{-1} U_l \mathbf{x} + \mathbf{y}^T R^{-1} \mathbf{y} - \right. \\ &\quad \left. (\mathbf{x}^T R^{-1} W_l + \mathbf{y}^T R^{-1}) V_l^{-1} (W_l R^{-1} \mathbf{x} + R^{-1} \mathbf{y})]\right) \\ &\quad (\text{where } V_l \triangleq I + R^{-1} + R^{-1} U_l) \\ &= \frac{c_l n \beta}{\sqrt{|V_l|}} \exp\left(-\frac{1}{2}[\mathbf{x}^T R^{-1} (U_l - W_l V_l^{-1} W_l R^{-1}) \mathbf{x} + \right. \\ &\quad \left. \mathbf{y}^T R^{-1} (I - V_l^{-1} R^{-1}) \mathbf{y} - 2\mathbf{x}^T R^{-1} W_l V_l^{-1} R^{-1} \mathbf{y}]\right) \\ &\triangleq c_{l+1} \exp\left(-\frac{1}{2}(\mathbf{x}^T R^{-1} U_{l+1} \mathbf{x} + \mathbf{y}^T R^{-1} U_{l+1} \mathbf{y} \right. \\ &\quad \left. - 2\mathbf{x}^T R^{-1} W_{l+1} \mathbf{y})\right), \end{aligned} \quad (\text{G29})$$

where we have again applied Eq. G25 to obtain the fourth equality. Given the ansatz in Eq. G28 to be satisfied for $l + 1$, and using $R V_l = I + R + U_l$, we can write the following set of recursive equations:

$$U_{l+1} = I - (I + R + U_l)^{-1}, \quad (\text{G30a})$$

$$W_{l+1} = W_l (I + R + U_l)^{-1}, \quad (\text{G30b})$$

$$c_{l+1} = c_l n \beta |I + R^{-1} + R^{-1} U_l|^{-\frac{1}{2}}. \quad (\text{G30c})$$

For the approximate closed-form SPLD: $\omega_1(\mathbf{x}, \mathbf{y}) = \nu(\mathbf{x}, \mathbf{y})$. Combining with the ansatz in Eq. G28 gives the base cases $U_l = W_l = I$ and $c_1 = \beta$, which can then be used to solve Eq. G30, and thus provide the expression for conditional PMF from Eq. G28.

Highly spatial Gaussian RGG. Consider a highly ‘‘spatial’’ Gaussian RGG, wherein the connection scales are much smaller than the variance, i.e. $R \rightarrow 0$. This simplifies solving Eq. G30, since as $R \rightarrow 0$, from Eq. G30 we get:

$$\begin{aligned} U_{l+1} &\rightarrow I - (I + U_l)^{-1} = (I + U_l)^{-1} U_l, \\ W_{l+1} &\rightarrow W_l (I + U_l)^{-1}, \\ c_{l+1} &\rightarrow c_l n \beta \sqrt{\frac{|R|}{|I + U_l|}}. \end{aligned} \quad (\text{G31})$$

where in the first limit we make use of WMI. Putting in the base cases, we obtain closed-forms:

$$\begin{aligned} U_l &\rightarrow \frac{1}{l} I, \\ W_l &\rightarrow \frac{1}{l} I, \\ c_l &\rightarrow \beta \left(n \beta \sqrt{|R|}\right)^{l-1} l^{-\frac{k}{2}}, \end{aligned} \quad (\text{G32})$$

Note from Eq. G27 that the mean degree approaches

$$\langle d \rangle \rightarrow n \beta \sqrt{|R|} 2^{-\frac{k}{2}}.$$

Putting in Eq. G28 yields the expression for the approximate closed-form of the conditional PMF of the SPLD in Eq. 70.

b. Percolation threshold

Consider the percolation threshold for Gaussian RGGs. Let T be the integral operator defined by Eq. 40, then the percolation criterion is $r(T) > 1$, i.e. its spectral radius. Let $f \in F$ be an eigenfunction of T in the function space $F : \mathbb{R}^k \rightarrow \mathbb{R}$. Given the form of the node distribution in Eq. 66 being a Gaussian centered at 0, we restrict F to the space of functions which map the input to the exponential of negative of its quadratic form with respect to some (positive-definite) matrix. That is, f has the form:

$$f(\mathbf{x}; \alpha, C) = \alpha \exp\left(-\frac{1}{2} \mathbf{x}^T C^{-1} \mathbf{x}\right), \quad (\text{G33})$$

where $\alpha \in \mathbb{R} \setminus \{0\}$ and C is a positive-definite matrix. Applying T on f using Eqs. 40, G33, 65 and 66, we obtain:

$$\begin{aligned}
(Tf)(x) &= n \int_{\mathbb{R}^k} \nu(\mathbf{x}, \mathbf{y}) f(\mathbf{y}) d\mu(\mathbf{y}) \\
&= \frac{\alpha n \beta}{(2\pi)^{\frac{k}{2}}} \exp\left(-\frac{\mathbf{x}^T R^{-1} \mathbf{x}}{2}\right) \int_{\mathbb{R}^k} \exp \\
&\quad \left(-\frac{1}{2} \left[\mathbf{y}^T (I + R^{-1} + C^{-1}) \mathbf{y} \right] + \mathbf{x}^T R^{-1} \mathbf{y} \right) d\mathbf{y} \\
&= \frac{\alpha n \beta}{\sqrt{|S|}} \exp\left(-\frac{1}{2} \left[\mathbf{x}^T R^{-1} (I - S^{-1} R^{-1}) \mathbf{x} \right]\right), \tag{G34}
\end{aligned}$$

where $S \triangleq I + R^{-1} + C^{-1}$, and $|\cdot|$ indicates the matrix determinant. Putting this and Eq. G33 in Eq. 91 results in:

$$\begin{aligned}
(Tf)(\mathbf{x}) &= \lambda f(\mathbf{x}) \\
\Rightarrow \frac{n\beta}{\sqrt{|S|}} \exp\left(-\frac{1}{2} \left[\mathbf{x}^T R^{-1} (I - S^{-1} R^{-1}) \mathbf{x} \right]\right) &= \\
\lambda \exp\left(-\frac{1}{2} \mathbf{x}^T C^{-1} \mathbf{x}\right) & \\
\Rightarrow \lambda = \frac{n\beta}{\sqrt{|S|}}, \tag{G35}
\end{aligned}$$

where $R^{-1} - C^{-1} = R^{-1} S^{-1} R^{-1}$.

To estimate the spectral radius λ , we need to solve for C . From the constraint in Eq. G35, and noting that R and C are positive-definite, we can write:

$$\begin{aligned}
R^{-1} - C^{-1} &= R^{-1} (I + R^{-1} + C^{-1})^{-1} R^{-1} \\
\Rightarrow (R^{-1} - C^{-1})(I + R + RC^{-1}) &= R^{-1} \\
\Rightarrow \cancel{R^{-1}} + I + \cancel{C^{-1}} - \cancel{C^{-1}} - C^{-1} R - C^{-1} R C^{-1} &= \cancel{R^{-1}} \\
\Rightarrow C^2 - RC - R = 0. \tag{G36}
\end{aligned}$$

Since both R and C are symmetric matrices, for the constraint in Eq. G36 to be satisfied, RC must be symmetric too, i.e. $RC = (RC)^T$. We can always write $(RC)^T = C^T R^T = CR$, which implies that $RC = CR$, i.e. R and C are commuting matrices, and they must have the same eigenvectors. Thus, the matrix constraint translates into k quadratic equations for the (positive) eigenvalues of C , in terms of eigenvalues of R . Alternatively, since we are concerned with the determinant of $S = I + R^{-1} + C^{-1}$, we can formulate an equation for the inverse instead, by re-writing Eq. G36 as:

$$\begin{aligned}
C^2 - RC - R = 0 \\
\Rightarrow R^{-1} C^2 - C - I = 0 \\
\Rightarrow C^{-2} + C^{-1} - R^{-1} = 0 \tag{G37}
\end{aligned}$$

Consequently, let (τ_i, \mathbf{v}_i) be an eigenpair of R^{-1} , then the corresponding eigenpair for C^{-1} is given by (γ_i, \mathbf{v}_i) , such

that γ_i satisfies the scalar quadratic constraint analogous to Eq. G37: $\gamma_i^2 + \gamma_i - \tau_i = 0$, i.e. $\gamma_i = \frac{\sqrt{1+4\tau_i}-1}{2}$. (The second root is rejected since C is positive-definite and therefore $\gamma_i > 0$.) Since I commutes with every matrix, we can express $|S| = |I + C^{-1} + R^{-1}|$ entirely in terms of the eigenvalues of R^{-1} as $|I + C^{-1} + R^{-1}| = \prod_{i=1}^k (1 + \tau_i + \gamma_i) = \prod_{i=1}^k \left(\tau_i + \frac{\sqrt{1+4\tau_i}+1}{2} \right)$. Combining this with the spectral condition $r(T) > 1$, Eq. 104 yields the percolation condition in Eq. 105.

c. Relationship between degree and percolation

Finally, we explore what the percolation threshold in Gaussian RGGs implies for the expected degree at different locations in \mathbb{R}^k , which allows for a comparison to the fiducial constraint of $\langle d \rangle > 1$ in ER graphs [23].

Let $\{(\tau_i, \mathbf{v}_i)\}_{i=1}^k$ be the eigenpairs of R^{-1} . Then from Eq. G26, the expected degree at \mathbf{x} is given by:

$$\begin{aligned}
\hat{d}(\mathbf{x}) &= \frac{n\beta}{\sqrt{|I + R^{-1}|}} \exp\left(-\frac{\mathbf{x}^T (I + R)^{-1} \mathbf{x}}{2}\right) \\
&= \frac{n\beta}{\prod_i \sqrt{1 + \tau_i}} \exp\left(-\frac{\sum_i (1 + \tau_i^{-1})^{-1} (\mathbf{x}^T \mathbf{v}_i)^2}{2}\right) \\
&= n\beta \prod_i (1 + \tau_i)^{-\frac{1}{2}} \exp\left(-\frac{\tau_i \hat{x}_i^2}{2(1 + \tau_i)}\right), \tag{G38}
\end{aligned}$$

where $\hat{x}_i \triangleq \mathbf{x}^T \mathbf{v}_i$ is the projection of \mathbf{x} on the i^{th} eigenvector of R^{-1} . Consequently, the percolation threshold from Eq. 105 can be written in terms of the expected degree at \mathbf{x} as:

$$\hat{d}(\mathbf{x}) > \prod_i \left[\frac{1 + 2\tau_i + \sqrt{1 + 4\tau_i}}{2(1 + \tau_i)} \right]^{\frac{1}{2}} \exp\left(-\frac{\tau_i \hat{x}_i^2}{2(1 + \tau_i)}\right). \tag{G39}$$

Evidently, for $\tau_i \rightarrow 0$, the i^{th} eigenvalue contributes 1 to the RHS of Eq. G39, regardless of the projection \hat{x}_i . Then, if $\tau_i \rightarrow 0$ for all i , which implies that the connectivity scales tend to infinity, then the RHS is simply 1, which is the ER constraint. In general, we find that the ‘‘contribution’’ to the expected-degree-at- \mathbf{x} -constraint is 1 for a value dependent on both τ_i and \hat{x}_i , however existing *only* in the regime where $0 < |\hat{x}_i| < 1$ —see Fig. G3c. That is,

1. for $0 < |\hat{x}_i| < 1$, there is an interval of the eigenvalue τ_i given by $I_{\hat{x}_i} \triangleq (0, \tau_{\hat{x}_i})$ for which the ‘‘contribution’’ of an additional eigenvalue is greater than 1, i.e. higher than for ER graphs, and is less than 1 outside of it;
2. for $|\hat{x}_i| > 1$, the ‘‘contribution’’ of an additional eigenvalue is always lesser than 1, i.e. lower than for ER graphs;

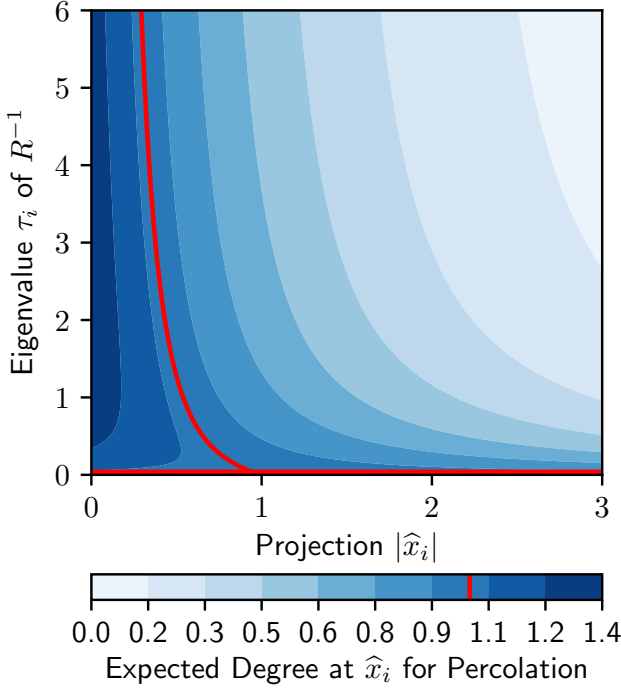


FIG. 27. Regimes of percolation behavior for a node \mathbf{x} in Gaussian RGGs of arbitrary dimension. Contour plot indicates contribution of an eigenvalue τ_i of R^{-1} to the constraint on expected-degree-at- \mathbf{x} as indicated by Eq. G39, with red curves indicating a contribution of 1. “Peripheral” nodes, which have a projection on the corresponding eigenvector larger than 1 in absolute value, always receive a lower contribution from τ_i than 1—the fiducial value for ER graphs [23]. “Central” nodes, on the other hand, have an interval of τ_i for which the contribution is greater than 1, but is smaller than 1 outside of it. Thus, every additional dimension can only reduce the constraint on expected-degree-at- \mathbf{x} for peripheral nodes.

3. for $\hat{x}_i = 0$, the “contribution” of an additional eigenvalue is always greater than 1, i.e. higher than for ER graphs.

In other words, nodes which are closer to the centre—and thus with the smallest projections—“bear the burden” of percolation in lieu of the nodes at the periphery. Consequently, as the number of dimensions increases, the expected degree constraint for central nodes goes up, while that for peripheral nodes goes down.

However, as we saw in Sec. IVD, the overall effect is that the percolation constraint on the mean degree of the

network itself goes down. From Eq. G27:

$$\begin{aligned}
 \langle d \rangle &= \frac{n\beta}{\sqrt{|I + R^{-1}| |I + (I + R)^{-1}|}} \\
 &= n\beta \prod_i \left\{ (1 + \tau_i) \left[1 + (1 + \tau_i^{-1})^{-1} \right] \right\}^{-\frac{1}{2}} \\
 &= n\beta \prod_i \left[(1 + \tau_i) \left(1 + \frac{\tau_i}{1 + \tau_i} \right) \right]^{-\frac{1}{2}} \\
 &= n\beta \prod_i (1 + 2\tau_i)^{-\frac{1}{2}}
 \end{aligned} \tag{G40}$$

Consequently, the percolation threshold from Eq. 105 can be written in terms of the mean network degree as:

$$\begin{aligned}
 \langle d \rangle &> \prod_i \left[\frac{1 + 2\tau_i + \sqrt{1 + 4\tau_i}}{2(1 + 2\tau_i)} \right]^{\frac{1}{2}} \\
 &= 2^{-\frac{n}{2}} \prod_i \left(1 + \frac{\sqrt{1 + 4\tau_i}}{1 + 2\tau_i} \right).
 \end{aligned} \tag{G41}$$

which is the inequality in Eq. 106.

4. Scale-free graphons

a. General properties

Consider the real-interval $[h, 1]$ where $0 < h \ll 1$ on which nodes are distributed uniformly. (Conventionally, nodes are distributed uniformly on $[0, 1]$ in a graphon, but we curtail the interval to prevent unbounded node degrees in this “scale-free” graphon.)

$$\mu(x) = \begin{cases} \frac{1}{1-h} & \text{if } h \leq x \leq 1, \\ 0 & \text{otherwise.} \end{cases} \tag{G42}$$

Next, (undirected) edges are added according to the connectivity kernel:

$$\nu(x, y) = \beta \left(\frac{xy}{h^2} \right)^{-\alpha}, \tag{G43}$$

where $0 < \alpha \leq 1$, $\beta > 0$ and $\beta = O(n^{-1})$. In terms of the multiplicative graphons definition from Sec. IVE:

$$\nu(x, y) = W_{\times}(x, y) \triangleq f(x)f(y),$$

where:

$$f(x) = \sqrt{\beta} \left(\frac{x}{h} \right)^{-\alpha}. \tag{G44}$$

Then we know that the expected degrees and geodesic length distribution are given by making use of $\zeta \triangleq$

$$\frac{1}{1-h} \int_h^1 f(x) dx:$$

$$\begin{aligned} \zeta &= \frac{1}{1-h} \int_h^1 f(x) dx \\ &= \frac{\sqrt{\beta} h^\alpha}{1-h} \int_h^1 x^{-\alpha} dx \\ &= \begin{cases} \frac{\sqrt{\beta} h}{1-h} \log x|_h^1 & \text{if } \alpha = 1, \\ \frac{\sqrt{\beta} h^\alpha}{1-h} \frac{x^{1-\alpha}}{1-\alpha} \Big|_h^1 & \text{otherwise} \end{cases} \quad (\text{G45}) \\ &= \begin{cases} \sqrt{\beta} \frac{h \log h^{-1}}{1-h} & \text{if } \alpha = 1, \\ \sqrt{\beta} \frac{h^\alpha - h}{(1-h)(1-\alpha)} & \text{otherwise,} \end{cases} \end{aligned}$$

$$\text{and } \eta \triangleq \frac{n}{1-h} \int_h^1 f(x)^2 dx:$$

$$\begin{aligned} \eta &= \frac{n}{1-h} \int_h^1 f(x)^2 dx \\ &= \frac{n\beta h^{2\alpha}}{1-h} \int_h^1 x^{-2\alpha} dx \\ &= \begin{cases} \frac{n\beta h}{1-h} \log x|_h^1 & \text{if } \alpha = 1/2, \\ \frac{n\beta h^{2\alpha}}{1-h} \frac{x^{1-2\alpha}}{1-2\alpha} \Big|_h^1 & \text{otherwise} \end{cases} \quad (\text{G46}) \\ &= \begin{cases} n\beta \frac{h \log h^{-1}}{1-h} & \text{if } \alpha = 1/2, \\ n\beta \frac{h^{2\alpha} - h}{(1-h)(1-2\alpha)} & \text{otherwise.} \end{cases} \end{aligned}$$

Degree distribution. Using Eqs. 73a, G44, G45 the expected degree at location \mathbf{x} is given by:

$$\begin{aligned} \widehat{d}(x) &= n\zeta f(x) \\ &= \begin{cases} x^{-1} n\beta \frac{h^2 \log h^{-1}}{1-h} & \text{if } \alpha = 1, \\ x^{-\alpha} n\beta \frac{h^{2\alpha} - h^{1+\alpha}}{(1-h)(1-\alpha)} & \text{otherwise} \end{cases} \quad (\text{G47}) \\ &\triangleq c(\alpha) x^{-\alpha}, \end{aligned}$$

where $c(\alpha)$ functions as a constant independent of x . To see how expected degrees are distributed by a power law, consider Eq. G47 as a monotonically decreasing transformation of random variable x to $\widehat{d}(x)$.

$$\begin{aligned} P(\widehat{d}(x) \leq k) &= P(x \geq \widehat{d}^{-1}(k)) \\ &= 1 - P(x \leq \widehat{d}^{-1}(k)) \\ &= \begin{cases} 1 & \text{if } \widehat{d}^{-1}(k) < h, \\ \frac{1 - \widehat{d}^{-1}(k)}{1-h} & \text{if } \widehat{d}^{-1}(k) \in [h, 1], \\ 0 & \text{if } \widehat{d}^{-1}(k) > 1 \end{cases} \\ &= \begin{cases} 1 & \text{if } k > c(\alpha) h^{-\alpha}, \\ \frac{1 - (\frac{k}{c(\alpha)})^{-\frac{1}{\alpha}}}{1-h} & \text{if } k \in [c(\alpha), c(\alpha) h^{-\alpha}], \\ 0 & \text{if } k < c(\alpha) \end{cases} \\ P(\widehat{d}(x) = k) &= \begin{cases} \frac{\theta-1}{1-h} c(\alpha)^{\theta-1} k^{-\theta} & k \in [c(\alpha), c(\alpha) h^{-\alpha}], \\ 0 & \text{otherwise,} \end{cases} \quad (\text{G48}) \end{aligned}$$

i.e. $\widehat{d} \sim \widehat{d}^{-\theta}$ where $\theta \triangleq (1 + \frac{1}{\alpha})$ is the power law exponent which can take values $\theta \in [2, \infty)$. This power law distribution is over a bounded interval $[c(\alpha), c(\alpha) h^{-\alpha}]$ unlike more conventional ones which are unbounded from above. We emphasize that this is the distribution of *expectation of degrees* in the network and not, strictly speaking, the empirical degree distribution. The network generation process of adding independent edges will asymptotically impose a Poisson degree distribution at a given location x , whose expectation is given by $\widehat{d}(x)$, which follows the power law as shown in Eq. G48. But it can be shown that the empirical degree distribution will also follow this power law behavior.

Let $d(x)$ be the degree of node at x , then $d(x) \sim \text{Poisson}(\widehat{d}(x))$. If d represent the degree of any node in the network, then its distribution is given by:

$$\begin{aligned} P(d = k) &= \int_h^1 P(d(x) = k) d\mu(x) \\ &= \frac{1}{1-h} \int_h^1 \frac{[c(\alpha) x^{-\alpha}]^k \exp(-c(\alpha) x^{-\alpha})}{k!} dx \\ &= \frac{c(\alpha)^{\frac{1}{\alpha}}}{\alpha(1-h)k!} \left[\Gamma\left(k - \frac{1}{\alpha}, c(\alpha)\right) - \Gamma\left(k - \frac{1}{\alpha}, c(\alpha) h^{-\alpha}\right) \right] \quad (\text{if } k > \alpha^{-1}) \\ &= \frac{\theta - 1}{1-h} c(\alpha)^{\theta-1} \\ &= \frac{\Gamma(k + 1 - \theta, c(\alpha)) - \Gamma(k + 1 - \theta, c(\alpha) h^{-\alpha})}{\Gamma(k + 1)}. \quad (\text{G49}) \end{aligned}$$

Now, assuming that $c(\alpha) \rightarrow 0$ and $c(\alpha) h^{-\alpha} \rightarrow \infty$ i.e. the interval bounding the expected degree $\widehat{d}(x)$ is very wide, we get:

$$\begin{aligned} P(d = k) &\approx \frac{\theta - 1}{1-h} c(\alpha)^{\theta-1} \frac{\Gamma(k + 1 - \theta)}{\Gamma(k + 1)} \\ &\approx \frac{\theta - 1}{1-h} c(\alpha)^{\theta-1} \frac{(k - \theta)^{k + \frac{1}{2} - \theta}}{k^{k + \frac{1}{2}}} e^\theta \\ &= \frac{\theta - 1}{1-h} c(\alpha)^{\theta-1} \left(1 - \frac{\theta}{k}\right)^{k + \frac{1}{2} - \theta} e^\theta k^{-\theta} \quad (\text{G50}) \\ &\approx \frac{\theta - 1}{1-h} c(\alpha)^{\theta-1} e^{\frac{\theta}{k}(\theta - \frac{1}{2})} k^{-\theta} \\ &\approx \frac{\theta - 1}{1-h} c(\alpha)^{\theta-1} k^{-\theta}. \end{aligned}$$

i.e. $d \sim d^{-\theta}$ where in the second approximation we apply Stirling's formula for the Gamma function i.e. $\Gamma(z + 1) \approx \sqrt{2\pi z} \left(\frac{z}{e}\right)^z$; in the last two approximations we make a stronger use of $k \gg \theta$. These assumptions make it apparent that the power law holds for the empirical degree distribution in this "scale-free" graphon for large degrees when a broad degree distribution is possible, and the form obtained in Eq. G50 matches that of

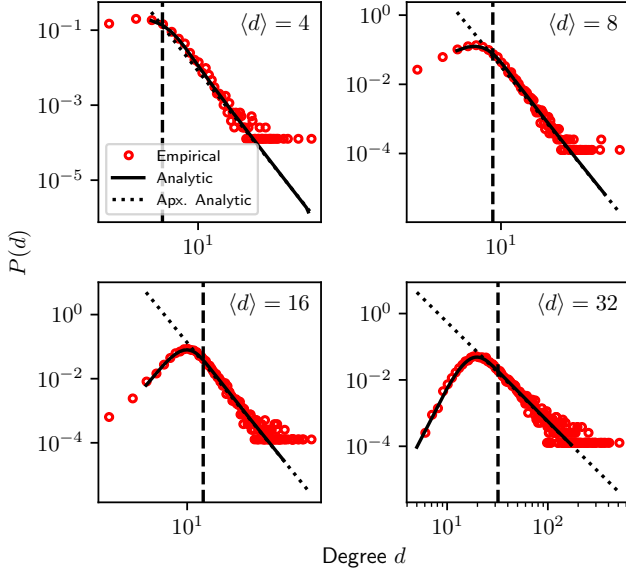


FIG. 28. Degree distribution for “scale-free” graphons with power law exponent $\theta = 3$ (i.e. $\alpha = \frac{1}{2}$), corresponding to BA graphs, for $n = 8192$ nodes, free-parameter $\beta = 1$, with varying mean degree $\langle d \rangle$. Markers indicate empirical distribution from a single network sample, while the solid line indicates the analytic estimate from Eq. G49, and the dotted line is the approximate analytic estimate from Eq. G50. In each subplot, the power law is apparent for degrees above a certain cut-off—evidently above $\langle d \rangle$ indicated by the dashed line—but these are not *pure* power law behaviours.

the expected degree distribution in Eq. G48, as depicted in Fig. 28. Also, using Eqs. 73b, G45 the average degree of the whole network is given by

$$\begin{aligned} \langle d \rangle &= n\zeta^2 \\ &= \begin{cases} n\beta \left(\frac{h \log h^{-1}}{1-h} \right)^2 & \text{if } \alpha = 1, \\ n\beta \left[\frac{h^\alpha - h}{(1-h)(1-\alpha)} \right]^2 & \text{otherwise.} \end{cases} \end{aligned} \quad (\text{G51})$$

b. Special cases: BA and highly scale-free graphons

Next, we consider some special cases of the “scale-free” graphon, as described in Sec. IVE. But first, it will be useful to define the solution to the following equation:

$$x \log x = a. \quad (\text{G52})$$

We know that for real numbers y, a , the solution to

$$ye^y = a, \quad (\text{G53})$$

is given by:

$$y = \begin{cases} W_0(a) & \text{if } a \geq 0, \\ W_{-1}(a) & \text{if } -\frac{1}{e} \leq a < 0, \end{cases} \quad (\text{G54})$$

where W_0 and W_{-1} are the principal and non-principal branches of the Lambert W function, and have the following asymptotic expansions [122]:

$$W_0(x) \approx \log x - \log \log x \quad (\text{for large } x > 0), \quad (\text{G55a})$$

$$W_{-1}(-x) \approx \log(-x) - \log(-\log(-x)) \quad (\text{for small } x < 0). \quad (\text{G55b})$$

Consequently, the solution for Eq. G52 is given by substituting y with $\log x$ in Eq. G53 to obtain:

$$\begin{aligned} x &= \begin{cases} e^{W_0(a)} & \text{if } a \geq 0, \\ e^{W_{-1}(a)} & \text{if } -\frac{1}{e} \leq a < 0 \end{cases} \\ &= \begin{cases} \frac{a}{W_0(a)} & \text{if } a \geq 0, \\ \frac{a}{W_{-1}(a)} & \text{if } -\frac{1}{e} \leq a < 0 \end{cases} \\ &\approx \begin{cases} \frac{a}{\log a - \log \log a} & \text{for large positive } a, \\ \frac{-a}{\log(-\log(-a)) - \log(-a)} & \text{for small negative } a, \end{cases} \end{aligned} \quad (\text{G56})$$

where in the first equality we use the identity satisfied by the Lambert W function in Eq. G53, and in the second one we use the asymptotic expression from Eq. G55.

Given that formulations in terms of the network’s mean degree are easier to interpret, we consider the special cases of scale-free graphons and use Eqs. G51, G46 along with the constraint $h \ll 1$, to express h and η in terms of $\langle d \rangle, n, \beta$ as follows:

1. For ER graphs, we have $\theta \rightarrow \infty \implies \alpha \rightarrow 0$:

$$\begin{aligned} \langle d \rangle &\rightarrow n\beta, \quad \eta \rightarrow n\beta, \\ &\implies \eta = v. \end{aligned} \quad (\text{G57})$$

2. For BA graphs the power law exponent is $\theta = 3$ [84], and therefore $\alpha = 1/2$

$$\begin{aligned} \langle d \rangle &= n\beta \left(2 \frac{\sqrt{h}}{1 + \sqrt{h}} \right)^2 \approx 4n\beta h, \\ \eta &\approx n\beta h \log h^{-1}, \\ &\implies h \approx \frac{\langle d \rangle}{4n\beta}, \\ &\implies \eta \approx \frac{\langle d \rangle}{4} \log \frac{4n\beta}{\langle d \rangle}. \end{aligned} \quad (\text{G58})$$

3. For “highly scale-free” networks where power law

exponent $\theta \rightarrow 2 \implies \alpha \rightarrow 1$:

$$\begin{aligned}
\langle d \rangle &\approx n\beta(h \log h^{-1})^2, \quad \eta = n\beta h, \\
\implies h \log h &= -\sqrt{\frac{\langle d \rangle}{n\beta}} \\
\implies h &\approx \frac{\sqrt{\frac{\langle d \rangle}{n\beta}}}{\log \log \sqrt{\frac{n\beta}{\langle d \rangle}} + \log \sqrt{\frac{n\beta}{\langle d \rangle}}} \approx \frac{\sqrt{\frac{\langle d \rangle}{n\beta}}}{\log \sqrt{\frac{n\beta}{\langle d \rangle}}}, \\
\implies \eta &\approx \frac{\sqrt{n\beta \langle d \rangle}}{\log \sqrt{\frac{n\beta}{\langle d \rangle}}},
\end{aligned} \tag{G59}$$

where we use the result in Eq. G56, and asymptotically $\log \log n \ll \log n$.

Bond percolation threshold. Consider the percolation threshold for a multiplicative graphon, which we saw in Sec. V is given by $\eta > 1$. Using Eq. G57, we obtain the usual criterion for ER graphs that $\langle d \rangle > 1$. Consider the BA graphon, with free-parameter $\beta = 1$, for which we get from Eq. G58:

$$\begin{aligned}
\frac{\langle d \rangle}{4} \log \frac{4n}{\langle d \rangle} &> 1 \\
\implies \frac{\langle d \rangle}{4n} \log \frac{\langle d \rangle}{4n} &< -\frac{1}{n} \\
\implies \frac{\langle d \rangle}{4n} &> \frac{n^{-1}}{\log n + \log \log n} \\
\implies \langle d \rangle &> \frac{4}{\log n + \log \log n},
\end{aligned} \tag{G60}$$

where we use the result in Eq. G56. Next, consider the highly scale-free graphons, with free-parameter $\beta = 1$, for which we get from Eq. G59 by setting $\eta > 1$:

$$\begin{aligned}
\frac{\sqrt{n \langle d \rangle}}{\log \sqrt{\frac{n}{\langle d \rangle}}} &> 1 \\
\implies \sqrt{\frac{n}{\langle d \rangle}} \log \sqrt{\frac{n}{\langle d \rangle}} &< n \\
\implies \sqrt{\frac{n}{\langle d \rangle}} &< \frac{n}{\log n - \log \log n} \\
\implies \langle d \rangle &> \frac{(\log n - \log \log n)^2}{n},
\end{aligned} \tag{G61}$$

where we again use the result in Eq. G56.

Mean geodesic length. Consider the expression for mean geodesic lengths from Eq. 111, from which, for large η , we obtain:

$$\langle \lambda \rangle \approx \frac{1}{2} - \frac{2\mathbb{E}_\mu[\log f(x)] + \gamma}{\log \eta}. \tag{G62}$$

Then, plugging Eqs. 117, G57, G58, G59 into Eq. G62, results in the following:

$$\langle \lambda \rangle = \frac{1}{2} + \begin{cases} \frac{\log \frac{n}{d} - \gamma}{\log d} & \text{if } \alpha = 0, \\ \frac{\log \frac{4n}{d} - (\gamma+1)}{\log(\frac{d}{4} \log \frac{4n}{d})} & \text{if } \alpha = \frac{1}{2}, \\ 2 \frac{\log n + \log(\frac{1}{d} \log^2 \sqrt{\frac{n}{d}}) - (\gamma+2)}{\log n - \log(\frac{1}{d} \log^2 \sqrt{\frac{n}{d}})} & \text{if } \alpha = 1. \end{cases} \tag{G63}$$

Asymptotically then, for large n this leads to Eq. 118.

Appendix H: Mean geodesic lengths and path-based centralities

In this section, we elaborate on deriving global and node-level path-based statistics, such as the mean geodesic length (Appendix H1) and node closeness centrality (Appendix H2), analytically and in closed-form (Appendix H3). We also draw connections to the literature on matrix-function based network centralities (Appendix H4).

1. Analytic estimate of mean geodesic length

First, we consider the ensemble average model of Sec. II. The average geodesic length in a network with n nodes can be finite only after conditioning on nodes i, j being on the same (giant) component. We use the notation $\langle \cdot | \cdot \rangle$ for conditional expectation over the ensemble.

$$\begin{aligned}
\langle \lambda_{ij} | \phi_i, \phi_j \rangle &= \sum_{l=0}^{\infty} l P(\lambda_{ij} = l | \phi_i, \phi_j) = \\
&\sum_{l=1}^{\infty} l [P(\lambda_{ij} > l-1 | \phi_i, \phi_j) - P(\lambda_{ij} > l | \phi_i, \phi_j)] \\
&= \sum_{l=0}^{\infty} P(\lambda_{ij} > l | \phi_i, \phi_j) = \sum_{l=0}^{\infty} \frac{P(l < \lambda_{ij} < \infty | \phi_i)}{P(\phi_j | \phi_i)} \\
&= \frac{\sum_{l=0}^{\infty} [P(\lambda_{ij} > l | \phi_i) - P(\lambda_{ij} = \infty | \phi_i)]}{P(\phi_j)},
\end{aligned} \tag{H1}$$

where the 3rd equality is due to the sum of the telescoping series preceding it, and the 4th equality arises from $\phi_i \cap \phi_j \implies \lambda_{ij} < \infty$. Let λ be the geodesic length between any two randomly selected nodes in the network. Then its expectation, i.e. the average geodesic length for the

whole network, is given by

$$\begin{aligned}
\langle \lambda | \lambda < \infty \rangle &= \sum_l l P(\lambda = l | \lambda < \infty) = \sum_l \frac{l P(\lambda = l)}{P(\lambda < \infty)} \\
&= \frac{\sum_l l \mathbb{E}_{\mu^2} [P(\lambda_{ij} = l)]}{\mathbb{E}_{\mu^2} [P(\lambda_{ij} < \infty)]} \\
&= \frac{\mathbb{E}_{\mu^2} [\sum_l l P(\lambda_{ij} = l | \phi_i, \phi_j) P(\phi_i, \phi_j)]}{\mathbb{E}_{\mu^2} [P(\phi_i, \phi_j)]} \\
&= \frac{\mathbb{E}_{\mu^2} [\langle \lambda_{ij} | \phi_i, \phi_j \rangle P(\phi_i) P(\phi_j)]}{\mathbb{E}_{\mu} [P(\phi_i)]^2}
\end{aligned} \tag{H2}$$

Together, Eqs. H1 and H2 allow us to compute the expected geodesic length in a network. Consider the average ensemble model and the definition of the survival

$$\langle \lambda | \lambda < \infty \rangle = \frac{\int_V \int_V [\sum_{l=0}^{\infty} \psi_l(x, y) - \psi_{\infty}(x, y)] [1 - \psi_{\infty}(y, x)] d\mu(x) d\mu(y)}{\int_V \int_V [1 - \psi_{\infty}(x, y)] [1 - \psi_{\infty}(y, x)] d\mu(x) d\mu(y)}. \tag{H5}$$

If the network is almost surely connected, then $\Psi_{\infty} \rightarrow 0$. This simplifies the expression in Eq. H4 to:

$$\langle \lambda \rangle = \frac{1}{n^2} \mathbf{u}^T \left(\sum_{l=0}^{\infty} \Psi_l \right) \mathbf{u}, \tag{H6}$$

where we drop the conditioning on $\lambda < \infty$ since $P(\lambda = \infty) \rightarrow 0$. Similarly, for the general random graph model in node space V , we obtain from Eq. H5 the analogous Eq. 107.

2. Analytic expectation of closeness centrality

First, we consider a given ensemble average model of Sec. II with n nodes. Given that we have a random graph model, the closeness centrality of a node is itself a random variable. Consider then the expectation of node k 's closeness in Eq. 120 over the ensemble:

$$\begin{aligned}
\bar{\gamma}_k &\triangleq \langle \gamma_k \rangle = \langle \mathbb{E} [\lambda_{ik}^{-1}] \rangle = \mathbb{E} [\langle \lambda_{ik}^{-1} \rangle] \\
&= \mathbb{E} [\langle \lambda_{ik}^{-1} | \phi_i \rangle P(\phi_i) + \langle \lambda_{ik}^{-1} | \neg \phi_i \rangle (1 - P(\phi_i))] \tag{H7} \\
&= \mathbb{E} [\langle \lambda_{ik}^{-1} | \phi_i \rangle P(\phi_i)],
\end{aligned}$$

where, in the first line, the order of expectations can be changed due to finite λ_{ik}^{-1} , and in the last equality we use the fact that asymptotically if i is not on the giant component then its expected reciprocal distance to any node k is 0. We use the survival function of the geodesic length distribution and the definition in Eq. 7a to obtain $P(\lambda_{ik} = l | \phi_i) = P(\lambda_{ik} > l - 1 | \phi_i) - P(\lambda_{ik} > l | \phi_i) =$

function matrix Ψ_l from Eq. 7a. Define the matrix Ψ_{∞} where

$$[\Psi_{\infty}]_{ij} \triangleq P(\lambda_{ij} = \infty | \phi_i) = \lim_{l \rightarrow \infty} P(\lambda_{ij} > l | \phi_i), \tag{H3}$$

using Eq. 14. From Eq. 15, recall that we can write the percolation probability of j as $1 - P(\lambda_{ij} = \infty | \phi_i)$. Putting Eq. H3 in Eqs. H1 and H2, the expected geodesic length λ for the whole network is given by:

$$\langle \lambda | \lambda < \infty \rangle = \frac{\mathbf{u}^T \{ [\sum_{l=0}^{\infty} (\Psi_l - \Psi_{\infty})] \odot (\mathbf{u} \mathbf{u}^T - \Psi_{\infty}^T) \} \mathbf{u}}{\mathbf{u}^T [(\mathbf{u} \mathbf{u}^T - \Psi_{\infty}) \odot (\mathbf{u} \mathbf{u}^T - \Psi_{\infty}^T)] \mathbf{u}}, \tag{H4}$$

where \mathbf{u} is the all-ones vector of length n , which is straightforward to compute for most models. Using Eqs. H1, H2, 15, and the definition of $\psi_{\infty}(x, y)$ from Eq. 89, the expected geodesic length for the network of a general family is analogously given by:

$[\Psi_{l-1} - \Psi_l]_{ik}$, yielding:

$$\langle \lambda_{ik}^{-1} | \phi_i \rangle = \sum_{l=1}^{\infty} \frac{[\Psi_{l-1} - \Psi_l]_{ik}}{l} = 1 - \sum_{l=1}^{\infty} \frac{[\Psi_l]_{ik}}{l(l+1)}, \tag{H8}$$

which has a value between 0—when k is very likely to not be on the giant component and thus $[\Psi_l]_{ik} \approx 1$ for any l —and 1—when k is very likely to be an immediate neighbour of i and thus $[\Psi_l]_{ik} \approx 0$ for any $l > 0$. Let $\bar{\gamma}$ be the vector encoding expected closeness of nodes. Inserting Eq. 15, and the definition in Eq. H3 into Eqs. H7 and H8, we obtain

$$\bar{\gamma} = \frac{1}{n} \left(\left\{ \mathbf{u} \mathbf{u}^T - \sum_{l=1}^{\infty} [l(l+1)]^{-1} \Psi_l^T \right\} \odot (\mathbf{u} \mathbf{u}^T - \Psi_{\infty}) \right) \mathbf{u}, \tag{H9}$$

where \mathbf{u} is the all-ones vector of length n . Analogously, we can write an expression for the general random graph model in node space V . Let $\psi_{-1}(x, y) \triangleq \sum_{l=0}^{\infty} [l(l+1)]^{-1} \psi_l(x, y)$ for nodes $x \in V, y \in V$, then using the definition from Eq. 89, the expected closeness centrality of a node at $z \in V$ is:

$$\bar{\gamma}(z) = \int_V [1 - \psi_{-1}(x, z)] [1 - \psi_{\infty}(z, x)] d\mu(x). \tag{H10}$$

3. Poisson summation for mean geodesic length

Consider a re-parametrized form of the (approximate) closed-form of the survival function of the distribution of shortest path length λ_{xy} between nodes x, y belonging to

the same percolating subspace of the node space V —see Theorem 3 in Appendix D 2—given by $\tilde{\psi}_{xy}(l) \triangleq P(\lambda_{xy} > l | \phi_x, \phi_y)$. We wish to estimate the expected length of the shortest path between x, y , which from Eq. 108a is given as:

$$\langle \lambda_{xy} \rangle = \sum_{l=0}^{\infty} \tilde{\psi}_{xy}(l). \quad (\text{H11})$$

Consider the Poisson summation formula, which expresses the relationship of summation of a function f to the summation of its continuous Fourier transform [123]:

$$\sum_{n=n_1}^{n_2} f(n) = \frac{f(n_1^+) + f(n_2^-)}{2} + \sum_{m=-\infty}^{\infty} \int_{n_1^+}^{n_2^-} f(z) e^{-2\pi i m z} dz. \quad (\text{H12})$$

First, we remark that $\forall l < 0, \tilde{\psi}_{xy}(l) = 0, \tilde{\psi}_{xy}(0) = 1$ and $\tilde{\psi}_{xy}(l)$ is a positive decreasing function in l , since it is a survival function. Second, since we have conditioned on the nodes being on the same percolating subspace, $\lim_{l \rightarrow \infty} \tilde{\psi}_{xy}(l) = 0$. Third, we will assume $\tilde{\psi}_{xy}(l)$ to be infinitely-differentiable in the domain $[0, \infty)$. (This assumption is naturally satisfied by the smooth analytic forms of the survival function that we derive in this paper, such as Eq. 78b for multiplicative graphons.) In Eq. H12, setting n_1 as 0, n_2 as ∞ , then by the above properties of $\tilde{\psi}_{xy}(l)$ we can write:

$$\begin{aligned} \sum_{l=0}^{\infty} \tilde{\psi}_{xy}(l) &= \frac{1}{2} + \sum_{m=-\infty}^{\infty} \int_0^{\infty} \tilde{\psi}_{xy}(z) e^{-2\pi i m z} dz \\ &= \frac{1}{2} + \int_0^{\infty} \tilde{\psi}_{xy}(z) dz + \\ &\quad 2 \sum_{m=1}^{\infty} \int_0^{\infty} \tilde{\psi}_{xy}(z) \cos(2\pi m z) dz, \end{aligned} \quad (\text{H13})$$

where the second equality makes use of Euler's formula $e^{i\theta} = \cos \theta + i \sin \theta$. Consider the integral in the summation on the RHS. Using integration by-parts, and making use of $\lim_{l \rightarrow \infty} \tilde{\psi}_{xy}(l) = 0$, we can write:

$$\begin{aligned} \int_0^{\infty} \tilde{\psi}_{xy}(z) \cos(2\pi m z) dz &= -\frac{1}{4\pi^2 m^2} \left[\tilde{\psi}'_{xy}(0) + \right. \\ &\quad \left. \int_0^{\infty} \tilde{\psi}''_{xy}(z) \cos(2\pi m z) dz \right] \\ &= \sum_{k=1}^{\infty} \left(\frac{-1}{4\pi^2 m^2} \right)^k \tilde{\psi}_{xy}^{2k-1}(0), \end{aligned} \quad (\text{H14})$$

where $f^n(0)$ refers to the n th derivative of f at 0, we have made use of $\lim_{l \rightarrow \infty} \tilde{\psi}_{xy}^n(l) = 0$ due to the smooth saturation of the SPLD for large l , and the second equality follows by recursion to infinity. Because of the sparsity assumption, $\tilde{\psi}_{xy}(l)$ should be a very slowly-changing

function close to $l = 0$, since most of the probability mass is away from the shortest path lengths. For instance, for Eq. 78b, all of the higher-order derivatives with respect to l will be proportional to the connectivity kernel $W_{\times}(x, y)$, which scales as $O(n^{-1})$. Thus, setting $\tilde{\psi}_{xy}^{2k-1}(0) \approx 0$ on RHS of Eq. H14 $\forall k \in \{1, 2, \dots\}$ allows us to write $\int_0^{\infty} \tilde{\psi}_{xy}(z) \cos(2\pi m z) dz \approx 0$ which holds $\forall m \in \{1, 2, \dots\}$, which translates Eq. H13 to

$$\sum_{l=0}^{\infty} \tilde{\psi}_{xy}(l) \approx \frac{1}{2} + \int_0^{\infty} \tilde{\psi}_{xy}(z) dz. \quad (\text{H15})$$

Rank-1 models. In essence, this allows for an approximation of the expectation of the discrete distribution of shortest path lengths by an integral of the continuous analogue of the distribution's survival function. In particular, consider the case of rank-1 models like the multiplicative graphons $W_{\times}(x, y)$ from Eq. 71, that are equivalent to a canonical degree-configuration model. From Eqs. 78b, 71 and 74a, assuming the supercritical regime $\eta > 1$ (from Eq. 93), we have

$$\tilde{\psi}_{xy}(l) = \exp\left(-\frac{\eta^l - 1}{\eta - 1} W_{\times}(x, y)\right),$$

which when combined with Eqs. H11, H15 leads to:

$$\begin{aligned} \langle \lambda_{xy} \rangle &\approx \frac{1}{2} + \exp\left(\frac{W_{\times}(x, y)}{\eta - 1}\right) \\ &\quad \times \int_0^{\infty} \exp\left(-\frac{W_{\times}(x, y)}{\eta - 1} \eta^z\right) dz \\ &= \frac{1}{2} - \exp\left(\frac{W_{\times}(x, y)}{\eta - 1}\right) \frac{\text{Ei}\left(-\frac{W_{\times}(x, y)}{\eta - 1}\right)}{\log(\eta)} \\ &\approx \frac{1}{2} + \frac{\log(\eta - 1) - \gamma - \log(f(x)f(y))}{\log(\eta)} \end{aligned} \quad (\text{H16})$$

where $\text{Ei}(\cdot)$ in the second equality is the exponential integral function whose value for small negative arguments $x < 0$ is given by $\text{Ei}(x) \approx \log(-x) + \gamma$ [124] where γ is the Euler-Mascheroni constant whose value is given by $\gamma \approx 0.57222$, and we make use of $W_{\times}(x, y) = O(n^{-1})$.

Rank-1 models with asymmetric kernel. Due to the correspondence between rank-1 models and multiplicative graphons (see Theorem 6 in Appendix F 4), we can express mean geodesic lengths in rank-1 models analogously to Eq. H16. In Sec. VIA, Eq. 119 demonstrates this equivalence for symmetric kernels. This result also holds in the asymmetric setting, where for a rank-1 model with integral operator T (in Eq. 40), the dependence is on its eigenfunction φ , and eigenfunction $\varphi^{\#}$ of its adjoint $T^{\#}$ (in Eq. F12):

$$\langle \lambda \rangle = \frac{1}{2} + \frac{\log(n(1 - \tau^{-1})) - \gamma - \mathbb{E}_{\mu}[\log \varphi] - \mathbb{E}_{\mu}[\log \varphi^{\#}]}{\log \tau}. \quad (\text{H17})$$

To illustrate, consider the directed degree-configuration model from Sec. V A. Using Eq. 97 the (normalized) right and left eigenvectors are given by $\left\{ \frac{\langle d_i^+ \rangle}{\sqrt{\langle d^- d^+ \rangle}} \right\}_{i=1}^n$ and $\left\{ \frac{\langle d_i^- \rangle}{\sqrt{\langle d^- d^+ \rangle}} \right\}_{i=1}^n$. Putting in Eq. H17, alongside τ from Eq. 97, we obtain:

$$\langle \lambda \rangle = \frac{1}{2} + \frac{\log(n(\langle d^- d^+ \rangle - \langle d \rangle)) - \gamma - \mathbb{E}[\log \langle d^- \rangle] - \mathbb{E}[\log \langle d^+ \rangle]}{\log \left(\frac{\langle d^- d^+ \rangle}{\langle d \rangle} \right)}, \quad (\text{H18})$$

which recovers known scaling of typical distances in directed degree-configuration graphs as $\log_b n$ where $b \triangleq \frac{\langle d^- d^+ \rangle}{\langle d \rangle}$ [19]. We note that the mean geodesic length depends on the mean degree, covariance of in- and out-degrees, and mean logarithm of the expected in- and out-degrees—and not on the variance of in-/out-degrees.

Higher rank models with positive definite kernels. For graph models where the integral operator T , as defined in Eq. 40, has more than 1 non-zero eigenvalue, no closed-form integral of the approximate closed-form survival function exists. However, if the non-leading eigenvalues are “small enough”, then we can apply a suitable “rank-1 approximation” to T and make use of the closed-form of mean geodesic lengths, as in Eq. H16. Consider a general random graph model with a symmetric kernel ν . Since the network is supercritical, we have $r(T) = \tau_1 > 1$ from Theorem 2. We assume a homophilous connectivity kernel, i.e. ν is positive definite, and T has small non-leading eigenvalues:

$$\forall i \in \{2, 3, \dots, N\} : 0 < \tau_i < 1, \quad (\text{H19})$$

where N is the rank of T . Consider the approximate closed-form survival function for nodes at $x, y \in V$ from Eq. 47, where we suppress the dependence on node locations:

$$a_i \triangleq \frac{\tau_i \varphi_i(x) \varphi_i(y)}{n(\tau_i - 1)}, \quad (\text{H20a})$$

$$b_i \triangleq \log \tau_i, \quad (\text{H20b})$$

and re-parametrize the survival function as a function of geodesic length l :

$$\begin{aligned} \tilde{\psi}(l) &= \exp \left(- \sum_{i=1}^N a_i [\exp(b_i l) - 1] \right) \\ &= \exp \left(\sum_{i=1}^N a_i \right) \exp \left(- \sum_{i=1}^N a_i \exp(b_i l) \right) \\ &\approx \exp \left(\sum_{i=1}^N a_i \right) \exp(-a_1 e^{b_1 l}) \left[1 - \sum_{i=2}^N a_i \exp(b_i l) \right], \\ &\approx \exp(-a_1 e^{b_1 l}) - \sum_{i=2}^N a_i \exp(-a_1 e^{b_1 l} + b_i l). \end{aligned} \quad (\text{H21})$$

In the third equality, we have used a first-order approximation for the exponential, which is asymptotically applicable since Eqs. H19 and H20 yield for

$$\forall i \in \{2, 3, \dots, N\} : b_i < 0, \quad (\text{H22a})$$

$$\forall i \in \{1, 2, \dots, N\} : a_i = O(n^{-1}). \quad (\text{H22b})$$

To integrate Eq. H21 with respect to l from 0 to ∞ , it is useful to define a function that encodes the “additive correction” offered by non-leading eigenvalues to a putative rank-1 approximation:

$$q_i(l) \triangleq -a_i \exp(-a_1 e^{b_1 l} + b_i l). \quad (\text{H23})$$

Following the change of variable $u = a_1 e^{b_1 l} \implies dl = \frac{du}{u b_1}$, we can write from Eq. H23:

$$\begin{aligned} \int_0^\infty q_i(l) dl &= -\frac{a_i}{b_1} a_1^{-\frac{b_i}{b_1}} \int_{a_1}^\infty u^{\frac{b_i}{b_1}-1} \exp(-u) du \\ &= -\frac{a_i}{b_1} \frac{\Gamma\left(\frac{b_i}{b_1}, a_1\right)}{a_1^{\frac{b_i}{b_1}}}, \end{aligned} \quad (\text{H24})$$

where $\Gamma(s, x)$ is the upper incomplete gamma function. Due to the result in Eq. H22, we can apply for $s < 0$: $\lim_{x \rightarrow 0} \frac{\Gamma(s, x)}{x^s} = -\frac{1}{s}$ to Eq. H24 to asymptotically yield:

$$\int_0^\infty q_i(l) dl \approx \frac{a_i}{b_i} = \frac{\tau_i \varphi_i(x) \varphi_i(y)}{n(\tau_i - 1) \log \tau_i}, \quad (\text{H25})$$

where we apply the definitions in Eq. H20. Thus for small positive eigenvalue τ_i , the “higher-rank correction” scales as $O\left(\frac{\tau_i}{\log \tau_i}\right)$, which tends to 0.

4. Connections to other centralities

In the ensemble average model of Sec. II, we saw from Eq. 29 that the approximate closed-form of the survival function of the geodesic length distribution is given by

a sum of powers of $\langle A \rangle$. Here, we show how the expressions for expected closeness and betweenness centralities on the giant component relate closely to other centrality measures in literature which consider powers of the adjacency matrix A .

Closeness centrality. Asymptotically, for any finite l , we can apply a first-order approximation to the survival function of the SPLD in Eq. 29 to obtain for nodes i, j :

$$[\tilde{\Psi}_l]_{ij} \approx 1 - \sum_{k=1}^l [\langle A \rangle^k]_{ij}. \quad (\text{H26})$$

Since we are using the approximate closed-form of the survival function in the supercritical regime, Eq. 46 has a limiting value of zero and we can drop the conditioning on the giant component. From Eqs. H7, H8, H26 obtain the expected (harmonic) closeness of j :

$$\bar{\gamma}_j = \sum_i \sum_{l=1}^{\infty} \frac{[\tilde{\Psi}_{l-1} - \tilde{\Psi}_l]_{ij}}{l} = \sum_{l=1}^{\infty} \frac{[\mathbf{u}^T \langle A \rangle^l]_j}{l}, \quad (\text{H27})$$

where \mathbf{u} is the all-ones vector. Since the network is percolating, from Theorem 2 we have $r(\langle A \rangle) > 1$. Consequently, the sum of the infinite series on the RHS of Eq. H27 is unbounded, being well-defined only if the sum is up to a finite l , which is also where the approximation in Eq. H26 holds. Therefore, consider a scaled version of $\langle A \rangle \mapsto \alpha \langle A \rangle$, such that $0 < \alpha < \frac{1}{r(\langle A \rangle)}$ that allows for interpolation between short and long scales. Then, we define α -closeness as the closeness defined in Eq. H27, except with the scaled ensemble average matrix $\alpha \langle A \rangle$. Then we can write an “ α -closeness vector” for the nodes in the network as:

$$\begin{aligned} \bar{\gamma}^\alpha &\triangleq \left[\sum_{l=1}^{\infty} \frac{(\alpha \langle A \rangle^T)^l}{l} \right] \mathbf{u} \\ &= -\log(I - \alpha \langle A \rangle^T) \mathbf{u} \\ &= \log \left((I - \alpha \langle A \rangle^T)^{-1} \right) \mathbf{u}, \end{aligned} \quad (\text{H28})$$

where I is the identity matrix, and \log refers to the matrix logarithm, whose series expansion converges since $r(\alpha \langle A \rangle^T) < 1$ due to the constraint on α to be smaller than the inverse of the spectral radius of $\langle A \rangle$. For a symmetric model we can eigendecompose $\langle A \rangle = Q\Lambda Q^T$, where Q is an orthogonal matrix whose columns are the eigenvectors, with the corresponding elements in diagonal matrix Λ being the eigenvalues, and compute the real symmetric matrix $\log M = Q \log(I - \alpha\Lambda)^{-1} Q^T$, which can be inserted into Eq. H28. Evidently, the matrix M resembles the matrix used to compute Katz centralities [40] for nodes in a network given by A , where the centrality of nodes is given by the vector:

$$\boldsymbol{\kappa} \triangleq \left[(I - \alpha A^T)^{-1} - I \right] \mathbf{u},$$

where $0 < \alpha < \frac{1}{r(\langle A \rangle)}$. While there is no direct analogue to Eq. H28 in the centrality literature, if we were to define a centrality for A by the row sums of $C \triangleq \log((I - \alpha A^T)^{-1})$, then it corresponds to the series expansion $C = \sum_{l=1}^{\infty} \frac{(\alpha A^T)^l}{l}$. That is, $[C]_{ij}$ accounts for the number of paths between nodes i and j , down-weighted by a factor of $\frac{\alpha^l}{l}$ such that shorter paths contribute more to this centrality. Consequently, while $\bar{\gamma}^\alpha$ as defined in Eq. H28 does not exactly measure closeness as defined by Refs. [102, 103], it measures a weighted-closeness such that shorter paths contribute more than longer ones. This is in the same vein as measures given by arbitrary matrix functions of A [106]—such as the subgraph centrality [107] or communicability [125] which use the matrix exponential function, i.e. down-weight paths of length l by $l!$, or Katz centrality [40] which down-weights them by α^l .

Betweenness centrality. Similarly, consider the (approximate) bridging probabilities $\hat{\chi}_{ijk}(p; l)$ from Lemma 3, which is a good estimate for finite l asymptotically. Consider Eq. A5, while suppressing the conditioning on the giant component:

$$\begin{aligned} \hat{\chi}_{ijk}(p; l) &= P(\lambda_{ik} = l - p)P(\lambda_{kj} = p)P(\lambda_{ij} \geq l) \\ &\approx P(\lambda_{ik} = l - p)P(\lambda_{kj} = p) \\ &= ([\tilde{\Psi}_{l-p-1} - \tilde{\Psi}_{l-p}]_{ik})([\tilde{\Psi}_{p-1} - \tilde{\Psi}_p]_{kj}), \end{aligned}$$

where we apply the fact that for any finite l , the likelihood that the geodesic is larger than l is asymptotically close to unity, and the definition from Eq. 7a. Then, inserting into Eq. 125, alongside Eq. H26, the expected betweenness of nodes is encoded by the vector:

$$\boldsymbol{\beta} \approx \sum_{l=2}^{\infty} \sum_{p=1}^{l-1} \left(\langle A \rangle^T \right)^{l-p} \mathbf{u} \odot \langle A \rangle^p \mathbf{u}, \quad (\text{H29})$$

where \odot is element-wise multiplication. To ensure that the expression in Eq. H29 is well-defined, consider the same scaling as above, i.e. $\langle A \rangle \mapsto \alpha \langle A \rangle$, then by a change of variables $l - p \mapsto x$, $p \mapsto y$, define an “ α -betweenness vector” as

$$\begin{aligned} \boldsymbol{\beta}^\alpha &\triangleq \sum_{x=1}^{\infty} \sum_{y=1}^{\infty} \left(\alpha \langle A \rangle^T \right)^x \mathbf{u} \odot (\alpha \langle A \rangle)^y \mathbf{u} \\ &= \left[\sum_{x=1}^{\infty} \left(\alpha \langle A \rangle^T \right)^x \mathbf{u} \right] \odot \left[\sum_{y=1}^{\infty} (\alpha \langle A \rangle)^y \mathbf{u} \right] \\ &= \left[(I - \alpha \langle A \rangle^T)^{-1} - I \right] \mathbf{u} \odot \left[(I - \alpha \langle A \rangle)^{-1} - I \right] \mathbf{u}, \end{aligned} \quad (\text{H30})$$

where we have applied the formula for geometric series of a matrix. From above, the RHS can be seen as the product of “incoming” and “outgoing” Katz centralities—except on the expectation of A i.e. $\langle A \rangle$ —thus encoding the idea of “in-betweenness”. Again, we emphasize that

while β^α does not exactly measure betweenness as defined by Freeman [105], it measures a weighted notion of in-betweenness as given by net incoming and outgoing geodesics. Measures which build on this concept of accounting for both incoming and outgoing paths via powers of A and A^T have been previously defined, especially in the context of directed networks, to determine node roles and consequently node similarities based on them [108].

Appendix I: Empirical networks

We elaborate below on the approach to apply the SPLD formalism to empirical networks.

1. MLE of labeled graphs as SBMs

Say we have a given graph represented by the adjacency matrix A with known node labels given by the assignment matrix Z . The most trivial label assignment would be to assume a single block to which every node belongs, i.e. $k = 1$, which assumes an underlying ER graph model. For most empirical networks, labels can be retrieved from domain knowledge—like nodes in a social network will have associated socio-demographic characteristics. Assuming that the network is generated by an SBM with parameters $\boldsymbol{\pi}, B$, we can use the model definition in Eq. 50 to obtain a maximum likelihood estimate (MLE) of the parameters. For ease of notation let $\kappa : \{1, 2, \dots, n\} \rightarrow \{1, 2, \dots, k\}$ define the label assignment for a given graph A . Then the likelihood function, given the SBM model defined in Eq. 50 is given by:

$$\begin{aligned} L(\boldsymbol{\pi}, B) &= \prod_{i \neq j} P(A_{ij} | Z_{i\kappa(i)} = 1, Z_{j\kappa(j)} = 1, B_{\kappa(i)\kappa(j)}) \\ &\quad \prod_i P(Z_{i\kappa(i)} = 1 | \boldsymbol{\pi}) \\ &= \prod_{i \neq j} \left(\frac{B_{\kappa(i)\kappa(j)}}{n} \right)^{A_{ij}} \left(1 - \frac{B_{\kappa(i)\kappa(j)}}{n} \right)^{1-A_{ij}} \\ &\quad \prod_i \pi_{\kappa(i)}. \end{aligned} \tag{I1}$$

To maximize the log-likelihood, subject to the constraint $\sum_x \pi_x = 1$, apply the method of Lagrange multipliers. Define the Lagrangian $\mathcal{L}(\boldsymbol{\pi}, B, \lambda) \triangleq \log L(\boldsymbol{\pi}, B) + \lambda(1 - \sum_x \pi_x)$, where λ is the Lagrange multiplier, which

from Eq. I1 is given by:

$$\begin{aligned} \mathcal{L}(\boldsymbol{\pi}, B, \lambda) &= \sum_{x,y} \left[[Z^T A Z]_{xy} \log \left(\frac{B_{xy}}{n} \right) + \right. \\ &\quad \left. [Z^T (\mathbf{u}\mathbf{u}^T - A - I) Z]_{xy} \log \left(1 - \frac{B_{xy}}{n} \right) \right] \\ &\quad + \sum_x ([Z^T \mathbf{u}]_x \log \pi_x - \lambda \pi_x) + \lambda \end{aligned} \tag{I2}$$

For finding the stationary points, consider the first-order partial derivatives:

$$\frac{\partial \mathcal{L}}{\partial B_{xy}} = \frac{[Z^T A Z]_{xy}}{B_{xy}} - \frac{[Z^T (\mathbf{u}\mathbf{u}^T - A - I) Z]_{xy}}{n - B_{xy}} \tag{I3a}$$

$$\frac{\partial \mathcal{L}}{\partial \pi_x} = \frac{[Z^T \mathbf{u}]_x}{\pi_x} - \lambda \tag{I3b}$$

$$\frac{\partial \mathcal{L}}{\partial \lambda} = 1 - \sum_x \pi_x \tag{I3c}$$

Setting the partial derivatives with respect to the parameters to zero, i.e. RHS of Eq. I3 to 0, along with looking at the Hessian condition, yields:

$$\hat{\boldsymbol{\pi}} = \frac{Z^T \mathbf{u}}{n}, \tag{I4a}$$

$$\hat{B} = n Z^T A Z \oslash [Z^T (\mathbf{u}\mathbf{u}^T - I) Z], \tag{I4b}$$

where \mathbf{u} is an all-ones vector of length n , and $I \triangleq \text{diag}(\mathbf{u})$ is the identity matrix. Evidently, $\hat{\boldsymbol{\pi}}$ corresponds to the normalized total node-count of every block, and \hat{B} to the normalized total edge-count of every block pair, which is useful especially when we may not have access to the full adjacency structure. This formalism allows us to define an SBM for any given (A, Z) pair, regardless of how Z itself was inferred, with no computational cost except for summation of edge counts.

2. Empirical network datasets

All network datasets used in this work were obtained from the SNAP dataset library [58]. We only consider networks with fewer than 10,000 nodes but spanning a range of domains, and thus connectivities. We apply two pre-processing steps: (1) if networks are directed, they are converted to their undirected versions by assuming edges both ways, and (2) the network is restricted to only its giant component.

To obtain “labels” for the nodes to coarsen into SBMs, we use the graph-tool library [63] and infer hierarchical SBMs [54] to obtain a multi-level coarsening, i.e. SBMs with progressively increasing number of blocks. We restrict our analysis to SBMs with fewer than 64 blocks. Alternatively, we may apply modularity maximization [61]—as we do in Appendix I1 using the implementation

TABLE III. Empirical networks and associated statistic after pre-processing: number of nodes n , mean degree $\langle d \rangle$, mean geodesic length $\langle \lambda \rangle$, and number of blocks at multiple levels of coarsening obtained by inferring a hierarchical SBM.

Name	Description	n	$\langle d \rangle$	$\langle \lambda \rangle$	Blocks ^a
soc-sign-bitcoin-otc	Trust networks of people trading on Bitcoin OTC and	5875	7.32	3.57	1,4,14,56
soc-sign-bitcoin-alpha	Bitcoin Alpha platforms [126, 127]	3775	7.48	3.57	1,4,14,48
ca-GrQc	Collaboration networks of authors submitting to the	4158	6.46	6.05	1,2,5,14,34
ca-HepTh	“gr-qc” and “hep-th” categories of arXiv [57]	8638	5.74	5.95	1,4,14,48
CollegeMsg	Message network of an online college social network [128]	1893	14.62	3.06	1,2,12,61
email-Eu-core	Email network within a research institution [56, 57]	986	32.58	2.59	1,5,10,36
ego-Facebook	Friendship network from Facebook “friends lists” [101]	4039	43.69	3.69	1,2,3,5,9,23
p2p-Gnutella05	“Peer-to-peer” sharing network from Gnutella collected as snapshots on multiple dates within a week of each other [57, 129]	8842	7.20	4.60	1,3,6
p2p-Gnutella06		8717	7.23	4.57	1,2,6,16
p2p-Gnutella08		6299	6.60	4.64	1,2,5
p2p-Gnutella09		8104	6.42	4.77	1,3,6
feather-lastfm-social	Mutual-follower network of LastFM users from Asia [130]	7624	7.29	5.23	1,2,4,15,51
musae-twitch-DE	Friendship network from Twitch collected across 6 different countries [131]	9498	32.25	2.72	1,24
musae-twitch-EN		7126	9.91	3.68	1,3,18
musae-twitch-ES		4648	25.55	2.88	1,4,23
musae-twitch-FR		6549	34.41	2.68	1,4,20
musae-twitch-PT		1912	32.74	2.53	1,9,54
musae-twitch-RU		4385	17.01	3.02	1,2,11
wikispeedia		Hyperlink network of a subset of Wikipedia [132, 133]	4589	46.43	2.53
wiki-Vote	Voting network for Wikipedia admins and users [134, 135]	7066	28.51	3.25	1,9,38

^a showing levels below the cut-off of 64 blocks

in the NetworkX library [62]—to obtain “community labels” for nodes. To discourage very small communities, we post-process the labels obtained via modularity maximization by agglomerating communities containing fewer than 1% of the nodes.

Finally, empirical mean geodesic length is obtained using Dijkstra’s algorithm [136] implemented in the NetworkX library [62]. In Tab. III, we describe these networks and their associated statistics.

-
- [1] S. H. Strogatz, *Nature* **410**, 268 (2001).
- [2] R. Albert and A.-L. Barabási, *Reviews of Modern Physics* **74**, 47 (2002).
- [3] M. E. Newman, *SIAM Review* **45**, 167 (2003).
- [4] S. Wasserman and K. Faust, *Social Network Analysis: Methods and Applications*, Vol. 8 (Cambridge University Press, 1994).
- [5] M. E. Newman, *Nature Physics* **14**, 542 (2018).
- [6] A. Goldenberg, A. X. Zheng, S. E. Fienberg, and E. M. Airoldi, *Foundation and Trends in Machine Learning* **2**, 129 (2010).
- [7] T. P. Peixoto, *Physical Review Letters* **123**, 128301 (2019).
- [8] A. Godoy-Lorite and N. S. Jones, *Science Advances* **7**, eabb8762 (2021).
- [9] T. Hoffmann, L. Peel, R. Lambiotte, and N. S. Jones, *Science Advances* **6**, eaav1478 (2020).
- [10] T. P. Peixoto, *Physical Review X* **8**, 041011 (2018).
- [11] R. Cohen, K. Erez, D. Ben-Avraham, and S. Havlin, *Physical Review Letters* **85**, 4626 (2000).
- [12] D. S. Callaway, M. E. Newman, S. H. Strogatz, and D. J. Watts, *Physical Review Letters* **85**, 5468 (2000).
- [13] M. E. Newman, S. H. Strogatz, and D. J. Watts, *Physical Review E* **64**, 026118 (2001).
- [14] T. Nishikawa, A. E. Motter, Y.-C. Lai, and F. C. Hoppensteadt, *Physical Review Letters* **91**, 014101 (2003).
- [15] J. K. Harris, *An Introduction to Exponential Random Graph Modeling*, Vol. 173 (Sage Publications, 2013).
- [16] V. D. Blondel, J.-L. Guillaume, J. M. Hendrickx, and R. M. Jurgens, *Physical Review E* **76**, 066101 (2007).
- [17] E. Katzav, M. Nitzan, D. Ben-Avraham, P. Krapivsky, R. Kühn, N. Ross, and O. Biham, *Europhysics Letters* **111**, 26006 (2015).
- [18] R. van der Hofstad, G. Hooghiemstra, and P. Van Mieghem, *Random Structures & Algorithms* **27**, 76 (2005).
- [19] P. van der Hoorn and M. Olvera-Cravioto, *The Annals of Applied Probability* **28**, 1739 (2018).
- [20] A. Fronczak, P. Fronczak, and J. A. Holyst, *Physical Review E* **70**, 056110 (2004).
- [21] K. Françoisse, I. Kivimäki, A. Mantrach, F. Rossi, and M. Saerens, *Neural Networks* **90**, 90 (2017).
- [22] M. O. Jackson, B. W. Rogers, and Y. Zenou, *Journal of Economic Literature* **55**, 49 (2017).
- [23] P. Erdős and A. Rényi, *Publ. Math. Inst. Hung. Acad. Sci* **5**, 17 (1960).
- [24] R. Cohen and S. Havlin, *Physical Review Letters* **90**, 058701 (2003).
- [25] M. Molloy and B. Reed, *Random Structures & Algorithms* **6**, 161 (1995).

- [26] M. Molloy and B. Reed, *Combinatorics Probability and Computing* **7**, 295 (1998).
- [27] M. E. Newman, *Physical Review E* **76**, 045101 (2007).
- [28] I. Kryven, *Physical Review E* **95**, 052303 (2017).
- [29] B. Söderberg, *Physical Review E* **66**, 066121 (2002).
- [30] B. Söderberg, *Physical Review E* **68**, 026107 (2003).
- [31] B. Bollobás, S. Janson, and O. Riordan, *Random Structures & Algorithms* **31**, 3 (2007).
- [32] A. Allard, L. Hébert-Dufresne, J.-G. Young, and L. J. Dubé, *Physical Review E* **92**, 062807 (2015).
- [33] B. Karrer, M. E. J. Newman, and L. Zdeborová, *Phys. Rev. Lett.* **113**, 208702 (2014).
- [34] K. E. Hamilton and L. P. Pryadko, *Phys. Rev. Lett.* **113**, 208701 (2014).
- [35] L. C. Freeman, *Social Networks* **1**, 215 (1978).
- [36] S. P. Borgatti and M. G. Everett, *Social Networks* **28**, 466 (2006).
- [37] A. P. Giles, O. Georgiou, and C. P. Dettmann, in *2015 IEEE International Conference on Communications (ICC)* (IEEE, 2015) pp. 6450–6455.
- [38] M. Avella-Medina, F. Parise, M. T. Schaub, and S. Segarra, *IEEE Transactions on Network Science and Engineering* **7**, 520 (2018).
- [39] P. Bonacich, *Journal of mathematical sociology* **2**, 113 (1972).
- [40] L. Katz, *Psychometrika* **18**, 39 (1953).
- [41] M. Newman, *Networks*, 2nd ed. (Oxford University Press, 2018).
- [42] P. W. Holland, K. B. Laskey, and S. Leinhardt, *Social Networks* **5**, 109 (1983).
- [43] M. Penrose, *Random Geometric Graphs*, Vol. 5 (Oxford University Press, 2003).
- [44] S. J. Young and E. R. Scheinerman, in *International Workshop on Algorithms and Models for the Web-Graph* (Springer, 2007) pp. 138–149.
- [45] B. Bollobás and O. Riordan, *Random Structures & Algorithms* **39**, 1 (2011).
- [46] F. Riesz and B. Sz. Nagy, *Functional Analysis*, 2nd ed. (Frederick Ungar, 1955).
- [47] J. M. McPherson and L. Smith-Lovin, *American Sociological Review* , 370 (1987).
- [48] M. McPherson, L. Smith-Lovin, and J. M. Cook, *Annual Review of Sociology* **27**, 415 (2001).
- [49] B. Gnedenko, *Annals of Mathematics* , 423 (1943).
- [50] I. Tishby, O. Biham, and E. Katzav, *Journal of Physics A: Mathematical and Theoretical* **49**, 285002 (2016).
- [51] J. L. W. V. Jensen, *Acta Mathematica* **30**, 175 (1906).
- [52] B. Karrer and M. E. Newman, *Physical Review E* **83**, 016107 (2011).
- [53] J. Moody, *American Journal of Sociology* **107**, 679 (2001).
- [54] T. P. Peixoto, *Physical Review X* **4**, 011047 (2014).
- [55] M. E. Newman and A. Clauset, *Nature Communications* **7**, 1 (2016).
- [56] H. Yin, A. R. Benson, J. Leskovec, and D. F. Gleich, in *Proceedings of the 23rd ACM SIGKDD international conference on knowledge discovery and data mining* (2017) pp. 555–564.
- [57] J. Leskovec, J. Kleinberg, and C. Faloutsos, *ACM Transactions on Knowledge Discovery from Data (TKDD)* **1**, 2 (2007).
- [58] J. Leskovec and A. Krevl, *SNAP Datasets: Stanford large network dataset collection*, <http://snap.stanford.edu/data> (2014).
- [59] M. Girvan and M. E. Newman, *Proceedings of the National Academy of Sciences* **99**, 7821 (2002).
- [60] M. E. Newman, *Proceedings of the National Academy of Sciences* **103**, 8577 (2006).
- [61] A. Clauset, M. E. Newman, and C. Moore, *Physical Review E* **70**, 066111 (2004).
- [62] A. A. Hagberg, D. A. Schult, and P. J. Swart, in *Proceedings of the 7th Python in Science Conference*, edited by G. Varoquaux, T. Vaught, and J. Millman (Pasadena, CA USA, 2008) pp. 11 – 15.
- [63] T. P. Peixoto, [figshare 10.6084/m9.figshare.1164194](https://arxiv.org/abs/10.6084/m9.figshare.1164194) (2014).
- [64] M. Kraetzl, C. Nickel, and E. R. Scheinerman, *Preliminary manuscript* (2005).
- [65] W. L. Hamilton, R. Ying, and J. Leskovec, *IEEE Data Engineering Bulletin* **40**, 52– (2017).
- [66] H. Cai, V. W. Zheng, and K. C.-C. Chang, *IEEE Transactions on Knowledge and Data Engineering* **30**, 1616 (2018).
- [67] P. Goyal and E. Ferrara, *Knowledge-Based Systems* **151**, 78 (2018).
- [68] A. Ahmed, N. Shervashidze, S. Narayanamurthy, V. Josifovski, and A. J. Smola, in *Proceedings of the 22nd international conference on World Wide Web* (2013) pp. 37–48.
- [69] A. Grover and J. Leskovec, in *Proceedings of the 22nd ACM SIGKDD International Conference on Knowledge Discovery and Data Mining* (2016) pp. 855–864.
- [70] J. Mercer, *Philosophical Transactions of the Royal Society of London Series A* **209**, 415 (1909).
- [71] A. Rahimi and B. Recht, in *Advances in Neural Information Processing Systems*, Vol. 3 (2007) p. 5.
- [72] L. Barnett, E. Di Paolo, and S. Bullock, *Physical Review E* **76**, 056115 (2007).
- [73] M. Penrose, *The Annals of Applied Probability* **26**, 986 (2016).
- [74] C. P. Dettmann and O. Georgiou, *Physical Review E* **93**, 032313 (2016).
- [75] D. Krioukov, F. Papadopoulos, M. Kitsak, A. Vahdat, and M. Boguná, *Physical Review E* **82**, 036106 (2010).
- [76] M. Barthélemy, *Physics Reports* **499**, 1 (2011).
- [77] M. Garrod and N. S. Jones, *Physical Review E* **98**, 052316 (2018).
- [78] L. Lovász and B. Szegedy, *Journal of Combinatorial Theory, Series B* **96**, 933 (2006).
- [79] L. Lovász, *Large Networks and Graph Limits*, Vol. 60 (American Mathematical Society, 2012).
- [80] P. Orbanz and D. M. Roy, *IEEE Transactions on Pattern Analysis and Machine Intelligence* **37**, 437 (2014).
- [81] C. Borgs, J. Chayes, L. Lovász, V. Sós, and K. Vesztegombi, *European Journal of Combinatorics* **32**, 985 (2011).
- [82] F. Klimm, N. S. Jones, and M. T. Schaub, *arXiv preprint arXiv:2101.00503* (2021).
- [83] B. Bollobás, *Random Graphs*, 73 (Cambridge University Press, 2001).
- [84] A.-L. Barabási and R. Albert, *Science* **286**, 509 (1999).
- [85] G. Caldarelli, A. Capocci, P. De Los Rios, and M. A. Munoz, *Physical Review Letters* **89**, 258702 (2002).
- [86] K. Hashimoto, in *Automorphic Forms and Geometry of Arithmetic Varieties*, *Advanced Studies in Pure Mathematics*, Vol. 15, edited by K. Hashimoto and Y. Namikawa (Academic Press, 1989) pp. 211–280.
- [87] R. Cohen, K. Erez, D. Ben-Avraham, and S. Havlin,

- Physical Review Letters **86**, 3682 (2001).
- [88] N. H. Bingham, C. M. Goldie, and J. L. Teugels, *Regular Variation*, 27 (Cambridge University Press, 1989).
- [89] C. Cooper and A. Frieze, *Combinatorics, Probability and Computing* **13**, 319–337 (2004).
- [90] H. Schawe and A. K. Hartmann, *Physical Review E* **102**, 052108 (2020).
- [91] P. Van Mieghem, J. Omic, and R. Kooij, *IEEE/ACM Transactions On Networking* **17**, 1 (2008).
- [92] B. Bollobás, C. Borgs, J. Chayes, and O. Riordan, *The Annals of Probability* **38**, 150 (2010).
- [93] J. Dall and M. Christensen, *Physical Review E* **66**, 016121 (2002).
- [94] V. G. Cerf, D. D. Cowan, R. C. Mullin, and R. G. Stanton, *Networks* **4**, 335 (1974).
- [95] A. J. Hoffman and R. R. Singleton, *IBM Journal of Research and Development* **4**, 497 (1960).
- [96] M. Miller and J. Sirán, *The Electronic Journal of Combinatorics*, DS14 (2012).
- [97] F. Chung and L. Lu, *Proceedings of the National Academy of Sciences* **99**, 15879 (2002).
- [98] J.-C. Delvenne and A.-S. Libert, *Physical Review E* **83**, 046117 (2011).
- [99] Z. Burda, J. Duda, J.-M. Luck, and B. Waclaw, *Physical Review Letters* **102**, 160602 (2009).
- [100] R. Lambiotte, J.-C. Delvenne, and M. Barahona, *IEEE Transactions on Network Science and Engineering* **1**, 76 (2014).
- [101] J. J. McAuley and J. Leskovec, in *Advances in Neural Information Processing Systems*, Vol. 2012 (2012) pp. 548–56.
- [102] M. Marchiori and V. Latora, *Physica A: Statistical Mechanics and its Applications* **285**, 539 (2000).
- [103] Y. Rochat, *Closeness centrality extended to unconnected graphs: The harmonic centrality index*, Tech. Rep. (Institute of Applied Mathematics University of Lausanne, Switzerland, 2009).
- [104] A. Bavelas, *The Journal of the Acoustical Society of America* **22**, 725 (1950).
- [105] L. C. Freeman, *Sociometry*, 35 (1977).
- [106] E. Estrada and D. J. Higham, *SIAM Review* **52**, 696 (2010).
- [107] E. Estrada and J. A. Rodriguez-Velazquez, *Physical Review E* **71**, 056103 (2005).
- [108] K. Cooper and M. Barahona, *arXiv preprint arXiv:1012.2726* (2010).
- [109] P. Li, Y. Wang, H. Wang, and J. Leskovec, *Advances in Neural Information Processing Systems* **33** (2020).
- [110] P. W. Holland and S. Leinhardt, *Comparative Group Studies* **2**, 107 (1971).
- [111] P. W. Holland and S. Leinhardt, *Sociological Methodology* **7**, 1 (1976).
- [112] L. Le Cam, *Pacific Journal of Mathematics* **10**, 1181 (1960).
- [113] O. Perron, *Mathematische Annalen* **64**, 248 (1907).
- [114] C. D. Meyer, *Matrix Analysis and Applied Linear Algebra*, Vol. 71 (SIAM, 2000).
- [115] F. G. Frobenius, *Sitzung der physikalisch-mathematischen* (1912).
- [116] A. Broder, R. Kumar, F. Maghoul, P. Raghavan, S. Rajagopalan, R. Stata, A. Tomkins, and J. Wiener, in *The Structure and Dynamics of Networks* (Princeton University Press, 2011) pp. 183–194.
- [117] C. R. Johnson and R. A. Horn, *Matrix Analysis* (Cambridge University Press, 1985).
- [118] N. J. Higham, *Functions of Matrices: Theory and Computation* (SIAM, 2008).
- [119] B. Wang, W. Shi, and Z. Miao, *PloS One* **10**, e0118537 (2015).
- [120] M. H. Stone, *Linear Transformations in Hilbert Space and their Applications to Analysis*, Vol. 15 (American Mathematical Society, 1932).
- [121] S. Kotz, N. Balakrishnan, and N. L. Johnson, *Continuous Multivariate Distributions, Volume 1: Models and Applications* (John Wiley & Sons, 2004) p. 488.
- [122] R. M. Corless, G. H. Gonnet, D. E. Hare, D. J. Jeffrey, and D. E. Knuth, *Advances in Computational Mathematics* **5**, 329 (1996).
- [123] O. A. Civi, P. H. Pathak, and H.-T. Chou, *IEEE Transactions on Antennas and Propagation* **47**, 958 (1999).
- [124] M. Abramowitz and I. A. Stegun, *Handbook of Mathematical Functions with formulas, graphs, and mathematical table* (National Bureau of Standards Applied Mathematics series 55, 1965) p. 229.
- [125] E. Estrada and N. Hatano, *Physical Review E* **77**, 036111 (2008).
- [126] S. Kumar, F. Spezzano, V. Subrahmanian, and C. Faloutsos, in *IEEE 16th International Conference on Data Mining (ICDM)* (2016) pp. 221–230.
- [127] S. Kumar, B. Hooi, D. Makhija, M. Kumar, C. Faloutsos, and V. Subrahmanian, in *Proceedings of the Eleventh ACM International Conference on Web Search and Data Mining* (ACM, 2018) pp. 333–341.
- [128] P. Panzarasa, T. Opsahl, and K. M. Carley, *Journal of the American Society for Information Science and Technology* **60**, 911 (2009).
- [129] M. Ripeanu and I. Foster, in *International Workshop on Peer-to-peer Systems* (Springer, 2002) pp. 85–93.
- [130] B. Rozemberczki and R. Sarkar, in *Proceedings of the 29th ACM International Conference on Information and Knowledge Management (CIKM)* (ACM, 2020) p. 1325–1334.
- [131] B. Rozemberczki, C. Allen, and R. Sarkar, *Multi-scale attributed node embedding* (2019), arXiv:1909.13021 [cs.LG].
- [132] R. West, J. Pineau, and D. Precup, in *Twenty-First International Joint Conference on Artificial Intelligence* (2009).
- [133] R. West and J. Leskovec, in *Proceedings of the 21st international conference on World Wide Web* (2012) pp. 619–628.
- [134] J. Leskovec, D. Huttenlocher, and J. Kleinberg, in *Proceedings of the SIGCHI conference on human factors in computing systems* (2010) pp. 1361–1370.
- [135] J. Leskovec, D. Huttenlocher, and J. Kleinberg, in *Proceedings of the 19th international conference on World wide web* (2010) pp. 641–650.
- [136] E. W. Dijkstra *et al.*, *Numerische Mathematik* **1**, 269 (1959).